

**Spatial and temporal aspects of
PI(4,5)P₂ and SNAREs in exocytosis studied using
isolated membrane sheets and capacitance measurements**

Ph.D. Thesis

in partial fulfilment of the requirements for the degree
“Doctor of Philosophy (PhD)/Dr. rer. nat.”
in the Neuroscience Program at the Georg August University Göttingen
Faculty of Biology

submitted by

IRA MILOSEVIC

born in

SINJ, CROATIA

Göttingen 2005

Advisor, first member of FAC:

Prof. Dr. Erwin Neher

Advisor, second member of FAC:

Prof. Dr. Reinhard Jahn

Third member of FAC:

Prof. Dr. Detlev Schild

Date of submission of the Ph.D. thesis:

December 15th, 2005

Date of thesis defence:

I hereby declare that I prepared the Ph.D. thesis “Spatial and temporal aspects of PI(4,5)P₂ and SNAREs in exocytosis studied using isolated membrane sheets and capacitance measurements” on my own and with no other sources and aids than quoted.

Göttingen, December 12th, 2005

Ira Milosevic

LIST OF CONTENTS

PUBLISHING NOTE.....	1
1. GENERAL INTRODUCTION.....	2
1.1. Key steps of regulated exocytosis.....	3
1.2. Molecular machinery involved in the late steps of regulated exocytosis.....	5
1.2.1. Proteins involved in regulated exocytosis.....	5
1.2.1.1. SNARE proteins.....	5
1.2.1.2. Exocytic regulatory proteins.....	10
1.2.2. Lipids involved in regulated exocytosis.....	13
1.2.2.1. PI(4,5)P ₂ regulation and cellular functions.....	16
1.3. Aims and experimental approach.....	21
1.3.1. Chromaffin cell as a model system for studying regulated exocytosis...21	
1.3.2. Evaluation of regulated exocytosis in chromaffin cells.....	22
1.3.3. Evaluation of exocytic proteins and lipids in the plasma membrane.....	26
1.3.4. The aims of my studies.....	27
2. PUBLICATIONS.....	30
2.1. Plasmalemmal phosphatidylinositol-4,5-bisphosphate level regulates the releasable vesicle pool size in chromaffin cell.....	30
2.1.1. Additional data.....	40
A proportion of PI(4,5)P ₂ -clusters colocalise with syntaxin 1 in chromaffin cells.....	40
Exocytic proteins which may mediate PI(4,5)P ₂ regulation of chromaffin cell secretion.....	42
The role of PI4P5K-I γ in Ca ²⁺ -dependent priming.....	44
2.2. Alternative splicing of SNAP-25 regulates secretion through non-conservative substitutions in the SNARE domain.....	46
2.3. Sequential N- to C-terminal „zipping-up“ of the SNARE complex drives priming and fusion of secretory vesicles.....	58
3. GENERAL DISCUSSION.....	105

3.1. Plasma membrane sheet as an assay to study plasmalemmal proteins and lipids.....	106
3.2. Plasma membrane clusters of proteins and lipids involved in exocytosis.....	108
PI(4,5)P ₂ clusters.....	109
SNARE protein clusters.....	113
3.3. The role of PI(4,5)P ₂ in chromaffin cell exocytosis.....	115
3.4. The role of SNAP-25 isoforms in chromaffin cell exocytosis.....	119
3.5. The mechanism of the SNARE complex action in exocytosis.....	121
3.6. Future perspectives.....	122
4. SUMMARY.....	126
5. REFERENCES.....	128
Abbreviations.....	148
CURRICULUM VITAE.....	150

PUBLISHING NOTE

The experimental part of this doctoral thesis was performed at the Max Planck Institute for Biophysical Chemistry (Göttingen, Germany) in the Department of Membrane Biophysics and the Department of Neurobiology.

The thesis is based on the following publications referred to by their corresponding Roman numerals:

- I. Milosevic I., Sørensen J. B., Lang T., Krauss M., Nagy G., Haucke V., Jahn R., Neher E. (2005) Plasmalemmal phosphatidylinositol-4,5-bisphosphate level regulates the releasable vesicle pool size in chromaffin cells. *J Neurosci* 25 (10), 2557-2565
- II. Nagy G.*, Milosevic I.*, Fasshauer D., Müller M., de Groot B., Lang T., Wilson M.C., Sørensen J. B. (2005) Alternative splicing of SNAP-25 regulates secretion through non-conservative substitutions in the SNARE domain. *Mol. Biol. Cell* 16, 5675-5685
*equal contribution
- III. Sørensen J. B., Wiederhold K., Müller M., Milosevic I., Nagy G., de Groot B., Grubmüller H., Fasshauer D. (2006) Sequential N- to C-terminal „zipping-up“ of the SNARE complex drives priming and fusion of secretory vesicles. *EMBO J.*

In addition, some unpublished data are presented and discussed.

1. GENERAL INTRODUCTION

Biological membranes are cohesive but flexible barriers separating two fluid compartments. They constitute the boundaries of cells, and moreover, define compartments and localise cellular processes (Jain, 1972). Membrane lipids establish the unique liquid-crystalline organisation of membranes by virtue of the hydrophobic interactions and the elasticity of phospholipid acyl chains (Jain, 1972). Yet, membranes are more than barriers; they harbour the integral membrane proteins which catalyse the selective transfer of information and material between compartments. The head groups of some lipids serve as ligands for specific protein domains, and others carry a net negative charge that in a less specific manner attract positively charged protein domains to the membrane/solution interface (Alberts *et al.*, 2002). The polar head groups thus serve to direct and organize protein targeting to different compartmental interfaces. Hence, membrane lipids provide a structural scaffold for the organization of cellular enzymatic machineries and for the anchoring of the cytoskeleton. In addition, some membrane lipids have an important function in cellular signalling due to their active metabolism, leading to transient accumulation in the target membranes (Alberts *et al.*, 2002). Consequently, even though membrane lipids have no intrinsic catalytic activity, they are key participants in the regulation of cell metabolism and function due to their fast turnover.

As a consequence of this membrane-based organisation of life, cells have developed processes by which they can shuttle molecules between compartments and release them to the extracellular space. This latter process, named exocytosis, is of particular importance since it enables the cell to communicate with its surroundings. It can occur constitutively or in a regulated manner, triggered by a specific signal (Alberts *et al.*, 2002). For neurons and neuroendocrine cells, the specialized cells whose main function is to produce and secrete signalling molecules rapidly on demand, this signal is an increase in the intracellular calcium (Ca^{2+}) concentration (Douglas, 1968; Kandel *et al.*, 2000).

Ca^{2+} -triggered exocytosis is a complex and highly controlled process (Südhof, 2004). It is based on the cycling of secretory vesicles, modules that contain defined amount of molecules destined to be released. Small non-peptide molecules mainly accumulate in the synaptic vesicles (SVs), while peptides and biogenic amines are stored in the large dense-core vesicles (LDCVs; Kandel *et al.*, 2000). The distribution of secretory vesicles depends on the cell type: SVs are hallmark of neurons and LDCVs of neuroendocrine cells (e.g. chromaffin cells). Although SVs and LDCVs differ in a number of aspects, they share the common fundamental mechanism of release (De Camilli and Jahn, 1990). The mature secretory

vesicles wait in close proximity to the plasma membrane, until directed to undergo exocytosis. The exocytic process involves targeted translocation of vesicles to the sites of release, the initial contact with the plasma membrane (docking), the preparation of vesicles for the fusion (priming) and the Ca^{2+} -triggered fusion of membranes that results in the release of vesicular content (Südhof, 2004). Finally, to compensate for the added membrane during exocytosis, the cells maintain the net surface area by recycling the proteins and lipids, through a process called endocytosis (Slepnev and De Camilli, 2000). During the last decade exocytosis and endocytosis have been studied independently in great details. Although it unclear how, it is currently believed that these processes are tightly coupled (Gundelfinger *et al.*, 2003).

This doctoral thesis describes the investigation of two molecules involved in the regulated transfer of information and material across the plasma membrane. One molecule is a membrane lipid, phosphatidylinositol 4,5-bisphosphate [$\text{PI}(4,5)\text{P}_2$], and the other is a membrane protein, synaptosomal-associated protein of 25 kDa (SNAP-25). Although these two relatively simple molecules have multiple cellular functions, this thesis focuses only on their role in regulated exocytosis.

1.1. Key steps of regulated exocytosis

Regulated exocytosis consists of a cascade of protein-protein and lipid-protein interactions leading to the externalisation of the secretory molecules (Südhof, 2004). As mentioned above, the key steps of exocytosis are vesicular recruitment to the plasma membrane, docking, priming and fusion (Figure 1). In this section a general overview of these steps is presented, and in the next two sections I present the proteins and lipids which mediate them.

A pool of mature secretory vesicles (referred to as the reserve pool) is localised in close proximity to the plasma membrane. Vesicles are imbedded in a network of cortical actin, whose rearrangement triggered by stimulation-induced Ca^{2+} entry allows movement of secretory vesicles to exocytic sites (Vitale *et al.*, 1995; Gil *et al.*, 2000). Therefore, it is thought that the actin network regulates the availability of vesicles and other regulatory molecules (Sankaranarayanan *et al.*, 2003).

Docking in mammalian secretory cells is defined as the initial contact of the secretory vesicle with the plasma membrane. In neurons it mainly occurs at the active zone (reviewed by Südhof, 2004). Specific release zones or “hot spots” of exocytosis in neuroendocrine cells have been detected, but generally neuroendocrine cells lack the highly localised specialisations (reviewed by Mansvelder and Kits, 2000; see Discussion). Nevertheless, many

neuroendocrine cells (e.g. chromaffin cells in adrenal medulla, but not in cell culture) are polarised and the secretory vesicles dock accordingly. Interestingly, the spatial organisation of certain plasmalemmal proteins may preferentially recruit vesicles. In the plasma membrane of pheochromocytoma cells (PC12, a neuroendocrine tumor cell line), it was shown that the protein syntaxin 1 is organised in cholesterol-enriched clusters to which a population of secretory vesicles can dock and fuse (Lang *et al.*, 2001).

Not all secretory vesicles located at the plasma membrane of neurosecretory cells are able to undergo fusion in response to an increase in intracellular Ca^{2+} concentration ($[\text{Ca}^{2+}]_i$; Steyer *et al.*, 1997; Oheim *et al.*, 1998). Therefore, secretory vesicles targeted to their release site are not initially fusion competent. To become responsive to Ca^{2+} increase they must undertake a complex set of reversible interactions involving vesicular and plasma membrane proteins and lipids. In other words, they need to undergo priming. Priming requires Ca^{2+} , ATP and some cytoplasmic factors (reviewed by Martin, 2003). It is currently believed that the initiation of the SNARE (soluble *N*-ethylmaleimide-sensitive factor (NSF) attachment protein receptor) complex assembly is probably the key molecular event underlying the priming process.

The final step of exocytosis is the release of the vesicle content into the extracellular space. This can be achieved either by the complete fusion of the secretory vesicle with the plasma membrane or by a “kiss-and-run” mechanism (An and Zenisek, 2004). The latter involves the formation of a transient fusion pore which allows the partial release of the vesicle content (Aravanis *et al.*, 2003; Gandhi and Stevens, 2003). Since the release of neurotransmitters by neurons or hormones by some neurosecretory cells (e.g. catecholamines by chromaffin cells) occurs in the millisecond range after the stimulus, the fusion machinery must be assembled to a point in which only few additional molecular interactions are required (Südhof, 1995; Shao *et al.*, 1997). Given that the stimulus is a sudden increase in $[\text{Ca}^{2+}]_i$, the process assumes binding of Ca^{2+} -cations to the Ca^{2+} -sensor(s) to trigger the irreversible fusion reaction. It has been observed that the secretory vesicles display heterogeneous release probability (Rosenmund *et al.*, 1993; Voets, 2000), which suggests the existence of distinct vesicle populations with different Ca^{2+} -sensors. Present biophysical models indicate that the cooperative binding of at least five Ca^{2+} -cations to the Ca^{2+} -sensor is needed to release the vesicular content into the extracellular space (Beutner *et al.*, 2001; Wölfel and Schneggenburger, 2003).

1.2. Molecular machinery involved in the late steps of regulated exocytosis

1.2.1. Proteins involved in regulated exocytosis

Regulated exocytosis relies on the same basic proteinaceous machinery as other membrane trafficking events (Jahn *et al.*, 2003). In addition, the sophisticated control that characterises regulated exocytosis in neurons and neuroendocrine cells requires the existence of regulatory proteins. Here I present an outline on the basic and regulatory apparatus.

1.2.1.1. SNARE proteins

The SNARE protein superfamily is presently considered central to the late steps of regulated exocytosis and bilayer fusion. Originally described as soluble NSF attachment protein (SNAP) receptors, most members of the SNARE family have been identified by their possession of a conserved homologous stretch of 60-70 amino acids, referred to as the SNARE motif (Terrian and White, 1997; Weimbs *et al.*, 1998). Four SNARE motifs assemble spontaneously into a thermostable, sodium dodecyl sulfate and protease resistant coiled-coil bundle, called the SNARE core complex (Figure 1; Sutton *et al.*, 1998; Fasshauer *et al.*, 1998; Antonin *et al.*, 2002). Heptad repeats in components of the core complex form 16 conserved layers of interacting amino acid side chains which are arranged perpendicular to the axis of the complex. All layers except one contain hydrophobic amino acids. The unique central layer, termed the “0-layer”, is hydrophilic and consists of three glutamines (Qs) and one arginine (R) stabilised by ionic interactions. Based on this characteristic, SNARE proteins are classified into four subfamilies: Q_a-, Q_b-, Q_c- and R-SNAREs (Fasshauer *et al.*, 1998; Bock *et al.*, 2001). All analysed SNARE complexes that contain three or four SNARE proteins have a Q_aQ_bQ_cR composition. It is believed that this arrangement contributes to specific SNARE pairing, and consequently to the fusion of appropriate membranes (McNew *et al.*, 2000; Parlati *et al.*, 2000).

To date, 35 SNARE proteins have been identified in humans (Bock *et al.*, 2001). Despite the large number of SNAREs, the members of the neuronal synaptic SNARE complex have been the most intensely studied. This complex, first purified by Sönnner and collaborators (1993), is comprised of three proteins: syntaxin 1 (Bennett *et al.*, 1992), synaptosome-associated protein of 25 kDa (SNAP-25; Oyler *et al.*, 1989) and synaptobrevin 2/vesicle associated membrane protein (VAMP) 2 (Trimble *et al.*, 1988; Baumert *et al.*, 1989). These three proteins are described in detail below.

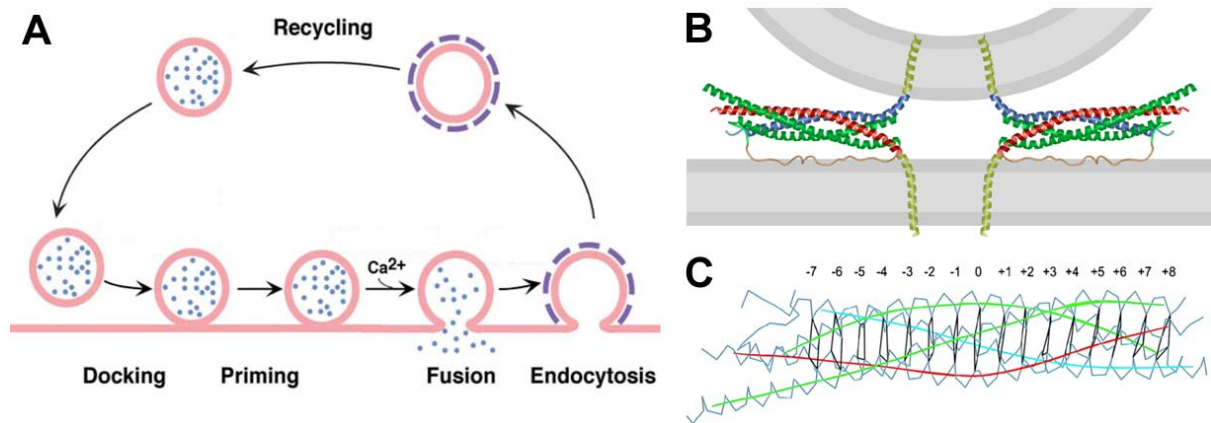


Figure 1. (A) The secretory vesicle cycle depicting the key steps of secretory vesicle fusion. (B) Neuronal SNARE complexes. Based on the crystal structure (Sutton *et al.*, 1998), the schematic shows a vesicle brought into close proximity to the plasma membrane by the SNARE complexes. The SNARE motif of syntaxin 1 is depicted in red, synaptobrevin 2 in blue, and the two SNAP-25 SNARE motifs are green. (C) The localisation of 15 hydrophobic layers and the central hydrophilic “0-layer”. From Fasshauer *et al.*, 1998.

Syntaxin

Syntaxin 1 is a prototypic Q_a -SNARE and it contributes one of the four α -helices forming the neuronal exocytic SNARE complex (Sutton *et al.*, 1998; Fasshauer *et al.*, 1998). This 35 kDa plasma membrane protein consists of a transmembrane domain, a SNARE motif and an N-terminal H_{abc} -domain (Bennett *et al.*, 1992). Two alternatively spliced isoforms, syntaxin 1A and syntaxin 1B, share high homology and localisation to the plasma membrane (Bennett *et al.*, 1992). While their expression pattern largely overlaps, with only subtle changes in distribution, it is essentially restricted to neuronal and neuroendocrine cells (Ruiz-Montasell *et al.*, 1996). Interestingly, an increase in syntaxin 1B level has been detected during the process of learning (Davis *et al.*, 1998).

The N-terminal H_{abc} -domain of syntaxin 1 is implicated in the regulation of protein accessibility. This region reversibly binds to the SNARE motif and can maintain two distinct syntaxin 1 conformations. In the “open” conformation (H_{abc} -domain not bound to the SNARE motif) protein is able to form a functional SNARE complex, whereas in the “closed” conformation (H_{abc} -domain bound to the SNARE motif) it is not (Dulubova *et al.*, 1999). A regulatory protein Munc18, a member of the conserved Sec1/Munc18 (SM)-related protein family, is believed to stabilise the “closed” conformation of syntaxin 1 and control its accessibility (Dulubova *et al.*, 1999; Yang *et al.*, 2000; Misura *et al.*, 2000). In this particular model syntaxin 1 may also be involved in the priming process. However, it has also recently

been suggested that multiple syntaxin 1 transmembrane domains may act as the subunits of a proteinaceous fusion pore (Han *et al.*, 2004).

The Q_a-SNAREs syntaxin family has a total of 15 members in mammals. They are found in numerous intracellular organelles where they function in a wide range of intracellular membrane fusion pathways (Teng *et al.*, 2001). In addition to syntaxin 1, three other syntaxins (2–4) are also localised to the plasma membrane and function in exocytosis in different cell types (Teng *et al.*, 2001).

SNAP-25

SNAP-25 is a Q_{bc}-SNARE and contributes two of the four α -helices of the neuronal exocytic SNARE complex (Sutton *et al.*, 1998; Fasshauer *et al.*, 1998). The SNARE motifs are present at the N- and C-termini of SNAP-25 and are separated by a central cysteine-rich membrane targeting domain (also called a linker domain; Sutton *et al.*, 1998). SNAP-25 is highly conserved among species with little variation in length. The two alternatively spliced variants, SNAP-25a and SNAP-25b, have high homology, differing only in 9 amino acids (Bark and Wilson, 1994). They are efficiently targeted to the plasma membrane due to the palmitoylation of the four cysteine residues in the linker domain (Hess *et al.*, 1992; Bark and Wilson, 1994). The position of one of these four cysteines is different in the SNAP-25 isoforms and it has been speculated that this variation could target the two isoforms to different sites on the plasma membrane (Bark and Wilson, 1994; Bark *et al.*, 1995). Where the SNAP-25 isoforms are palmitoylated in the cell is speculative - it presumably occurs either in the Golgi or at the plasma membrane (Gonzalo and Linder, 1998). Moreover, even a single cysteine substitution is known to reduce the level of palmitoylation and membrane association (Veit *et al.*, 1996; Lane and Liu, 1997).

The SNAP-25 isoforms have a restricted expression pattern, being most abundant in neuronal and neuroendocrine cells (Bark *et al.*, 1995; Borschert *et al.*, 1996). However, an interesting developmental shift in the expression of the isoforms has been described: SNAP-25a is more abundant in embryonic brain, whereas the expression of SNAP-25b increases robustly after birth to become the predominant isoform in most, but not all, adult brain areas (Bark *et al.*, 1995; Boschert *et al.*, 1996). Impairment of this switch towards the SNAP-25b isoform in mice leads to premature mortality and a change in short-term plasticity in hippocampal synapses (Bark *et al.*, 2004). In contrast, SNAP-25a remains the predominant isoform in adult chromaffin cells (Grant *et al.*, 1999).

Ablation of the SNAP-25 gene in mice results in embryonic lethality of the mutant animal (Washbourne *et al.*, 2002). The SNAP-25 *null* embryos are morphologically abnormal, but the major brain structures are unchanged (Washbourne *et al.*, 2002). Ca^{2+} -triggered secretion from SNAP-25 *null* chromaffin cells is nearly abolished (Sørensen *et al.*, 2003a). Both SNAP-25 isoforms can rescue secretion when expressed in SNAP-25 *null* chromaffin cells, but interestingly the SNAP-25b isoform is two to three times more efficient in this respect than the SNAP-25a isoform (Sørensen *et al.*, 2003a).

Two other proteins belong to this family, SNAP-23 and SNAP-29. SNAP-23 shares nearly 60% identity with SNAP-25 and is ubiquitously expressed (Ravichandran *et al.*, 1996; Wang *et al.*, 1997). Similarly to SNAP-25, SNAP-23 is targeted to the plasma membrane by palmitoylation of five cysteine residues (Wang *et al.*, 1997) and it forms a SNARE complex with synaptobrevin 2 and several syntaxin isoforms (Ravichandran *et al.*, 1996). It has been implicated in both constitutive and regulated exocytosis in non-neuronal cells (Leung *et al.*, 1998; Rea *et al.*, 1998; Vaidyanathan *et al.*, 2001). In chromaffin cells it can partially substitute SNAP-25 function (Sørensen *et al.*, 2003a). On the other hand, SNAP-29 shares less identity with SNAP-25 and lacks the conserved palmitoylated residues (Steeigmaier *et al.*, 1998). It has been suggested that SNAP-29 acts as a negative modulator for neurotransmitter release, probably by slowing synaptic vesicle turnover (Pan *et al.*, 2005).

Synaptobrevin

Synaptobrevin is a prototypic R-SNARE and contributes one of the four α -helices which compose the neuronal exocytic SNARE complex (Sutton *et al.*, 1998; Fasshauer *et al.*, 1998). It is an abundant 13 kDa vesicle protein with a central SNARE motif, a C-terminal transmembrane region and a proline-rich N-terminus (Elferink *et al.*, 1989; Trimble *et al.*, 1990). Two of the best studied isoforms, synaptobrevin/VAMP 1 and synaptobrevin/VAMP 2, mainly differ in the hydrophobic C-terminus and in the poorly conserved N-terminus (Elferink *et al.*, 1989; Trimble *et al.*, 1990). Although a partial overlap in their expression pattern is apparent, synaptobrevin 1 and 2 are differentially distributed in the brain, suggesting specialised functions for each isoform. Synaptobrevin 2 is in general more evenly distributed, while synaptobrevin 1 expression is located predominantly in neurons with somatomotor function (Trimble *et al.*, 1990). In addition, these two isoforms are differently distributed in the mouse retina (Sherry *et al.*, 2003).

Ablation of the synaptobrevin 2 gene is lethal post-natally (Schoch *et al.*, 2001). Evoked synaptic exocytosis from synaptobrevin 2 *null* hippocampal neurons is severely

deceased, but fusion is not completely abolished (Schoch *et al.*, 2001). The vesicles which fuse even in the absence of synaptobrevin 2 are unable to endocytose and recycle quickly, suggesting that synaptobrevin 2 is also necessary for rapid synaptic vesicle endocytosis (Deak *et al.*, 2004).

The function of SNARE proteins in regulated exocytosis

The central role of the SNARE complex in regulated exocytosis of neurons and neuroendocrine cells is well documented. The first, and maybe the most impressive demonstration, came from studies with neurotoxins which selectively cleave SNAREs and potently inhibit exocytosis (Blasi *et al.*, 1993a; 1993b; Niemann *et al.*, 1994). Tetanus toxin cleaves synaptobrevin, while botulinum neurotoxins (BoNT) A, B and C cleave SNAP-25, synaptobrevin and syntaxin, respectively (Niemann *et al.*, 1994). Reconstitution studies of purified proteins in liposomes indicated that SNAP-25, syntaxin 1 and synaptobrevin 2 are sufficient to fuse membranes and can be considered to represent a "minimal fusion machinery" (Weber *et al.*, 1998). Another study expressed the same SNARE proteins on the cellular surface and detected spontaneous cell fusion, showing that SNAREs are sufficient to fuse biological membranes as well (Hu *et al.*, 2003). Finally, the genetic ablations of SNAP-25 and synaptobrevin 2 in mice strongly inhibit exocytosis, but not completely (see above). The residual exocytosis observed in synaptobrevin 2 *null* animals suggested the existence of SNARE-independent membrane fusion (Schoch *et al.*, 2001). There is however no experimental proof to support this, and it may be possible that the related SNARE proteins present in the *null* cells are mediating the observed exocytosis (Borisovska *et al.*, 2005).

The formation of the SNARE complex was originally suggested to execute docking of secretory vesicles (Söllner *et al.*, 1993). However, morphological docking of vesicles is normal after the neurotoxin treatment (Schiavo *et al.*, 2000), suggesting a downstream role for SNAREs, possibly both in priming and fusion. The SNARE complex may serve as a core for the regulatory proteins and the energy liberated during its formation may be needed to overcome the energy barrier for membrane fusion (Chen and Scheller, 2001; Rizo and Südhof, 2002; also see Discussion). The mechanism of the SNARE complex formation and the relative timing of this process with respect to the Ca^{2+} -trigger is unclear. Hanson, Heuser and Jahn (1997) suggested that the SNARE complex assembles or "zips-up" progressively from the N-terminus towards the membrane anchors of syntaxin 1 and synaptobrevin 2. Several experiments using different systems support such a model (Xu *et al.*, 1999; Chen *et al.*, 2001; Melia *et al.*, 2002; Matos *et al.*, 2003). However, two studies report that the C-

terminal part of synaptobrevin is inserted into the vesicular membrane, and as such cannot participate in the SNARE complex formation (Hu *et al.*, 2002; Kweon *et al.*, 2003).

In short, the three neuronal SNARE proteins represent the minimal fusion machinery. However, fusion mediated by SNAREs only is relatively slow and uncoordinated. On the other hand, neurons and neuroendocrine cells require high levels of spatially and temporally coordinated activity. In these cells, SNARE proteins are tightly regulated at different stages of their generation and action: transcriptional regulation of gene expression, targeting to the correct compartment membranes, functionality in targeted membranes, posttranslational modification (e.g. phosphorylation), assembly, activity and disassembly of the SNARE complex. Consequently, many accessory factors that modulate the SNARE-driven exocytosis are necessary.

1.2.1.2. Exocytic regulatory proteins

The molecular action of accessory proteins is presently under intense study. As they are not the focus of this doctoral thesis, I shall give a superficial overview of the present knowledge on several important protein families implicated in the exocytic process.

As mentioned above, the SNARE complex assembly is tightly regulated and two conserved SNARE-interacting protein families play a major role in this process: Rab and SM proteins.

Rab proteins are small cytosolic GTPases. Among the 70 members identified in humans, Rab3 has been implicated in the regulation of multiple steps of exocytosis (reviewed by Südhof, 2004). When bound to membranes, Rab proteins operate as molecular switches which are active in the GTP-bound form and inactive in the GDP-bound form. The active Rabs presumably recruit a number of proteins and bridge the membranes designed to fuse. However, Rab proteins may also coordinate the downstream reactions which result in the formation of the SNARE complex (Waters and Hughson, 2000).

SM-proteins represent a small family of conserved soluble 60-70 kDa proteins. Similar to SNAREs, SM-proteins are essential for exocytosis and they seem to be required for several steps of the exocytic pathway (Toonen, 2003). SM-proteins bind SNAREs, preferably of the Q_a-subfamily, implying that they may function in the SNARE assembly regulation. As mentioned above, Munc18, the SM-protein involved in neuronal exocytosis, binds to the “closed” syntaxin 1 conformation and presumably prevents the formation of SNARE complexes (Dulubova *et al.*, 1999; Yang *et al.*, 2000; Misura *et al.*, 2000). Consequently, Munc18/syntaxin 1 interaction is expected to be a negative regulator of the exocytic process.

However, functional data do not support such model. With the exception of Schulze *et al.* (1994), Munc18 overexpression does not inhibit exocytosis (Graham *et al.*, 1997; Voets *et al.*, 2001; Fisher *et al.*, 2001). In addition, Munc18-1 *null* cells do not exocytose (Verhage *et al.*, 2000; Voets *et al.*, 2001), suggesting a more complex role for this protein in the exocytic process.

Naturally, the assembled SNARE protein complexes need to disassemble after membrane fusion. The ATPase NSF and the adaptor protein α/β -SNAP are required for this task (Söllner *et al.*, 1993; Littleton *et al.*, 2001).

In contrast to SNAREs, NSF, Rabs and SM-proteins which are present in all eukaryotic cells, a number of proteins are specific for neurons and/or neuroendocrine cells. Presumably these proteins are responsible for the fast Ca^{2+} -triggered exocytosis that characterises these cells (neurons 2 ms, chromaffin cells 20 ms; Schneggenburger and Neher, 2000). Here I describe several of the best characterised of these: Munc13s, complexins, Ca^{2+} -dependent activator proteins for secretion (CAPSs) and synaptotagmins.

Munc13s are conserved 200 kDa proteins containing a diacylglycerol (DAG) binding C_1 -domain, two or three C_2 -domains, and a syntaxin 1 binding domain (Brose *et al.*, 1995; Betz *et al.*, 1997; Betz *et al.*, 1998). Three isoforms are presently known in humans: Munc13-1, -2 and -3 (Brose *et al.*, 2000). Munc13s are essential for both spontaneous and evoked release and, as shown by gene ablation studies in worms, flies and mice, function after docking in the regulation of the releasable pool size (Richmond *et al.*, 1999; Aravamudan *et al.*, 1999; Augustin *et al.*, 1999; Rosenmund *et al.*, 2002). Mutations in syntaxin 1, which result in a constitutively “open” conformation, can overcome a requirement for UNC-13 in worms, suggesting that UNC-13 promotes the formation of the “open” syntaxin 1 form (Richmond *et al.*, 2001). However, it still remains to be shown in functional assays whether Munc13s exert their priming activity by regulating the availability of syntaxin 1 for the SNARE complex formation.

Complexins are soluble, conserved 15 kDa proteins (McMahon *et al.*, 1995). Two isoforms, complexin I and II, are enriched in the brain and spinal cord, and complexin II is also present in secretory cells (McMahon *et al.*, 1995). Soluble complexins are largely unstructured, but they gain a helical conformation upon binding and stabilising assembled SNARE complexes (Pabst *et al.*, 2000; Chen *et al.*, 2002). Complexins I and II *null* cells are impaired in Ca^{2+} -regulated exocytosis, but they show normal docking (Reim *et al.*, 2001). Therefore, complexins function after docking, probably during vesicle priming and fusion, and future studies are needed to reveal the mechanism of their action.

That Ca^{2+} represents an exocytic trigger has been known for nearly half a century (Douglas, 1968); however, the longstanding debate regarding the identity of the Ca^{2+} -sensor(s) persists. Several Ca^{2+} -binding proteins which could potentially serve as Ca^{2+} -sensors have been identified. Here I describe two of them: CAPSs and synaptotagmins.

CAPS1 is a cytoplasmic 145 kDa protein originally described as essential in Ca^{2+} -triggered release from permeabilised PC12 cells, where it is required for a secretory step following ATP-dependent priming (Walent *et al.*, 1992; Hay and Martin, 1992; Ann *et al.*, 1997). It consists of a C-terminal membrane-association domain which mediates LDCV binding, a pleckstrin homology (PH) domain which binds acidic phospholipids, a Munc homology domain and a C_2 -domain (Grishanin *et al.*, 2002). The second structurally and functionally similar isoform, CAPS2, exhibits a different cellular and developmental expression pattern (Cisternas *et al.*, 2003; Speidel *et al.*, 2003). While CAPS1 is specific for neuronal and neuroendocrine cells, CAPS2 is more uniformly distributed (Speidel *et al.*, 2003). Initially, CAPS1 is described to act during the Ca^{2+} -triggering step of regulated LDCV exocytosis (Elhamdani *et al.*, 1999; Rupnik *et al.*, 2000). However, a recent study revealed its function in the catecholamine loading of LDCVs (Speidel *et al.*, 2005; see Discussion).

Presently the best candidates for the Ca^{2+} -sensors are the members of synaptotagmin family (Sugita *et al.*, 2002). Sixteen family members have been identified (Craxton, 2004). Most of them comprise an N-terminal transmembrane domain, a variable linker and the two C-terminal C_2 -domains which bind Ca^{2+} , SNAREs and phospholipids (Brose *et al.*, 1992; Südhof, 2002). The precise cellular localisation of all members is not clear; presumably synaptotagmins 1, 2 and 9 are vesicular, whereas the others are plasma membrane proteins (Südhof, 2002). Synaptotagmin 1 is the best characterised family member. The deletion of this 65 kDa protein causes the loss of the rapidly released pool of vesicles in chromaffin cells (Voets *et al.*, 2001), and the fast synchronous neurotransmitter release in hippocampal neurons (Geppert *et al.*, 1994), suggesting that synaptotagmin 1 represents the Ca^{2+} -sensor for the fastest component of release. In the proposed model the Ca^{2+} -independent interaction of synaptotagmin 1 with SNARE complex and phospholipids (preferentially $\text{PI}(4,5)\text{P}_2$) positions synaptotagmin for subsequent Ca^{2+} -sensing (Figure 2; Bai *et al.*, 2004; Bai and Chapman, 2004). Upon increase of $[\text{Ca}^{2+}]_i$, Ca^{2+} -binding to synaptotagmin 1 C_2 -domains results in their partial insertion into the phospholipid layers thereby triggering vesicle fusion (Figure 2; Chapman, 2002).

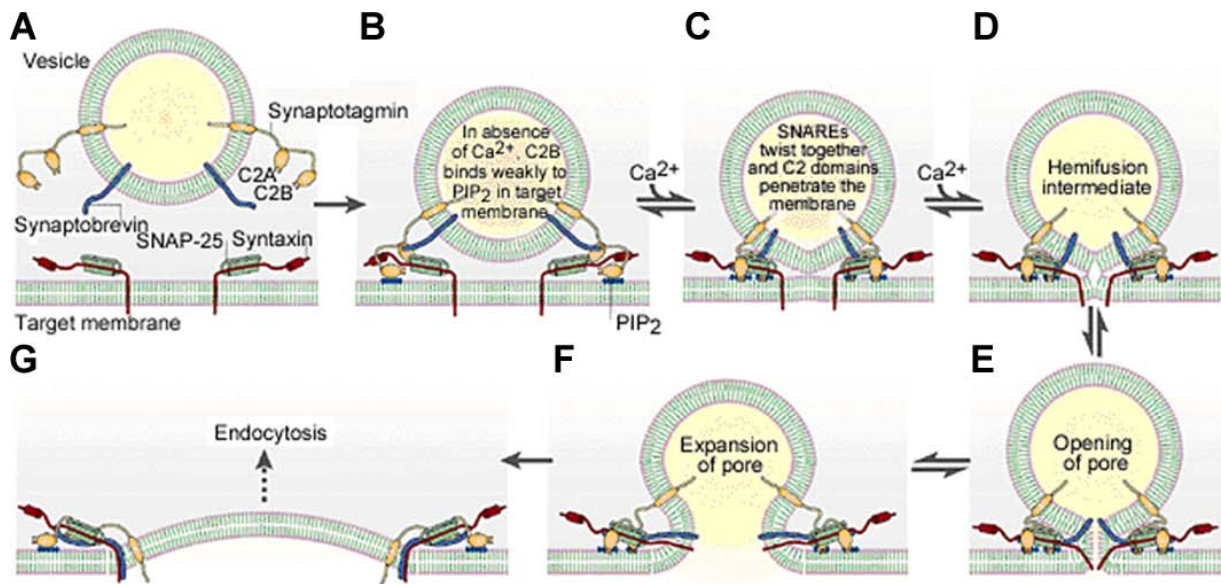


Figure 2. Putative model for the function of synaptotagmin and SNARE proteins in Ca^{2+} -triggered exocytosis. In the docked vesicle (A), SNAREs and synaptotagmin presumably do not interact directly. During priming (B-C), the SNARE complex assembles and synaptotagmin associates with it and negatively charged phospholipids (preferentially $\text{PI}(4,5)\text{P}_2$). Subsequently, Ca^{2+} -influx (D-E) triggers the partial insertion of synaptotagmin C_2 -domains into the phospholipid layers thereby causing a mechanical perturbation in the membrane which (F-G) opens and dilatates the fusion pore. From Chapman, 2002.

The Ca^{2+} -sensor for release of the slow component still remains to be identified. Several results indicate that other members of synaptotagmin family, in particular, synaptotagmin 3, 7 and 9 may contribute to the Ca^{2+} -triggering of the slow component (Sugita *et al.*, 2002; Hui *et al.*, 2005). Future studies will probably address this.

1.1.2. Lipids involved in regulated exocytosis

Membrane lipids have an important regulatory function in exocytosis and membrane traffic in general (Cremona and De Camilli, 2001). It has been known since the 1950s that stimulation of pancreatic cell secretion leads to increased phosphorylation of phospholipids (Hokin and Hokin, 1953). Ten years later, Larrabee and collaborators (1963) revealed that this modification is limited to a minor fraction of phospholipids, the phosphatidylinositides (PIs). These observations linked PIs to membrane trafficking. However, only recently has it been shown that PIs, and not their cleavage products, play a role in exocytosis (Eberhard *et al.*, 1990). To date it remains unclear which PI molecules are necessary for the exocytic process and their molecular mechanism of action.

PIs are present in some bacteria and all eukaryotic cells where they generally constitute less than 10% of total cellular phospholipids (Janssens, 1988; Rana and Hokin, 1990). The importance of these molecules is best illustrated by the longstanding research that has accompanied them. The intense research on (1) membrane structure (~1930-1950) coincided with the characterisation of PIs, (2) cell signalling (~1950-1980) with phosphatidylinositol-4-phosphate [PI(4)P] and PI(4,5)P₂, and (3) membrane trafficking and the cytoskeleton (~1980-2005) with the remaining PIs. The molecules of the PI family are ancient, very stable and versatile (Irvine, 2005). The inositol head group of PI can be reversibly phosphorylated at various positions, resulting in seven naturally occurring PIs. All forms can be rapidly interconverted by specialised lipid kinases and phosphatases, which add or remove specific phosphate groups. Some forms are also broken down by phospholipases. Hundreds of proteins have domains which recognise particular PIs and the continual changes in the relative population of these lipids profoundly affect cellular activities.

PI-responsive proteins can be grouped into two classes (Suh and Hille, 2005). The first class comprises cytoplasmic enzymes, vesicle trafficking factors and proteins involved in cytoskeletal rearrangement. These proteins have recognition domains (e.g. phox homology (PX), PH, E/ANTH, FERM, FYVE, Tubby; reviewed by Lemmon, 2003) which interact with lipid head groups facing the cytoplasm. They are attracted to target membranes through their lipid ligand, and shuttle between membrane and cytoplasm as the PI composition changes. The second class of proteins comprises intrinsic membrane proteins and includes ion channels and transporters. Their activity is either dependent on or blocked by specific PIs. They presumably recognise the PI head group and interact laterally with their phospholipid ligand in the inner leaflet of the plasma membrane.

Since PIs are heterogeneously distributed in the cellular membranes, it is assumed that these lipids determine which proteins are recruited to each membrane and when they are active (De Matteis and Godi, 2004). In addition, the different membrane-restricted PIs may serve to program/control vesicular trafficking, which in turn may regulate a multitude of cellular signalling events. PI(4)P is mainly detected on the Golgi apparatus, PI(3)P on early endosomes, PI(3,5)P₂ on late endosomes and PI(3,4)P₂, PI(4,5)P₂ and PI(3,4,5)P₃ on the plasma membrane (De Matteis and Godi, 2004; Figure 3). Enzymes of PI metabolism often serve as molecular switches; they are interconnected and precisely regulated. The PI phosphatases eliminate inappropriate PI synthesis products and terminate the signal, which may in itself create a messenger for a different trafficking event. Because different PI kinases are localised to specific target sites, PI turnover regulates exocytosis, endocytosis and

intracellular membrane trafficking. To further understand the spatial and temporal regulation of membrane turnover, it is necessary to understand which of the numerous PI kinases and phosphatases are involved, and how they are regulated.

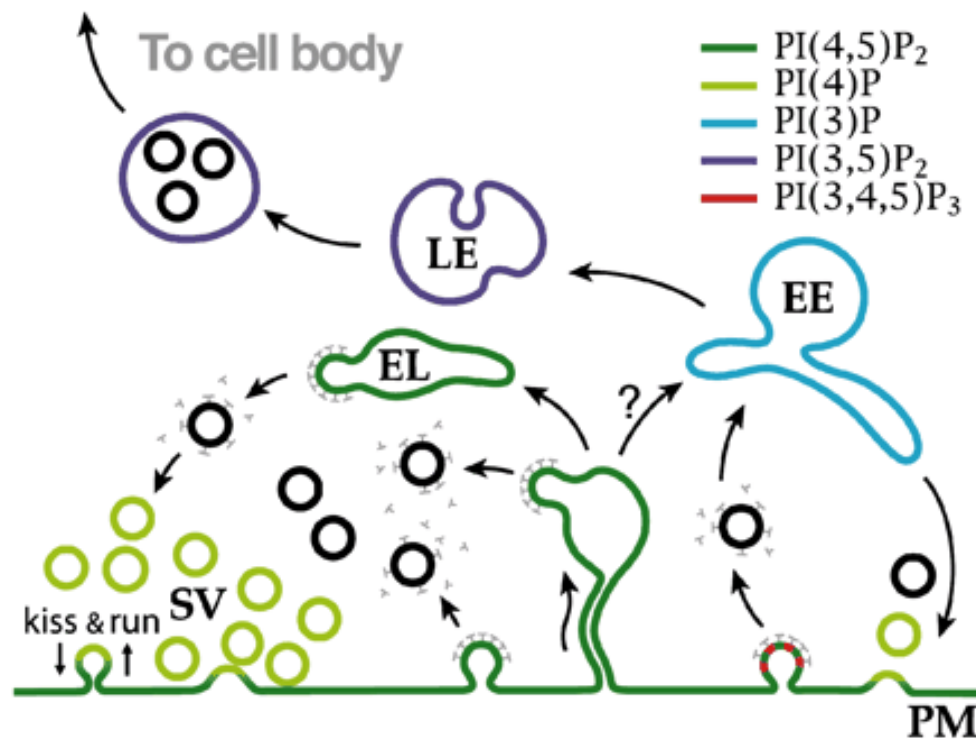


Figure 3. Putative scheme depicting the relationship between vesicle traffic and PI metabolism in nerve terminals. Membranes are colour-coded based on their supposed PI content. PI(4)P (light green) is present mainly on SVs, whereas PI(4,5)P₂ (dark green) is selectively concentrated in the plasma membrane (PM). PI(4,5)P₂ presence is also suggested in the deep plasma membrane invaginations and endosome-like (EL) structures generated during intense activity. Presence of PI(3)P (light blue) and PI(3,5)P₂ (dark blue) on early (EE) and late (LE) endosomes, respectively, is proposed. PI(3,4,5)P₃ (red) is generated by PI3Ks associated with growth factor receptor signalling. From Wenk and De Camilli, 2004.

In addition to PIs in membranes, all eukaryotic cells also contain soluble inositol phosphates (IPs) in the cytoplasm. IPs are more numerous than PIs; their synthesis and turnover is complex and presently not well understood (Irvine, 2005). These pathways have emerged as a multifaceted ensemble of cellular switches that regulate a number of processes well beyond inositol 1,4,5-triphosphate [I(1,4,5)P₃]-mediated Ca²⁺ release and include membrane trafficking, channel activity and nuclear function (Huisamen and Lochner, 1996; Balla, 2001; Shears *et al.*, 2004; Hammond *et al.*, 2004). It has been shown that inositol 1,2,3,4,5,6-hexakisphosphate (IP₆) can modulate insulin exocytosis presumably by recruiting secretory vesicles (Efanov *et al.*, 1997).

1.2.2.1. PI(4,5)P₂ regulation and cellular functions

PI(4,5)P₂, the best characterised PI, was first isolated from the brain and had been originally described as a brain lipid (Folch, 1949; Tomlinson and Ballou, 1961; Ellis and Hawthorne, 1961; Dittmer and Dawson, 1960). Three decades ago PI(4,5)P₂ was recognised as a precursor of two signalling molecules, I(1,4,5)P₃ and DAG (Berridge and Irvine, 1984), and for many years it was assumed that PI(4,5)P₂ simply represent the source of these molecules. Nevertheless, a large body of evidence describing additional functions of this phospholipid accumulated over the years. PI(4,5)P₂ is presently considered to be one of the most important signalling molecules in mammalian cells.

Regulation of PI(4,5)P₂ in mammalian cells

PI(4,5)P₂ is found predominantly in the inner layer of the plasma membrane of all eukaryotic cells; however, traces of this lipid are also detectable on intracellular membranes, the nuclear envelope and in the nucleus (Watt *et al.*, 2002). The reported PI(4,5)P₂ abundance in cells varies between 0.5 and 1.5% of membrane phospholipids (Singh, 1992; Nasuhoglu *et al.*, 2002). Nevertheless it is assumed that in a quiescent cell, PI(4,5)P₂ is sparse enough that changes in its level can be recognised as a signal. Probably due to its signalling potential, the regulation of PI(4,5)P₂ in mammalian cells is very complex and tightly controlled. The level of PI(4,5)P₂ depends on its synthesis, hydrolysis and dephosphorylation (Figure 4). There are several sources of PI(4,5)P₂ and numerous distinct enzymes are involved in its synthesis (Weernink *et al.*, 2004). The canonical pathway of PI metabolism places PI(4)P as the precursor of PI(4,5)P₂. In this pathway, PI4-kinases (PI4Ks) phosphorylate PI to produce PI(4)P, which then serves as a substrate for PIP5-kinases (PI5Ks; Figure 4). Two types of PIP5Ks are responsible for the PI(4,5)P₂ synthesis and each exists as several isoforms which can use multiple substrates. Depending on the cell type, a particular isoform directs PI(4,5)P₂ synthesis at the required cellular site. For example, phosphatidylinositol 4-phosphate 5-kinase I γ (PI4P5K-I γ) is the major isoform that produces PI(4,5)P₂ at the neuronal active zone (Wenk *et al.*, 2001). To account for the complex demands for PI(4,5)P₂ at the active zone, PI4P5K-I γ is tightly regulated by Ca²⁺, Arf6, phosphorylation and phosphatidic acid (PA), the product of phospholipase D (PLD) activity (Fruman *et al.*, 1998; Aikawa and Martin, 2003).

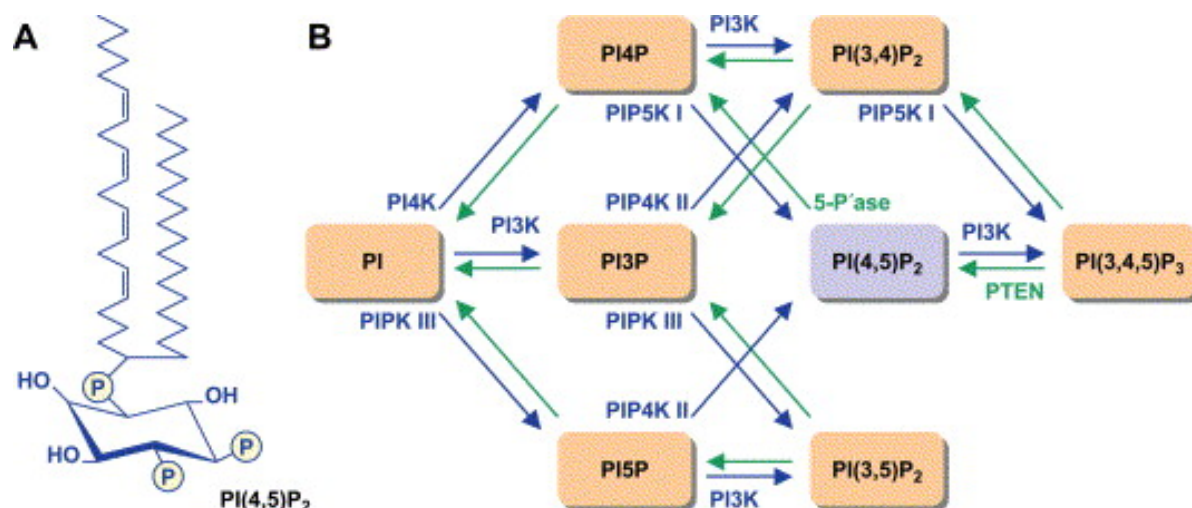


Figure 4. PI(4,5)P₂ and PI metabolism. (A) Chemical structure of PI(4,5)P₂. The acronym PI(4,5)P₂ considers the positions *D*-4 and *D*-5 of the inositol ring that are phosphorylated. (B) The PI network. The inositol ring of PI can be reversibly phosphorylated either at one or any combination of the *D*-3, *D*-4 and *D*-5 positions, resulting in seven identified PIs that can be interconverted by the action of distinct kinase (blue) and phosphatase (green) reactions. Note that PI(4,5)P₂ can be generated by the phosphorylation of PI(4)P and PI(5)P as well as by the dephosphorylation of PI(3,4,5)P₃, and that PIP5K type I catalyses the synthesis of PI(4,5)P₂ as well as PI(3,4,5)P₃ *in vivo*. From Weernink *et al.*, 2004.

In addition to kinases, PI phosphatases play an important role in regulating the functions and concentration of PI(4,5)P₂ (Figure 4). The family of inositol polyphosphate 5'-phosphatases (5'-Pase) is capable of dephosphorylating both PIs and inositol polyphosphate (Mitchell *et al.*, 1996). One of these enzymes, synaptojanin, has a prominent 5'-phosphatase activity and it can rapidly dephosphorylate PI(4,5)P₂ and PI(3,4,5)P₃ in neurons (Woscholski *et al.*, 1997). In addition, although not depicted in Figure 4, three families of phospholipase C (PLC) enzymes, β , γ and δ , are responsible for the hydrolysis of PI(4,5)P₂ and the regulation of many cellular functions (Rhee and Bae, 1997; see next chapter).

Cellular functions of PI(4,5)P₂

PI(4,5)P₂ affects a wide range of physiological functions (Czech, 2000; Yin and Janmey, 2003; Wenk and De Camilli, 2004). Below I have described the most significant roles of plasmalemmal PI(4,5)P₂.

1. Production of second messengers

PI(4,5)P₂ is a precursor of many second messengers, of which the most familiar are I(1,4,5)P₃, DAG and PI(3,4,5)P₃. As mentioned before, receptor-mediated activation of PLC

catalyzes hydrolysis of PI(4,5)P₂ to I(1,4,5)P₃ and DAG (Berridge and Irvine, 1984). Cytosolic I(1,4,5)P₃ stimulates the release of Ca²⁺ from intracellular stores (Clapham, 1995), whereas DAG remains in the plasma membrane and activates protein kinase C (PKC) family members (Hurley and Misra, 2000). Phosphorylation of PI(4,5)P₂ by a PI3-kinase (PI3K) results in production of PI(3,4,5)P₃ which functions as a membrane anchor for a number of proteins (Czech, 2000; see Discussion). Since the level of PI(3,4,5)P₃ in a quiescent cell is very low (Vanhaesebroeck *et al.*, 2001), activating a PI3K results in rapid signal amplification.

2. Enzyme activation

PI(4,5)P₂ also serves to directly activate or modulate the activity of many cellular enzymes. The level of PI(4,5)P₂ itself can be controlled through complex positive and negative feedback loops as a consequence of the activation of PI modulating enzymes (reviewed by Czech, 2000). Here I present just one example of a positive feedback loop, which may ultimately result in massive PI(4,5)P₂ synthesis and a subsequent change in membrane lipid composition. PI(4,5)P₂ is required for activation of PLD which generates PA (Liscovitch *et al.*, 1994). PA in return affects the major PI(4,5)P₂ synthesis pathway in mammalian cells by strongly activating PIP5Ks (Fruman *et al.*, 1998). This positive feedback loop is particularly important in specific regions of the plasma membrane such as membrane ruffles (Honda *et al.*, 1999).

3. Actin cytoskeleton attachment and reorganisation

The importance of PI(4,5)P₂ in cytoskeletal attachment and reorganisation has been extensively investigated and is well documented (reviewed by Yin and Janmey, 2003). A decrease in the PI(4,5)P₂ level is known to result in a dramatic release of the actin cytoskeleton from the membrane (Raucher *et al.*, 2000). PI(4,5)P₂ binding of many actin capping and severing proteins, such as profilin, cofilin, gelsolin, destrin, α -actinin, filamin and vinculin, directly influences actin assembly (Yin and Janmey, 2003). In addition, PI(4,5)P₂ induces conformational changes in Wiskott-Aldrich syndrome protein (WASP) and ezrin/radixin/moesin (ERM) proteins, which also trigger the remodelling of the actin cytoskeleton (Sechi and Wehland, 2000). Similarly, myristoylated alanine-rich C kinase substrate (MARCKS) and pleckstrin are PI(4,5)P₂-binding proteins associated with the cytoskeleton that promote the formation of actin based structures such as lamellipodia and membrane ruffles (Honda *et al.*, 1999).

4. Membrane targeting

PI(4,5)P₂ is considered an important plasma membrane marker and changes in its concentration regulate dynamic targeting of a number of proteins. Such membrane-cytosol shuffling of proteins is an important aspect of cellular function, as it influences their spatial and temporal localisation in response to a signal (Hurley and Meyer, 2001). Several PI(4,5)P₂-binding domains mediate membrane targeting and consequently the localisation and activity of hundreds of proteins (Lemmon, 2003). Of particular relevance is the PH-domain. Found in over 100 proteins, this domain anchors proteins to membranes by mediating protein-lipid and protein-protein interactions. In particular, PH-domains of pleckstrin, spectrin, dynamin and PLCδ₁ are shown to bind PI(4,5)P₂ specifically and with the high affinity. The PH-domain of PLCδ₁ binds strongly to PI(4,5)P₂ and even more efficiently to I(1,4,5)P₃ which may be important for PLCδ₁ regulation *in vivo* (Lemmon *et al.*, 1995). PH-PLCδ₁ fused to green fluorescent protein (GFP) is a useful experimental tool and it has often been used to probe PI(4,5)P₂ localisation *in vivo* (Stauffer *et al.*, 1998; Várnai and Balla 1998; Holz *et al.*, 2000; Micheva *et al.*, 2001; Watt *et al.*, 2002).

5. Regulation of ion channels and transporters

Many families of ion channels and transporters are regulated by PI(4,5)P₂ and in most cases PI(4,5)P₂ enhances their activity (reviewed by Hilgemann *et al.*, 2001; Suh and Hille, 2005). The best studied examples include inward-rectifier K⁺-channels (Rohacs *et al.*, 2003), voltage-gated K⁺-channels (Zhang *et al.*, 2003; Oliver *et al.*, 2004), voltage-gated Ca²⁺-channels (Wu *et al.*, 2002; Gamper *et al.*, 2004), sensory transduction channels (Hirono *et al.*, 2004), cardiac Na⁺/Ca²⁺ exchangers (Hilgemann and Ball, 1996) and Na⁺/H⁺-exchangers (Aharonovitz *et al.*, 2000).

6. Regulation of exocytosis and endocytosis

PI(4,5)P₂ has been suggested to be a key player in regulated exocytosis and endocytosis in neurons and neuroendocrine cells (reviewed by Cremona and de Camilli, 2001; Martin, 2001; Wenk and De Camilli, 2004). In this section I summarise the knowledge available when I started my doctoral work.

The first clue suggesting a direct role of PI(4,5)P₂ in regulated exocytosis came from studies on permeabilised chromaffin cells which showed that PI(4,5)P₂, and not its hydrolysis products I(1,4,5)P₃ and DAG, was required for an ATP-dependent priming step preceding Ca²⁺-triggered fusion (Holz *et al.*, 1989; Eberhard *et al.*, 1990). A search for the cytosolic

factors required for this energy requiring priming step in permeabilised neuroendocrine cells led to the identification of two enzymes involved in the PI metabolism: a phosphatidylinositol transfer protein (PITP; Hay and Martin, 1993) and a PI4P5K (Hay *et al.*, 1995). A latter study suggested a model in which PI was delivered to the vesicle membrane via PITP, phosphorylated to PI(4)P by vesicular protein PI4K-II, and finally converted to PI(4,5)P₂ by PI4P5K recruited from the cytoplasm (Hay *et al.*, 1995; implemented in Figure 5). In subsequent work it was observed that the PI(4,5)P₂-binding PH-domain from PLCδ₁ was localised to the plasma membrane and inhibited Ca²⁺-dependent exocytosis in chromaffin cells (Holz *et al.*, 2000).

Additionally, many exocytic proteins had been shown to interact with PI(4,5)P₂ *in vitro* (reviewed by Wenk and De Camilli, 2004). Based on these interactions it was postulated that PI(4,5)P₂ had a function in vesicle docking, priming and/or fusion reactions. PI(4,5)P₂ binds to synaptotagmin family members and CAPS proteins, as mentioned above (Schiavo *et al.*, 1996; Loyet *et al.*, 1998). Other relevant interactions included binding of PI(4,5)P₂ to Mints, which bind Munc18s and are implicated in docking (Okamoto and Südhof, 1997), and rabphilin 3, an effector of Rab3 proteins postulated to control SNARE complex formation (Chung *et al.*, 1998). Moreover, PI(4,5)P₂ inhibited vesicular protein casein kinase I, which phosphorylated among other vesicular proteins, synaptic vesicle protein 2 (Gross *et al.*, 1995). It was however not known which of these interactions were physiologically relevant *in vivo*.

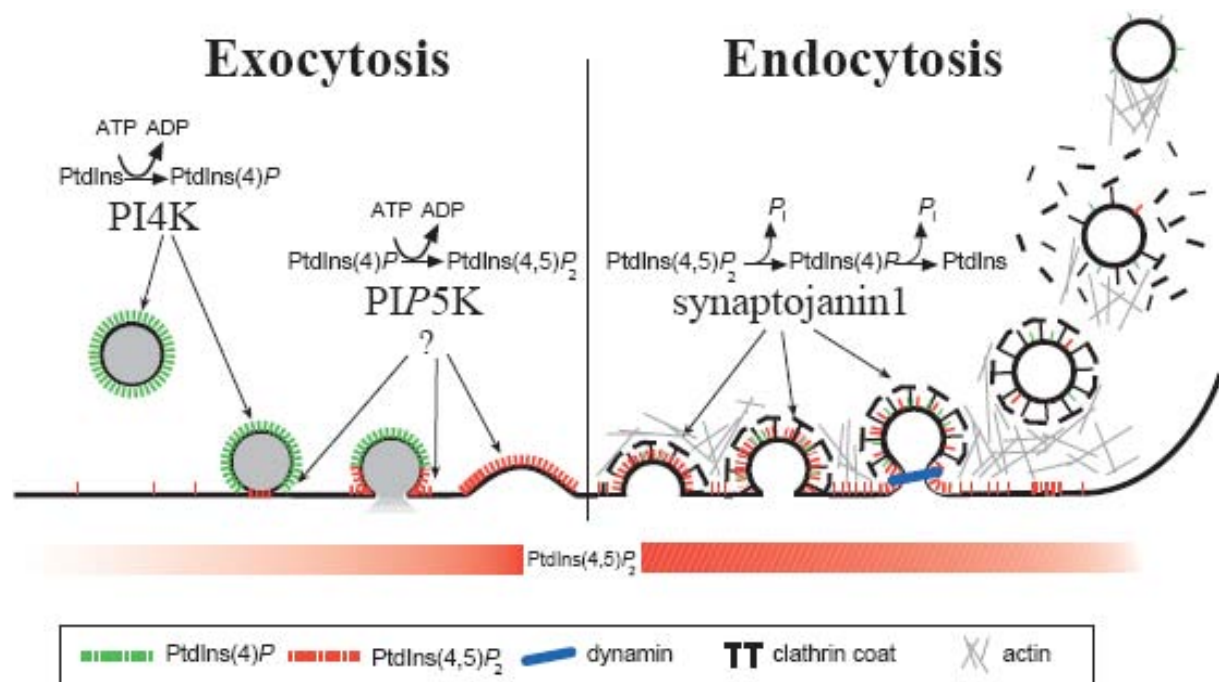


Figure 5. Schematic representation of a putative link between exocytosis, endocytosis and PI(4,5)P₂ synthesis/dephosphorylation. From Cremona and De Camilli, 2001.

Similar to the above mentioned exocytic proteins, many proteins involved in clathrin-mediated endocytosis also bound PI(4,5)P₂. In addition to dynamin, a key protein in the fission reaction of endocytosis, clathrin adaptor proteins such as AP-1, AP-2, AP180, Hip1 and epsin have a high affinity for PI(4,5)P₂ (Traub, 2003). The importance of PI(4,5)P₂ in the recruitment of endocytic proteins has been demonstrated by several functional studies. The clathrin coat could assemble on PI(4,5)P₂ liposomes *in vitro* (Takei *et al.*, 1998), and manipulations which stimulated clathrin coat nucleation were shown to act through PI(4,5)P₂ synthesis (Cremona *et al.*, 1999; Ford *et al.*, 2001). Dephosphorylation of PI(4,5)P₂ by overexpression of a membrane-tagged inositol 5'-phosphatase domain of synaptojanin 1 (IPP1-CAAX) or PI(4,5)P₂-masking by PH-PLCδ₁ and neomycin inhibited clathrin-mediated endocytosis (Jost *et al.*, 1998; Krauss *et al.*, 2003). Furthermore, neurons from synaptojanin 1 *null* mouse had elevated PI(4,5)P₂ levels and defective synaptic vesicle recycling, presumably due to a delay in clathrin coat disassembly (Cremona *et al.*, 1999). In short, PI(4,5)P₂ seems to play an important role in all steps of endocytic process (Figure 5): clathrin coat recruitment (through clathrin adaptor proteins), fission of endocytic pits (through dynamin) and clathrin uncoating (through synaptojanin 1).

Dual roles of PI(4,5)P₂ in exocytosis and endocytosis suggested that this lipid may control the plasma membrane trafficking and a model in which a PI cycle is nestled within the secretory vesicle cycle was proposed (Cremona and De Camilli, 2001; Figure 5).

1.3. Aims and the experimental approach

1.3.1. Chromaffin cell as a model system for studying regulated exocytosis

The neuroendocrine system links behaviour with hormone secretion. In turn hormones act on all organs to regulate functions such as reproduction, fluid and mineral intake and balance, metabolism and activity of the immune system. Examples of hormones are catecholamines which play a role in the cardiovascular and metabolic adaptations of the body to stress. In mammals, the adrenal gland medulla is the principal site of catecholamine synthesis, namely adrenaline and noradrenaline (also called epinephrine and norepinephrine, respectively). The adrenal medulla is mainly composed of chromaffin cells which are derived from the embryonic neural crest and as such are simply modified neurons. In particular, chromaffin cells are postganglionic cells of the sympathetic nervous system, receiving innervations from the corresponding preganglionic fibres. Reflecting their common origin, chromaffin cells use the same fusion machinery as neurons (De Camilli and Jahn, 1990).

As an experimental model for studying the basic concepts of stimulation-dependent exocytosis, chromaffin cells are used in preference to neurons as they allow direct measurements of exocytosis. Consequently, chromaffin cells are widely used in exocytic research (Rettig and Neher, 2002; Bader *et al.*, 2002). They also offer the following additional benefits:

- 1) a sudden increase in $[Ca^{2+}]_i$ to the micromolar range can trigger a rapid release of catecholamines from LDCVs,
- 2) $[Ca^{2+}]_i$ can be precisely measured with fluorescent dyes,
- 3) $[Ca^{2+}]_i$ can be controllably elevated using photolysable Ca^{2+} -caged compounds,
- 4) $[Ca^{2+}]_i$ can be kept spatially homogenous with Ca^{2+} -buffers,
- 5) the fusion of LDCVs can be monitored by membrane capacitance measurements,
- 6) the released catecholamines can be measured with carbon fiber amperometry,
- 7) the cultured chromaffin cells can be efficiently transfected to overexpress different proteins,
- 8) functional cell culture can be generated from transgenic animals,
- 9) the number and spatial distribution of the LDCVs can be studied with complementary methods such as electron and light microscopy,
- 10) the live imaging of vesicular movement can be performed by total internal reflection microscopy (TIRF; Steyer *et al.*, 1997).

The first six points enable a quantitative investigation of secretory vesicle pool dynamics as a function of $[Ca^{2+}]_i$. Points 7 and 8 permit the coupling of genetics with overexpression techniques and allow studies of the exocytic molecular machinery in a genetically “clean” system.

1.3.2. Evaluation of regulated exocytosis in chromaffin cells

Due to the speed of vesicular release, techniques with the temporal resolution in the millisecond range are required for the direct study of exocytosis in real time *in vivo*. Fast electrophysiological and electrochemical techniques provide the required resolution (Rettig and Neher, 2002). All functional analyses presented in this thesis were performed on chromaffin cells using a combination of whole-cell membrane capacitance and amperometric measurements accompanied by the simultaneous measurements of $[Ca^{2+}]_i$ while exocytosis is triggered by a spatially uniform Ca^{2+} signal (Figure 6 and 7).

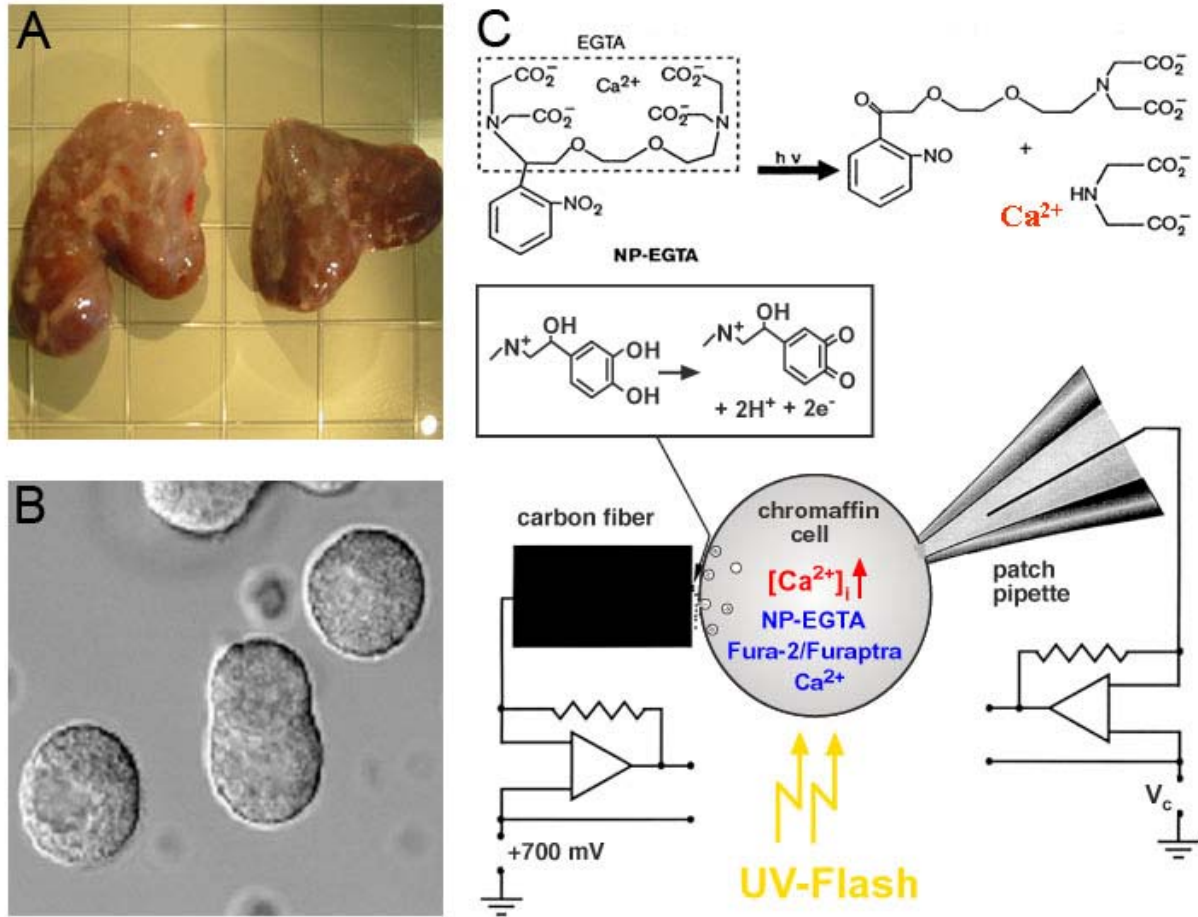


Figure 6. (A) Bovine adrenal glands. (B) Bovine chromaffin cells in primary culture. (C) Schematic depicting the combined measurement of membrane capacitance and amperometric in chromaffin cells. A chromaffin cell is loaded with Ca^{2+} -sensitive fluorescent dyes (e.g. fura-2 and furaptra) and a Ca^{2+} -caged compound (e.g. nitrophenyl-EGTA) through the patch pipette. A flash of UV-light liberates Ca^{2+} from the nitrophenyl-EDTA (top), which triggers the fusion of secretory vesicles with the plasma membrane. An increase in the membrane surface is measured as an increase in membrane capacitance (bottom right), while the secreted catecholamines are detected as an oxidation current through the carbon fibre electrode (bottom left).

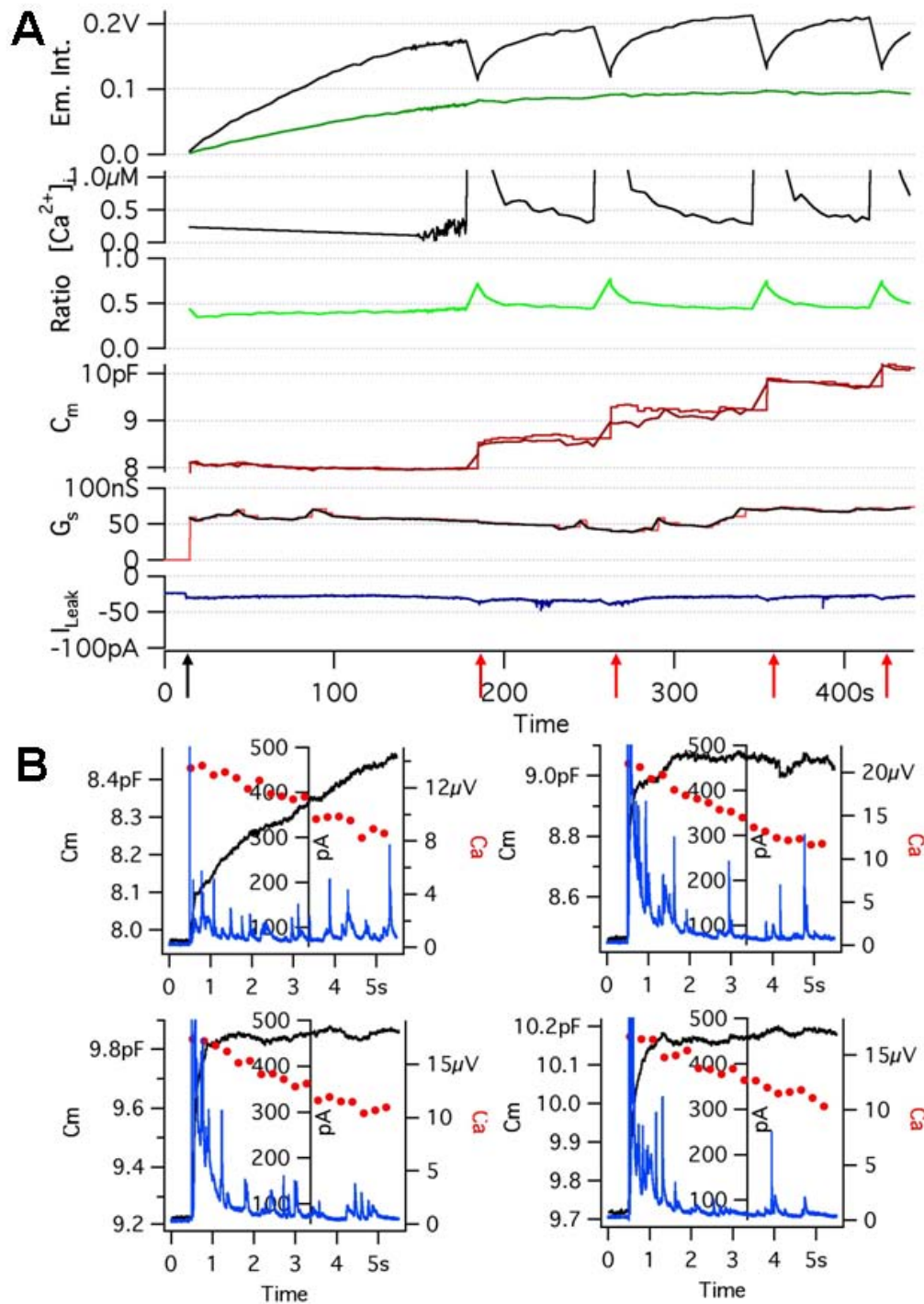


Figure 7. Exocytic data as a recording example obtained from bovine chromaffin cell. (A) Monitored parameters: emitted light intensity (black trace: at 380 nm; green trace: at 350 nm), $[Ca^{2+}]_i$ calculated from calibration parameters, fluorescence emission ratio, membrane capacitance (C_m), series conductance (G_s) and leak current (I_{leak}). The black arrow indicates the time point when the whole-cell configuration is established, the four consecutive red arrows indicate the application of four stimuli (UV-flashes). (B) Example of four consecutive high-time resolution recordings of exocytic response. Red dots: postflash Ca^{2+} concentration calculated from calibration parameters; black trace: membrane capacitance change; blue trace: amperometry. A potentiation of exocytic release is often seen during the second stimulus.

Morphological studies have showed that as many as 1000 secretory vesicles are located near the plasma membrane in an adult bovine chromaffin cell (BCC; Plattner *et al.*, 1997). However, electrophysiological measurements indicated that only a fraction of these vesicles can rapidly fuse with the membrane to release their content upon stimulation (Neher and Zucker, 1993; Parsons *et al.*, 1995). In addition, the high-time resolution membrane capacitance measurements have revealed the existence of different kinetic phases of exocytosis in a variety of neuronal and neuroendocrine cells. A rapid increase in $[Ca^{2+}]_i$ triggers an exocytic burst followed by a sustained phase of secretion (Xu *et al.*, 1998; Voets *et al.*, 1999). The burst can be further resolved into two kinetically distinct components, a fast and a slow burst, suggesting the presence of two release-competent vesicle pools (Voets, 2000). Based on these observations the existence of four vesicle pools was postulated (Figure 8; Ashery *et al.*, 2000; Rettig and Neher, 2002). According to the model, vesicles from the reserve pool translocate to the plasma membrane to enter the docked but unprimed pool, UPP. Vesicles in the UPP are primed into the slowly releasable pool, SRP, from where they can form the rapidly releasable pool, RRP. Vesicles in the both SRP and RRP can fuse with the plasma membrane, but with different rate constants ($\sim 3s^{-1}$ versus $\sim 30s^{-1}$; Voets, 2000; Ashery *et al.*, 2000). The size of the pools and the rate of vesicle transition between them can be regulated by $[Ca^{2+}]_i$ and the number of proteins involved in exocytosis (Sørensen, 2004).

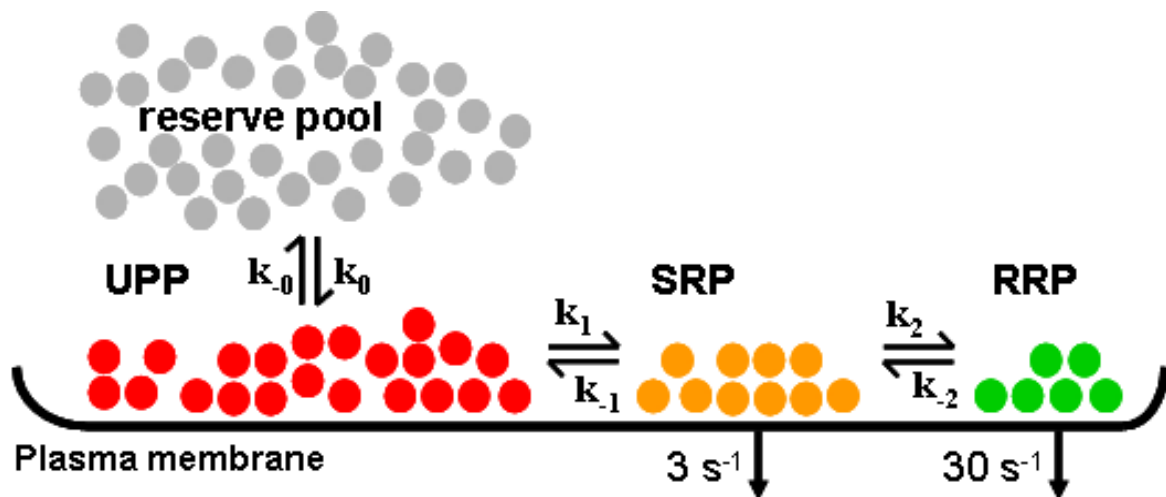


Figure 8. A pool model of LDCV exocytosis. Secretory vesicles are depicted in four different stages. Vesicles of the depot pool (about 2000) enter the unprimed pool (UPP) when they dock at the membrane. A total of 850 morphologically docked vesicles (as observed in electron micrographs) are subdivided into the unprimed pool (UPP; about 650 vesicles) and the primed pool. The primed pool is subdivided into the slowly releasable pool (SRP) and rapidly releasable pool (RRP), each containing about 100 vesicles. Figure modified from Rettig and Neher, 2002.

1.3.3. Evaluation of exocytic proteins and lipids in the plasma membrane

Few techniques are amenable for the study of exocytic molecules in their natural environment with the required spatial resolution (Steyer and Almers, 2001). A method that has an excellent spatial resolution sufficient for the imaging of both small synaptic vesicles and the dynamics of single protein molecules is TIRF microscopy (reviewed by Steyer and Almers, 2001). This technique has proven to be valuable for studying the recruitment, docking and fusion of secretory vesicles (Steyer *et al.*, 1997; Oheim *et al.*, 1998). However, although TIRF microscopy is well suited to imaging plasma membrane constituents and associated organelles in living cells, it does not allow direct biochemical access to the plasma membrane itself.

The method with an analogous spatial resolution but which also allows access to the plasma membrane is a cell-free assay refined by Avery and collaborators (2000; Figure 9). This assay is based on shearing cultured PC12 cells with ultrasonic pressure waves which remove the cell organelles leaving carrier-attached “cellular footprints” behind. These footprints are several nanometers thick and are referred to as plasma membrane sheets (Avery *et al.*, 2000). Due to thickness of the preparation, there is no interference of labelled structures above or below the focal plane which minimises the noise to signal ratio. Therefore, similar to TIRF microscopy, the plasma membrane proteins and lipids can be investigated with exceptional spatial resolution limited only by the physics of light microscopy.

The plasma membrane sheet preparation can be used to monitor the fate of a single secretory vesicle - vesicles are found both to remain attached to the membrane sheets and moreover, to retain exocytic competence (Avery *et al.*, 2000; Holroyd *et al.*, 2002). In addition, the exocytic machinery can be studied using biochemical tools such as clostridial neurotoxins, fluorescently labelled recombinant proteins or antibodies raised against exocytic proteins. Studies performed on membrane sheets revealed that the SNARE proteins are highly reactive and clustered in the plasma membrane and that such clusters are the sites where secretory vesicles preferentially dock and fuse (Lang *et al.*, 2001; Lang *et al.*, 2002).

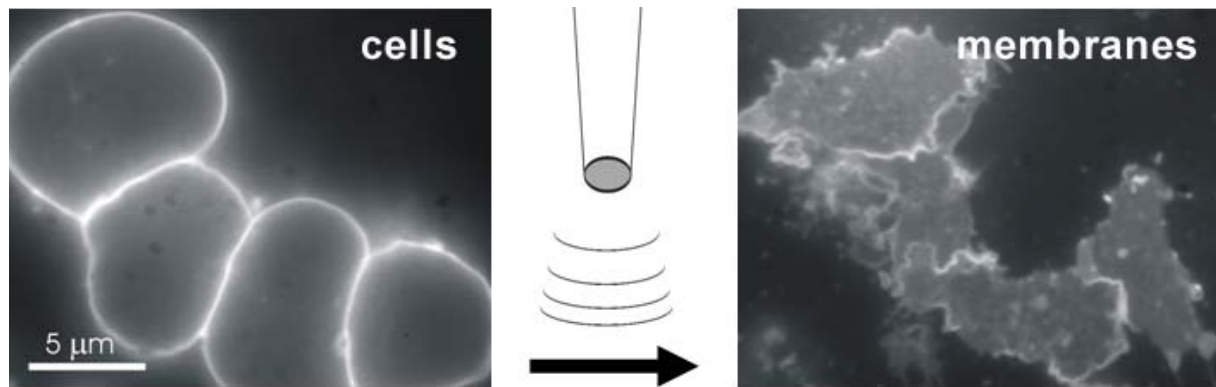


Figure 9. Plasma membrane sheets from bovine chromaffin cells in primary culture generated in the field of view of a fluorescent microscope. The membranes can be viewed are using 1-(4-trimethylamoniumpheyl)-6-phenyl-1,3,5-hexatriene (TMA-DPH), a lipophylic styryl dye that intercalates between phospholipids.

1.3.4. The aims of my studies

Prior to my doctoral work, the information on several key proteins involved in neuronal and neuroendocrine cell exocytosis (e.g. exocytic SNAREs, synaptotagmin 1, Munc13, Munc18) was integrated into the previously described four-pool model. Nevertheless, many open questions remained and it became evident that focusing on proteins alone may not be sufficient to explain all the features of the exocytic process. For example, many regulatory proteins modify just particular vesicular pools and the kinetics of release was affected only by synaptotagmin 1, a protein possessing C_2 -domains with an affinity for negative phospholipids, particularly $PI(4,5)P_2$ (Bai and Chapman, 2004). Hence, the question arose whether phospholipids could regulate exocytosis and specifically whether they could control the release kinetics. The knowledge of lipid involvement in exocytosis was modest (see chapter 1.2.2.). Several studies had indirectly suggested the involvement of $PI(4,5)P_2$ in the process (Eberhard *et al.*, 1990; Hay and Martin, 1993; Hay *et al.*, 1995; Holz *et al.*, 2000; Micheva *et al.*, 2001; reviewed by Cremona and De Camilli, 2001). Yet, it was not clear whether this multi-functional phospholipid was essential for the exocytic process or it whether just regulated it. Further, if $PI(4,5)P_2$ had a regulatory role, it was not known where in the exocytic pathway it was required. The first aim of my doctoral project was to address these questions.

SNARE proteins are known both to be essential for exocytosis and to regulate the exocytic process (see chapter 1.2.1.1.). For example, both SNAP-25 isoforms rescue exocytosis when expressed in SNAP-25 *null* chromaffin cells, but interestingly SNAP-25b is

two to three times more efficient than SNAP-25a (Sørensen *et al.*, 2003a). The molecular basis for this difference was the next specific objective my doctoral project.

I wanted to address these aims by studying both spatial and temporal aspects of PI(4,5)P₂ and SNAREs involvement in exocytosis. A decades-long investigation of exocytosis has resulted in the establishment of many assays for studying different properties of this process. Electrophysiological techniques, methods of choice in functional studies, record the response of the entire cell, providing temporal information required for resolving fast exocytic events *in vivo* (Rettig and Neher, 2002). However, they provide no spatial information with respect to vesicles or other factors involved in exocytosis. On the other hand, imaging techniques such as TIRF microscopy and the plasma membrane sheet assay, have spatial resolution that allows monitoring of secretory vesicle fate (Steyer and Almers, 2001; Lang, 2003), but cannot compete with the exceptional temporal resolution of electrophysiology. As no single technique is able to fulfil both the spatial and temporal requirements, a combination of different methods was necessary. This doctoral work represents the first example where fast electrophysiological techniques have been combined with the plasma membrane sheet assay to monitor and record the spatial and temporal features of exocytic lipids and proteins.

To be able to combine the aforementioned techniques in the suitable form for my project, I needed to refine the plasma membrane sheet assay. PC12 cells originally used in the assay display relatively long latencies and slow kinetics of release (Ninomiya *et al.*, 1997), probably because cells lack primed vesicle pools. Consequently, these cells cannot perform the rapid exocytosis which characteristic of neurons and chromaffin cells. Moreover, by choosing chromaffin cells as a model system, my investigations gained all the benefits of studying exocytosis from a temporal point of view. Therefore, I adapted the membrane sheet assay to primary culture of bovine and mouse chromaffin cells, and was able to inspect the spatial organisation of the exocytic machinery in this powerful model system.

The spatial distribution of membrane lipids is of particular interest (Edidin, 2003a). The currently very active and challenging field of lipid microdomain research has produced quite contradictory opinions. Similarly to other lipids, the organisation of PI(4,5)P₂ in the plasma membrane is questionable (van Rheenen *et al.*, 2005; see Discussion). However, information on the distribution and dynamics of this phospholipid is an important requirement for understanding its multiple roles in the cell. To obtain such knowledge it was critical to use better membrane lipid detection probes. A PH-domain of PLCδ₁ is a monovalent probe which specifically binds to PI(4,5)P₂ with high affinity *in vivo* (Stauffer *et al.*, 1998; Várnai and Balla 1998). Therefore, a chimera of PH-PLCδ₁ and GFP was a required tool. When applied

to the plasma membrane sheets, GFP-PH-PLC δ_1 allowed an inspection of the level and the spatial organisation of PI(4,5)P₂ within the limits of light microscopy. This permitted further studies on how the level of PI(4,5)P₂ influenced exocytic regulation and a direct comparison of the PI(4,5)P₂ and SNARE protein distributions.

In the following chapters I present three studies that employed the combination of the plasma membrane sheet and fast physiological assays. These studies investigated some basic aspects of the exocytic process by recording both spatial and temporal information. The first study investigates the regulation of the releasable vesicle pool size by plasmalemmal PI(4,5)P₂, the second explores the basis of differential exocytic regulation by SNAP-25 splice variants, and the third reveals how the “zipping” of the SNARE complex drives exocytosis. In addition, I include some unpublished data addressing the molecular mechanisms by which PI(4,5)P₂ regulates neuroendocrine cell exocytosis.

2. PUBLICATIONS

2.1. Paper I.

Plasmalemmal phosphatidylinositol-4,5-bisphosphate level regulates the releasable vesicle pool size in chromaffin cells

Ira Milosevic, Jakon B. Sørensen, Thorsten Lang, Michael Krauss, Gabor Nagy,
Volker Haucke, Reinhard Jahn and Erwin Neher

The Journal of Neuroscience Vol. 25 (10): 2557-2565, March 9th, 2005

Plasmalemmal Phosphatidylinositol-4,5-Bisphosphate Level Regulates the Releasable Vesicle Pool Size in Chromaffin Cells

Ira Milosevic,^{1,2} Jakob B. Sørensen,¹ Thorsten Lang,² Michael Krauss,³ Gábor Nagy,¹ Volker Haucke,³ Reinhard Jahn,² and Erwin Neher¹

Departments of ¹Membrane Biophysics and ²Neurobiology, Max Planck Institute for Biophysical Chemistry, D-37077 Göttingen, Germany, and ³Institute of Chemistry–Biochemistry, Freie Universität Berlin, D-14195 Berlin, Germany

During exocytosis, certain phospholipids may act as regulators of secretion. Here, we used several independent approaches to perturb the phosphatidylinositol-4,5-bisphosphate [PI(4,5)P₂] level in bovine chromaffin cells to investigate how changes of plasmalemmal PI(4,5)P₂ affect secretion. Membrane levels of PI(4,5)P₂ were estimated by analyzing images of lawns of plasma membranes labeled with fluorescent probes specific for PI(4,5)P₂. The specific PI(4,5)P₂ signal was enriched in submicrometer-sized clusters. In parallel patch-clamp experiments on intact cells, we measured the secretion of catecholamines. Overexpression of phosphatidylinositol-4-phosphate-5-kinase I γ , or infusion of PI(4,5)P₂ through the patch pipette, increased the PI(4,5)P₂ level in the plasma membrane and potentiated secretion. Expression of a membrane-targeted inositol 5-phosphatase domain of synaptojanin 1 eliminated PI(4,5)P₂ from the membrane and abolished secretion. An inhibitor of phosphatidylinositol-3 kinase, 2-(4-morpholinyl)-8-phenyl-4H-1-benzopyran-4-one, led to a transient increase in the PI(4,5)P₂ level that was associated with a potentiation of secretion. After prolonged incubation, the level of PI(4,5)P₂ decreased and secretion was inhibited. Kinetic analysis showed that changes in PI(4,5)P₂ levels led to correlated changes in the size of two releasable vesicle pools, whereas their fusion kinetics remained unaffected. We conclude that during both short- and long-term manipulations of PI(4,5)P₂ level secretion scales with plasma membrane PI(4,5)P₂ content and that PI(4,5)P₂ has an early effect on secretion by regulating the number of vesicles ready for release.

Key words: exocytosis; phosphatidylinositol-4,5-bisphosphate; chromaffin cell; phosphatidylinositol 4-phosphate 5-kinase; plasmalemmal microdomains; LY294002

Introduction

Neuroendocrine exocytosis is a highly regulated process comprising translocation of secretory vesicles to the plasma membrane (docking), the formation of an exocytotic machinery between vesicles and membrane (priming), and, finally, fusion resulting in the release of the vesicular contents into the extracellular space. The fusion of large dense-core vesicles (LDCVs) in chromaffin cells is often used to study the basic concepts of exocytosis (Rettig and Neher, 2002).

In chromaffin cells, it was found that an ATP-dependent priming step precedes the ATP-independent Ca²⁺-triggered fusion step (Holz et al., 1989). Additional experiments revealed that the presence of phosphatidylinositides, but not of phospholipase

C cleavage products, is necessary for Ca²⁺-dependent exocytosis in chromaffin cells (Eberhard et al., 1990). A screening of cytoplasmic factors required for ATP-dependent priming in PC12 cells identified two enzymes involved in phosphoinositide metabolism: phosphatidylinositol transfer protein (PITP α) (Hay and Martin, 1993) and phosphatidylinositol 4-phosphate 5-kinase (PI4P5K) (Hay et al., 1995). Because PI4P5K uses ATP to synthesize phosphatidylinositol-4,5-bisphosphate [PI(4,5)P₂], a role for PI(4,5)P₂ in exocytosis was hypothesized (Hay et al., 1995; Martin et al., 1997). Later, it was found that the overexpressed pleckstrin homology domain of phospholipase C- δ_1 (PH-PLC δ_1), which specifically binds PI(4,5)P₂, localized to the plasma membrane and inhibited Ca²⁺-dependent exocytosis (Holz et al., 2000). Olsen et al. (2003) used capacitance measurements in pancreatic β -cells and showed that infusion of phosphatidylinositol 4-phosphate [PI(4)P] or PI(4,5)P₂ increased the size of the readily releasable pool (RRP) of vesicles. Recently, Aikawa and Martin (2003) demonstrated that overexpression of a constitutively active ARF6 mutant caused redistribution of PI(4,5)P₂ and PI4P5K1 γ from plasma membrane to endosomal membranes and inhibited LDCV secretion.

The above studies indicate that PI(4,5)P₂ is intimately involved in exocytosis of LDCVs. One idea is that PI(4,5)P₂ recruits

Received Sept. 10, 2004; revised Jan. 24, 2005; accepted Jan. 24, 2005.

This work was supported by grants from the Deutsche Forschungsgemeinschaft (SFB 523/TP B4 to E.N., SPP 1128 and SFB 406/TP B8 to T.L. and R.J., SFB 523/TP B8 and SFB 366/TP B11 to V.H.), INTAS (01-2095 to E.N.), and the Fonds der Chemischen Industrie (to V.H.). V.H. is a European Molecular Biology Organization Young Investigator. I.M. is a PhD student of the International MD-PhD/PhD Program in the Neurosciences of the International Max Planck Research School and holds a Boehringer-Ingelheim Fond Fellowship. We thank Ina Herfort and Dirk Reuter for expert technical assistance and Dr. Ralf B. Nehring for cloning consulting.

Correspondence should be addressed to Dr. Sørensen at the above address. E-mail: jsoreen@gwdg.de.

DOI:10.1523/JNEUROSCI.3761-04.2005

Copyright © 2005 Society for Neuroscience 0270-6474/05/252557-09\$15.00/0

proteins to the plasma membrane and thereby acts as a nucleation center for an exocytosis apparatus (Hay et al., 1995), in line with a relatively early role in exocytosis. On the other hand, a recent *in vitro* study showed that binding of synaptotagmin 1, the Ca²⁺ sensor for exocytosis, to PI(4,5)P₂-containing membranes via its C2B domain increased the speed of insertion of synaptotagmin 1 side chains into that membrane after the addition of Ca²⁺ (Bai et al., 2004). It was suggested that changes in the PI(4,5)P₂ level could regulate release rates, which would imply PI(4,5)P₂ in regulating the last Ca²⁺-dependent step in exocytosis. Thus, it remains to be established where exactly in the exocytosis pathway PI(4,5)P₂ is required.

We have used several independent approaches to upregulate and downregulate PI(4,5)P₂ levels in bovine chromaffin cells (BCCs). The effects of these manipulations were assessed semi-quantitatively by detection of PI(4,5)P₂ in isolated plasma membrane lawns by exogenous green fluorescent protein (GFP)-tagged PH domain. In parallel experiments, exocytosis of LDCVs was monitored by patch-clamp capacitance measurements and amperometry. We discovered that the size of the releasable vesicle pools, but not their release kinetics, scales with the amount of PI(4,5)P₂ in the plasma membrane, no matter whether PI(4,5)P₂ is regulated acutely or chronically, suggesting that PI(4,5)P₂ is a key physiological regulator of chromaffin cell secretion.

Materials and Methods

Antibodies, expression constructs, and virus generation. Mouse monoclonal antibody was used to detect PI(4,5)P₂ (Assay Design, Ann Arbor, MI), and the primary antibody was visualized using cyanine 5 (Cy5)-conjugated goat anti-mouse secondary antibody (Jackson ImmunoResearch, West Grove, PA). Unless indicated otherwise, the chemicals used were purchased from Sigma (Taufkirchen, Germany).

For protein expression, pET28a-His₆-GFP-PH-PLCδ₁ was generated by subcloning the fusion construct between the PH domain from PLCδ₁ and enhanced GFP (EGFP) (attached to the C-terminal end of the PH domain) into pET28a. The triple mutation K30A, K32A, W36N of GFP-PH-PLCδ₁, which does not bind to PI(4,5)P₂, was generated by PCR and also cloned into pET28a. For the construction of a vector encoding the proteins tagged with monomeric red fluorescent protein (mRFP) at their N terminus, mRFP containing an initiator, ATG, but no stop codon was amplified from pmRFP (a gift from Dr. H.-D. Söling, Göttingen, Germany) and inserted into the mammalian expression vector pcDNA3 (Invitrogen, San Diego, CA) yielding pcmRFP. The coding sequences for PI4P5KIγ and the membrane-tagged 5-inositol phosphatase domain of synaptotagmin 1 (IPPI-CAAX) (Krauss et al., 2003) were inserted into pcmRFP. For infection of BCCs, the viral constructs pSFV1-PI4P5KIγ-IRES-GFP and pSFV1-IPPI-CAAX-IRES-GFP were generated: a viral pSFV1 vector (Invitrogen) was modified by the introduction of an internal ribosome entry site from poliovirus and EGFP. PI4P5KIγ was cut from pGFP-C1-PI4P5KIγ (Krauss et al., 2003) and subcloned into the modified pSFV1 using the *PmeI* site. IPPI-CAAX was cut from pcDNA-IPPI-CAAX (Krauss et al., 2003) and cloned into the modified pSFV1 using the *BamHI/PmeI* sites. The sequences of all constructs were verified by DNA sequencing. Virus production was performed as described previously (Ashery et al., 1999).

Expression and purification of wild-type and mutated GFP-PH-PLCδ₁. *Escherichia coli* BL21 (DE3) cells transformed with wild-type (wt) or mutated pET28a-His₆-GFP-PH-PLCδ₁ were grown in Luria broth medium containing 50 μg/ml kanamycin at 37°C to an OD₆₀₀ of 0.8. Protein expression was induced by the addition of 0.5 mM isopropyl-1-thio-β-D-galactopyranoside for 4 h. The cell pellet was resuspended in 35 ml of ice-cold PBS containing 1 mM phenylmethylsulfonyl fluoride and incubated with lysozyme for 10 min on ice. After sonification, 1% Triton X-100 and 1% 3-[(3-cholamidopropyl)dimethylammonio]-1-propanesulfonate were added. The mixture was incubated for another 10 min and then centrifuged at 25,000 × g for 15 min. The supernatant was supple-

mented with 20 mM imidazol and incubated with nickel-nitrilotriacetic acid-agarose (Qiagen, Hilden, Germany) for 2 h at 4°C. The collected beads were washed twice with PBS buffer containing 20 mM imidazol, once with PBS buffer containing 40 mM imidazol, and once with K-Glu buffer (in mM: 120 potassium glutamate, 20 potassium acetate, 20 HEPES, and 4 MgCl₂, pH 7.2). The beads were subsequently resuspended in 2 ml of K-Glu buffer supplemented with 10 mM EDTA, and after 30 min, thrombin (30 U; Sigma) was added and incubated for at least 4 h. The supernatant containing His₆-tag-cleaved protein was dialyzed twice against 0.5 L K-Glu buffer supplemented with 1 mM dithiothreitol. Finally, the dialyzed solution was sedimented in a microcentrifuge (14,000 rpm for 30 min at 4°C), and the protein concentration of the supernatant was determined by the method of Bradford. The protein was analyzed by SDS-PAGE and Coomassie staining. Two bands were detected: one of the appropriate size (~75% of the total protein amount) and another significantly smaller. Only the bigger band associated specifically with PI(4,5)P₂ liposomes.

Liposome binding with wt and triple mutated GFP-PH-PLCδ₁. Liposomes containing 70% phosphatidylcholine, 20% phosphatidylethanolamine, and 10% PI or 10% PI(4,5)P₂ were prepared as described previously (Rohde et al., 2002). Fifty microliters of each liposome suspension (100 μg) were incubated in cytoplasmic buffer (in mM: 25 HEPES, pH 7.2, 25 KCl, 2.5 magnesium acetate, and 150 potassium glutamate) with 3 μg of wt or mutated GFP-PH-PLCδ₁ for 15 min at room temperature in a final volume of 100 μl. The mixture was centrifuged at 35,000 × g for 1 h at 4°C. The pellet was resuspended in Laemmli sample buffer.

Cell culture and transfection. The primary culture of BCCs was prepared as described previously (Nagy et al., 2002). The neuroendocrine cell line PC12 (clone 251) was maintained and propagated as described previously (Lang et al., 1997). Viral infection was performed on cultured BCCs 12–36 h after plating. Transfection of PC12 cells with wt and mutated GFP-PH-PLCδ₁, mRFP-PI4P5KIγ, and mRFP-IPPI-CAAX was performed as described previously (Lang et al., 1997).

Electrophysiological and electrochemical measurements. Whole-cell patch-clamp capacitance, amperometry, flash photolysis of caged calcium, and intracellular Ca²⁺ measurements were performed as described previously (Nagy et al., 2002). PI(4,5)P₂ isolated from bovine spinal cord was obtained from Calbiochem (Darmstadt, Germany) and dissolved in the pipette-filling solution by sonification for 15 min on ice. During the recordings, the BCCs were maintained in extracellular solution (145 mM NaCl, 2.8 mM KCl, 2 mM CaCl₂, 1 mM MgCl₂, 10 mM HEPES, and 2 mg/ml D-glucose, pH 7.20, 305 mOsm/kg). In the experiments with short-term 2-(4-morpholinyl)-8-phenyl-4H-1-benzopyran-4-one (LY294002) application, a local perfusion system was used. Kinetic analysis was performed fitting individual capacitance traces with a triple-exponential function as described previously (Nagy et al., 2004). The amplitudes and time constants of the two faster exponentials define the size and release kinetics of the slowly releasable pool (SRP) and the RRP, respectively, whereas the slowest exponential was included to correct for the sustained component of release. Because the time constant of the sustained component is too slow to be measured accurately in this way, this third exponential was not used directly. Instead, we subtracted the amplitudes of the fast and slow burst from the total amount of secretion during 5 s and calculated the linear rate of sustained release. Statistical testing of amplitudes and time constants of the kinetics components was performed by the nonparametric Mann–Whitney *U* test. Each experimental condition has been compared with control cells obtained from the same cell preparations. The values given represent the mean ± SEM.

Generation of plasma membrane sheets from BCCs and PC12 cells. BCCs were plated on 25 mm glass coverslips that had been pretreated with a 0.1 mg/ml poly-L-lysine (Sigma) for 30 min (5 × 10⁵ to 7 × 10⁵ cells/coverslip) and kept at 37°C in 8% CO₂. Cells were used for experiments 24–36 h after plating. For chromaffin cells, membrane sheets were made by placing the coverslip into 150 ml of ice-cold sonication buffer (120 mM potassium glutamate, 20 mM potassium acetate, 20 mM HEPES, 2 mM ATP, 100 μM GTP, 4 mM MgCl₂, 4 mM EGTA, 6 mM Ca-EGTA, and 300 nM [Ca²⁺]_{free}, pH 7.2, 310 mOsm/kg; bubbled with N₂ for 30 min) in a round glass beaker with a final volume of 300 ml. A coverslip with attached cells was centered 12 mm under the sonication tip (2.5 mm), and

the cells were disrupted applying a single ultrasound pulse (Sonifier 450, power setting at 1.8 and a duty cycle of 100 ms; Branson Ultrasonics, Danbury, CT). Apart from chromaffin cells, the primary culture contained a low number of other cell types, mainly endothelial cells and erythrocytes. However, the membrane sheets generated from these cells differed in their size and level of staining for syntaxin 1, so that they were easily recognized and excluded from analysis. Membrane sheets from PC12 cells were generated as described previously (Avery et al., 2000).

Fluorescence on plasma membrane sheets generated from BCCs and PC12 cells. In experiments with recombinant GFP-PH-PLC δ_1 , freshly prepared membrane sheets from BCCs or PC12 cells were incubated for 10 or 15 min with 3 μ M GFP-PH-PLC δ_1 in K-Glu buffer with 3% BSA. Subsequently, the sheets were washed for 100 s in K-Glu buffer and fixed for at least 2 h in 4% paraformaldehyde in PBS at room temperature. For visualizing the plasma membrane, 1-(4-trimethyl-ammoniumphenyl)-6-phenyl-1,3,5-hexatriene (TMA-DPH) or 1,1'-dihexadecyl-3,3',3'-tetramethylindocarbocyanine perchlorate (DiI_{C16}) (Molecular Probes, Eugene, OR) were used. Immunofluorescence on PC12 membrane sheets was performed as described previously (Lang et al., 2001).

All samples were examined with an Axiovert 100 TV fluorescence microscope (Zeiss, Oberkochen, Germany) with a 100 \times , 1.4 numerical aperture plan achromate objective using the appropriate fluorescence filters (excitation filter G 365, BS 395 and emission filter LP 420 were used for TMA-DPH dye; excitation filter BP 480/40, BS 505 and emission filter BP 527/30 were used for GFP; excitation filter BP 590/60, BS 660 and emission filter BP 662/76 were used for Cy5 dye). Throughout all experiments, the focal position of the objective was controlled using a low-voltage piezo translator driver and a linear variable transformer displacement controller (Physik Instrumente, Walldbronn, Germany). The images were taken with a back-illuminated frame transfer CCD camera (2x512x512-EEV chip, 13 \times 13 μ m pixel size; Princeton Instruments, Trenton, NJ) with a magnifying lens (1.6 \times or 2.5 \times Optovar) to avoid spatial undersampling by the larger pixels. Digital image analysis was performed using MetaMorph software (Universal Imaging, West Chester, PA). The size of PI(4,5)P₂ clusters was estimated by fitting one-dimensional Gaussians to a line-scan profile through the center of selected fluorescent spots as described previously (Lang et al., 2001). The point-spread function was identified by fitting two-dimensional Gaussian functions to the fluorescence intensity profile of 220 nm beads (TetraSpeck microfluorospheres; Molecular Probes) and was determined to be 246 nm. To perform comparative quantitation of fluorescence intensity, plasma membrane sheets were identified in the TMA-DPH images. A 3.3 \times 3.3 μ m (40 \times 40 pixels; 1 pixel corresponding to 81.25 nm) region of interest was defined on the randomly selected membrane and transferred to the other channels. The fluorescence intensity was quantified by measuring the average intensity of the area. The local background was measured in the area outside the membrane sheets and subtracted. For each condition, at least 30 membrane sheets were analyzed in each experiment. Intensity values are given as mean \pm SEM. Images for display are presented on a linear intensity scale, usually scaled between the minimal and maximal value present in the region of interest. In some cases, the maximal value was decreased, resulting in local image saturation, to make finer structures (microdomains) visible.

Results

A spatially resolved assay for PI(4,5)P₂ in the plasma membrane of chromaffin and PC12 cells

We aimed at comparing the amount of PI(4,5)P₂ in the plasma membrane with LDCV secretion from chromaffin cells as measured electrophysiologically. To measure PI(4,5)P₂ levels in the plasma membrane, we adapted a microscopic assay that has recently been developed for PC12 cells and fibroblasts to measure the amount and spatial distribution of plasma membrane constituents (Lang et al., 2001, 2002). Cells grown on coverslips are disrupted by a brief ultrasonic pulse, leaving behind lawns of plasma membrane with the cytosolic face being directly accessible to external probes. In addition, some intact cells are usually still present. To visualize PI(4,5)P₂, we incubated membrane sheets

prepared from PC12 cells with exogenously added PI(4,5)P₂-binding PH domain of PLC δ_1 fused to GFP (GFP-PH-PLC δ_1) that was previously shown to bind selectively to PI(4,5)P₂ (Stauffer et al., 1998; Várnai and Balla, 1998). We observed strong labeling of membrane sheets (Fig. 1B), whereas intact cells were not labeled (data not shown), in agreement with the general finding that PI(4,5)P₂ is only present in the inner plasma membrane leaflet. The labeling exhibited a punctate staining pattern distributed over the entire plasma membrane. To confirm the integrity of the membrane sheets, the sheets were visualized using TMA-DPH, a lipophilic styryl dye (Fig. 1A). Punctate labeling by GFP-PH-PLC δ_1 was detected in areas where the TMA-DPH membrane staining was uniform (Fig. 1C,D), revealing that it was not attributable to local increases in the membrane area (e.g., attributable to infoldings). Similar results were obtained when the lipid dye DiI_{C16} instead of TMA-DPH was used (data not shown).

Several experiments were performed to ensure that GFP-PH-PLC δ_1 labeling of the membrane sheets can be used to detect PI(4,5)P₂. First, we constructed a triple mutant of GFP-PH-PLC δ_1 deficient in PI(4,5)P₂ binding (K30A, K32A, W36N GFP-PH-PLC δ_1). In contrast to the wt GFP-PH-PLC δ_1 , this mutant did not bind PI(4,5)P₂ liposomes (Fig. 1E,F). When applied to membrane sheets, no labeling by the triple mutant was observed (<0.3% of the wt signal) (Fig. 1G,H). Next, we compared labeling with a PI(4,5)P₂-specific antibody to GFP-PH-PLC δ_1 staining. When applied to the same membrane sheets simultaneously, the two PI(4,5)P₂ ligands showed similar staining patterns (Fig. 1I,K), which partly overlapped. Finally, we tested whether binding of GFP-PH-PLC δ_1 competes with antibody binding. When PC12 cell membrane sheets were incubated with a mixture of anti-PI(4,5)P₂ antibody and increasing amounts of GFP-PH-PLC δ_1 , a gradual decrease of anti-PI(4,5)P₂ antibody labeling was observed (Fig. 1L). Hence, we conclude that GFP-PH-PLC δ_1 is a reliable reporter of plasmalemmal PI(4,5)P₂. An alternative reporter would be the anti-PI(4,5)P₂ antibody, but to avoid probe-mediated PI(4,5)P₂ clustering or coalescence of clusters, we preferred to use GFP-PH-PLC δ_1 , which binds PI(4,5)P₂ with a one-to-one stoichiometry.

GFP-PH-PLC δ_1 labeling was very stable in membrane sheets: the level of fluorescent probe remained unchanged for at least 30 min after staining, also in experiments in which membrane sheets were not fixed after the addition of GFP-PH-PLC δ_1 . We estimated the size of the clusters by fitting Gaussians to a line-scan profile through the center of selected fluorescent puncta (Lang et al., 2001). That method gave a size of 306 \pm 13 nm after correction for point-spread function (n = 60 puncta). The clustering of the GFP-PH-PLC δ_1 signal was disrupted when cholesterol was extracted from the membrane using methyl- β -cyclodextrin (data not shown). Clustering was evident in most experiments, but uniform GFP-PH-PLC δ_1 staining was observed in some cells, particularly on sheets with very intense TMA-DPH staining.

In the above, we used the easily accessible PC12 cells and the previously published method for membrane sheet generation to define the basal properties of the PI(4,5)P₂ assay. However, for electrophysiological experiments, we preferred to use chromaffin cells, because chromaffin cells, in contrast to PC12 cells, display fast secretion of LDCVs on the millisecond time scale as detected electrophysiologically. This property allows us to address the question at which step PI(4,5)P₂ acts in the secretory cascade. We therefore developed a membrane sheet assay for chromaffin cells by enhancing cell attachment by poly-L-lysine coating of the glass coverslips and modifying the sonication procedure (see Materials and Methods). When membrane sheets from chromaffin cells

were incubated with GFP-PH-PLC δ_1 , we again observed a punctate distribution of PI(4,5)P₂ in the membrane (see Fig. 5C). The specificity of the GFP-PH-PLC δ_1 signal in chromaffin cells was verified by repeating the experiments in Figure 1, G and H, which gave indistinguishable results. The estimated size of PI(4,5)P₂ clusters in BCCs was comparable with the one calculated in PC12 cells (319 ± 12 nm; $n = 50$ puncta). Indeed, in every aspect tested, we obtained similar results with the PI(4,5)P₂ assay in PC12 cells and chromaffin cells.

We conclude that PI(4,5)P₂ can be specifically detected in isolated membrane sheets by the addition of exogenous GFP-PH-PLC δ_1 . Hence, we used this method to semiquantitatively evaluate the effect of manipulations on plasma membrane PI(4,5)P₂ content.

An increase in the plasma membrane PI(4,5)P₂ level potentiated LDCV secretion in chromaffin cells

PI4P5KI γ is preferentially expressed in the nervous system and concentrated at synapses where it has been implicated in the synthesis of the PI(4,5)P₂ pool relevant for membrane trafficking (Wenk et al., 2001). We first examined the consequences of expressing PI4P5KI γ fused to mRFP (mRFP-PI4P5KI γ) in PC12 cells. For convenience, we used PC12 cells for these measurements, because they can be transfected more easily than BCCs, without the need for a viral transfection system, and because all tested properties of GFP-PH-PLC δ_1 staining were very similar between PC12 cells and BCCs. Plasma membrane sheets were generated from transfected as well as from nontransfected cells and incubated with GFP-PH-PLC δ_1 . Expressed mRFP-PI4P5KI γ was localized to the plasma membrane (Fig. 2B), in agreement with previous observations (Arioka et al., 2004). The fluorescence quantification revealed nearly threefold higher GFP-PH-PLC δ_1 binding to membrane sheets from transfected cells (Fig. 2A–C). A similar increase in plasmalemmal PI(4,5)P₂ was detected using anti-PI(4,5)P₂ antibody instead of GFP-PH-PLC δ_1 (data not shown). These data show that overexpression of PI4P5KI γ increased the level of PI(4,5)P₂ in the plasma membrane. Note that the GFP-PH-PLC δ_1 labeling of the membrane sheets in Figure 2A appears more uniform than in Figure 1B; this impression is caused by the scaling of the image to represent the very different fluorescence intensities present. After rescaling according to the intensity present within either sheet, both sheets showed inhomogeneous staining, although in the expressing cells, the inhomogeneities no longer appeared punctate (data not shown). When we compared the staining for GFP-PH-PLC δ_1 (in the green channel) with the PI4P5KI γ signal (in the red channel), we observed a significant correlation (Pearson correlation coefficient, $r = 0.65$; $p < 0.0001$) between the binding of GFP-PH-PLC δ_1 and the level of PI4P5KI γ overexpression (Fig. 2D).

PI4,5P₂ in the plasma membrane

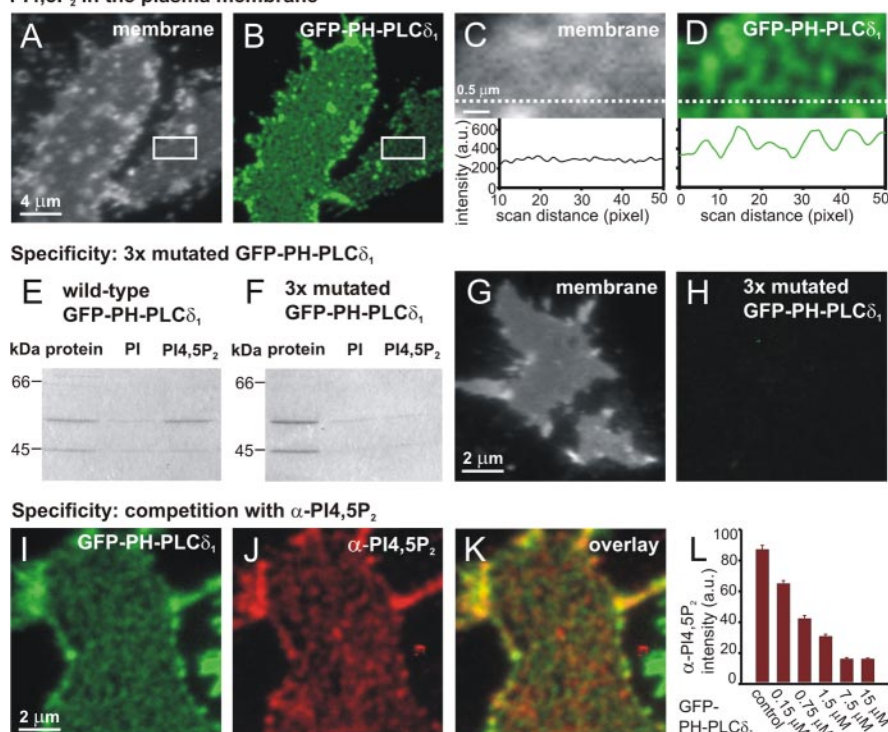


Figure 1. Punctate PI(4,5)P₂-specific staining of PC12 membrane sheets. **A–D**, Plasma membrane sheets were generated from PC12 cells, labeled with GFP-PH-PLC δ_1 , washed, and fixed. The samples were imaged in two channels: membranes were identified in the presence of TMA-DPH dye in the blue channel (**A**) and GFP-PH-PLC δ_1 in the green channel (**B**). **C, D**, Magnified view from **A** and **B** (rectangle). Punctate GFP-PH-PLC δ_1 staining was detected in areas where the TMA-DPH membrane staining was uniform. Bottom panels, The fluorescence intensities recorded along a line scan (dashed line) through the images (the fluorescence background was measured outside of the sheet and subtracted). **E–F**, Specificity of GFP-PH-PLC δ_1 binding. **E, F**, PI and PI(4,5)P₂ liposomes were incubated with wt GFP-PH-PLC δ_1 and triple-mutated GFP-PH-PLC δ_1 . The triple mutation eliminated binding to PI(4,5)P₂ liposomes. **G, H**, No staining ($<0.3\%$) was detected in the green channel when membrane sheets were incubated with triple-mutated GFP-PH-PLC δ_1 . **I, K**, Simultaneous binding of PI(4,5)P₂ antibody and GFP-PH-PLC δ_1 . Freshly prepared membrane sheets from PC12 cells were incubated for 10 min with GFP-PH-PLC δ_1 (3 μ M) and PI(4,5)P₂ antibody (1:50 dilution). **I**, GFP-PH-PLC δ_1 -stained sheet in the green channel. **J**, The same sheet, stained with Cy5-PI(4,5)P₂ antibody and imaged in the dark red channel. **K**, Overlay of **I** and **J**. Note that for display, each of the images **I–K** was scaled between the local minimum and maximum intensity (see Materials and Methods), so that the intensity of different displayed images are not comparable (e.g., **B** and **J** are not comparable as far as absolute intensities are concerned). **L**, Quantification of fluorescence intensities: GFP-PH-PLC δ_1 could compete with PI(4,5)P₂ antibody binding. In the presence of a constant antibody concentration (1:50 dilution) and increasing GFP-PH-PLC δ_1 concentrations, the staining intensity of random images in the dark red [Cy5-PI(4,5)P₂ antibody] channel decreased with increasing GFP-PH-PLC δ_1 concentration.

To achieve high efficiency of BCC transfection, we expressed PI4P5KI γ and GFP (as an expression marker) using Semliki Forest virus (SFV). Transfected cells were loaded via a patch pipette with the photolabile Ca²⁺ chelator nitrophenyl-EGTA and two Ca²⁺-sensitive dyes that enable accurate Ca²⁺ measurements during the whole-cell patch-clamp experiments (Voets, 2000). Flash photorelease of caged calcium commonly increased the intracellular calcium concentration ([Ca²⁺]_i) from several hundred nanomolars to >10 μ M, which resulted in robust secretion assayed by the increase in membrane capacitance and amperometric current (Fig. 3A). Measured by capacitance increase, exocytosis in the cells overexpressing PI4P5KI γ was strongly enhanced (on average, 235%) compared with control cells. Larger amperometric currents from PI4P5KI γ -overexpressing cells revealed that this strong increase in capacitance was mediated by fusion of catecholamine-filled LDCVs. A similar increase was observed as a result of a second stimulation executed 100 s after the first one (on average, 241%). As described previously, BCC secretion elicited under these conditions consists of a burst phase

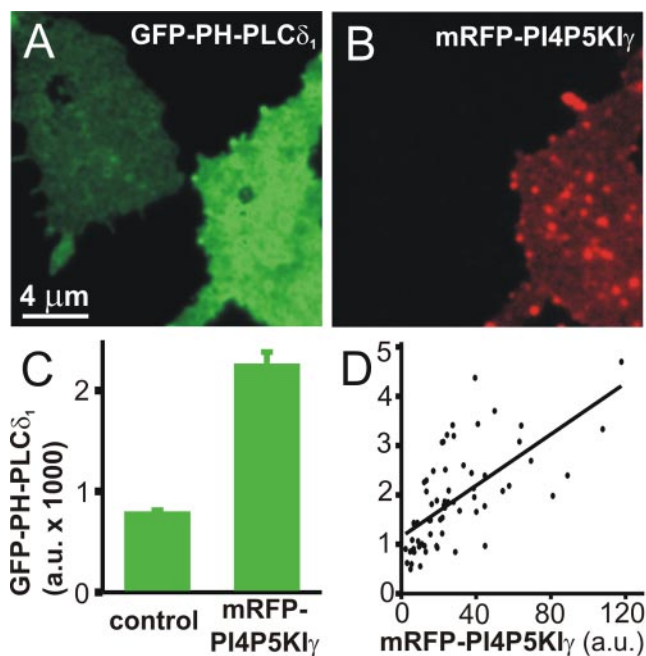


Figure 2. Overexpression of mRFP-PI4P5KI γ increased the concentration of PI(4,5)P₂ in the plasma membrane. Plasma membrane sheets were generated from PC12 cells overexpressing mRFP-PI4P5KI γ for 24–36 h, reacted with GFP-PH-PLC δ_1 , fixed, and imaged in the green (**A**) and red (**B**) channels. An increased PI(4,5)P₂ level was detected on the membrane sheets generated from mRFP-PI4P5KI γ -expressing cells. **C**, Quantitative determination of GFP-PH-PLC δ_1 fluorescence intensity on membrane sheets from control and transfected cells from 65 sheets from two separate experiments (mean \pm SEM). **D**, On membrane sheets such as those shown in **A** and **B**, the staining intensity of random images in the green channel (GFP-PH-PLC δ_1) was measured and plotted against the staining intensity in the red channel (mRFP-PI4P5KI γ). The line is a linear regression.

that corresponds to the emptying of two pools of release-competent vesicles (the RRP and the SRP, respectively) and a sustained phase that represents vesicle recruitment and subsequent fusion (Xu et al., 1998; Voets, 2000). In accordance with this model, we performed a kinetic analysis to determine the pool sizes (the amplitudes of the exponential fits) and fusion kinetics (time constants of the exponential fits) (Nagy et al., 2004). The sizes of both releasable pools, the RRP and the SRP, were increased by approximately a factor of 2 in PI4P5KI γ -overexpressing cells (Fig. 3A). Also, the sustained component of release, which measures the refilling of the pools, was significantly increased (Fig. 3A). In contrast, the time constants of RRP and SRP fusion did not differ significantly between control and PI4P5KI γ -overexpressing cells (Fig. 3A). These data indicate that the increased PI(4,5)P₂ level had an influence on the size and refilling of the releasable pools but not on their rate constant of fusion with the plasma membrane under conditions of elevated calcium concentrations.

We wanted to investigate whether a short-term (acute) increase in PI(4,5)P₂ would also modulate secretion. Therefore, we applied 5 μ M PI(4,5)P₂ suspension through the patch pipette (Olsen et al., 2003). Cells loaded with PI(4,5)P₂ exhibited a large increase in secretion, both as a result of the first (on average, 275% increase) (Fig. 3B) and the second (on average, 270% increase) stimulus. Further kinetic analysis revealed that PI(4,5)P₂-loaded cells had a significantly larger exocytotic burst than the control, and, as in the case of PI4P5KI γ -overexpressing cells, this was a result of a twofold increase in the size of the RRP and the SRP in the absence of a change in fusion kinetics (Fig. 3B). The

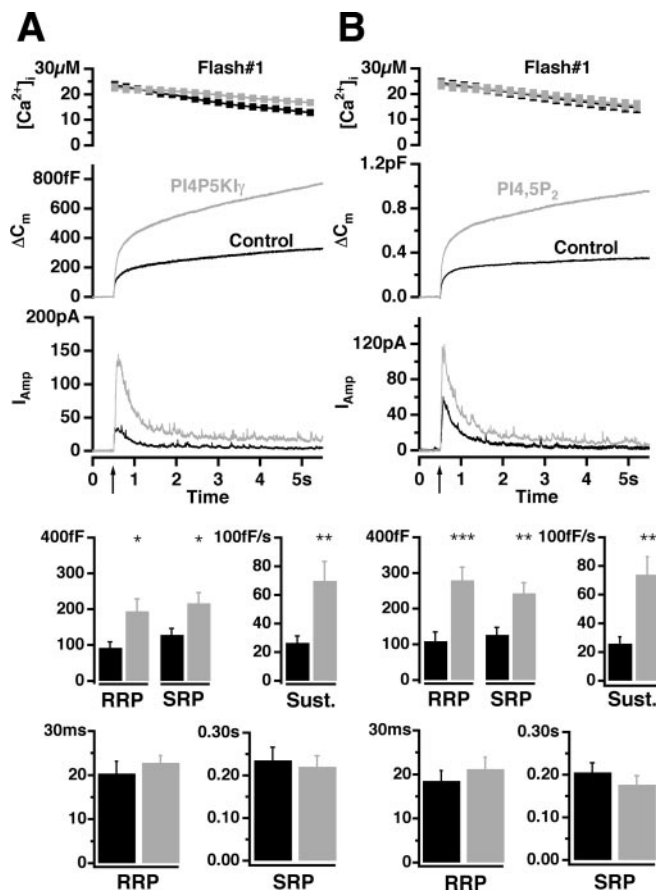


Figure 3. Overexpression of PI4P5KI γ or loading of BCCs with PI(4,5)P₂ potentiated LDCV secretion. **A**, **B**, Top, Mean [Ca²⁺]_i (top; error bars represent SEM), capacitance change (middle), and amperometric current (bottom) were measured simultaneously after a step-like elevation of [Ca²⁺]_i caused by flash photolysis of caged Ca²⁺ (flash at arrow). The traces are averages of many experiments, so the individual fusion events (spikes) are not recognizable in the amperometric signal. **A**, Secretion from BCCs after the first flash photorelease of calcium. The means of 34 control cells (black) and 34 cells overexpressing PI4P5KI γ for 12–16 h (gray) are shown. There was no difference in preflash [Ca²⁺]_i between the two groups (data not shown). Secretion in transfected cells was strongly potentiated. Bottom, amplitudes and time constants of exponential fits to individual responses. The amplitudes (mean \pm SEM) of the two releasable pools (RRP and SRP) and the rate of sustained component were significantly increased in cells overexpressing PI4P5KI γ (gray bars) (* p < 0.05; ** p < 0.01; *** p < 0.001). In contrast, time constants were similar between control cells and BCCs overexpressing PI4P5KI γ . **B**, Intracellular application of PI(4,5)P₂ strongly potentiated secretion. The response to a first flash stimulation in control cells (black trace; n = 26) and cells loaded with 5 μ M PI(4,5)P₂ (gray trace; n = 27) is shown. Bottom, Significant increase in amplitudes of the RRP and the SRP as well as in the rate of sustained component was detected. Time constants were unchanged.

increase in the rate of sustained release from PI(4,5)P₂-loaded cells was also highly significant (Fig. 3B). Given that intracellular application of PI(4,5)P₂ affects exocytosis, we inspected whether PI(4,5)P₂ could be incorporated in the plasma membrane when incubated *in vitro* with plasma membrane sheets generated from BCCs and PC12 cells. The sheets were incubated with different concentrations of PI(4,5)P₂ suspension and subsequently reacted with GFP-PH-PLC δ_1 . We detected fluorescent particles attached to the membrane sheets, but plasmalemmal PI(4,5)P₂ was not significantly increased, indicating that insertion of PI(4,5)P₂ was not very efficient in this *in vitro* experiment (data not shown). Nevertheless, we expect that in an *in vivo* situation, cytoplasmic proteins such as PITP would mediate insertion of PI(4,5)P₂ into the membrane.

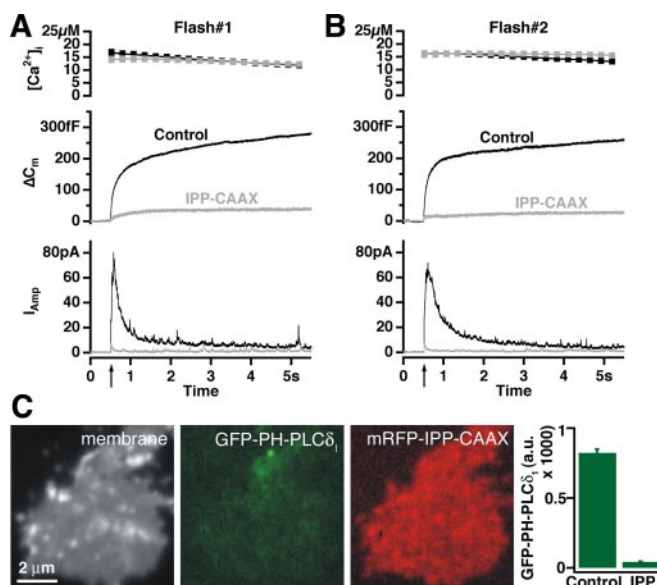


Figure 4. Depletion of plasma membrane PI(4,5)P₂ abolished LDCV secretion in BCCs. **A**, Response to a first flash stimulation in control cells (black trace; $n = 53$) and cells overexpressing IPP1-CAAX for 9–13 h (gray trace; $n = 52$). Secretion in transfected cells was almost abolished. **B**, A second flash stimulation given 2 min after the first one gave the same result (black trace, 54 control cells; gray trace, 53 cells overexpressing IPP1-CAAX). **C**, PI(4,5)P₂ depletion from plasma membrane of PC12 cells. Plasma membrane sheets were generated from PC12 cells overexpressing mRFP-IPP1-CAAX for 30 h, reacted with GFP-PH-PLC δ_1 , fixed, and imaged in the presence of TMA-DPH dye in the blue, green, and red channels. Barely any GFP-PH-PLC δ_1 signal could be detected on membrane sheets generated from mRFP-IPP1-CAAX-expressing cells. The graph shows quantitative determination of GFP-PH-PLC δ_1 fluorescence on membrane sheets from control (71 sheets) and transfected (58 sheets) cells from two experiments (mean \pm SEM).

Together, these data demonstrate that increasing the amount of plasmalemmal PI(4,5)P₂ over control conditions caused a higher level of LDCV secretion and that this increase is attributable to a larger number of primed vesicles.

Deprivation of PI(4,5)P₂ from plasma membrane abolished LDCV secretion in chromaffin cells

We next asked whether normal secretion in resting chromaffin cells depends on the presence of PI(4,5)P₂. To decrease the PI(4,5)P₂ concentration in the plasma membrane, we overexpressed a PI(4,5)P₂ degrading enzyme, the membrane-targeted inositol 5-phosphatase domain of synaptojanin 1 (IPP1-CAAX) fused to mRFP (mRFP-IPP1-CAAX) (Krauss et al., 2003) in PC12 cells. Plasma membrane sheets were generated from these as well as from nontransfected cells and reacted with GFP-PH-PLC δ_1 . The fluorescence quantification revealed that almost no signal could be detected on the membrane sheets generated from mRFP-IPP1-CAAX-expressing cells (on average, 5.2% of control values) (Fig. 4C). Similar data were obtained using an anti-PI(4,5)P₂ antibody (data not shown). Thus, overexpression of mRFP-IPP1-CAAX almost completely deprived PI(4,5)P₂ from PC12 cell plasma membrane.

We constructed SFV encoding IPP1-CAAX and GFP and transfected BCCs in primary culture. Ca²⁺-induced secretion from BCCs expressing IPP1-CAAX was nearly abolished, when evaluated as both a capacitance change and as amperometric current (Fig. 4A). The total secretion over the first 5 s recording period added up to \sim 13% of that seen in control cells. Also, a second stimulation \sim 2 min after the first one failed to elicit secretion (Fig. 4B). We therefore conclude that PI(4,5)P₂ is essen-

tial for Ca²⁺-induced LDCV secretion. Because of the low amount of remaining secretion, a kinetic analysis was not possible.

Next, we examined whether the Ca²⁺-induced secretion in BCCs overexpressing IPP1-CAAX could be rescued by loading the cells with 5 μM PI(4,5)P₂ through the patch pipette. In approximately one-quarter of the experimental cells, we managed to rescue secretion up to normal levels, whereas in approximately three-quarters of the cells, this was not the case (data not shown), probably because of the continuous action of IPP1-CAAX to break down PI(4,5)P₂.

The previous two sections show that the resting level of PI(4,5)P₂ in the inner leaflet of the plasma membrane is intermediate between the levels that would result in minimal and maximal secretion. Thus, the level of secretion can be changed in both directions by a change in PI(4,5)P₂, making PI(4,5)P₂ a likely key physiological regulator of chromaffin cell secretion.

Dual effect of LY294002 on the plasma membrane PI(4,5)P₂ level and LDCV secretion in chromaffin cells

Besides PI(4,5)P₂, other phosphoinositides may have a role in secretion (Cremona and De Camilli, 2001). Based on the use of phosphatidylinositol 3-kinase (PI3K) inhibitors, several studies suggested PI3K and 3-phosphorylated phosphatidylinositides in regulating exocytosis and synaptic transmission (Chasserot-Golaz et al., 1998; Hong and Chang, 1999; Rizzoli and Betz, 2002; Cousin et al., 2003). Therefore, we examined the effect of the most commonly used PI3K inhibitor, LY294002, on catecholamine secretion in BCCs. Acute application of 100 μM LY294002 was performed through a local perfusion system. Measured by capacitance increase, the first Ca²⁺-releasing stimulus applied 4 min after the beginning of LY294002 application showed strongly enhanced secretion in treated cells (on average, 235%) (Fig. 5A). The sizes of both the releasable pools were increased; the rate of the sustained component was, on average, higher in LY294002-treated cells, but this was not statistically significant. The time constants for fusion of the releasable pools were indistinguishable from control cells (Fig. 5A). The second flash given 100 s after the first one also evoked an increased exocytotic response (on average, 242%). These findings are surprising, because it was previously shown that LY294002 inhibited secretion in chromaffin cells (Chasserot-Golaz et al., 1998); in that study, longer incubation times were used. Therefore, we increased the preincubation time to 30–70 min and indeed this resulted in a 58% reduction of secretion at the first stimulus and a 72% reduction at the second one (Fig. 5B). Kinetic analysis revealed that the sizes of both releasable pools as well as the rate of sustained secretion were significantly decreased after prolonged application of LY294002 (Fig. 5B). Moreover, inspection of the time constants revealed no differences in fusion kinetics with respect to control for both the RRP and the SRP (Fig. 5B).

We wanted to determine whether the effect of LY294002 could be accounted for by changes in the PI(4,5)P₂ level. We therefore measured the corresponding PI(4,5)P₂ levels in plasma membrane sheets from BCCs (Fig. 5C) or PC12 cells treated with LY294002 for defined time periods. For both BCC and PC12 cell plasma membranes, a nearly twofold increase in GFP-PH-PLC δ_1 binding was observed after short-term incubation with LY294002 (3–5 min) (Fig. 5D, data from BCC; data from PC12 cells were similar). Prolonged incubation with LY294002 resulted in a \sim 50% decrease in GFP-PH-PLC δ_1 binding (30–60 min) (Fig. 5D). We performed the same experiment with 100 μM 2-(4-piperazinyl)-8-phenyl-4H-1-benzopyran-4-one (LY303511), an

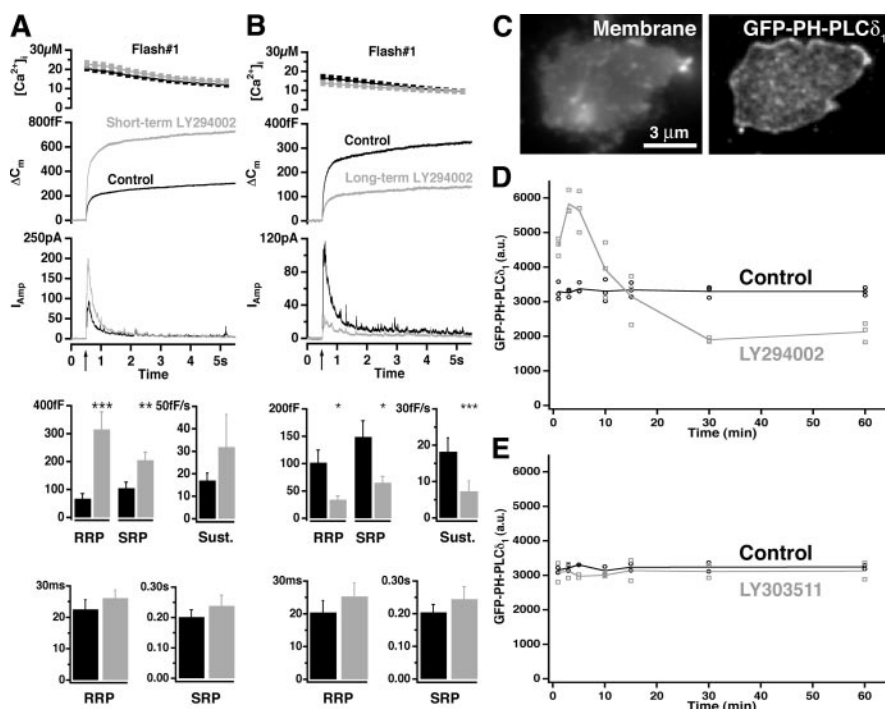


Figure 5. Dual effect of LY294002 on the plasma membrane PI(4,5)P₂ level and LDCV secretion in chromaffin cells. **A**, Short-term (4 min) application of 100 μ M LY294002. The response to the first stimulation in control cells (black; 33 cells) and BCCs perfused with LY294002 (gray; 31 cells) is shown. For an explanation, see the legend to Figure 3. A significant increase in RRP and SRP amplitudes was seen when LY294002 was applied, but no difference in the rate of the sustained component or time constants was found. **B**, Long-term application (30–70 min) of 100 μ M LY294002. The response to the first flash stimulation in control cells (black; 29 cells) and BCCs preincubated with LY294002 (gray; 30 cells) is shown. A significant decrease in the total secretion was found; the time constants were indistinguishable from control cells. **C**, Example plasma membrane sheets generated from BCCs and labeled with GFP-PH-PLC δ_1 . The samples were imaged in two channels: membranes were identified in the presence of TMA-DPH dye in the blue channel and GFP-PH-PLC δ_1 in the green channel. **D**, LY294002 induced a transient increase that was followed by a decrease of PI(4,5)P₂ content in the plasma membrane. BCCs were incubated with 100 μ M LY294002 in extracellular buffer or extracellular buffer only (control) for the time intervals indicated, and membrane sheets were generated, labeled with GFP-PH-PLC δ_1 , and fixed. The experiment was repeated three times. The staining intensity of >50 sheets from each experiment was measured in the green channel and plotted against time. **E**, The same sheet experiment was performed with 100 μ M LY303511, an inactive analog of LY294002. No difference in GFP-PH-PLC δ_1 binding compared with control was detected.

inactive analog of LY294002, and observed no difference in GFP-PH-PLC δ_1 binding compared with control (Fig. 5E). Therefore, we conclude that changes of the PI(4,5)P₂ level in the plasma membrane were because of the specific activities of LY294002.

In conclusion, LY294002 has a biphasic effect on secretion: acute application leads to increased PI(4,5)P₂ levels and potentiation of secretion, whereas chronic application decreases PI(4,5)P₂ levels and inhibits secretion.

Discussion

By comparing secretion from chromaffin cells using electrophysiological methods with inner membrane leaflet PI(4,5)P₂ levels using a membrane sheet assay, we have shown that the PI(4,5)P₂ level determines the extent of chromaffin cell secretion. If PI(4,5)P₂ is depleted from the plasma membrane by phosphatase overexpression or long-term LY294002 application, secretion is reduced. If PI(4,5)P₂ levels are increased by PI4P5KI γ overexpression, PI(4,5)P₂ infusion, or short-term LY294002 application, secretion is increased. This shows that (1) short-term (acute) and long-term (chronic) changes in PI(4,5)P₂ levels are equally effective at modulating secretion, therefore (2) the cells do not seem to compensate for a change in the PI(4,5)P₂ level but rather use it as an input signal to determine the extent of secretion, and (3) in the normal, resting chromaffin cells the PI(4,5)P₂

level is suboptimal, so that an increase can upregulate secretion. All of these features make PI(4,5)P₂ a potential key physiological regulator of secretion.

Spatial distribution of PI(4,5)P₂ in the plasma membrane

We wanted to develop methods for assaying plasma membrane PI(4,5)P₂ levels and distribution. In many studies, it is hard to distinguish between the roles of PI(4,5)P₂ and that of related phosphatidylinositides [PI(4)P, PI(3,4,5)P₃] on secretion. Likewise, the question of the spatial distribution of PI(4,5)P₂ in the membrane remains unresolved. The presence of PI(4,5)P₂ domains has been proposed by several groups (for review, see Caroni, 2001; Martin, 2001). However, the results of overexpression studies using PH domains are diverse. In the first studies, a nearly uniform distribution over the plasma membrane was found (Stauffer et al., 1998; Várnai and Balla, 1998). Some later studies that revealed local accumulations in plasma membrane “ruffles” (Honda et al., 1999; Botelho et al., 2000; Tall et al., 2000) were recently reinterpreted after the demonstration of colocalization with lipophilic membrane dyes, implying that the apparent PI(4,5)P₂ enrichments might have been local membrane infoldings (van Rheenen and Jalink, 2002). Várnai et al. (2002) found that another PH domain from the PLC-like protein p130 did not become localized to the plasma membrane, although it showed selective binding to PI(4,5)P₂ *in vitro*. It was suggested that a proteinaceous factor contributes to the plasma membrane localization of GFP-PH-PLC δ_1 . However, the interpretation of expression studies is difficult, because the localization of a soluble protein in a living cell is determined by the relative affinities, amounts, and accessibilities of all of the different ligands [for PH-PLC δ_1 and PH-p130, also the soluble inositol(1,4,5)triphosphate], the concentration of the overexpressed protein, and the way that the cell responds to the sequestering of the ligands.

We therefore favored to detect plasmalemmal PI(4,5)P₂ by an *in vitro* assay in which exogenous probe was added to isolated membrane sheets, in which only a single high-affinity ligand is present [PI(4,5)P₂]. Our experiments show that PI(4,5)P₂ binding of PH-PLC δ_1 is necessary for membrane binding, that PH-PLC δ_1 competes with an anti-PI(4,5)P₂ antibody for plasma membrane binding, and that the assay could detect chronic as well as acute increases in PI(4,5)P₂. The following features characterize the spatial organization of PI(4,5)P₂ in the membrane sheets of chromaffin and PC12 cells: (1) PI(4,5)P₂ was apparently enriched in abundant submicrometer-sized clusters; and (2) cholesterol was necessary for the organization of PI(4,5)P₂ clusters. Our GFP-PH-PLC δ_1 clusters in the plasma membrane did not correspond to local increases in membrane area, as shown by TMA-DPH or DiI_{C16} staining (Fig. 1A–D). Being approximately punctate, these domains appear similar to those that were de-

scribed by Laux et al. (2000) to colocalize with PI(4,5)P₂-binding GAP43, MARCKS, and CAP23 (the GMC proteins) in PC12 cells. It should be pointed out that the punctate staining of GFP-PH-PLC δ_1 can be interpreted in several ways: the most obvious is that it reflects a punctate PI(4,5)P₂ distribution in the plasma membrane. However, it is also possible that it reflects varying accessibility of the probe to plasmalemmal PI(4,5)P₂, caused by steric hindrance attributable to endogenous PI(4,5)P₂-associated proteins. In this case, the punctate labeling may reflect an inhomogeneous protein distribution in the membrane, rather than an inhomogeneous PI(4,5)P₂ distribution.

PI(4,5)P₂ and exocytosis

We found that PI(4,5)P₂ positively modulates secretion in neuroendocrine cells, in agreement with previous studies (Eberhard et al., 1990; Holz et al., 2000; Aikawa and Martin, 2003; Olsen et al., 2003). A number of different manipulations of the PI(4,5)P₂ level all showed that PI(4,5)P₂ stimulates exocytosis by increasing the number of vesicles residing in the releasable vesicle pools and increasing the sustained rate of release, which is assumed to be indicative of an increased refilling rate of the releasable pools. This is in agreement with the finding that PI(4,5)P₂ infusion into pancreatic β -cells increases the RRP size (Olsen et al., 2003).

Overexpression of PI4P5KI γ , the kinase that generates PI(4,5)P₂, caused an increase in the plasmalemmal PI(4,5)P₂ level, whereas overexpression of a membrane-tagged PI(4,5)P₂ phosphatase, IPP1-CAAX, eliminated plasmalemmal PI(4,5)P₂ and secretion. Thus, the balance between generation and degradation rates of plasmalemmal PI(4,5)P₂ directly regulates the extent of LDCV secretion from chromaffin cells. The implication is that PI(4,5)P₂ is more than an obligatory-permissive factor that needs to be present at sufficient levels in order for exocytosis to occur. Rather, PI(4,5)P₂ levels are limiting secretion in the control situation, and therefore changes in this level regulate secretion directly and dynamically.

A time-dependent correlation between the plasma membrane PI(4,5)P₂ level and primed vesicle pool size was found in our experiments with LY294002. Two previous studies addressed the effect of LY294002 on neuroendocrine secretion. When applied for 30 min, LY294002 did not significantly affect secretion in permeable PC12 cells (Martin et al., 1997). However, Chasserot-Golaz et al. (1998) described a dose-dependent inhibition of catecholamine secretion in chromaffin cells after a 30 min incubation with LY294002 and implied that PI3K is involved in secretion. In agreement with the latter study, we found that preincubation (30–70 min) with LY294002 inhibited secretion. However, in addition we discovered that short-term application of LY294002 (up to 6–7 min) caused a more than twofold increase in the number of fused vesicles. Taking advantage of our PI(4,5)P₂ assay, we found that the short-term application of LY294002 induced a transient increase in the level of PI(4,5)P₂ in the plasma membrane, whereas a longer preincubation decreased it significantly. Together with the overexpression studies, this correlation suggests that the effect of LY294002 on secretion is mediated through a change in the plasmalemmal PI(4,5)P₂ level. However, the pathway through which this biphasic change in the PI(4,5)P₂ level comes about was not identified by our experiments. LY294002 is an inhibitor of PI3K that uses PI(4,5)P₂ as a substrate to generate PI(3,4,5)P₃ (Vlahos et al., 1994). PI(3,4,5)P₃ may affect the PI(4,5)P₂ metabolism by activating PLC γ (Bae et al., 1998). However, LY294002 also inhibits PI4K, which generates PI(4)P, the precursor for PI(4,5)P₂ (Downing et al., 1996; Sorensen et al., 1998). Therefore, LY294002 inhibits at least two pathways of phosphatidylinositol metabolism, which could lead

to complex time-dependent effects on the PI(4,5)P₂ level. In addition, LY294002 affects other kinases (e.g., casein kinase 2) (Davies et al., 2000), which may have indirect effects on PI(4,5)P₂ metabolism. Whatever the pathway for LY294002 action, our data show that the effect of this inhibitor on secretion may be accounted for by changes in PI(4,5)P₂ levels, without the need to invoke a direct role for 3-phosphorylated phosphatidylinositides in exocytosis. In addition, this experiment shows that the size of the primed vesicle pools in chromaffin cells can respond to transient changes in the PI(4,5)P₂ level on the minute time scale. This is consistent with a function of PI(4,5)P₂ as an acute regulator of secretion.

Several proteins involved in exocytosis specifically bind PI(4,5)P₂: the family of synaptotagmin proteins (Schiavo et al., 1996), Ca²⁺-dependent activator protein for secretion (CAPS) (Loyet et al., 1998), Mint (Okamoto and Sudhof, 1997), and rabphilin 3 (Chung et al., 1998). Which of these interactions are physiologically relevant remains to be explored. The recent finding that synaptotagmin 1 binds to PI(4,5)P₂-containing membranes via its C2B domain, and thereby increases its speed of insertion into that membrane, led to the suggestion that changes in the PI(4,5)P₂ level could regulate release rates (Bai et al., 2004). We found that under conditions of increased or decreased PI(4,5)P₂ levels, the releasable vesicle pool sizes were changed but the release rate constants were not. It was previously shown that fusion of vesicles from the RRP is dependent of synaptotagmin 1 (Voets et al., 2001) and that the release rate constant can be modified by synaptotagmin 1 mutation (Sorensen et al., 2003). Therefore, the simplest explanation for our findings is that PI(4,5)P₂ binding of synaptotagmin 1 is not rate limiting for fusion triggering under our conditions. An interesting possibility would be that PI(4,5)P₂ binding of synaptotagmin 1 is involved in upstream reactions. Additional studies are required to answer this question.

In conclusion, we report that PI(4,5)P₂ is in a position to be a key physiological regulator of the size and the refilling rate of the primed vesicle pools but not the fusion rate constants. As a secretion regulator, PI(4,5)P₂ has several advantages over proteins with the same task: plasmalemmal PI(4,5)P₂ molecules could recruit and activate a large number of different proteins to create a local environment in which exocytosis takes place. At the same time, the rapid enzymatic production and degradation of PI(4,5)P₂ allows the cell to remain flexible: by changing the PI(4,5)P₂ level, physiological function can be modified within seconds or minutes without the need for protein synthesis or degradation.

References

- Aikawa Y, Martin TFJ (2003) ARF6 regulates a plasma membrane pool of phosphatidylinositol(4,5)bisphosphate required for regulated exocytosis. *J Cell Biol* 162:647–659.
- Arioka M, Nakashima S, Shibasaki Y, Kitamoto K (2004) Dibasic amino acid residues at the carboxy-terminal end of kinase homology domain participate in the plasma membrane localization and function of phosphatidylinositol 5-kinase γ . *Biochem Biophys Res Commun* 319:456–463.
- Ashery U, Betz A, Xu T, Brose N, Rettig J (1999) An efficient method for infection of adrenal chromaffin cells using the Semliki Forest virus gene expression system. *Eur J Cell Biol* 78:525–532.
- Avery J, Ellis DJ, Lang T, Holroyd P, Riedel D, Henderson RM, Edwardson JM, Jahn R (2000) A cell-free system for regulated exocytosis in PC12 cells. *J Cell Biol* 148:317–324.
- Bae YS, Cantley LG, Chen CS, Kim SR, Kwon KS, Rhee SG (1998) Activation of phospholipase C γ by phosphatidylinositol 3,4,5-trisphosphate. *J Biol Chem* 273:4465–4469.
- Bai J, Tucker WC, Chapman ER (2004) PIP₂ increases the speed of response of synaptotagmin and steers its membrane-penetration activity toward the plasma membrane. *Nat Struct Mol Biol* 11:36–44.

- Botelho RJ, Teruel M, Dierckman R, Anderson R, Wells A, York JD, Meyer T, Grinstein S (2000) Localized biphasic changes in phosphatidylinositol-4,5-bisphosphate at sites of phagocytosis. *J Cell Biol* 151:1353–1368.
- Caroni P (2001) New EMBO members' review: actin cytoskeleton regulation through modulation of PI(4,5)P(2) rafts. *EMBO J* 20:4332–4336.
- Chasserot-Golaz S, Hubert P, Thierse D, Dirrig S, Vlahos CJ, Aunis D, Bader M-F (1998) Possible involvement of phosphatidylinositol 3-kinase in regulated exocytosis: studies in chromaffin cells with inhibitor LY294002. *J Neurochem* 70:2347–2355.
- Chung SH, Song WJ, Kim K, Bednarski JJ, Chen J, Prestwich GD, Holz RW (1998) The C2 domains of Rabphilin3A specifically bind phosphatidylinositol 4,5-bisphosphate containing vesicles in a Ca²⁺-dependent manner. In vitro characteristics and possible significance. *J Biol Chem* 273:10240–10248.
- Cousin MA, Malladi CS, Tan TC, Raymond CR, Smillie KJ, Robinson PJ (2003) Synapsin I-associated phosphatidylinositol 3-kinase mediates synaptic vesicle delivery to the readily releasable pool. *J Biol Chem* 278:29065–29071.
- Cremona O, De Camilli P (2001) Phosphoinositides in membrane traffic at the synapse. Phosphoinositides in membrane traffic at the synapse. *J Cell Sci* 1041–1052.
- Davies SP, Reddy H, Caivano M, Cohen P (2000) Specificity and mechanism of action of some commonly used protein kinase inhibitors. *Biochem J* 351:95–105.
- Downing GJ, Kim S, Nakanishi S, Catt KJ, Balla T (1996) Characterization of a soluble adrenal phosphatidylinositol 4-kinase reveals wortmannin sensitivity of type III phosphatidylinositol kinases. *Biochemistry* 35:3587–3594.
- Eberhard DA, Cooper CL, Low MG, Holz RW (1990) Evidence that the inositol phospholipids are necessary for exocytosis. Loss of inositol phospholipids and inhibition of secretion in permeabilized cells caused by a bacterial phospholipase C and removal of ATP. *Biochem J* 268:15–25.
- Hay JC, Martin TF (1993) Phosphatidylinositol transfer protein required for ATP-dependent priming of calcium activated secretion. *Nature* 366:572–575.
- Hay JC, Fiset PL, Jenkins GH, Fukami K, Takenawa T, Anderson RA, Martin TF (1995) ATP-dependent inositide phosphorylation required for calcium activated secretion. *Nature* 34:173–177.
- Holz RW, Bittner MA, Peppers SC, Senter RA, Eberhard DA (1989) MgATP-independent and MgATP-dependent exocytosis. Evidence that MgATP primes adrenal chromaffin cells to undergo exocytosis. *J Biol Chem* 264:5412–5419.
- Holz RW, Hlubek MD, Sorensen SD, Fisher SK, Balla T, Ozaki S, Prestwich GD, Stuenkel EL, Bittner MA (2000) A pleckstrin homology domain specific for phosphatidylinositol 4,5-bisphosphate (PtdIns-4,5-P2) and fused to green fluorescent protein identifies plasma membrane PtdIns-4,5-P2 as being important in exocytosis. *J Biol Chem* 275:17878–17885.
- Honda A, Nogami M, Yokozeki T, Yamazaki M, Nakamura H, Watanabe H, Kawamoto K, Nakayama K, Morris AJ, Frohman MA, Kanaho Y (1999) Phosphatidylinositol 4-phosphate 5-kinase α is a downstream effector of the small G protein ARF6 in membrane ruffle formation. *Cell* 99:521–532.
- Hong SJ, Chang CC (1999) Inhibition of quantal release from motor nerve by wortmannin. *Br J Pharmacol* 128:142–148.
- Krauss M, Kinua M, Wenk MR, De Camilli P, Takei K, Haucke V (2003) ARF6 stimulates clathrin/AP-2 recruitment to synaptic membranes by activating phosphatidylinositol phosphate kinase type I γ . *J Cell Biol* 162:113–124.
- Lang T, Wacker I, Steyer J, Kaether C, Wunderlich I, Soldati T, Gerdes HH, Almers W (1997) Ca²⁺-triggered peptide secretion in single cells imaged with green fluorescent protein and evanescent-wave microscopy. *Neuron* 18:857–863.
- Lang T, Bruns D, Wenzel D, Riedel D, Holroyd P, Thiele C, Jahn R (2001) SNAREs are concentrated in cholesterol-dependent clusters that define docking and fusion sites for exocytosis. *EMBO J* 20:2202–2213.
- Lang T, Margittai M, Holzler H, Jahn R (2002) SNAREs in native plasma membranes are active and readily form core complexes with endogenous and exogenous SNAREs. *J Cell Biol* 158:751–760.
- Laux T, Fukami K, Thelen M, Golub T, Frey D, Caroni P (2000) GAP43, MARCKS, and CAP23 modulate PI(4,5)P(2) at plasmalemmal rafts, and regulate cell cortex actin dynamics through a common mechanism. *J Cell Biol* 149:1455–1472.
- Loyet KM, Kowalchuk JA, Chaudhary A, Chen J, Prestwich GD, Martin TF (1998) Specific binding of phosphatidylinositol 4,5-bisphosphate to calcium-dependent activator protein for secretion (CAPS), a potential phosphoinositide effector protein for regulated exocytosis. *J Biol Chem* 273:8337–8343.
- Martin TF (2001) PI(4,5)P(2) regulation of surface membrane traffic. *Curr Opin Cell Biol* 13:493–499.
- Martin TF, Loyet KM, Barry VA, Kowalchuk JA (1997) The role of PtdIns(4,5)P₂ in exocytotic membrane fusion. *Biochem Soc Trans* 25:1137–1141.
- Nagy G, Matti U, Nehring RB, Binz T, Rettig J, Neher E, Sorensen JB (2002) Protein kinase C-dependent phosphorylation of synaptosome-associated protein of 25 kDa at Ser187 potentiates vesicle recruitment. *J Neurosci* 22:9278–9286.
- Nagy G, Reim K, Matti U, Brose N, Binz T, Rettig J, Neher E, Sorensen JB (2004) Regulation of releasable vesicle pool sizes by protein kinase A-dependent phosphorylation of SNAP-25. *Neuron* 41:417–429.
- Okamoto M, Sudhof TC (1997) Mints, Munc18-interacting proteins in synaptic vesicle exocytosis. *J Biol Chem* 272:31459–31464.
- Olsen HL, Hoy M, Zhang W, Bertorello AM, Bokvist K, Capito K, Efanov AM, Meister B, Thams P, Yang SN, Rorsman P, Berggren PO, Gromada J (2003) Phosphatidylinositol 4-kinase serves as a metabolic sensor and regulates priming of secretory granules in pancreatic beta cells. *Proc Natl Acad Sci USA* 100:5187–5192.
- Rettig J, Neher E (2002) Emerging roles of presynaptic proteins in calcium triggered exocytosis. *Science* 298:781–785.
- Rizzoli SO, Betz WJ (2002) Effects of 2-(4-morpholinyl)-8-phenyl-4H-1-benzopyran-4-one on synaptic vesicle cycling at the frog neuromuscular junction. *J Neurosci* 22:10680–10689.
- Rohde G, Wenzel D, Haucke V (2002) A phosphatidylinositol (4,5)-bisphosphate binding site within μ 2-adaptin regulates clathrin-mediated endocytosis. *J Cell Biol* 158:209–214.
- Schiavo G, Gu QM, Prestwich GD, Sollner TH, Rothman JE (1996) Calcium-dependent switching of the specificity of phosphoinositide binding to synaptotagmin. *Proc Natl Acad Sci USA* 93:13327–13332.
- Sørensen JB, Fernandez-Chacon R, Sudhof TC, Neher E (2003) Examining synaptotagmin 1 function in dense core vesicle exocytosis under direct control of Ca²⁺. *J Gen Physiol* 122:265–276.
- Sorensen SD, Linseman DA, McEwen EL, Heacock AM, Fisher SK (1998) A role for a wortmannin-sensitive phosphatidylinositol-4-kinase in the endocytosis of muscarinic cholinergic receptors. *Mol Pharmacol* 53:827–836.
- Stauffer TP, Ahn S, Meyer T (1998) Receptor-induced transient reduction in plasma membrane PtdIns(4,5)P₂ concentration monitored in living cells. *Curr Biol* 8:343–346.
- Tall EG, Spector I, Pentyala SN, Bitter I, Rebecchi MJ (2000) Dynamics of phosphatidylinositol 4,5-bisphosphate in actin-rich structures. *Curr Biol* 10:743–746.
- van Rheenen J, Jalink K (2002) Agonist-induced PIP₂ hydrolysis inhibits cortical actin dynamics: regulation at a global but not at a micrometer scale. *Mol Biol Cell* 13:3257–3267.
- Várnai P, Balla T (1998) Visualization of phosphoinositides that bind pleckstrin homology domains: calcium- and agonist-induced dynamic changes and relationship to myo-[3H]inositol-labeled phosphoinositide pools. *J Cell Biol* 143:501–510.
- Várnai P, Lin X, Lee SB, Tuymetova G, Bondeva T, Spät A, Rhee SG, Hajnóczky G, Balla T (2002) Inositol lipid binding and membrane localization of isolated pleckstrin homology (PH) domains. Studies on the PH domains of phospholipase C δ_1 and p130. *J Biol Chem* 277:27412–27422.
- Vlahos CJ, Matter WF, Hui KY, Brown RF (1994) A specific inhibitor of phosphatidylinositol 3-kinase, 2-(4-morpholinyl)-8-phenyl-4H-1-benzopyran-4-one (LY294002). *J Biol Chem* 269:5241–5248.
- Voets T (2000) Dissection of three calcium-dependent steps leading to secretion in chromaffin cells from mouse adrenal slices. *Neuron* 28:537–545.
- Voets T, Moser T, Lund PE, Chow RH, Geppert M, Sudhof TC, Neher E (2001) Intracellular calcium dependence of large dense-core vesicle exocytosis in the absence of synaptotagmin I. *Proc Natl Acad Sci USA* 98:11680–11685.
- Wenk MR, Pellegrini L, Klenchin VA, Di Paolo G, Chang S, Daniell L, Arioka M, Martin T, De Camilli P (2001) PIP kinase Iggamma is the major PI(4,5)P(2) synthesizing enzyme at the synapse. *Neuron* 32:79–88.
- Xu T, Binz T, Niemann H, Neher E (1998) Multiple kinetic components of exocytosis distinguished by neurotoxin sensitivity. *Nat Neurosci* 1:192–200.

2.1.1. Additional data

A proportion of PI(4,5)P₂-clusters colocalise with syntaxin 1 in chromaffin cells

The SNARE protein syntaxin 1 clusters in a cholesterol-dependent manner in neuroendocrine cells and these clusters define the sites of regulated exocytosis (Lang *et al.*, 2001; Ohara-Imaizumi *et al.*, 2004). Hence, I determined the extent to which syntaxin 1 and PI(4,5)P₂-clusters overlap. When membrane sheets of BCCs were double labelled with anti-syntaxin 1 antibody and GFP-PH-PLC δ 1 (Fig. 10A-C), abundant labelling was observed in both detection channels, making it difficult to assess the degree of syntaxin 1 and GFP-PH-PLC δ 1 colocalisation by visual inspection. I therefore calculated the cross-correlation function between the syntaxin 1 and GFP-PH-PLC δ 1 images (shown in Fig. 10E as a function of displacement distance) and used the value at zero displacement as a measure of the correlation between the signals (for method description see II). This value, 0.26 ± 0.02 (37 sheets from 3 experiments), indicates a moderate, but significant degree of colocalisation. Provided that both signals consisted of the same number of randomly distributed identical two dimensional (2D) Gaussian spots, one can conclude that 26% of the spots (i.e. the labelling) are colocalised, whereas the rest are not. This value of 26% represents an underestimate because first, there is uncorrelated noise between channels and second, the number of spots (Gaussians) in the two channels differs from each other.

To estimate the size of the PI(4,5)P₂-clusters in BCCs, I calculated the 2D auto-correlation function of PI(4,5)P₂ images, such as the one in Figure 10A. The half-width of the two-sided auto-correlation function was found to be 564 ± 24 nm (38 membrane sheets from 3 experiments, Fig. 10D). Assuming that the PI(4,5)P₂-specific signal consists of partly overlapping identical Gaussian distributions, the half-width of the diameter of these spots would then be calculated to be approximately 314 nm after correcting for the point-spread-function. For comparison, I used the previously published method of fitting 1D Gaussians to a line-scan profile through the centre of selected fluorescent spots (Lang *et al.*, 2001). That method gave the half-width size of 319 nm after correction for the point-spread-function. It should be noted that the advantage in using the auto-correlation function for determining the size of clusters lies in the fact that the whole membrane sheet is analysed, whereas selecting single spots for analysis can result in error if the signal (as in this case) is very abundant and the spots partly overlap.

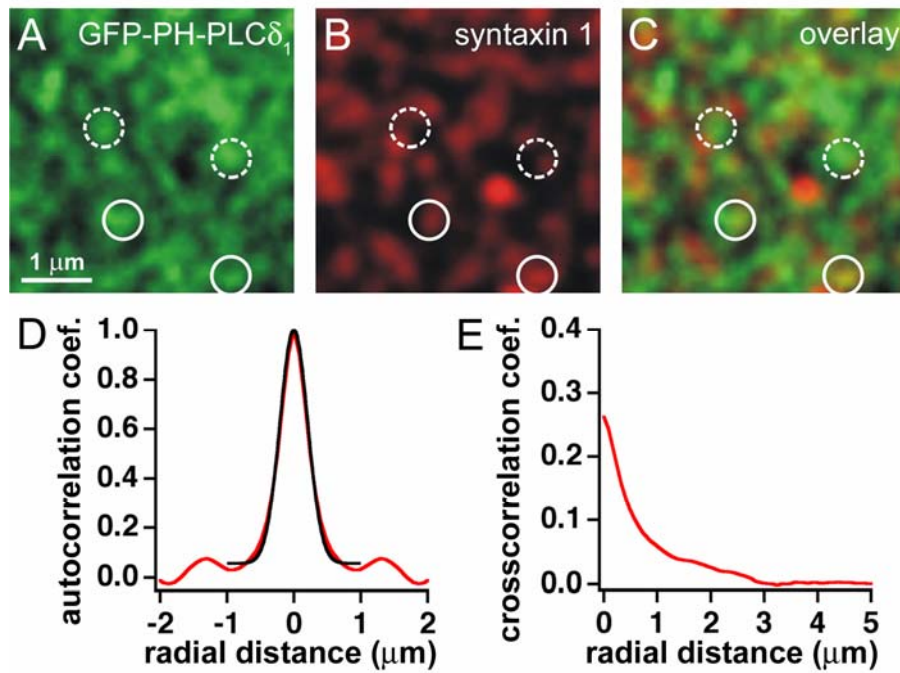


Figure 10. PI(4,5)P₂-clusters partially colocalise with syntaxin 1-clusters in chromaffin cells. (A-C) Syntaxin 1 and PI(4,5)P₂ are clustered in the plasma membrane of BCC. Freshly prepared membrane sheets from BCC were incubated with 3 μ M GFP-PH-PLC δ_1 (panel A: visualised using the green channel) for 10 min at 37°C, washed in K-Glu buffer for 100 s, fixed and immunostained for syntaxin 1 (panel B: visualised using the red channel). (C) Overlay of A and B. Circles indicate identical pixel locations in different channels. Closed circles: PI(4,5)P₂-clusters with a corresponding syntaxin 1-signal; dashed circles: PI(4,5)P₂-clusters that lack a corresponding syntaxin 1-signal. (D) Example of the two-sided auto-correlation function of the GFP-PH-PLC δ_1 -signal (red curve). The shape of the peak is approximately Gaussian, as shown by the fit (black curve). (E) The mean cross-correlation function of the GFP-PH-PLC δ_1 - and syntaxin 1-signal (red curve).

Exocytic proteins which may mediate PI(4,5)P₂ regulation of chromaffin cell secretion

Several proteins involved in exocytosis specifically bind PI(4,5)P₂ *in vitro* (Wenk and De Camilli, 2004). To explore which of these interactions are physiologically relevant and may account for PI(4,5)P₂ control the vesicle pool size, I investigated whether the chronic increase in PI(4,5)P₂ level changes the plasmalemmal amount of several proteins involved in exocytosis. I tested CAPS1, CAPS2 and Munc18-1 as they represent cytosolic proteins transiently associated with the plasma membrane (Speidel *et al.*, 2003; Pevsner *et al.*, 1994), and synaptotagmin 1 and 7 which are vesicular proteins (Perin *et al.*, 1990; localisation of synaptotagmin 7 is doubtful: Sugita *et al.*, 2001; Fukuda *et al.*, 2004).

Plasma membrane sheets were generated from control and BCC overexpressing GFP-PI4P5K-I γ and immunostained for CAPS1, CAPS2, synaptotagmin 1, synaptotagmin 7 and Munc18-1. All inspected proteins revealed punctate staining on the BCC plasma membrane (Figure 11A-E). Interestingly, synaptotagmin 1 showed sparse staining characteristic for LDCVs, while synaptotagmin 7 displayed abundant plasmalemmal labelling, implying that synaptotagmin 7 is at least partly a plasma membrane protein as reported by Sugita *et al.* (2001; Figure 11C-D). Quantification of the membrane signal from uninfected and PI4P5K-I γ infected BCCs revealed that synaptotagmin 1, synaptotagmin 7 and Munc18-1, but not CAPS1 and CAPS2, are significantly enriched on the plasma membranes containing an increased PI(4,5)P₂ level (Figure 11G). Even though the effects are modest, these data imply that the regulatory role of PI(4,5)P₂ in exocytosis may be mediated through members of synaptotagmin family and/or Munc18-1 (see Discussion).

Since the cortical actin network regulates the availability of secretory vesicles (Sankaranarayanan *et al.*, 2003), I investigated whether the amount of cortical actin remaining on the plasma membrane sheets was altered by a chronic increase in plasmalemmal PI(4,5)P₂ level. Plasma membrane sheets generated from control and BCC overexpressing GFP-PI4P5K-I γ were incubated with fluorescently labelled phalloidin (Figure 11F). The increased amount of actin was detected on the plasma membranes containing an increased PI(4,5)P₂ level, suggesting that PI(4,5)P₂ levels control actin dynamics in primary neuroendocrine cells, in agreement with Bittner and Holz (2005).

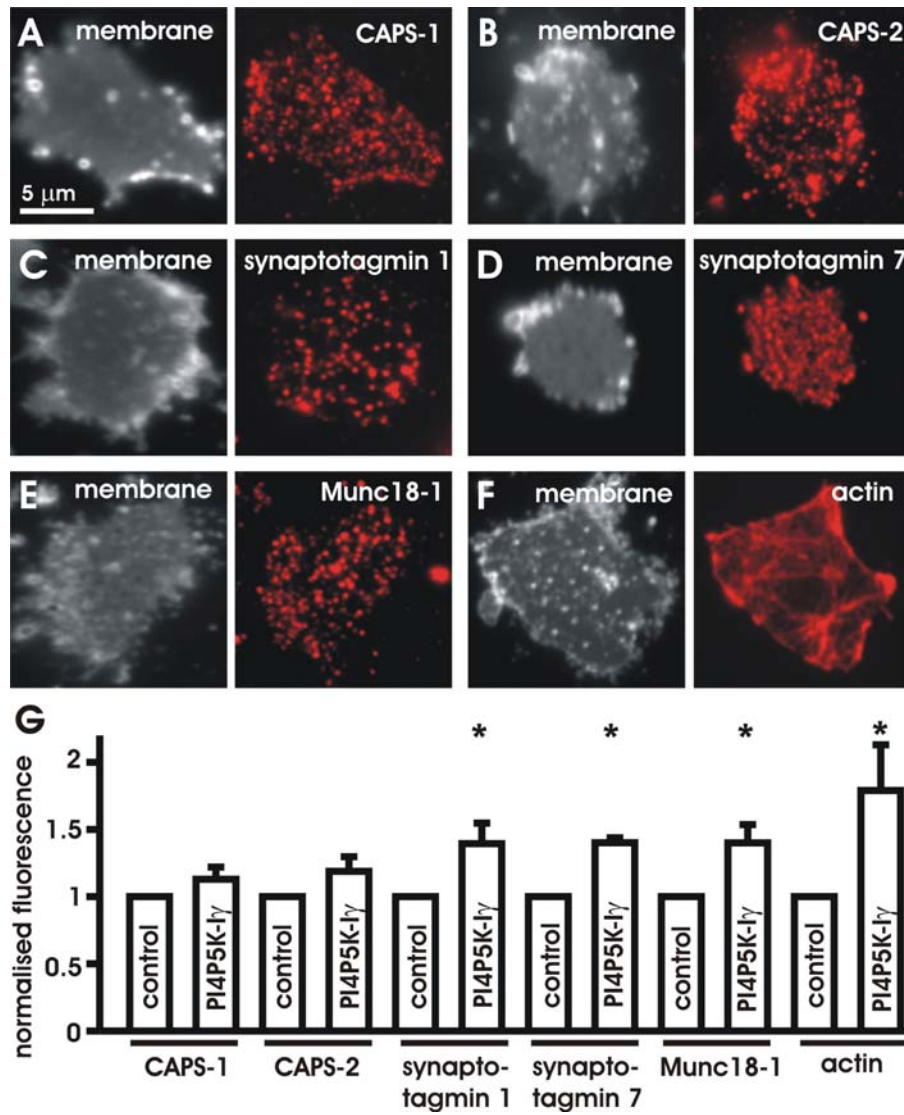


Figure 11. Synaptotagmin 1, synaptotagmin 7, Munc18-1 and actin are significantly enriched on the plasma membrane of BCCs expressing PI4P5K-Iy. Plasma membrane sheets were generated from BCC infected for 12h with Semliki Forest Virus encoding GFP-PI4P5K-Iy and fixed. Immunostaining of CAPS1, CAPS2, synaptotagmin 1, synaptotagmin 7 and Munc18-1 was achieved using the appropriate antibodies. Actin was labelled with phalloidin conjugated to rhodamine. Membranes were visualised in the presence of TMA-DPH dye using the blue channel and all probes were detected using the red channel. (A) CAPS1, (B) CAPS2, (C) synaptotagmin 1, (D) synaptotagmin 7, (E) Munc18-1, (F) actin, (G) Quantification of the membrane proteins and normalisation to the signal detected on the plasma membrane sheets generated from uninfected BCC.

The role of PI4P5K-I γ in Ca²⁺-dependent priming

PI4P5K-I γ is preferentially expressed in the nervous system and concentrated at synapses where it synthesizes the PI(4,5)P₂-pool relevant for membrane trafficking (Wenk *et al.*, 2001; Di Paolo *et al.*, 2004). This enzyme is regulated by Ca²⁺, phosphorylation and ARF6-dependent mechanisms (Aikawa and Martin, 2003). As PI4P5K-I γ overexpression increases the releasable vesicle pool size in chromaffin cells (I), it is possible that Ca²⁺-regulated PI(4,5)P₂ synthesis by PI4P5K-I γ underlines the Ca²⁺-dependent priming in these cells. To test this hypothesis, I constructed Semliki Forest Virus (SFV) encoding non-phosphorylatable S264A (this is activated kinase form as it associates constitutively with Arf6 in Ca²⁺-independent way; Aikawa and Martin, 2003) as well as S264E (presumably non-activated kinase form as no association with Arf6 is expected) mutants of PI4P5K-I γ and analysed BCC secretion upon infection.

I stimulated BCCs using flash photolysis of photolabile Ca²⁺-cage nitrophenyl-EGTA. This resulted in stepwise, uniform increases in [Ca²⁺]_i to 20–30 μ M (Figure 12A, top) and triggered Ca²⁺-dependent exocytosis of LDCVs, which was monitored by electrochemical detection of liberated catecholamines (Figure 12A, middle) and an increase in membrane capacitance (ΔC_m ; Figure 12A, bottom). The stimulation was performed from a low [Ca²⁺]_i (~200 nM) to minimise the Ca²⁺-dependent priming. Under such conditions, a twofold higher secretion was obtained from BCC expressing wild-type PI4P5K-I γ (Figure 12A). In agreement with study I, both the exocytic burst and the rate of the sustained release were significantly increased (Figure 12B-C). Interestingly, an even larger increase in secretion was detected upon PI4P5K-I γ S264A overexpression (Figure 12), suggesting that the primed pools can be even further enlarged exclusively through PI4P5K-I γ activity. However, the exocytic burst and the rate of the sustained release were also significantly increased upon overexpression of PI4P5K-I γ S264E, but overall secretion was lower than of wild-type PI4P5K-I γ or PI4P5K-I γ S264A overexpressing BCCs (Figure 12). Assuming that PI4P5K-I γ S264E indeed mimics non-activated kinase, these data would imply that LDCVs can be primed independently of Ca²⁺-regulated activity. Nevertheless, without additional information on the plasmalemmal PI(4,5)P₂ level in PI4P5K-I γ S264E expressing cells and the confirmation of complete kinase inactivity, it is hard to interpret the significance of this observation. Altogether, these experiments provides a hint, but alone cannot answer the question as whether Ca²⁺-dependent priming is, at least partially, a direct result of Ca²⁺-activated PI(4,5)P₂ synthesis by PI4P5K-I γ (see Discussion).

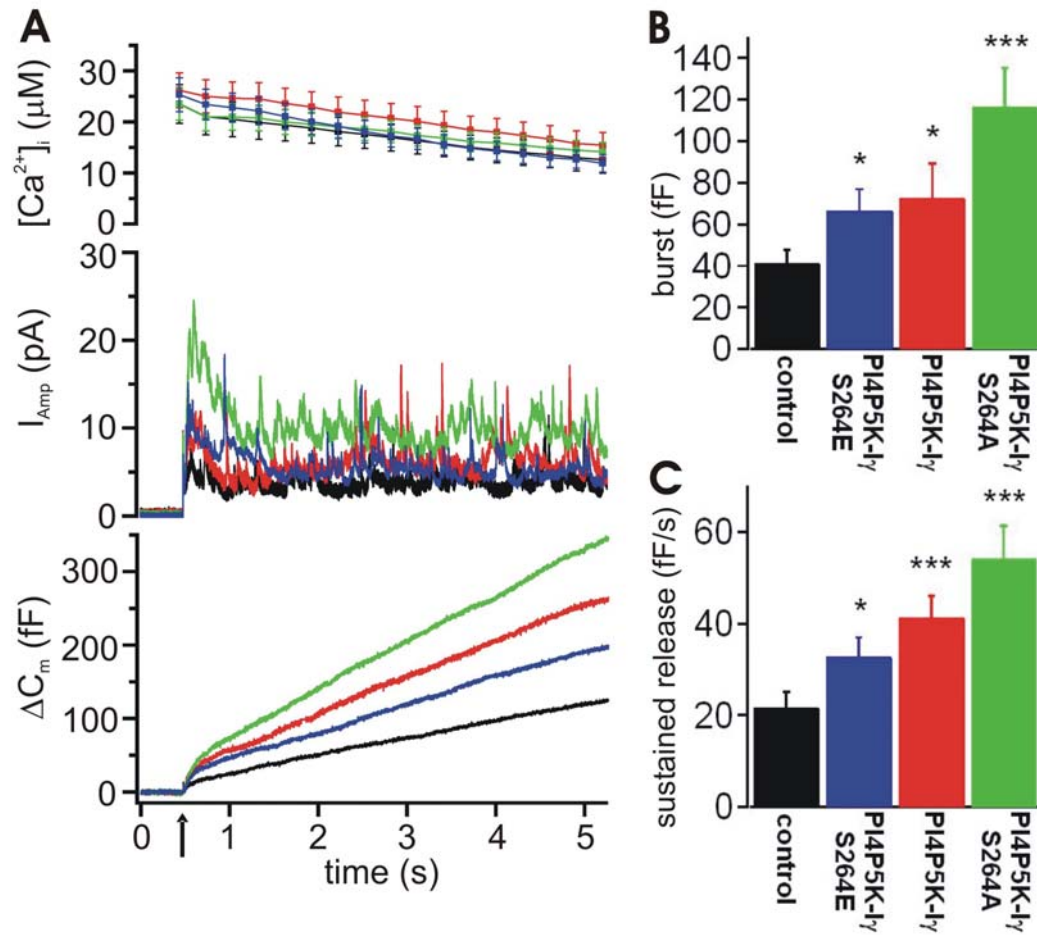


Figure 12. Exocytosis in BCCs overexpressing wild-type PI4P5K-I γ , PI4P5K-I γ S264E and PI4P5K-I γ S264A mutants. (A) Average [Ca²⁺]_i (top), amperometry (middle) and ΔC_m (bottom) in response to the first stimulus in control (N=31; black traces), PI4P5K-I γ S264E (N=31; blue traces), wild-type PI4P5K-I γ (N=29; red traces) and PI4P5K-I γ S264A (N=31; green traces) overexpressing cells. The first flash was delivered from a low [Ca²⁺]_i (~200 nM). Comparison of (B) the exocytic burst and (C) rate of sustained release in control, PI4P5K-I γ S264E, wild-type PI4P5K-I γ and PI4P5K-I γ S264A overexpressing cells. Error bars show the SEM, significant differences (Mann-Whitney U-test) are indicated (*p < 0.05; ***p < 0.001).

2.2. Paper II.

Alternative splicing of SNAP-25 regulates secretion through non-conservative substitutions in the SNARE domain

Gabor Nagy*, Ira Milosevic*, Dirk Fasshauer, Matthias Müller,
Bert L. de Groot, Thorsten Lang, Michael C. Wilson and Jakob B. Sørensen

*equal contribution

Molecular Biology of the Cell, Vol 16: 5675-5685, December 2005

Alternative Splicing of SNAP-25 Regulates Secretion through Nonconservative Substitutions in the SNARE Domain

Gábor Nagy,^{*†} Ira Milosevic,^{*†‡} Dirk Fasshauer,[‡] E. Matthias Müller,[§]
Bert L. de Groot,[§] Thorsten Lang,[‡] Michael C. Wilson,^{||} and Jakob B. Sørensen^{*}

Departments of ^{*}Membrane Biophysics, [‡]Neurobiology, and [§]Theoretical and Computational Biophysics, Max-Planck-Institute for Biophysical Chemistry, 37077 Göttingen, Germany; and ^{||}Department of Neurosciences, University of New Mexico Health Science Center, Albuquerque, NM 87131

Submitted July 5, 2005; Revised September 6, 2005; Accepted September 20, 2005
Monitoring Editor: Vivek Malhotra

The essential membrane fusion apparatus in mammalian cells, the soluble *N*-ethylmaleimide-sensitive factor attachment protein receptor (SNARE) complex, consists of four α -helices formed by three proteins: SNAP-25, syntaxin 1, and synaptobrevin 2. SNAP-25 contributes two helices to the complex and is targeted to the plasma membrane by palmitoylation of four cysteines in the linker region. It is alternatively spliced into two forms, SNAP-25a and SNAP-25b, differing by nine amino acids substitutions. When expressed in chromaffin cells from SNAP-25 *null* mice, the isoforms support different levels of secretion. Here, we investigated the basis of that different secretory phenotype. We found that two nonconservative substitutions in the N-terminal SNARE domain and not the different localization of one palmitoylated cysteine cause the functional difference between the isoforms. Biochemical and molecular dynamic simulation experiments revealed that the two substitutions do not regulate secretion by affecting the property of SNARE complex itself, but rather make the SNAP-25b-containing SNARE complex more available for the interaction with accessory factor(s).

INTRODUCTION

The identity of the proteinaceous machinery responsible for fusing intracellular membranes is rapidly being unraveled (Jahn *et al.*, 2003). Among the molecular players the soluble *N*-ethylmaleimide-sensitive factor attachment protein receptor (SNARE) proteins assume a special position, because they seem to form the essential fusion apparatus on which the other proteins work. Reconstituted SNARE proteins suffice to fuse vesicles *in vitro* (Weber *et al.*, 1998), and many of the other proteins regulating membrane fusion (e.g., Sec1p/Munc18-proteins, synaptotagmins, and complexins) may be recruited to the fusion apparatus through binding to SNAREs. A simple model would be that the SNARE complex executes the membrane fusion reaction itself, whereas accessory proteins would provide the necessary regulation of the process. However, the situation seems more complicated, because the neuronal SNARE proteins that act in fast neuroexocytosis to release neurotransmitter in the synapse are present in alternative isoforms (Elferink *et al.*, 1989; Archer *et al.*, 1990; Bennett *et al.*, 1992; Bark and Wilson, 1994). The question how these isoforms regulate secretion has not been resolved.

The core of the neuronal SNARE complex is a twisted coiled-coil structure composed of amphipathic helices contributed by the plasma membrane attached proteins syntaxin 1 and synaptosome-associated protein of 25 kDa (SNAP-25), and the vesicular synaptobrevin 2 (Sutton *et al.*, 1998; Figure 1). SNAP-25 provides two of the four α -helices to the complex and is attached to the plasma membrane via palmitoylation of four cysteine residues in the linker region between the two SNARE domains. In contrast, both syntaxin 1 and synaptobrevin 2 have transmembrane domains and contribute to the SNARE complex with one α -helix each. The orientation of the four α -helices is parallel, so that the membrane anchors of syntaxin and synaptobrevin are located on the same side of the complex. This structure led to the suggestion that the SNARE complex when formed in trans would act as a molecular zipper, such that formation toward the transmembrane anchors brings the membranes into contact and eventually leads to fusion (Hanson *et al.*, 1997). This model for SNARE action would predict that assembly of the SNARE complex might be rate limiting for secretion. Considering that fast chemical neurotransmission depends on the extremely tight temporal coupling (<0.5 ms) between the calcium trigger for exocytosis and neurotransmitter release, this raises the question whether residues in the SNARE domains are modified to enable physiological regulation of synaptic transmission or whether they are conserved so as not to compromise the basic fusogenic function of SNARE complexes.

SNAP-25 is expressed as two isoforms that differ by nine amino acid substitutions. The substitutions cluster within the N-terminal region of the first SNARE domain and in the adjacent sequence and include a relocation of one of the four cysteine residues that are required for membrane association

This article was published online ahead of print in *MBC in Press* (<http://www.molbiolcell.org/cgi/doi/10.1091/mbc.E05-07-0595>) on September 29, 2005.

[†] These authors contributed equally to this work.

Address correspondence to: Jakob B. Sørensen (jsorensen@gwdg.de).

Abbreviations used: SNARE, soluble *N*-ethylmaleimide-sensitive factor attachment protein receptor; SNAP-25, synaptosome-associated protein of 25 kDa.

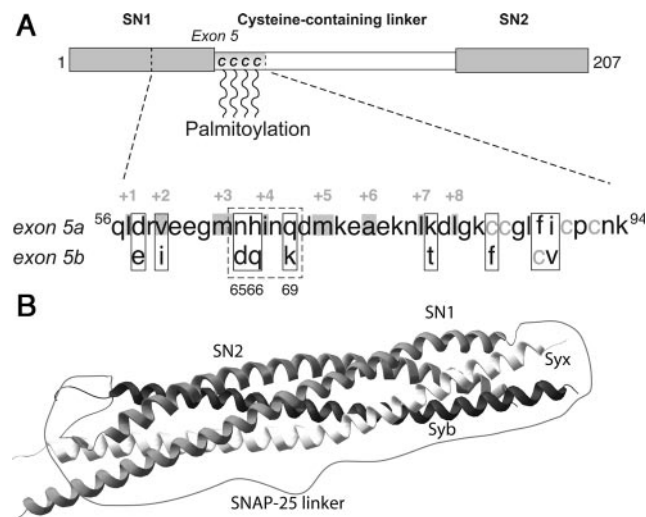


Figure 1. Alternative splicing of exon 5 introduces nine amino acid substitutions in SNAP-25. (A) The substitutions are located in the C-terminal end of the first SNARE motif and the first part of the linker and include a relocation of one of the palmitoylated cysteines. The gray boxes and numbers show residues that are buried in the inside of the complex. (B) Crystal structure of the ternary SNARE complex (Sutton *et al.*, 1998). The membrane anchors of syntaxin and synaptobrevin would attach at the right side. The linker between the two SNAP-25 SNARE domains (SN1 and SN2) was added using a drawing program. The structure was downloaded from PubMed (ISFC) and drawn using Swiss-Pdb viewer (Guex and Peitsch, 1997; <http://www.expasy.org/spdbv/>).

(Figure 1). The substitutions in the N-terminal SNARE domain of the two SNAP-25 isoforms include three charge changes (Figure 1). This is remarkable because in those syntaxin and synaptobrevin isoforms that have been shown to enter alternatively into the neuronal SNARE complex, substitutions in the SNARE domains are either nonexistent or conservative (syntaxin 1A and 1B, Bennett *et al.*, 1992; synaptobrevin 1 and 2, Elferink *et al.*, 1989; Archer *et al.*, 1990; and synaptobrevin 2 and cellubrevin, McMahon *et al.*, 1993; Borisovska *et al.*, 2005). The two SNAP-25 isoforms are the product of developmentally regulated alternative splicing of duplicated but divergent copies of exon 5 (Bark and Wilson, 1994; Bark *et al.*, 1995). In the embryonic brain, SNAP-25a is the prevalent isoform, whereas the expression of SNAP-25b increases robustly through postnatal brain development to become the predominant isoform in most, but not all, adult brain areas (Bark *et al.*, 1995; Boschert *et al.*, 1996). Impairment of this switch toward the SNAP-25b isoform in mice leads to premature mortality and a change in short-term plasticity in CA1 hippocampal synapses (Bark *et al.*, 2004). In contrast, the SNAP-25a isoform remains the predominant species in adult rat and mouse adrenal chromaffin cells and in PC12 cells (Bark *et al.*, 1995; Grant *et al.*, 1999). Importantly, when expressed in chromaffin cells from SNAP-25 null mice, the two splice variants support different levels of secretion, due to differential regulation of the size of the releasable vesicle pools (Sørensen *et al.*, 2003).

Here, we used a number of approaches to investigate the question how the two SNAP-25 isoforms differentially regulate secretion from chromaffin cells. The answer to this question has important implications for the understanding of how the SNARE complex can both regulate and trigger vesicle fusion.

MATERIALS AND METHODS

Chromaffin Cell Preparation, Mutagenesis, and Expression

SNAP-25 null embryos (E17–19) were recovered by Cesarean section and chromaffin cells prepared as described previously (Sørensen *et al.*, 2003). Mutations were introduced into SNAP-25a- or SNAP-25b-containing pSFV1 plasmids (pSFV1 SNAP-25a-IRES-EGFP and pSFV1 SNAP-25b-IRES-EGFP) by using PCR mutagenesis, and all constructs were sequenced. Semliki Forest Virus (SFV) expressing SNAP-25 and enhanced green fluorescent protein (EGFP) were prepared as described previously (Ashery *et al.*, 1999).

Plasma Membrane Sheets from Embryonic Mouse Chromaffin Cells: Generation and Immunofluorescence

Mouse chromaffin cells were plated on Ø 25-mm glass coverslips pretreated with 0.1 mg/ml poly-L-lysine (Sigma-Aldrich, St. Louis, MO) for 30 min. Plasma membrane sheets were generated 22–28 h after cell plating and 7 h after viral infection by placing the coverslip into 150 ml of ice-cold sonication buffer (120 mM potassium glutamate, 20 mM potassium acetate, 20 mM HEPES, 0.5 mM dithiothreitol [DTT], 2 mM ATP, 100 µM GTP, 4 mM MgCl₂, 4 mM EGTA, 6 mM Ca²⁺-EGTA, [Ca²⁺]_{free} = 300 nM, pH 7.2, and 310 mOsm/kg; bubbled with N₂ for 30 min) in a round glass beaker with a final volume of 300 ml. The coverslip with the attached cells was centered 14 mm under the sonication tip (Ø 2.5 mm), and the cells were disrupted applying a single ultrasound pulse (Sonifier 450, power setting at 1.6–1.8 and a duty cycle of 100 ms; Branson, Danbury, CT). Apart from chromaffin cells, the primary culture contained a low number of other cell types (e.g., endothelial cells). However, the membrane sheets generated from these cells differed in size and had lower level of staining for syntaxin 1, so that they were easily recognized and excluded from analysis.

For immunolabeling, freshly prepared membrane sheets were fixed for 2 h at room temperature in phosphate-buffered saline (PBS) containing 4% paraformaldehyde. They were washed twice in PBS, incubated for 10 min with 50 mM NH₄Cl in PBS to block free aldehyde groups, and then washed once more with PBS. Sheets were incubated for 2 h with primary antibodies raised against SNAP-25 (mouse monoclonal C171.2, recognizing both SNAP-25a and b; Xu *et al.*, 1999) and syntaxin 1 (rabbit polyclonal R31; Lang *et al.*, 2001) diluted 1:100 in PBS containing 1% bovine serum albumin (PBS-bovine serum albumin). They were washed four times for 10 min each with PBS and then incubated for 1 h with secondary antibodies diluted 1:200 in PBS-bovine serum albumin (Cy3-coupled goat-anti-mouse and Cy5-coupled goat-anti-rabbit; Jackson ImmunoResearch Laboratories, West Grove, PA). Membrane sheets were washed four times in PBS and were then imaged in PBS containing 1-(4-trimethylammoniumphenyl)-6-phenyl-1,3,5-hexatriene (TMA-DPH; Invitrogen, Carlsbad, CA). TMA-DPH visualizes phospholipid membranes and therefore allows for the identification of membrane sheets. In addition, 0.2-µm TetraSpeck beads (Invitrogen) were added and allowed to adsorb to the glass coverslip, acting as a spatial reference to correct for vertical shifts that occur during filter changes.

Coverslips mounted in an open chamber were analyzed using a Zeiss Axiovert 100 TV fluorescence microscope with a 100× 1.4 numerical aperture plan achromate objective. Appropriate filter sets were used for TMA-DPH (BP 350/50, BS 395, and BP 420LP), Cy3 (BP 525/30, BS 550LP, and BP 575/30) and Cy5 (BP 620/60, BS 660LP, and BP 700/75). Throughout all experiments the focal position of the objective was controlled using a low-voltage piezo translator driver and a linear variable transformer displacement controller (Physik Instrumente, Walldorf, Germany). Recordings were performed with a back-illuminated charge-coupled device camera (512 × 512-EEV chip, 24 × 24-µm pixel size; Princeton Instruments, Trenton, NJ) with a 2.5× Optovar magnifying lens. Images were acquired and analyzed using the program MetaMorph (Molecular Devices, Sunnyvale, CA).

For comparative quantitation of fluorescence intensity, membrane sheets were identified and selected in the TMA-DPH channel in an unbiased manner. Regions of interest (40 × 40 pixels corresponding to 3.7 × 3.7 µm) were placed onto the sheets and then transferred to the Cy3- and Cy5-channels with corrections being made to avoid obvious artifacts such as highly fluorescent contaminating particles that were occasionally seen. In the Cy3- and Cy5-channels, the average fluorescence intensity was determined and corrected for the local background measured in an area outside the membrane sheets.

From each animal, at least 10 membrane sheets were analyzed, and the mean value normalized to the mean of +/+ animals from the same litter. The animal means were used to calculate population mean and SEM (number of animals = 7–12 for each condition). For image representation, a linear look-up-table was applied using the autoscale-function. In some cases, the maximal value was decreased to make the finer structures (clusters) visible.

Correlative Features of Fluorescent Spots

To investigate correlative properties of fluorescent spots we calculated the normalized correlation coefficient between pairs of same-sized images (or regions of interests) detected in different channels. If $f'(x, y)$ and $t'(x, y)$ are the

two images after subtraction of the respective means the normalized correlation coefficient is given by (Manders *et al.*, 1992)

$$\gamma = \left[\sum_{x,y} f(x,y)t'(x,y) \right] / \sqrt{\left(\sum_{x,y} f(x,y)^2 \right) \left(\sum_{x,y} t'(x,y)^2 \right)}$$

The calculations were carried out in a custom-written macro for Igor Prover 4.01 (WaveMetrics, Lake Oswego, Oregon). We used the fluorescence profile of TetraSpeck beads (Invitrogen) to align the images with another. To investigate the maximal degree of correlation that could be expected in our system between the two channels used for SNAP-25 and syntaxin 1 detection, given noise, image distortion, and so on, we calculated the correlation coefficient between images of artificial liposomes containing phosphatidylethanolamine-Oregon Green and Alexa594-synaptobrevin 2. This gave a correlation coefficient of 0.78 ± 0.02 ($n = 4$).

Electrophysiology and Electrochemistry

The cells were used 2–4 d after plating; 6–10 h after virus infection, whole-cell patch-clamp capacitance, amperometry, flash photolysis of caged calcium, and intracellular Ca^{2+} measurements were performed as described previously (Nagy *et al.*, 2002). During the recordings, the mouse chromaffin cells were maintained in extracellular solution (145 mM NaCl, 2.8 mM KCl, 2 mM CaCl_2 , 1 mM MgCl_2 , 10 mM HEPES, and 2 mg/ml D-glucose, pH 7.20, 305 mOsm/kg). Capacitance and amperometric measurements were carried out in parallel to ensure that the fusion of catecholamine-containing vesicles was being monitored. Capacitance traces were fitted with a sum of exponential functions to separate pool sizes (noted as amplitudes of the exponentials) from the kinetics of fusion triggering (noted as time constants of the exponentials), as described previously (Nagy *et al.*, 2002, 2004). Data are given as mean \pm SEM, and the nonparametric Mann–Whitney *U*-test or the Kruskal–Wallis multiple comparison test were used to test statistical difference, which is indicated by * $p < 0.05$, ** $p < 0.01$, and *** $p < 0.001$.

Protein Purification

The basic SNARE expression constructs in a pET28a vector (residues 1–206), the syntaxin 1A SNARE motif (residues 180–262), and synaptobrevin 2 (residues 1–96) have been described previously (Fasshauer and Margittai, 2004). For expression of SNAP-25b, the full-length gene was cloned into the pET28a vector. The recombinant SNARE proteins were isolated from *Escherichia coli* and purified by Ni^{2+} -nitrilotriacetic acid affinity chromatography followed by ion exchange chromatography on an Äkta system (GE Healthcare, Little Chalfont, Buckinghamshire, United Kingdom) essentially as described previously (Fasshauer and Margittai, 2004). All ternary SNARE complexes were assembled overnight and purified using a Mono Q-column (GE Healthcare). Protein concentration was determined by absorption at 280 nm.

Circular Dichroism (CD) Spectroscopy Measurements

CD measurements were performed using a model J-720 instrument (Jasco, Tokyo, Japan). All experiments were carried out in 20 mM sodium phosphate, 2 M guanidine-HCl, pH 7.4, in the presence of 100 mM NaCl and 1 mM DTT. For thermal denaturation experiments, $\sim 10 \mu\text{M}$ purified ternary SNARE complexes were heated in Hellma quartz cuvettes with a pathlength of 0.1 cm. The ellipticity at 222 nm was recorded between 25 and 95°C at a temperature increment of 30°C/h.

Molecular Dynamics Simulations

Molecular dynamics simulations of the SNAP-25a-containing SNARE complex were started from the x-ray structure of the neuronal SNARE complex (chains A–D from PDB code: 1SFC; Sutton *et al.*, 1998). The simulation system contained 3002 protein atoms, 27,785 SPC water molecules (Berendsen *et al.*, 1981), and 15 sodium ions, resulting in a system size of 86,357 atoms. The “mutated structure” was generated using the molecular modeling suite WHATIF (Vriend, 1990). The MUTATE routine was used to replace H66 with Q and Q69 with K in the x-ray structure (1SFC), before the polar hydrogens were attached with the ADDHYD routine. Due to these mutations, the simulation system of the mutated structure contains 3003 protein atoms and 27,782 SPC water molecules. Fourteen sodium ions were added to keep the simulation system neutral.

Molecular dynamics simulations were carried out using the GROMACS simulation package (Lindahl *et al.*, 2001). We used the GOMACS force field, which is the GROMOS 87 force field (van Gunsteren and Berendsen, 1987) with slight modifications (Van Buuren *et al.*, 1993) and explicit hydrogens on the aromatic side chains. To allow an integration time step of 2 ns, covalent bond lengths were constrained using Lincs and Settle (Miyamoto and Kollman, 1992; Hess *et al.*, 1997). Electrostatic interactions were calculated explicitly at a distance smaller than 1.0 nm. Long-range electrostatic interactions were calculated by particle-mesh Ewald summation (Darden *et al.*, 1993). The protein and the solvent were coupled separately to an external temperature bath of 300 K (Berendsen *et al.*, 1984) with a coupling constant of $\tau = 0.1$ ps.

The pressure was kept constant at 1 bar by weak coupling ($\tau = 1.0$ ps) to a pressure bath (Berendsen *et al.*, 1984).

RESULTS

Plasma Membrane Localization of SNAP-25 Isoforms

SNAP-25 is targeted to the plasma membrane by a stretch of 36 amino acids (85–120) localized in the linker region between the two SNARE domains (Gonzalo *et al.*, 1999). All four linker-cysteines are necessary for proper membrane localization because single-cysteine substitutions suffice to greatly diminish palmitoylation and membrane association (Veit *et al.*, 1996; Lane and Liu, 1997). Because the position of one of these clustered cysteine residues differs between SNAP-25a and SNAP-25b, it has been suggested that the arrangement of potential fatty acylation sites may contribute to targeting the two SNAP-25 isoforms to different sites on the plasma membrane (Bark and Wilson, 1994; Bark *et al.*, 1995). In general, targeting of SNARE proteins to distinct regions (e.g., lipid rafts) in the plasma membrane has been suggested to spatially control exocytosis (Chamberlain *et al.*, 2001; Salaün *et al.*, 2005). Thus, it is possible that the functional difference between SNAP-25a and SNAP-25b might simply reflect an altered targeting efficiency to exocytotic sites.

We addressed these questions by isolating plasma membrane sheets from SNAP-25 null cells overexpressing either SNAP-25 isoform using a SFV construct (see *Materials and Methods*). This technique allows examination of membrane proteins in their natural microenvironment defined by local lipid composition and bound proteins (Lang, 2003). Previously, by Western blot analysis we showed that the SNAP-25a/b SFV constructs express similar amounts of protein in bovine chromaffin cells (Sørensen *et al.*, 2003); however, the preparation of mouse chromaffin cells does not yield enough protein for Western blot analysis. Thus, another advantage of the membrane sheet technique is that it allows the comparison of the amount of membrane-targeted protein in embryonic mouse chromaffin cells. Membrane-associated SNAP-25 was visualized by immunostaining, together with syntaxin 1, to assay the distribution and amount of the interacting SNARE protein that might be different upon ablation or overexpression of SNAP-25. In Figure 2, we present images of membrane sheets from wild-type (+/+) cells and knock-out cells (–/–) overexpressing either isoform. On overexpression, the amount of SNAP-25 increased to beyond wild-type levels (see below); however, to preserve spatial information the images C and D in Figure 2 were scaled independently of A and B (for quantitation, see Figure 3). In wild-type mouse chromaffin cells, both SNAP-25 and syntaxin 1 were clustered (Figure 2A), as shown previously in PC12 cells (Lang *et al.*, 2001). In the plasma membrane of SNAP-25 null cells syntaxin 1 still formed clusters (Figure 2B), indicating that syntaxin 1 clusters do not depend on direct or indirect interactions between syntaxin 1 and SNAP-25. Importantly, in cells from SNAP-25 null mice overexpressing SNAP-25a (Figure 2C) or SNAP-25b (Figure 2D), a spotty pattern of SNAP-25 was observed, indistinguishable from that in wild-type cells. In overexpressing cells, this pattern was present on top of a stronger background level, which is not obvious at the image scaling chosen for presentation in Figure 2 (see *Discussion*). We compared the absolute fluorescence intensities per unit membrane area for both SNAP-25 isoforms and syntaxin 1 (Figure 3, A and B). The SNAP-25-specific signal was reduced by 33% in heterozygous (Snap-25 +/–) cells compared with wild-type (Snap-25 +/+) cells ($p < 0.05$ Tukey–

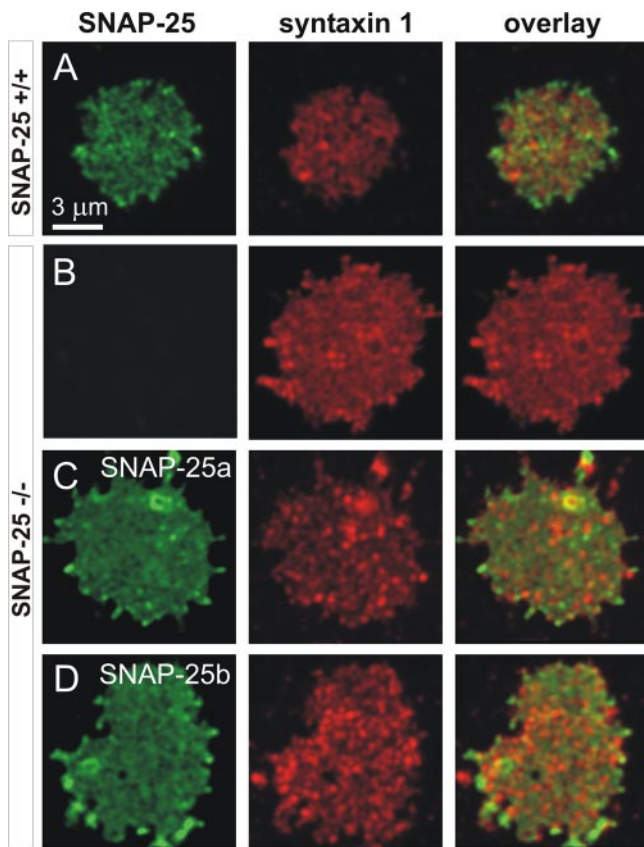


Figure 2. SNAP-25 and syntaxin 1 on membrane sheets from embryonic mouse chromaffin cells. Plasma membrane sheets were generated from SNAP-25 +/+ chromaffin cells (A), SNAP-25 null chromaffin cells (B), SNAP-25 null chromaffin cells expressing SNAP-25a (C), and SNAP-25 null chromaffin cells expressing SNAP-25b (D). Sheets were immediately fixed with paraformaldehyde and immunostained for SNAP-25 and syntaxin 1. The samples were imaged in three channels: membranes were identified in the presence of TMA-DPH dye in the blue (not shown), SNAP-25 signal was detected in the red and syntaxin 1 in the long red channel. Overlay from SNAP-25 and syntaxin 1 indicates partial colocalization of two proteins. Note that the SNAP-25 images in A, C, and D were scaled independently of each other to preserve spatial information; however, the absolute immunofluorescence intensities in C and D were much higher than in A (see Figure 3). The colocalization was quantified using correlation analysis (see text).

Kramer multiple comparison test), showing a gene-dose effect. In null cells overexpressing either SNAP-25a or SNAP-25b, the immunoreactivity was much higher than in wild-type cells but not significantly different between isoforms (SNAP-25a, 13.7 ± 1.0 -fold overexpression; SNAP-25b, 14.7 ± 2.2 -fold overexpression, $p > 0.05$, Tukey–Kramer multiple comparison test). The levels of syntaxin 1 immunofluorescence were not strongly affected by ablation or overexpression of SNAP-25 isoforms (Figure 3B; $p = 0.0393$, ANOVA, posttests showed that the difference between heterozygotes and knockouts was just significant). These data show no difference in targeting efficiency between the SNAP-25 isoforms. In addition, the 14- to 15-fold increase compared with wild-type levels excludes that limited availability at the plasma membrane of either isoform causes the difference in secretion.

However, the differences might occur at the level of microdomain organization. When the colocalization of

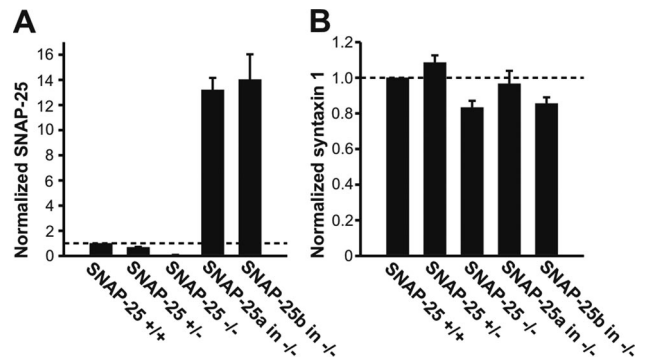


Figure 3. Quantification of SNAP-25 isoforms and syntaxin 1 in the plasma membrane of embryonic mouse chromaffin cells. The immunofluorescence of membrane sheets from 12 SNAP-25 null animals, 12 SNAP-25 WT(+/+) animals, 9 SNAP-25 heterozygous (+/-) animals, 9 SNAP-25 null animals expressing SNAP-25a and 7 SNAP-25 null animals expressing SNAP-25b were analyzed and plotted. A minimum of 10 sheets per animal were analyzed. The values indicate relative abundance (normalized to the mean of SNAP-25 +/+ animals from the same litter) \pm SEM of SNAP-25 (A) and syntaxin 1 (B) protein.

SNAP-25 and syntaxin 1 clusters was studied, findings ranged from only partial overlap (Lang *et al.*, 2001; Ohara-Imaizumi *et al.*, 2004) to nearly perfect colocalization (Rickman *et al.*, 2004), but all studies suggest that the sites of overlap represent fusion sites. To assay for a putative difference in the sorting of the SNAP-25 isoforms into the syntaxin 1-cluster, we quantified the colocalization by calculating the correlation coefficient of the two images (see *Materials and Methods*). First, the degree of overlap was characterized in homozygous wild-type cells, resulting in a correlation coefficient of 0.25 ± 0.02 ($n = 32$ membranes analyzed), indicating that a significant fraction of SNAP-25 is within or close to syntaxin 1 clusters. The correlation coefficients were similar when heterozygous and SNAP-25 null cells overexpressing SNAP-25a or SNAP-25b were analyzed (heterozygous cells, 0.26 ± 0.02 , $n = 34$; null cells overexpressing SNAP-25a, 0.25 ± 0.03 , $n = 24$; and null cells overexpressing SNAP-25b, 0.25 ± 0.02 , $n = 31$).

Finally, we conclude that the secretory difference between SNAP-25 isoforms cannot be explained by differential targeting efficiency to the plasma membrane or a change in microdomain organization as assayed by diffraction-limited light microscopy.

Identification of the Critical Amino Acid Substitutions Defining Neurosecretion Properties of SNAP-25a and SNAP-25b

To identify the amino acid substitutions responsible for the physiological differences in secretion mediated by SNAP-25 isoforms, we generated chimeric constructs and assayed their ability to rescue exocytosis in SNAP-25 null chromaffin cells. Secretion was assayed by simultaneous whole cell patch-clamp recordings to measure capacitance increase resulting from vesicular fusion (Figure 4A, middle) and amperometry (Figure 4A, bottom), which detects the release of oxidizable vesicle contents (adrenaline and noradrenaline). Viral-infected SNAP-25-expressing cells were recognized by the coexpression of green fluorescent protein (see *Materials and Methods*), and exocytosis was triggered by flash photolysis of caged Ca^{2+} (Figure 4A, at arrow). Because different preparations of chromaffin cells vary in secretory compe-

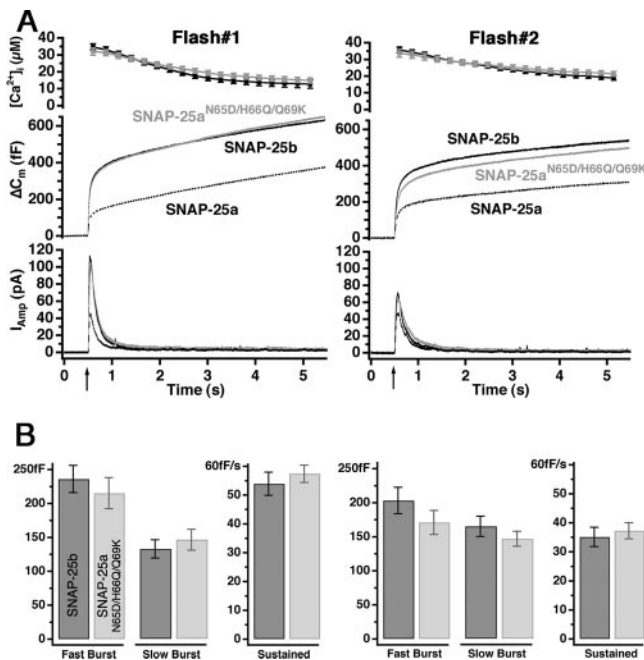


Figure 4. A group of three amino acids is sufficient to switch SNAP-25a to SNAP-25b phenotype. (A) Mean $[Ca^{2+}]_i$ (top, error bars represent SEM), capacitance change (middle), and amperometric current (bottom) were measured simultaneously after a step-like elevation of $[Ca^{2+}]_i$ caused by flash photolysis of caged Ca^{2+} (flash at arrow). The traces are averages of many experiments, so the individual fusion events (spikes) are not recognizable in the amperometric signal. Left, secretion after the first stimulation; right, secretion in response to the second stimulation (left). Shown are means of 38 SNAP-25 null cells expressing SNAP-25b cells (black) and 38 cells overexpressing SNAP-25a^{N65D/H66Q/Q69K} for 6–8 h (gray). There was no difference in preflash $[Ca^{2+}]_i$ between two groups (our unpublished data). The data for SNAP-25a overexpression were taken from another series of experiments and are shown here for comparison. Secretion from cells transfected with SNAP-25a^{N65D/H66Q/Q69K} and SNAP-25b was similar. (B) Amplitudes of exponential fits to individual responses. The amplitudes (mean \pm SEM) of the fast and the slow burst component and the rate of sustained component were similar in both stimuli (dark bars, SNAP-25b; gray bars, SNAP-25a^{N65D/H66Q/Q69K}).

tence, we adopted the strategy of dividing the chromaffin cells obtained from each SNAP-25 null embryo between several coverslips and performed rescue experiments with both mutated and control constructs on cells from the same animal on each experimental day. Only experiments done in parallel were compared statistically. Because we did not measure a difference in membrane targeting between the two isoforms, we reasoned that most likely the critical amino acid substitutions would be present in the SNARE domain, rather than in the linker. Hence, we first assayed the three nonconservative substitutions (from SNAP-25a to SNAP-25b; Figure 1) N65D, H66Q, and Q69K in the N-terminal SNARE domain, which could affect properties and function of the SNARE core complex.

As reported previously, expression of SNAP-25b in SNAP-25-deficient chromaffin cells resulted in a twofold increase in the size of the exocytotic burst, as determined by the secretion 0–1 s after flash photolysis of caged Ca^{2+} , compared with that supported by SNAP-25a overexpression (Figure 4A; note that the SNAP-25a trace is taken from a separate experimental series, and hence the quantification of

these experiments is not presented in Figure 4B; also see Sørensen *et al.*, 2003). The exocytotic burst phase represents the fusion of the two primed vesicle pools (the readily releasable and the slowly releasable pools, denoted RRP and SRP, respectively), whereas the sustained phase represents slower priming of new vesicles, followed by fusion as long as the intracellular calcium concentration ($[Ca^{2+}]_i$) stays high. By fitting of a sum of exponential functions to the capacitance trace, we can separate the size of the two releasable pools from their fusion time constants (Nagy *et al.*, 2002, 2004). The time constants for fusion from the two releasable pools were not different between SNAP-25a- and SNAP-25b-expressing cells (not shown; Sørensen *et al.*, 2003). In addition, the rate of sustained secretion was independent of the isoform of SNAP-25 expressed (1–5 s after Ca^{2+} release; Figure 4A and Sørensen *et al.*, 2003). However, it should be noted that by comparison with SNAP-25 null cells, it was shown that SNAP-25 expression is necessary for both the normal fusion rate constants and the rate of the sustained component (Sørensen *et al.*, 2003), indicating that SNAP-25 participates in all phases of release from chromaffin cells. However, the difference between SNAP-25 isoform is only evident on the size of the fast and slow exocytotic burst component, indicating that they only differ in their regulation of the size of the releasable vesicle pools.

Expression of a SNAP-25a variant in which the three amino acids in positions 65, 66, and 69 (Figure 1) were switched to SNAP-25b residues—N65D/H66Q/Q69K—resulted in a SNAP-25b-like secretory phenotype (Figure 4A). Kinetic analysis showed that the size of both burst components and the rate of the sustained component were indistinguishable from SNAP-25b overexpression (Figure 4B). In addition, providing a second flash stimulation ~ 100 s after the initial stimulus resulted in almost the same level of secretion as were recorded in SNAP-25b-expressing cells (Figure 4, A and B). The small reduction in secretion driven by the N65D/H66Q/Q69K construct during the second flash stimulation was not statistically significant (Figure 4B). This experiment tested the ability to refill depleted vesicle pools and confirmed that this component of secretion was also indistinguishable between cells expressing the triple SNAP-25a mutation and SNAP-25b. Thus, the three amino acid substitutions N65D/H66Q/Q69K were sufficient to provide SNAP-25a with the properties of SNAP-25b in mediating secretion from these chromaffin cells.

We next tested the effect of single mutations N65D, Q69K, and H66Q imposed on the SNAP-25a protein sequence background (Figure 5, A–D). The N65D mutation resulted in a level of secretion that was indistinguishable from SNAP-25a (Figure 5, A and B, red traces; compare with the trace for SNAP-25a in Figure 4). In contrast, the Q69K mutation resulted in an intermediate level of secretion, with an exocytotic burst that was significantly larger than in SNAP-25a N65D but smaller than for the N65D/H66Q/Q69K triple mutation (Figure 5, A and B). Kinetic analysis confirmed that the Q69K had intermediate sized RRP and SRP (Figure 5B). Note, that the sustained rate of release was not changed by any of these mutations (Figure 5B, bottom) –or by any of those that were studied in the following experiments. This is consistent with the difference between the SNAP-25a and SNAP-25b phenotype, where the burst size was changed, but the sustained rate was invariant (Figure 4; Sørensen *et al.*, 2003). The H66Q single mutation resulted in a SNAP-25a-like phenotype (Figure 5C, compare with trace for SNAP-25a in Figure 4). Therefore, the Q69K substitution was necessary for the stronger secretory phenotype produced by SNAP-25b, but in itself seemed not to be sufficient. Finally,

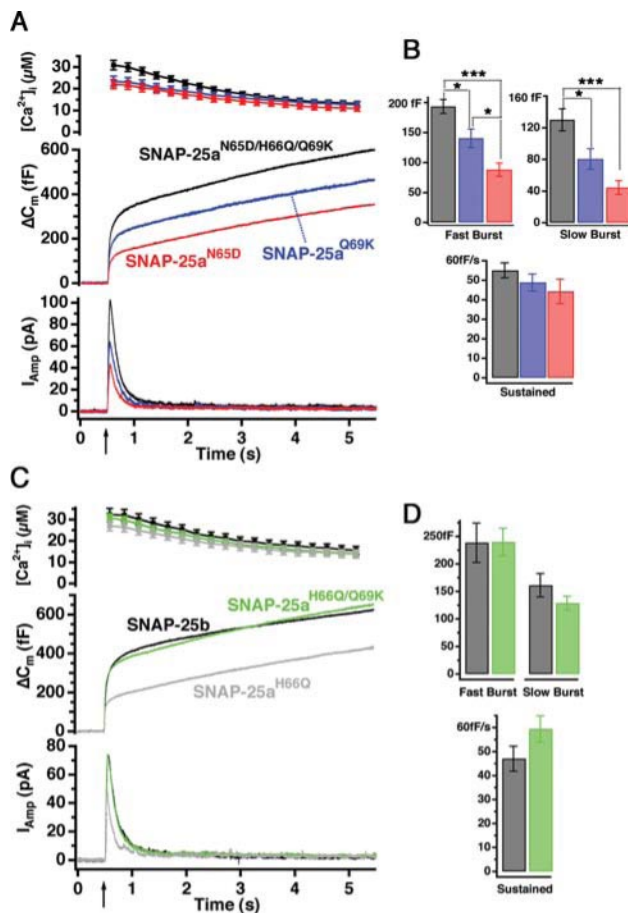


Figure 5. H66Q/Q69K: the minimal mutation in SNAP-25a that gives SNAP-25b phenotype. (A) Response to the first stimulation in SNAP-25 *null* cells expressing SNAP25a^{N65D} (red, 23 cells), SNAP25a^{Q69K} (blue, 30 cells) and SNAP25a^{N65D/H66Q/Q69K} (black, 40 cells). For explanation, see the legend to Figure 4. (B) Size of the burst (fast + slow burst) component and the rate of sustained secretion. The secretory phenotype of SNAP25a^{Q69K} is intermediate between SNAP25a^{N65D} and the triple mutation. No difference in the rate of the sustained component was detected. (C) Response to the first flash stimulation in SNAP-25 *null* cells expressing SNAP25a^{H66Q/Q69K} (green, 30 cells), SNAP25a^{H66Q} (gray, 16 cells) and SNAP25b (black, 23 cells). (D) The amplitudes of the burst components and the rate of sustained release in cells expressing SNAP25a^{H66Q/Q69K} were indistinguishable from cells expressing SNAP-25b.

we tested the effect of combining the Q69K with the H66Q substitution on secretion. Expression of the double substitution resulted in sizes of the fast and slow burst components that were indistinguishable from SNAP-25b (Figure 5, C and D). Together, these data indicate that the substitutions H66Q/Q69K define critical residues that distinguish the secretory properties attributed to SNAP-25 isoforms in chromaffin cells.

To confirm that these residues are sufficient to explain the difference in secretory phenotype between isoforms, we constructed the complementary substitution mutations in SNAP-25b. As shown in Figure 6, secretion rescued by the mutation Q66H/K69Q in SNAP-25b was almost indistinguishable from that obtained with SNAP-25a (Figure 6A, gray and black traces, respectively). Kinetic analysis confirmed that there was no statistical significant difference in

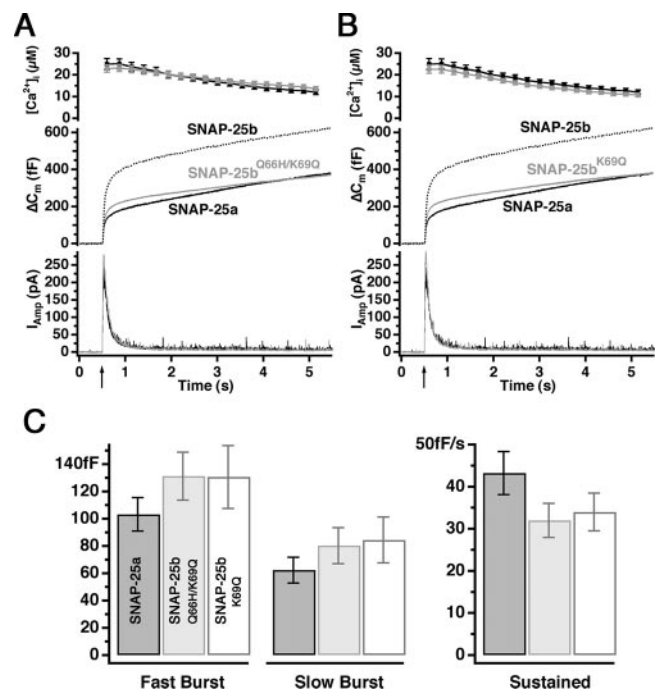


Figure 6. Q66H/K69Q mutation in SNAP-25b results in SNAP-25a-like phenotype. (A) The opposite experiment to the one shown in Figure 5. Here, we mutated the positions 66 and 69 in SNAP-25b into the residues found in SNAP-25a. Response to a first flash stimulation in SNAP-25 *null* cells expressing SNAP25b^{Q66H/K69Q} (gray, 26 cells) in comparison with SNAP25a (black, 26 cells). The data for SNAP-25b overexpression were taken from another series of experiments and are shown here for comparison. (B) Response to a first flash stimulation in SNAP-25 *null* cells expressing SNAP25b^{K69Q} (gray, 26 cells) in comparison with SNAP25a (black, 26 cells). Again, data for SNAP-25b overexpression were taken from another experimental series (C). Size of fast and slow burst and rate of the sustained component. Dark bars, SNAP-25a; gray bars, SNAP-25b Q66H/K69Q; and white bars, SNAP-25b K69Q. No significant changes were found between these three constructs (e.g., for the sustained component; $p = 0.13$, Kruskal-Wallis test).

the size of either burst component between cells expressing SNAP-25a and SNAP-25b Q66H/K69Q (Figure 6C, dark and gray bars). In fact, the single mutation K69Q in SNAP-25b was enough to secure the reversion to the SNAP-25a phenotype, as judged by the overall secretion (Figure 6B, dark and gray traces) and kinetic analysis of the burst sizes (Figure 6, B and C, dark and white). The fact that the Q69K mutation in the SNAP-25a background leads to an intermediate phenotype (Figure 5A), whereas the SNAP-25b K69Q mutation is indistinguishable from SNAP-25a, indicates that the two positions 66 and 69 have nonadditive effects on secretion. Given the complexity of protein-protein interaction such effects are not surprising.

In conclusion, by systematically swapping nonconservative amino acid differences between the isoforms, we find that the residue substitutions Q66H and K69Q, in SNAP-25a and SNAP-25b, respectively, are necessary and sufficient to account for the difference in secretory phenotype supported by these two isoforms in mouse chromaffin cells.

A Neighboring Residue, Asp-70, Defines a Hydrophilic Stretch of Amino Acids Regulating Secretion

One possible explanation for the difference in secretory phenotype between SNAP-25 isoforms is that an accessory fac-

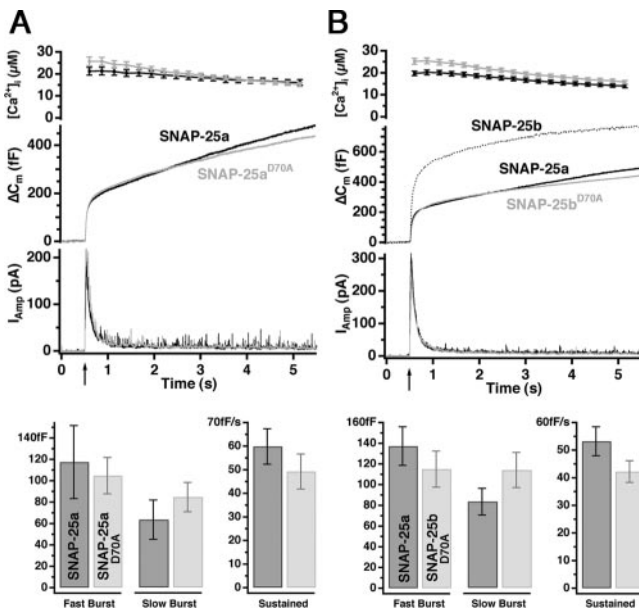


Figure 7. A neighboring aspartate (D70) present in both isoforms is necessary for the SNAP-25b-like phenotype. (A) Response to a first flash stimulation in SNAP-25 null cells expressing SNAP25a^{D70A} (gray, 22 cells) in comparison with SNAP25a (black, 21 cells). Bottom, size of fast and slow burst and rate of sustained component. (B) Response to a first flash stimulation in SNAP-25 null cells expressing SNAP25b^{D70A} (gray, 35 cells) in comparison with SNAP25a (black, 41 cells). The data for SNAP-25b overexpression were taken from another series of experiments and are shown here for comparison. Bottom, sizes of fast and slow burst of release, and rate of sustained component. No significant changes were found between SNAP-25a and SNAP-25b^{D70A}, showing that the aspartate at position 70 is necessary for the SNAP-25b secretory phenotype but not for the SNAP-25a-like secretory phenotype.

tor binds to the surface of the helical coiled-coil structure of the SNARE complex around positions 66 and 69 (see *Discussion*). If this is the case, then this factor may bind to a longer stretch than just these two residues. Alternatively, the difference in secretory phenotype might be explained by an interaction of the residues at positions 66 and 69 with neighboring residues in the SNARE complex, leading to different properties of the SNAP-25a- and SNAP-25b-containing SNARE core complexes. In both cases, structural neighbors of the amino acids at positions 66 and 69 might participate in the difference in secretory phenotype.

To identify other amino acids that could be involved, we mutated the neighboring aspartate D70, which is present in both SNAP-25a and SNAP-25b (Figure 1; also see Figure 9), and measured secretion after rescue of null cells. Mutation of D70 to alanine (D70A) in SNAP-25a did not compromise secretion, as shown in the overall secretion and following kinetic analysis of secretory components (Figure 7A). Strikingly, however, expression of the D70A SNAP-25b mutant resulted in a clear decrease in secretion compared with cells expressing native SNAP-25b (Figure 7B). The resulting secretion seemed indistinguishable from the level of vesicular fusion supported by SNAP-25a (Figure 7B). Moreover, we found no significant differences between the burst sizes between SNAP-25a and SNAP-25b D70A (Figure 7B, bottom). These data suggest that the neighboring amino acid D70 in SNAP-25 cooperates with K69 and Q66 in SNAP-25b to induce a stronger secretory phenotype for the SNAP-25b isoform.

Biochemical Properties of the Two Splice Variants of SNAP-25

We next investigated whether different biochemical properties of the SNARE complex formed with either SNAP-25 splice variant could account for the different secretory phenotypes. The pathway of SNARE complex formation in vitro involves a transient interaction between the N-terminal ends of the SNARE domains of syntaxin 1 and SNAP-25, which results in the formation of a 1:1 syntaxin 1:SNAP-25 precomplex (Fasshauer and Margittai, 2004) and serves as an acceptor for synaptobrevin. Therefore, mutations or changes in the N-terminal ends of the SNAP-25 SNARE domains can lead to slowdown of assembly, whereas C-terminal mutations do not (Fasshauer and Margittai, 2004; our unpublished data). The amino acid substitutions between the SNAP-25a and SNAP-25b isoforms are placed in the C-terminal end of the first SNARE motif (Figure 1); therefore, no difference in in vitro assembly rates can be expected.

The stability of the SNARE complex can be assayed by CD spectroscopy, which makes use of the fact that the α -helical structure of the SNARE domains is induced during complex formation, whereas uncomplexed SNARE domains are unstructured (Fasshauer *et al.*, 1997). To assess the consequences of the SNAP-25 isoform for the stability of the SNARE complex, we performed thermal denaturation experiments on in vitro assembled ternary SNARE core complexes. All analyzed complexes unfolded in a single, cooperative reaction (Figure 8). Interestingly, SNAP-25b-containing complexes melted at a slightly higher temperature (4–5°C) compared with those constituted with SNAP-25a, indicating that SNAP-25b increases the stability of the ternary SNARE complex. We next tested the stability of the SNAP-25a H66Q/Q69K double substitution that leads to a SNAP-25b-like secretory phenotype (see above). As shown in Figure 8, replacement of these residues in SNAP-25a resulted in a complex with the same stability as SNAP-25b, indicating that both the difference in stability and secretory phenotype can be attributed to these two amino acids. In contrast, complexes formed with SNAP-25a containing the Q69K single mutation did not affect the melting temperature, suggesting that this substitution cannot in isolation contribute to the differential stability of the isoforms. Finally, we tested the SNAP-25b mutation D70A. Remarkably, complexes containing SNAP-25b with the D70A substitution retained the higher melting temperature and thus stability characteristic of SNAP-25b, even though this single substitution was sufficient to provide a SNAP-25a-like secretory phenotype to SNAP-25b (Figure 7). These experiments suggest that despite a slight difference in stability of complexes containing either SNAP-25b or SNAP-25a, this change is probably not causal for the difference in secretory phenotype.

Structural Implications of the Replacement of Two Amino Acids in the SNARE Domains

To identify potential molecular interactions within the SNARE core complex involving the side chains of the two critical amino acid positions, we inspected the crystal structure of the SNARE core complex. The original crystal structure (Sutton *et al.*, 1998) and a later refined structure (Ernst and Brunger, 2003) both used the SNAP-25a isoform (note that in those publications this was denoted as SNAP-25b). By replacing H66 with Q and Q69 with K, we created a model structure to explore the possibilities for interaction with neighboring residues (Figure 9). Next, we performed molecular dynamics (MD) simulations of the wild-type (WT) crystal structure and the mutated structure. In both cases,

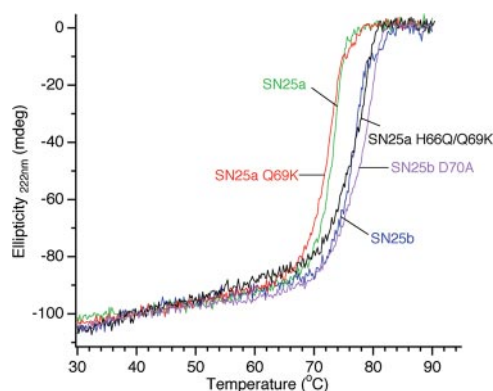


Figure 8. The thermal stability of the ternary SNARE complex is slightly higher in the presence of SNAP-25b. Thermal melts of purified ternary SNARE complexes containing different SNAP-25 variants or point mutations. Thermal stability of ternary SNARE complexes formed overnight was assayed by CD spectroscopy in the presence of 2 M guanidine hydrochloride. Complexes formed with SNAP-25b unfolded at a slightly higher temperature (4–5°C) than SNAP-25a-containing complexes. The double mutation H66Q/Q69K in SNAP-25a was sufficient to get a complex of higher stability, whereas the single mutation Q69K did not change stability. The D70A mutation in SNAP-25b led to a complex with SNAP-25b-like stability, but a SNAP-25a-like secretory phenotype (Figure 7B). This finding shows that the difference in stability is not causing the difference in secretory phenotype.

the crystal structure was solvated in a box of water molecules (Materials and methods) and simulated for 20 ns. The results show that in the WT (SNAP-25a-containing) crystal structure the side chains of the residues H66 and Q69 displayed more interactions (H-bonds) with neighboring residues than when mutated to the (SNAP-25b) residues Q66 and K69. In the SNAP-25a structure, the two nitrogen atoms (N δ 1 and N ϵ 2) in the imidazole ring of H66 participated in H-bonds 85 and 46% of the time, respectively, whereas the Q66 was hydrogen bound only 36% of the time. Similarly, at position 69, the Q residue of SNAP-25a participated in H-bonds 37% of the time, whereas K69 showed hydrogen bonds only 29% of the time. These simulations show that the substitution of histidine to glutamine at position 66 and glutamine to lysine at position 69 leads to decreased interaction of the side chains with neighboring amino acids within the SNARE complex. Together with the experimental findings, these computer simulations are consistent with the idea that the difference in secretory phenotype induced by the two amino acid substitutions is most likely caused by differential interaction with accessory factors on the surface of the coiled-coil structure of the SNARE complex.

DISCUSSION

Although there is considerable evidence that SNARE protein complexes participate in nearly all intracellular membrane fusion events, different opinions exist as to which step in the multiple-step process of membrane fusion is catalyzed by SNAREs. Similarly, the question of the physiological importance of different SNARE isoforms and how they may participate either in different membrane trafficking pathways or in the same vesicle fusion events has yet to be resolved. We have investigated these questions by comparing the two splice variants of SNAP-25, SNAP-25a and SNAP-25b, which can both support secretion when expressed in

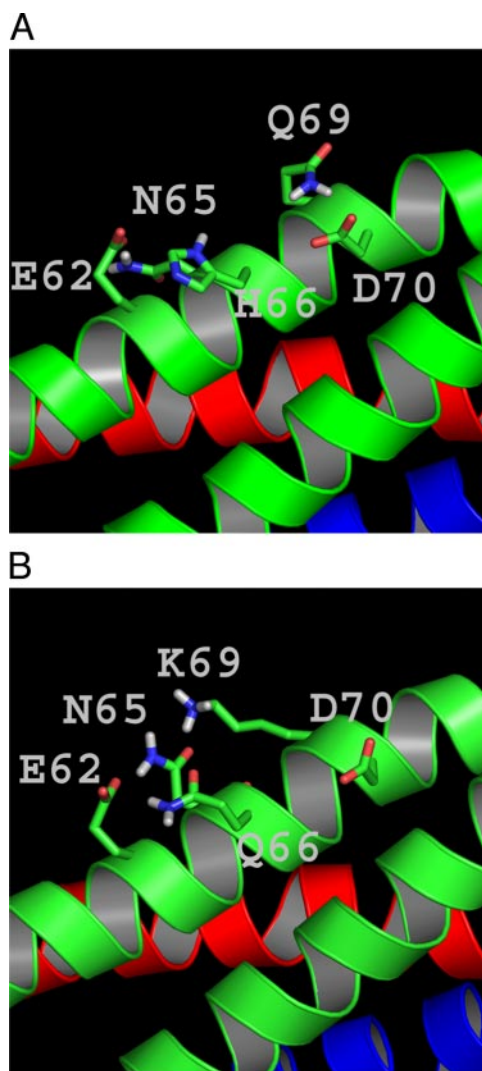


Figure 9. Structural arrangement of the SNARE complex around the SNAP-25 residues 66 and 69. A. Structure of the SNAP-25a-containing ternary SNARE complex (Sutton *et al.*, 1998) after MD simulation for 20 ns (as explained in the text). (B) Structure of the ternary SNARE complex after introduction of Q66 and K69 in the SNAP-25a-containing ternary SNARE complex and MD simulation for 20 ns. Note that the structural arrangements shown here are “snapshots” taken from a longer simulation and do not represent a preferred or typical arrangement of the side chains.

SNAP-25 *null* mutant chromaffin cells. In spite of only differing by nine amino acid substitutions, expression of the two splice variants results in a two- to threefold difference in the size of the exocytotic burst, indicating that they have a different ability to support the primed pool of vesicles. Here, we identify the two key amino acid residues that lead to the physiological differences in secretion. Biochemical and computer-assisted simulation analysis lead us to propose that the function of these residues, whose side chains face the external surface of the coiled-coil SNARE structure, is to interact with accessory proteins that may influence the stabilization or formation of the primed vesicle state.

Results from the plasma membrane sheet assay suggest that both SNAP-25 isoforms are targeted to the plasma membrane with the same efficiency, are available in excess, and colocalize to the same extent with syntaxin 1-clusters.

Concerning the latter conclusion, it should be noted that the antibody used for SNAP-25 detection is less sensitive for SNAP-25 in a complex with syntaxin 1 (Lang *et al.*, 2002), leading to a reduction of the signal-to-noise ratio for the detection of this pool compared with free SNAP-25. Nevertheless, the presence of significant positive correlations between the SNAP-25 and syntaxin 1 signals show that the proteins are targeted to the same subdomains in the plasma membrane. It might be surprising that a 14- to 15-fold increase of SNAP-25 leaves the correlation coefficient with syntaxin 1 unchanged compared with wild-type cells. However, it should be noted that correlation analysis was done on mean-subtracted images (see *Materials and Methods*). Therefore, the finding is consistent with two scenarios. First, independently of the SNAP-25 level always the same fraction of SNAP-25 ends up in clusters, or second, the mechanism that causes clustering has a limited capacity, and after saturation additional SNAP-25 is uniformly distributed in the membrane. Linescan analysis of the membrane sheets showed that after overexpression, the amplitude of the spotty signals is increased but that the background fluorescence level is increased even more (our unpublished data). Therefore, we suggest that the mechanism that causes clustering has a limited capacity, which, however, is not exhausted in control cells.

Although evidence has suggested that in some other cells coexpression with syntaxin 1 is required to retain SNAP-25 on intracellular membranes (Rowe *et al.*, 1999; Vogel *et al.*, 2000; Washbourne *et al.*, 2001), more recent studies have supported the view that targeting of SNAP-25 to the plasma membrane in neuronal cells does not require syntaxin 1 (Loranger and Linder, 2002). This model is in agreement with our finding that membrane associated SNAP-25 can be increased from nothing to >10-fold wild-type levels within 8 h without changing the plasma membrane syntaxin 1 level. The observation that the positioning of the four cysteines is rearranged between the two SNAP-25 isoforms had been suggested to provide a mechanism that might contribute to differences in membrane localization or targeting (Bark and Wilson, 1994). Our data show no discernible difference between the patterns of membrane-associated clusters formed by the two SNAP-25 isoforms. Furthermore, our search for the functionally relevant substitutions showed that the relocation of the cysteine does not contribute to the difference in secretory phenotype between SNAP-25 isoforms in chromaffin cells. Nevertheless, previous studies using tagged proteins expressed in nerve growth factor-differentiated PC12 cells indicated that SNAP-25b localized more to varicosities and terminals, whereas SNAP-25a showed a more diffuse localization (Bark *et al.*, 1995). Thus, this question should be reexamined in polarized neurons.

Our data demonstrate that the major functional distinction between the two SNAP-25 isoforms in neurosecretion is their ability to support the pool of releasable vesicles. By systematic mutagenesis, we identified the two nonconservative substitutions in the N-terminal SNARE domain (from SNAP-25a to SNAP-25b)—H66Q and Q69K—as being both necessary and sufficient for the functional difference between the isoforms. Thermal denaturation studies showed that SNAP-25b-containing complexes were somewhat (4–5°C) more stable than the SNAP-25a-containing complexes, which were used for structural studies (Sutton *et al.*, 1998) and that the difference in stability could be attributed to the same two amino acid substitutions. Moreover, further experiments demonstrated that a neighboring conserved aspartate (D70) also is required to obtain the stronger SNAP-25b secretory phenotype. Mutation of D70 to alanine in

SNAP-25b did not change the stability of the SNARE complex, even though the ability to support secretion was reduced to the level of SNAP-25a. Therefore, we conclude that the change in complex stability is most likely not causal for the functional difference between SNAP-25a and SNAP-25b.

The idea that the two substitutions H66Q and Q69K do not regulate secretion through a change in the property of the SNARE complex itself was corroborated by molecular dynamics simulations, which showed that Q66 and K69 participate less frequently in intracomplex interactions than the SNAP-25a residues H66 and Q69. It should be noted that this result is not in conflict with the higher thermostability of the SNAP-25b-containing complex measured biochemically. The thermostability of the SNARE complex does not depend strongly on hydrogen-bonding on the surface of the complex but more on the hydrophobic interactions in the interior of the complex, on the tendency of the SNARE domains to adopt different secondary structures, on the stability of partly unfolded states, and so on, which could all be changed in subtle ways by the H66Q and Q69K substitutions.

We thus suggest that the side chains of these two polar amino acids are available for interaction with accessory factor(s). Although the identity of such putative binding partner(s) is unknown, our findings suggest that the factor would bind to a stretch of amino acids at the N terminus of the coiled-coil SNARE structure. Two scenarios can be suggested: either this factor binds to only one of the two complexes (SNAP-25a or SNAP-25b containing), or it binds to both complexes, but with different affinities, which in turn regulates the size of the releasable vesicle pools. Because usually protein–protein interactions involve binding to multiple residues, but only two substitutions are necessary to explain the difference between isoforms, the latter scenario seems most likely. Interestingly, complexin proteins bind to the groove between syntaxin 1 and synaptobrevin 2 (Chen *et al.*, 2002), whereas Q66, K69 and D70 face the C-terminal SNAP-25 helix and syntaxin 1. Synaptotagmin 1 has been shown to bind to charged amino acids in the C-terminal end of the SNARE complex; however, the residues responsible for binding are found in the SN2 domain of SNAP-25 (refer to Figure 1; Zhang *et al.*, 2002). Furthermore, increasing the amount of synaptotagmin 1 in mouse chromaffin cells leads to a secretory phenotype, which is not consistent with the difference between SNAP-25 isoforms (our unpublished data). Finally, the accessory factor proposed here might, in fact, be the phospholipids themselves. Such an interaction may cause the SNARE complex to assume a more flat position on the plasma membrane, which could stabilize the primed vesicle state, but this notion remains speculative. The identification of the polar stretch of amino acids Q66, K69, and D70 should make it possible to identify the binding partner(s) by biochemical interaction experiments.

The effect of incorporating different SNAP-25 isoforms into the SNARE core complex is to regulate the size of the exocytotic burst, which represents the number of release-ready vesicles. Importantly, this is achieved without changing the rate of release from the releasable pools (either the slowly releasable pool or the readily releasable pool; our unpublished data; Sørensen *et al.*, 2003). This adds to our previous findings that alterations of protein kinase C or protein kinase A phosphorylation sites in SNAP-25 also modify upstream priming reactions, without affecting the fusion rate from the primed vesicle pools (Nagy *et al.*, 2002, 2004). Together, these results establish a function of SNAREs in regulating the priming reaction, which confers release competence to the vesicles. However, other studies have

involved the SNARE complex in exocytosis triggering and fusion pore formation (Gil *et al.*, 2002; Sørensen *et al.*, 2003; Han *et al.*, 2004; Borisovska *et al.*, 2005; our unpublished data). Collectively, these observations suggest that although the C-terminal end of the coiled-coil domain of the SNARE complex is involved in both vesicle priming and fusion triggering, these functions can be separately encoded within this small subdomain with certain residues being involved exclusively in one or the other reaction. Specifically, residues facing the surface of the SNARE bundle may regulate priming by binding to accessory factors, whereas residues facing the inside of the bundle will affect the assembly speed of the ternary complex and therefore may regulate the fusion rate, even though this has so far not been shown. The first of these steps (defining vesicle priming) may correspond to assembly of a precomplex between syntaxin 1 and SNAP-25, which in a later step serves as an acceptor for synaptobrevin 2 (An and Almers, 2004; Fasshauer and Margittai, 2004).

Thus, the SNAREs are not only required for the last steps in exocytosis (exocytosis triggering and fusion pore formation) but also for an upstream step (vesicle priming), and they can regulate the upstream reaction without compromising the fidelity and speed of the downstream fusion step. This arrangement allows regulation of the extent of exocytosis without compromising the exocytotic event itself, which is exactly what is required for the neuronal fusion apparatus.

ACKNOWLEDGMENTS

We are grateful to Erwin Neher for ongoing discussions and for commenting on the manuscript. We thank Ina Herfort and Dirk Reuter for expert technical assistance. This work was supported Deutsche Forschungsgemeinschaft Grants SFB523/TP4, SO 708/1-1 (to J.B.S.) and GRK521 (to G. N.) and by National Institutes of Health Grant MH-48989 (to M.C.W.). I. M. is a Ph.D. student of the International Ph.D./M.D.-Ph.D. Program in the Neurosciences of the International Max Planck Research School and holds a Boehringer-Ingelheim Fond Fellowship.

REFERENCES

- An, S. J., and Almers, W. (2004). Tracking SNARE complex formation in live endocrine cells. *Science* 306, 1042–1046.
- Archer, B. T., Özcelik, T., Jahn, R., Francke, U., and Südhof, T. C. (1990). Structures and chromosomal localizations of two human genes encoding synaptobrevins 1 and 2. *J. Biol. Chem.* 265, 17267–17273.
- Ashery, U., Betz, A., Xu, T., Brose, N., and Rettig, J. (1999). An efficient method for infection of adrenal chromaffin cells using the Semliki Forest virus gene expression system. *Eur. J. Cell Biol.* 78, 525–532.
- Bark, C., Bellinger, F. P., Kaushal, A., Mathews, J. R., Partridge, L. D., and Wilson, M. C. (2004). Developmentally regulated switch in alternatively spliced SNAP-25 isoforms alters facilitation of synaptic transmission. *J. Neurosci.* 24, 8796–8805.
- Bark, I. C., Hahn, K. M., Ryabinin, A. E., and Wilson, M. C. (1995). Differential expression of SNAP-25 protein isoforms during divergent vesicle fusion events of neural development. *Proc. Natl. Acad. Sci. USA* 92, 1510–1514.
- Bark, I. C., and Wilson, M. C. (1994). Human cDNA clones encoding two different isoforms of the nerve terminal protein SNAP-25. *Gene* 139, 291–292.
- Bennett, M. K., Calakos, N., and Scheller, R. H. (1992). Syntaxin: a synaptic protein implicated in docking of synaptic vesicles at presynaptic active zones. *Science* 257, 255–259.
- Berendsen, H.J.C., Postma, J. P., DiNola, A., and Haak, J. R. (1984). Molecular dynamics with coupling to an external bath. *J. Chem. Phys.* 81, 3684–3690.
- Berendsen, H.J.C., Postma, J.P.M., van Gunsteren, W. F., and Hermans, J. (1981). Interaction models for water in relation to protein hydration. In: *Intermolecular Forces*, ed. B. Pullman, Dordrecht, The Netherlands: D. Reidel Publishing Co., 331–342.
- Borisovska, M., Zhao, Y., Tsytisura, Y., Glyvuk, N., Takamori, S., Matti, U., Rettig, J., Südhof, T. C., and Bruns, D. (2005). v-SNAREs control exocytosis of vesicles from priming to fusion. *EMBO J.* 24, 2114–2126.
- Boschert, U., O'Shaughnessy, C., Dickinson, R., Tessari, M., Bendotti, C., Catsicas, S., and Pich, E. M. (1996). Developmental and plasticity-related differential expression of two SNAP-25 isoforms in the rat brain. *J. Comp. Neurol.* 367, 177–193.
- Chamberlain, L. H., Burgoyne, R. D., and Gould, G. W. (2001). SNARE proteins are highly enriched in lipid rafts in PC12 cells: implications for the spatial control of exocytosis. *Proc. Natl. Acad. Sci. USA* 98, 5619–5624.
- Chen, X., Tomchick, D. R., Kovrigin, E., Arac, D., Machius, M., Südhof, T. C., and Rizo, J. (2002). Three-dimensional structure of the complexin/SNARE complex. *Neuron* 33, 397–409.
- Darden, T., York, D., and Pedersen, L. (1993). Particle mesh Ewald - an $N \log(N)$ method for Ewald sums in large systems. *J. Chem. Phys.* 98, 10089–10092.
- Elferink, L. A., Trimble, W. S., and Scheller, R. H. (1989). Two vesicle-associated membrane protein genes are differentially expressed in the rat central nervous system. *J. Biol. Chem.* 264, 11061–11064.
- Ernst, J. A., and Brunger, A. T. (2003). High resolution structure, stability and synaptotagmin binding of a truncated neuronal SNARE complex. *J. Biol. Chem.* 278, 8630–8636.
- Fasshauer, D., Bruns, D., Shen, B., Jahn, R., and Brünger, A. T. (1997). A structural change occurs upon binding of syntaxin to SNAP-25. *J. Biol. Chem.* 272, 4582–4590.
- Fasshauer, D., and Margittai, M. (2004). A transient N-terminal interaction of SNAP-25 and syntaxin nucleates SNARE assembly. *J. Biol. Chem.* 279, 7613–7621.
- Gil, A., Guitérrez, L. M., Carrasco-Serrano, C., Alonso, M. T., Viniegra, S., and Criado, M. (2002). Modifications in the C terminus of the synaptosome-associated protein of 25 kDa (SNAP-25) and in the complementary region of synaptobrevin affect the final steps of exocytosis. *J. Biol. Chem.* 277, 9904–9910.
- Gonzalo, S., Greentree, W. K., and Linder, M. E. (1999). SNAP-25 is targeted to the plasma membrane through a novel membrane-binding domain. *J. Biol. Chem.* 274, 21313–21318.
- Grant, N. J., Hepp, R., Krause, W., Aunis, D., Oehme, P., and Langley, K. (1999). Differential expression of SNAP-25 isoforms and SNAP-23 in the adrenal gland. *J. Neurochem.* 72, 363–372.
- Guex, N., and Peitsch, M. C. (1997). SWISS-MODEL and the Swiss-Pdb-Viewer: an environment for comparative protein modeling. *Electrophoresis* 18, 2714–2723.
- Han, X., Wang, C. T., Bai, J., Chapman, E. R., and Jackson, M. B. (2004). Transmembrane segments of syntaxin line the fusion pore of Ca^{2+} -triggered exocytosis. *Science* 304, 289–292.
- Hanson, P. I., Roth, R., Morisaki, H., Jahn, R., and Heuser, J. E. (1997). Structure and conformational changes in NSF and its membrane receptor complexes visualized by quick-freeze/deep-etch electron microscopy. *Cell* 90, 523–535.
- Hess, B., Bekker, H., Berendsen, H.J.C., and Fraaije, J.G.E.M. (1997). LINCOS: a linear constraint solver for molecular simulations. *J. Comp. Chem.* 18, 1463–1472.
- Jahn, R., Lang, T., and Südhof, T. C. (2003). Membrane fusion. *Cell* 112, 519–533.
- Lane, S. R., and Liu, Y. (1997). Characterization of the palmitoylation domain of SNAP-25. *J. Neurochem.* 69, 1864–1869.
- Lang, T. (2003). Imaging SNAREs at work in “unroofed” cells –approaches that may be of general interest for functional studies on membrane proteins. *Biochem. Soc. Trans.* 31, 861–864.
- Lang, T., Bruns, D., Wenzel, D., Riedel, D., Holroyd, P., Thiele, C., and Jahn, R. (2001). SNAREs are concentrated in cholesterol-dependent clusters that define docking and fusion sites for exocytosis. *EMBO J.* 20, 2202–2213.
- Lang, T., Margittai, M., Holzler, H., and Jahn, R. (2002). SNAREs in native plasma membranes are active and readily form core complexes with endogenous and exogenous SNAREs. *J. Cell Biol.* 158, 751–760.
- Lindahl, E., Hess, B., and van der Spoel, D. (2001). GROMACS 3.0, a package for molecular simulation and trajectory. *J. Mol. Model.* 7, 306–317.
- Loranger, S. S., and Linder, M. E. (2002). SNAP-25 traffics to the plasma membrane by a syntaxin-independent mechanism. *J. Biol. Chem.* 277, 34303–34309.
- Manders, E.M.M., Stap, J., Brakenhoff, G. J., Van Driel, R., and Aten, J. A. (1992). Dynamics of three-dimensional replication patterns during the S-phase, analysed by double labelling of DNA and confocal microscopy. *J. Cell Sci.* 103, 857–862.

- McMahon, H. T., Ushkaryov, Y. A., Edelmann, L., Link, E., Binz, T., Niemann, H., Jahn, R., and Südhof, T. C. (1993). Cellubrevin is a ubiquitous tetanus-toxin substrate homologous to a putative synaptic vesicle fusion protein. *Nature* 364, 346–349.
- Miyamoto, S., and Kollman, P. A. (1992). SETTLE: an analytical version of the SHAKE and RATTLE algorithms for rigid water models. *J. Comp. Chem.* 13, 952–962.
- Nagy, G., Matti, U., Nehring, R. B., Binz, T., Rettig, J., Neher, E., and Sørensen, J. B. (2002) PKC-dependent phosphorylation of synaptosome-associated protein of 25 kDa at Ser187 potentiates vesicle recruitment. *J. Neurosci.* 22, 9278–9286.
- Nagy, G., Reim, K., Matti, U., Brose, N., Binz, T., Rettig, J., Neher, E., and Sørensen, J. B. (2004). Regulation of releasable vesicle pool sizes by protein kinase A-dependent phosphorylation of SNAP-25. *Neuron* 41, 351–365.
- Ohara-Imaizumi, M., Nishiwaki, C., Nakamichi, Y., Kikuta, T., Nagai, S., and Nagamatsu, S. (2004). Correlation of syntaxin-1 and SNAP-25 clusters with docking and fusion of insulin granules analysed by total internal reflection fluorescence microscopy. *Diabetologia* 47, 2200–2207.
- Rickman, C., Meunier, F. A., Binz, T., and Davletov, B. (2004). High affinity interaction of syntaxin and SNAP-25 on the plasma membrane is abolished by botulinum toxin E. *J. Biol. Chem.* 279, 644–651.
- Rowe, J., Corradi, N., Malosio, M. L., Taverna, E., Halban, P., Meldolesi, J., and Rosa, P. (1999). Blockade of membrane transport and disassembly of the Golgi complex by expression of syntaxin 1A in neurosecretion-incompetent cells: prevention by rbSEC1. *J. Cell Sci.* 112, 1865–1877.
- Salaün, C., Gould, G. W., and Chamberlain, L. H. (2005). Lipid raft association of SNARE proteins regulates exocytosis in PC12 cells. *J. Biol. Chem.* 280, 19449–19453.
- Sørensen, J. B., Nagy, G., Varoqueaux, F., Nehring, R. B., Brose, N., Wilson, M. C., and Neher, E. (2003). Differential control of the releasable vesicle pools by SNAP-25 splice variants and SNAP-23. *Cell* 114, 75–86.
- Sutton, R. B., Fasshauer, D., Jahn, R., and Brunger, A. T. (1998). Crystal structure of a SNARE complex involved in synaptic exocytosis at 2.4 Å resolution. *Nature* 395, 347–353.
- Van Buuren, A. R., Marrink, S.-J., and Berendsen, H.J.C. (1993). A molecular dynamics study of the decane/water interface. *J. Phys. Chem.* 97, 9206–9212.
- van Gunsteren, W. F., and Berendsen, H.J.C. (1987). GROMOS manual. BIOMOS, biomolecular Software, Laboratory of Physical Chemistry, University of Groningen, The Netherlands.
- Veit, M., Söllner, T. H., and Rothman, J. E. (1996). Multiple palmitoylation of synaptotagmin and the t-SNARE SNAP-25. *FEBS Lett.* 385, 119–123.
- Vogel, K., Cabaniols, J.-P., and Roche, P. A. (2000). Targeting of SNAP-25 to membranes is mediated by its association with the target SNARE syntaxin. *J. Biol. Chem.* 275, 2959–2965.
- Vriend, G. (1990). WHAT IF: a molecular modeling and drug design program. *J. Mol. Graph.* 8, 52–56.
- Xu, T., Rammner, B., Margittai, M., Artalejo, A. R., Neher, E., and Jahn, R. (1999). Inhibition of SNARE complex assembly differentially affects kinetic components of exocytosis. *Cell* 99, 713–722.
- Washbourne, P., Cansino, V., Mathews, J. R., Graham, M., Burgoyne, R. D., and Wilson, M. C. (2001). Cysteine residues of SNAP-25 are required for SNARE disassembly and exocytosis, but not for membrane targeting. *Biochem. J.* 357, 625–634.
- Weber, T., Zemelman, B. V., McNew, J. A., Westermann, B., Gmachl, M., Parlati, F., Söllner, T. H., and Rothman, J. E. (1998). SNAREpins: minimal machinery for membrane fusion. *Cell* 92, 759–772.
- Zhang, X., Kim-Miller, M. J., Fukuda, M., Kowalchuk, J. A., and Martin, T. F. (2002). Ca^{2+} -dependent synaptotagmin binding to SNAP-25 is essential for Ca^{2+} -triggered exocytosis. *Neuron* 34, 599–611.

2.3. Paper III.

Sequential N- to C-terminal “zipping-up” of the SNARE complex
drives priming and fusion of secretory vesicles

Jakob B. Sørensen, Katrin Wiederhold, Matthias Müller, Ira Milosevic,
Gabor Nagy, Bert L. de Groot, Helmut Grubmüller and Dirk Fasshauer

EMBO Journal, 2006

**Sequential N- to C-terminal ‘zipping-up’ of the SNARE complex
drives priming and fusion of secretory vesicles**

Jakob B. Sørensen¹, Katrin Wiederhold², E. Matthias Müller³, Ira Milosevic^{1,2}, Gábor Nagy¹, Bert L. de Groot³, Helmut Grubmüller³, Dirk Fasshauer²

¹Department of Membrane Biophysics

²Department of Neurobiology

³Department of Theoretical and Computational Biophysics

Max-Planck-Institute for Biophysical Chemistry, Am Fassberg 11, 37077 Göttingen,
Germany

Running title: Zipping of the SNARE complex drives exocytosis

60066 characters

Corresponding author:

Jakob B. Sørensen

Phone +49 551 2011297

Fax +49 551 2011688

jsoeren@gwdg.de

ABSTRACT

During exocytosis a four-helical coiled-coil is formed between the three SNARE proteins syntaxin, synaptobrevin and SNAP-25, bridging vesicle and plasma membrane. We have investigated the assembly pathway of this complex by interfering with the stability of the hydrophobic interaction layers holding the complex together. Mutations in the C-terminal end affected fusion triggering *in vivo* and led to two-step unfolding of the SNARE complex *in vitro*, indicating that the C-terminal end can assemble/disassemble independently. Free energy perturbation calculations showed that assembly of the C-terminal end could liberate substantial amounts of energy that may drive fusion. In contrast, similar N-terminal mutations were without effects on exocytosis, and mutations in the middle of the complex selectively interfered with upstream maturation steps (vesicle priming), but not with fusion triggering. We conclude that the SNARE complex forms in the N- to C-terminal direction, and that a partly assembled intermediate corresponds to the primed vesicle state.

INTRODUCTION

Formation of a tight, four-helical bundle (the SNARE complex) between the membranes is the decisive step during intracellular membrane fusion. The best-studied SNARE complex is involved in the exocytosis of neurotransmitter-filled vesicles in the synapse. This complex is a heterotrimer formed by synaptobrevin 2, syntaxin 1A and SNAP-25. SNAP-25 contributes two α -helices to the complex and is localized to the plasma membrane by palmitoylation, whereas synaptobrevin and syntaxin are anchored in the vesicular and plasma membrane, respectively, via transmembrane domains (Fig. 1).

The membrane anchors of synaptobrevin and syntaxin are both placed on the C-terminal side of the assembled complex (Hanson et al., 1997; Sutton et al., 1998). This arrangement gave rise to the idea that SNARE complex formation may occur in a ‘zipper-like’ fashion, proceeding from the (membrane-distal) N-terminal end towards the C-terminal membrane anchors (Hanson et al., 1997). According to this scenario, the formation energy of the *trans*-SNARE complex helps overcome the energy barrier for fusion of the membranes. Even though this model is highly attractive and has been investigated in a number of studies, it remains unproven. Using a single experimental system it has not been possible to bridge the description of the molecular mechanism with the physiological function. For example, ‘intact’ systems consisting of neurons or neurosecretory cells allow for the detailed study of high-speed exocytosis, but do not allow easy access to the underlying molecular machinery. *In vitro* studies, on the other hand, have so far failed to reconstitute membrane fusion with the speed and regulatory properties found in a living cell.

In vitro structural studies involving the soluble part of the SNAREs have shown that SNARE complex formation nucleates rather slowly through a N-terminal interaction between syntaxin and SNAP-25 (Fasshauer and Margittai, 2004). In turn, the 1:1 syntaxin:SNAP-25 complex serves as an acceptor site for synaptobrevin binding. The synaptobrevin binding site can be occupied by a second syntaxin; a step that is off-pathway, and is unlikely to occur in the cell. Yet, the competition of the second syntaxin with synaptobrevin so far has hindered the determination of the rate and mode of synaptobrevin binding. Structural studies of the homologous yeast SNAREs showed that the binary complex is partly unstructured in the C-terminal end, whereas the ternary complex is fully structured. It was thus suggested that a ternary

SNARE complex with a partly unstructured C-terminal end might be an intermediate on the pathway to secretion (Fiebig et al., 1999). Nevertheless, there is so far no direct evidence showing that the ternary complex can exist in a partly folded state.

SNAREs reconstituted into liposomes have been shown to drive membrane fusion, albeit with slow (minutes) kinetics (Weber et al., 1998). A C-terminal fragment of the synaptobrevin SNARE domain accelerated the fusion rate, and it was suggested that this effect is caused by the induction of structure into a partially formed ternary SNARE complex (Melia et al., 2002). However, the slow fusion rate *in vitro* may be due to the formation of an unproductive 2:1 syntaxin:SNAP-25 complex that is prevented by the synaptobrevin fragment (Fasshauer, 2004).

Closer to the *in vivo* situation are assay systems utilizing peptide infusion into permeabilized PC12 cells followed by detection of secreted catecholamines. Using a stage-specific assay for ATP-dependent vesicle priming and Ca^{2+} -dependent fusion it was found that SNARE complex assembly could not be dissociated from Ca^{2+} -triggering (Chen et al., 1999). Following priming both syntaxin and synaptobrevin fragments were able to inhibit secretion, and hence the existence of an intermediate SNARE complex consisting of synaptobrevin bound to SNAP-25 was suggested (Chen et al., 2001). However, these data are also in agreement with the formation during priming of a syntaxin:SNAP-25 1:1 precomplex, which can bind to either syntaxin or synaptobrevin. That syntaxin and SNAP-25 interact in intact PC12 cells has been demonstrated recently using FRET in intact PC12 cells (An and Almers, 2004). In another study infusion of syntaxin fragments was found to support N- to C-terminal formation of the SNARE complex, but it was argued that a partly formed complex is unlikely to exist (Matos et al., 2003). However, the slow secretion in PC12 cells ($\tau \sim 30$ s) compared to neurosecretory cells or neurons ($\tau \sim 20$ ms and ~ 2 ms, respectively) hampers the interpretation of results. This difference might be caused by the lack in PC12 cells of a population of vesicles that have matured to be 'release-ready' (Martin, 2003).

Fusion of this population of release-ready vesicles is usually assumed to underlie the first, fast secretory phase in neurosecretory cells and neurons. In these cells secretion can be measured with high time resolution using electrophysiological techniques. Kinetic consequences of SNARE cleavage (by neurotoxins), sequestering (by antibodies), elimination (by genetic techniques), or overexpression studies in

wildtype cells have all indicated that the SNAREs are intimately involved in the last steps of exocytosis (Capogna et al., 1997; Xu et al., 1998, 1999; Han et al., 2004; Hua and Charlton, 1999; Schoch et al., 2001; Sakaba et al., 2005), and some investigators have suggested the existence of partly folded intermediates (Xu et al., 1999; Hua and Charlton, 1999). However, with these approaches it was not possible to unambiguously identify intermediate steps in the fusion pathway.

Alternative models have been proposed for the SNARE assembly pathway. For example, it was suggested that the C-terminal end of the synaptobrevin SNARE domain is buried in the vesicular membrane, preventing SNARE complex formation (Hu et al., 2002; Kweon et al., 2003; Haro et al., 2004). This finding raised the possibility that SNARE complex formation may start from the C-terminal end (Kweon et al., 2003). In fact, the current data from intact cells do not allow distinguishing between this model and N- to C-terminal ‘zippering’.

In summary, despite many attempts, the pathway of SNARE assembly during membrane fusion has not been unambiguously resolved. In particular, two crucial aspects are unclear: does the complex indeed assemble in the N- to C-terminal direction, and does assembly occur in a single reaction, or through a partially assembled intermediate? To address this question, we have now combined analysis of SNARE assembly/stability *in vitro* with functional analysis of SNAREs in fast neurotransmitter release from chromaffin cells. In these cells vesicle maturation is arrested at the ‘release-ready’ state, where the vesicle awaits the calcium-trigger for fusion. Using electrophysiological methods it is possible to distinguish between ‘priming reactions’, which lead up to this state, and ‘triggering reactions’, which lead to fusion from this state. This makes it possible to study the assembly of the SNARE complex as it applies to these two steps. Three different scenarios can be envisioned: the SNARE complex may form completely either before (Fig. 1A), or after (Fig. 1B) Ca^{2+} -triggering. These scenarios do not allow the distinction of more than one assembly event, and would thus not provide information about the assembly direction or the existence of intermediates. However, in the third scenario the SNARE complex forms partly during the priming step, and then completes assembly simultaneously with the Ca^{2+} -triggering step (Fig. 1C). In this case an assembly intermediate coincides with the readily-releasable state, and localized interference with complex assembly should allow the determination of the assembly direction, i.e. if N- to C-

terminal assembly drives secretion (as in Fig. 1C), C-terminal interference would affect exocytosis triggering, whereas more N-terminal interventions would affect vesicle priming.

In order to obtain local destabilizations along the complex we interfered with the coiled coil interactions ('layers') in the interior of the 4-helical SNARE bundle. Layer mutants were tested in the *null* background of mouse chromaffin cells isolated from SNAP-25 knock-out embryos (Sørensen et al., 2003). Fast secretion is impaired by >85% in these cells, but it can be completely restored upon expression of SNAP-25A. This makes it possible to study the mutants in a gain-of-function framework without interference with wildtype SNAP-25. The electrophysiological measurements were supplemented by *in vitro* studies of SNARE complex assembly and stability and molecular dynamics simulations to estimate the energy that may be released by SNARE complex 'zippering'. We find that evidence from both *in vivo* and *in vitro* experiments supports two-step N-to-C terminal assembly of the SNARE complex (Fig. 1C).

RESULTS

In order to locally destabilize the SNARE complex we mutated layer residues to alanines, because its small apolar side chain would not introduce steric hindrance of SNARE complex formation, or change the surface charge of the complex. This is important, because several other proteins (synaptotagmins, complexins) bind to the surface of the SNARE complex through polar interactions. To evaluate secretion we expressed mutated SNAP-25 in SNAP-25 *null* embryonic chromaffin cells and performed parallel measurement of membrane capacitance and amperometric detection of liberated catecholamines. The use of embryonic tissue is necessary, since SNAP-25 knock-out mice die around birth (Washbourne et al., 2002). Secretion was elicited by flash photolysis of caged- Ca^{2+} , which led to a step-like increase of $[\text{Ca}^{2+}]_i$ (see e.g. Fig 2Aa). Flash-induced secretion happens in several phases, which are usually assumed to represent sequential events in the exocytotic cascade. A rapid burst of secretion within the first 0.5-1 s after the $[\text{Ca}^{2+}]_i$ increase is caused by fusion of vesicles that were release-ready before stimulation, whereas the much slower sustained component most likely represents the recruitment (referred to as priming) of new vesicles into the releasable pool (Sørensen, 2004). Kinetic analysis allows determination of the sizes of the two releasable pools (readily releasable pool, RRP, and slowly releasable pool, SRP), and the rate of the sustained component, all of which report on the priming process, and the fusion time constants, which report on the fusion triggering process.

Mutations in the C-terminal end of the complex: electrophysiology

In the first set of experiments we concentrated on the most C-terminal (membrane-proximal) hydrophobic layer of the complex (+8; Fig. 1D), which consists of a methionine (Met-202) and a leucine (Leu-81) from SNAP-25, a leucine from synaptobrevin and an alanine from syntaxin. When mutating Met-202 to Ala in SNAP-25, rescued chromaffin cells showed the same level of secretion as in cells rescued with wildtype (WT) SNAP-25 (Fig. 2Aa). Kinetic analysis revealed that neither the amplitude of the two exocytotic burst phases, nor the sustained rate of release was changed (Fig. 2Ab-c), indicating intact priming in these cells. The rate constant of release from the RRP ($=1/\tau$, where τ is the time constant of the fastest exponential) and the time delay (from the flash of UV-light until the start of the

capacitance increase) were unchanged by this mutation over the range of investigated $[Ca^{2+}]_i$ (Fig. 2Ad-e), indicating intact exocytosis triggering. When the single mutation Leu-81 to alanine (L81A) was tested, a roughly unchanged exocytosis pattern was found, except for a slight, but significant, decrease in the size of the RRP and a slower rate of exocytosis triggering in some cells (Suppl. Fig. 1).

Apparently, the introduction of a single alanine into layer +8 is insufficient to give a clear phenotype. We therefore combined the two mutations (Fig. 2B). The double mutation L81A/M202A led to a noticeable slow-down of the fastest phase of secretion (Fig. 2Ba). The amplitude of secretion within the first 1 s, or within the time period 1-5 s after the flash was, however, not significantly changed (Fig. 2Bc-d). We analyzed the fastest resolvable rate constant of secretion, and the secretory delay. This revealed substantially slower triggering kinetics with the double mutation, compared to WT (Fig 2Be-f). Alternatively, as a model-independent way of analyzing triggering speed we scaled the capacitance increase and the integrated amperometric charge in mutant and WT to the same amplitude at 1 s after the flash. This confirmed the slow-down of the fast-phase secretion by the double mutation (Fig. 2Bb).

We next combined the L81A/M202A mutation with a mutation in layer +7: L78A. The triple mutation L78A/L81A/M202A displayed substantial slow-down of secretion (Fig. 2Ca), and also reduced secretion at 1 s after the flash (Fig. 2Cc). This effect was more severe than for the double mutation, which was reflected in slower rates and longer delays (Fig. 2Ce-f). Slow-down of secretion was confirmed in the amperometric trace (Fig. 2Cb).

The flash photolysis data pointed to a more severe phenotype of the triple mutation compared to the double mutation. To investigate this further, we stimulated the cells using slowly increasing calcium concentrations (calcium ramps). The simultaneously measured capacitance change indicated that secretion was shifted to later times (or higher calcium concentrations) with the double mutation, but even more so with the triple mutation (Suppl. Fig. 2), indicating a graded effect of accumulating mutations in the C-terminal end of the SNARE complex.

With the triple mutation our possibilities for making alanine substitutions in the last layers were exhausted, since the other amino acids from SNAP-25 in layer +7 and +6 are already alanines (Fig. 1D). To further destabilize the last layers we deleted the last 9 amino acids ($\Delta 9$ mutant) in the C-terminal helix of SNAP-25, corresponding

to the Botulinum Neurotoxin A (BoNT/A) cleavage product. For comparison we also deleted the last 26 amino acids ($\Delta 26$ mutant), corresponding to cleavage by BoNT/E. When raising $[Ca^{2+}]_i$ to 20-30 μM , neither of these two mutants seemed to support secretion, when compared to SNAP-25 *null* cells (Fig. 3A). The $\Delta 26$ deletion actually acted as a dominant negative, depressing secretion to below SNAP-25 *null* levels. In the same cells we performed a second stimulation, increasing the post-flash $[Ca^{2+}]_i$ to $>100 \mu M$ (Fig. 3B). Under these conditions a large increase in cell membrane capacitance is normally observed, which does not correlate with the amperometric current and has been attributed to the fusion of another population of vesicles that does not contain catecholamines (Xu et al., 1998). Therefore, under these conditions we evaluated the integrated amperometric current as a measure of catecholamine secretion (Materials and methods). The released amperometric charge was significantly higher in the $\Delta 9$ mutation than in SNAP-25 *null* cells, whereas the $\Delta 26$ was still dominant-negative when comparing to the *null* (Fig. 3B lower panel) These data show that the $\Delta 9$ mutation can drive secretion of catecholamine-containing vesicles; however it does so at much higher $[Ca^{2+}]_i$ – even higher than the L78A/L81A/M202A triple mutation. The $\Delta 26$ mutation, on the other hand, seems unable to support secretion at all.

We then returned to alanine substitutions, and introduced mutations into layer +5 (M71A/I192A). This mutation showed a very dramatic phenotype (Fig. 3C-D): secretion was completely eliminated. In 18 cells from 3 preparations expressing this mutant only in one cell were a few amperometric spikes detected upon stimulation – secretion was also not restored when increasing $[Ca^{2+}]_i$ to $>100 \mu M$ (Fig. 3D). We noticed that these cells appeared to be smaller than normal, and this was confirmed by capacitance measurements (layer +5: 4.0 ± 0.2 pF, N=18; WT: 7.9 ± 0.4 pF, N=26, $P<0.001$). A similar mutation in layer +4 (I67A/N188A) also did not rescue secretion to anywhere near WT levels, even though amperometric spikes were seen frequently upon stimulation (total capacitance increase at 5 s after a flash: 35 ± 7.7 fF, N=18 cells, in the mutant compared to 370 ± 44 fF, N=24 cells in WT rescued cells, $P<0.001$). We also overexpressed the $\Delta 26$, layer +5 and layer +4 mutations in WT cells expressing endogenous SNAP-25, where all mutations led to a near-elimination of secretion (not shown). Thus, these mutations are dominant negative, indicating that

they can still interact with their cognate SNARE partners (syntaxin, synaptobrevin), but that the formed complexes are non-productive for fusion.

In conclusion, we have identified a number of C-terminal mutations leading to graded effects on the maximal rate of exocytosis triggering, establishing the sequence: layer +5 mutation < $\Delta 9$ < L78A/L81A/M202A < L81A/M202A < L81A \approx WT. In the following, we turned to biochemical measurements in order to investigate whether there is a correlation between these effects and the *in vitro* properties of the SNARE complex.

The SNARE complex contains two functional domains that can fold/unfold independently

SNARE assembly/disassembly exhibits pronounced hysteresis, indicative of a kinetic barrier between the assembled and unfolded states (Fasshauer et al., 2002). This feature makes it impossible to reach equilibrium within an experimentally accessible time scale, but at the same time it opens a rare possibility for studying both the assembly and disassembly reactions in isolation, without interconversions. Hence, thermal unfolding experiments give insights into the stability of the four-helix bundle, but do not reveal the free energy of the system, since at the temperatures at which the complex unfolds assembly is blocked. Similarly, the assembly reaction can be isolated by mixing the SNAREs at room temperature, at which disassembly is exceedingly slow. Since the formation of the complex is accompanied by a large increase in α -helical structure, CD spectroscopy can be used to monitor complex assembly and disassembly.

It has been shown that N-terminal truncations in SNAP-25 severely impair assembly of a ternary SNARE complex, whereas C-terminal deletions ($\Delta 9$ and $\Delta 26$) do not (Fasshauer and Margittai, 2004). This is because N-terminal nucleation is rate limiting for assembly *in vitro*. In line with these findings, all C-terminal alanine mutants were able to normally assemble into a binary syntaxin/SNAP-25 as well as into a ternary complex. (Fig. 4A). Next, thermal denaturation experiments on *in vitro* assembled ternary SNARE ‘core complexes’ were carried out. The WT complex unfolded in a single transition at $\sim 89^\circ\text{C}$ (Fig. 4B). The melting curve of the SNARE complex containing the single layer +8 mutation (L81A) was almost undistinguishable from wild type. When the double (L81A/M202A) or the triple

(L78A/L81A/M202A) SNAP-25 mutations were analyzed, a small deviation from a single step unfolding behavior was observed. This can be rationalized by postulating that the mutations lead to a loosening of the very C-terminal portion of the complexes, which appears to fall apart at slightly lower temperatures than the rest of the four-helix bundle. Remarkably, a very clear two-step unfolding process was detected for the $\Delta 9$ deletion and the layer +5 mutation (M71A/I192A) (Fig. 4B). The two-step unfolding process suggests that the C-terminal portion of the SNARE bundle can unfold independently of the N-terminal portion. This is the first clear structural evidence that two distinct domains do reside in the extended SNARE bundle. The first unfolding step occurred at different temperatures with the different mutations, establishing the sequence: layer +5 mutation < $\Delta 9$ < L78A/L81A/M202A < L81A/M202A < L81A \approx WT. Thereby, the temperature of the first unfolding step scales with the severity of the mutation for exocytosis, suggesting that the defect on secretion depends on the destabilization of the C-terminal end of the SNARE complex. However, we noticed that the layer +4 mutation (I67A/N188A) did not exhibit two-step unfolding, but rendered the entire four-helix bundle less stable ($\sim 81^\circ\text{C}$; not shown), even though it is a strong dominant-negative for secretion. It is possible that the layer +4 is so far removed from the C-terminal end that its mutation compromises the whole complex, rather than just the C-terminal end (see Discussion).

So far the mutations analyzed indicate that the fastest phase of exocytosis that we can resolve (denoted exocytosis triggering) is affected by mutations that specifically destabilize the C-terminal end of the SNARE complex, and that this end of the complex can fold/unfold independently of the rest. This suggests that SNARE assembly – probably of its C-terminal end – is intimately linked to exocytosis triggering and does not occur in an upstream priming step. This renders the first scenario for SNARE action (Fig. 1A) unlikely.

Expression and targeting of mutated SNAP-25 to the plasma membrane

An alternative explanation for the graded effect of our C-terminal mutations could be defective expression or targeting to the plasma membrane. This appeared unlikely, since most investigations have shown that palmitoylation in the SNAP-25 linker, and not binding to SNARE partners, is necessary and sufficient for correct plasma membrane targeting (Salaün et al., 2004). Nevertheless, we investigated membrane

targeting and the overexpression level of SNAP-25 mutations using isolated plasma membrane sheets. These data confirmed that similar amounts of SNAP-25 mutants were targeted to the plasma membrane (Fig. 5). The expression level was found to be ~10-fold over the level in wildtype cells. We have previously shown that overexpression of wildtype SNAP-25 does not impair secretion in chromaffin cells (Sørensen et al., 2003).

Alanine substitutions in the centre of the SNARE complex affect the priming reaction

In the next experimental series we introduced alanines pairwise into the central SNARE layers. The zero layer is special, because here a charged arginine from synaptobrevin interacts with three glutamines (Fig. 1D). Nevertheless, alanine substitutions into layers -1 (L50A/I171A), 0 (Q53A/Q174A), +1 (L57A/I178A) and +2 (V60A/I181A) had very similar effects on exocytosis (Fig. 6). In all cases the only parameters significantly changed were the sustained component of release (all mutations, Fig. 6Ac, Bc, Cc and Dc), and the size of the fast exocytotic burst (significantly affected in layer -1, 0, and +1, but not in layer +2 even though the same tendency was seen, Fig. 6Ab, Bb, Cb, Db). In contrast, the time constants of the fast and slow burst of release were unchanged (Fig. 6Ad-e, Bd-e, Cd-e, Dd-e). Inspection of capacitance and amperometric traces scaled to WT amplitude confirmed that the kinetics of fast phase secretion were unchanged (Fig. 6Af, Bf, Cf, Df). Thus, with mutations in the central part of the SNARE complex the sustained component of release is slowed down, which is an indication that priming of new vesicles for release is impaired. The reduction in the size of the fast burst leads to the same conclusion: fewer vesicles had been made ready for fast release before stimulation. However, the kinetics of fusion of those vesicles that were already primed at the time of stimulation remained unaffected. These data are qualitatively in agreement with overexpression experiments in bovine chromaffin cells targeting the zero layer (Wei et al., 2000). We show here that this effect is not special for the zero layer, but is shared by neighboring layers, and that the effect is seen with mutations that do not impose steric hindrance of SNARE complex formation.

Alanine substitutions in the N-terminal end of the SNARE complex fail to modify secretion

Interestingly, alanine substitutions in the outermost N-terminal layers: -7 (T29A/L150A) and -6 (M32A/V153A) only caused a small depression of mean secretion (Fig. 7). Upon kinetic analysis, however, neither the burst components nor the sustained rate of release were significantly reduced (Fig. 7Ab-c, Bb-c). Most importantly, the triggering phase of secretion was unchanged by both mutations (Fig. 7Ad-e, Bd-e). This conclusion is also reached when inspecting scaled capacitative and amperometric traces (Fig. 7Af, Bf). Thus, mutations in the very N-terminal layers did not significantly affect exocytosis.

Formation rate and stability of SNARE complexes with central and N-terminal mutations

We next investigated the assembly of SNARE complexes with mutations in the N-terminal end and in the middle. Both mutations in the N-terminal end of the complex (layers -6 and -7) strongly inhibited the formation of both the binary syntaxin/SNAP-25 complex and the ternary complex with synaptobrevin (layer -6 see Fig. 8A). The mutations in the central portion of the SNARE bundle also affected assembly: *e.g.* the layer -1 mutant slowed the binary and ternary SNARE interaction (Fig. 8A). These data show that N-terminal mutations change the rate of assembly of the binary and ternary SNARE complex, and at least part of this effect extends into the central portion of the SNARE bundle. It should be stressed that the measurements in Fig. 8A do not allow statements about the kinetics of synaptobrevin binding to the syntaxin:SNAP-25 1:1 complex, because of the spontaneous formation of a 2:1 syntaxin:SNAP-25 complex *in vitro*. Thermal denaturation experiments revealed that the mutations decreased the stability of the ternary SNARE complex compared to WT, however two-step disassembly was not observed, except for a tendency in the Layer 0 mutation (Fig. 8B).

The biochemical data thus show that all our alanine mutations destabilized the SNARE complex - also those mutations in layers -6 and -7 which did not have significant effects on secretion (Fig. 7). At the same time, those mutations led to a dramatic inhibition of *in vitro* SNARE complex formation, even though secretion was intact. This reveals the existence of a kinetic step in SNARE complex assembly that is rate limiting *in vitro* but not *in vivo* (see Discussion).

The energy available for fusing the membranes

The mutations in the N-terminal and the middle of the complex showed physiological effects on kinetic steps upstream of Ca^{2+} -triggering (priming), whereas C-terminal mutations led to two-step disassembly of the SNARE complex and effects on the Ca^{2+} -triggering step itself. This supports the two-step assembly model in Fig. 1C, in which fusion coincides with SNARE complex assembly across the C-terminal layers. This raises the question whether C-terminal SNARE assembly can exert force, which could be used to fuse the membranes. However, the formation energy of the SNARE complex cannot be measured biochemically, because of the folding/unfolding hysteresis (Fasshauer et al., 2002). Instead, we used free energy perturbation simulations to assess the change in structure and thermodynamic stability introduced by some of the C-terminal mutations that cause a slow-down of secretion. This gives a lower estimate of the total energy that can be made available by assembly across the last two layers. An assumption behind these calculations is that the mutations do not cause major structural changes. Based on the unfolding experiments in Fig. 4B this assumption appears reasonable when calculations are made at physiological temperatures and restricted to mutations in the last two hydrophobic layers.

Simulations were done by mutating the amino acids to alanines 'in silico' yielding free energy differences for the mutation in both the folded and the unfolded state (ΔG). The difference between the two ($\Delta\Delta G$) provides an estimate for the amount of destabilization of the complex. The results in Table 1 show that the single, double and triple C-terminal mutations progressively destabilize the complex. The amount of destabilization correlates with the experimentally observed slow-down of secretion for these mutations. The $\Delta\Delta G$ for the triple mutation of 45 kJ/mol indicates that assembly across the last layers may make substantial amounts of energy available for fusing of the membranes.

DISCUSSION

Sequential N- to C-terminal 'zipping-up' of the SNARE complex

In this study we have interfered systematically with the hydrophobic layers of the SNARE complex. We found that C-terminal mutations led to a slow-down of the fast phase of exocytosis, indicating that the C-terminal region of the complex is intimately coupled to exocytosis triggering. Thermal denaturation experiments of SNARE complexes formed with C-terminal mutations revealed a two-step unfolding process (Fig. 4B), indicating that these mutations specifically loosened the C-terminal end without affecting the remaining structure of the complex. This provides the first biochemical evidence that two functional domains reside in the extended SNARE bundle. Such a feature is a prerequisite for stepwise SNARE assembly (Fig. 1C). Free energy perturbation calculations showed that assembly of the C-terminal end of the complex might release substantial amounts of energy, which could be coupled to membrane fusion when the complex forms *in trans*. Weakening of the C-terminal portion would diminish this energy and eventually, with more disruptive mutations, SNARE assembly would surrender to the repulsive forces between two apposing membranes.

Mutations in the middle of the complex led to a specific slow-down of vesicle priming, but did not affect the fusion rate constant of primed vesicles. The simplest explanation for this finding is that chromaffin cells have at any time a certain number of vesicles with SNARE complexes in a state of assembly extending beyond the central layers. Consequently, during fusion triggering only the C-terminal layers have to assemble (Fig 1C), rendering the fusion of primed vesicles very fast, and not limited by the preceding slow N-terminal assembly process. Collectively, our findings strongly support the 'SNARE zipper model' (Hanson et al., 1997).

Mutation in the C-terminal end of the SNARE complex

The identification of a double alanine mutation in layer +5, which led to pronounced two-step unfolding in thermal melts, should make it possible to study the partly assembled ternary complex in detail using structural methods. The lack of two-step unfolding in the neighboring layer +4 mutation may mean that layer +4 is close to the interface between zipped and unzipped layers in the partially assembled complex. From the scenario in Fig. 1C, it might then be expected that the layer +4 mutation has

more upstream effects on secretion than the layer +5 mutation. However, it should be pointed out that since both mutations virtually abolished secretion it is not possible to determine whether they do so by interfering with different steps (priming or triggering). It is striking that the most deleterious mutation of a SNARE protein ever described (the layer +5 mutation) was obtained by the relative conservative substitution of alanines for two larger hydrophobic amino acids in the interior of the complex. This underlines the extreme importance of the assembly of the C-terminal end of the complex for secretion. The critical region around layer +5 has also been identified in other studies. Thus, genetic screens in *C. elegans* for individuals with defective acetylcholine secretion identified mutations in layers +4, +5 and +6 (Saifee et al., 1998; Nonet et al., 1998). In *Drosophila* a double mutation of syntaxin in layers +4 and +5 strongly reduced release (Fergestad et al., 2001), whereas more N-terminal layer mutations led to milder phenotypes (Wu et al., 1999; Rao et al., 2001). We suggest that this area defines the interface between two functional domains in the SNARE complex.

Previous work on mouse chromaffin cells showed that some secretion persists in the absence of SNAP-25 (Sørensen et al., 2003), possibly indicating substitution by another homologue (SNAP-23/SNAP-29). The identification in the present work of two constructs, the $\Delta 26$ deletion and the layer +5 mutation, which inhibited residual secretion, indicates that mutation of SNAREs can block secretion even more effectively than deletion. This is consistent with the idea that the residual fusion events in the SNAP-25 *null* also fuse using a SNARE complex. Functional substitution of one SNARE for another was recently shown for cellubrevin and synaptobrevin 2 (Borisovska et al., 2005).

Previous data on bovine chromaffin cells overexpressing the $\Delta 9$ deletion were interpreted as a selective loss of the RRP, whereas the other releasable vesicle pool – the SRP – persisted (Wei et al., 2000). Here we showed that when overexpressed in SNAP-25 *null* cells the $\Delta 9$ deletion cannot support secretion at 20–30 μM $[\text{Ca}^{2+}]$, but higher calcium concentrations can partly overcome the defect. This finding is in agreement with data obtained in neurons after BoNT/A-cleavage (Capogna et al., 1997; Trudeau et al., 1998; Gerona et al., 2000; Sakaba et al., 2005). Molecularly, this was explained by defective Ca^{2+} -dependent synaptotagmin binding to SNARE complexes containing truncated SNAP-25 (Gerona et al., 2000). In the

present investigation we have arranged the $\Delta 9$ -mutation into a sequence of mutations causing progressive destabilization of the C-terminal end of the complex. This makes it likely that the destabilization of the C-terminal end of the SNARE complex is causative also for the effect of the $\Delta 9$ deletion. However, if final zipping of the last couple of SNARE layers happens simultaneously with Ca^{2+} -binding to synaptotagmin (Fig. 1C), allosteric coupling between the two processes could make zipping of the SNARE complex dependent on binding of synaptotagmin to the SNARE complex and vice versa. In this case the two explanations for the effect of the $\Delta 9$ deletion do not exclude each other.

Mutation in the N-terminal end of the SNARE complex

In vitro, the nucleation step between syntaxin and SNAP-25 is rate-limiting for SNARE assembly and it can be disturbed easily by N-terminal mutations (Fig. 7A). The reason for the slow *in vitro* nucleation probably is that this step requires the coordinated parallel alignment of three helices (Fasshauer and Margittai, 2004). However, N-terminal alanine mutations were without significant effect on exocytosis (Fig. 7). In the cell, therefore, this step is not rate limiting. This is not surprising, since priming of new vesicles for release requires only seconds, whereas assembly of SNAREs *in vitro* requires many minutes (Fig. 8A). It is usually assumed that priming is driven by specific ‘priming factors’, however the molecular action of these factors is uncertain. We suggest that what they do is to catalyze initial N-terminal SNARE complex assembly. The N-terminal and central layer mutations in SNAP-25 could be used as a starting point to molecularly dissect this step of the exocytotic cascade.

Whereas mutations in the outmost N-terminal layers were without significant effect, mutations in the central layers slowed down vesicle priming. One possibility is that the N-terminal binding of synaptobrevin may be more robustly catalyzed, and followed by spontaneous zipping across the central layers, which may be more susceptible to disruption. Another possibility is that initial synaptobrevin binding involves a longer stretch of the syntaxin:SNAP-25 precomplex, so that the perturbation of individual layers is insufficient to elicit a clear phenotype.

How to render SNARE-driven membrane fusion calcium-dependent

Two especially interesting open questions are: what keeps the half-assembled SNARE complex from ‘zipping’ all the way up prematurely, and how is this last assembly step coupled to the calcium trigger for fast exocytosis (presumably synaptotagmin 1)? The concept of a ‘clamp on exocytosis’ have been put forward by several authors, and it has been suggested that this halt may be exerted by synaptotagmin, however, there is no indication that synaptotagmin can do such a job (discussed by Koh and Bellen, 2003). Another possibility is that the SNARE complex may be intrinsically unable to assemble all the way when it faces the energy barrier created by the repulsion of the two membranes. In this situation ‘zipping’ would come to a stop. Additional energy input would then be required to allow assembly to go forward and fuse the membranes. This energy could be provided by calcium-loaded synaptotagmin binding to the target membrane, to SNAREs, or to both. This would then lead to calcium-dependent fusion, driven by the collective effort of the SNAREs and synaptotagmin.

MATERIALS AND METHODS

Chromaffin cell preparation, mutagenesis and expression.

SNAP-25 *null* embryos (E17-E19) were recovered by Cesarean section and chromaffin cells prepared as described (Sørensen et al., 2003). Mutations were introduced into a SNAP-25a containing pSFV1 plasmid (pSFV1 SNAP-25a-IRES-EGFP) using PCR mutagenesis and all constructs were sequenced. Following production of Semliki Forest Virus (SFV), chromaffin cells were infected at days 2-4 after isolation and 6-8 h. were allowed for expression of the protein before starting experiments.

Semi-quantification of membrane-bound SNAP-25

Plasma membrane sheets from mouse embryonic chromaffin cells were prepared as described (Nagy et al., 2005). Membranes were visualized using 1-(4-trimethylammoniumphenyl)-6-phenyl-1,3,5-hexatriene (TMA-DPH; Molecular Probes, Eugene, OR) and SNAP-25 and syntaxin 1 were immuno-detected as described previously (Lang et al., 2001). The amount of membrane-bound SNAP-25 was semi-quantified by measuring the average intensity of a sheet (Nagy et al., 2005). Other cell types (e.g. endothelial cells) also present in the primary culture were excluded from analysis based on their size and the much lower level of syntaxin 1 staining. At least 10 membrane sheets from each animal were analyzed and the mean value for each animal used to calculate population mean and SEM (number of animals = 4-10).

Electrophysiology, electrochemistry.

Patch-clamp capacitance measurements, measurements of intracellular calcium concentration, flash photolysis of caged calcium and amperometry were carried out as described (Sørensen et al., 2003). Capacitance and amperometric measurements were carried out in parallel, to ensure that the fusion of catecholamine-containing vesicles was being monitored. For some of the more severe mutations (those displayed in Fig. 3) we used the integrated amperometric charge as a quantitative measurement of secretion. Since secretion was low in these cases, it was necessary to correct the amperometric measurements for current-artifacts caused by illumination of the carbon fiber by the flash light and the light used to measure calcium. This was done by removing the cell using the patch pipette after each experiment, followed by

stimulation of the carbon fiber with the standard protocol. The resulting amperometric trace was subtracted from the measurements. The remaining artifact amounts to an integrated current within ± 2 pC over the course of 5 s.

Kinetic analysis of capacitance data

Capacitance traces were fitted with a sum of exponential functions, in order to separate pool sizes (appear as amplitudes of the exponentials) from the kinetics of fusion triggering (appear as time constants of the exponentials), as previously described (Sørensen et al., 2003). Data are given as mean \pm SEM and Mann-Whitney U-test was used to test statistical difference; *: $p < 0.05$; **: $p < 0.01$; ***: $p < 0.001$.

Protein purification

The basic SNARE expression constructs in a pET28a vector, cysteine-free SNAP-25A (Cys84Ser, Cys85Ser, Cys90Ser, Cys92Ser; res. 1-206), the syntaxin 1A SNARE motif (res. 180-262), and synaptobrevin 2 (res. 1-96) have been described before (Fasshauer and Margittai, 2004). For all truncations and point mutations in SNAP-25A, the cysteine-free variant was used as template. The recombinant SNARE proteins were isolated from *E. coli* and purified by Ni-NTA affinity chromatography followed by ion exchange chromatography on an Äkta system (Amersham) essentially as described (Fasshauer and Margittai, 2004). All ternary SNARE complexes were assembled overnight and purified using a Mono Q-column. Protein concentration was determined by absorption at 280 nm.

CD spectroscopy measurements

CD measurements were performed using a Jasco model J-720 instrument. All experiments were carried out in 20 mM sodium phosphate or 20 mM TRIS, pH 7.4, in the presence of 100 mM NaCl and 1 mM DTT. For thermal denaturation experiments, about 10 mM purified ternary SNARE complexes were heated in Hellma quartz cuvettes with a pathlength of 0.1 cm. The ellipticity at 222 nm was recorded between 25 and 95°C at a temperature increment of 30 °C/h. Kinetic measurements were carried out in 1 cm quartz cuvettes at 25 °C. About 2 mM of the individual proteins were mixed and the increase in α -helical signal was followed at 222 nm.

Energy perturbation calculations

See supplementary Materials and methods.

ACKNOWLEDGEMENTS

We thank Reinhard Jahn, Thorsten Lang and Erwin Neher for critically commenting on the manuscript and for on-going discussions. We thank Dirk Reuter and Wolfgang Berning-Koch for expert technical assistance and Hartmut Sebesse for artwork. This work was supported by the Boehringer Ingelheim Foundation (I.M.), the Deutsche Forschungsgemeinschaft (DFG): SFB523/TP4, SO 708/1-1 (J.B.S.), and GRK521 (G.N.).

REFERENCES

- An SJ, Almers W (2004) Tracking SNARE complex formation in live endocrine cells. *Science* **306**: 1042-1046.
- Borisovska M, Zhao Y, Tsytsyura Y, Glyvuk N, Takamori S, Matti U, Rettig J, Südhof T, Bruns D (2005) v-SNAREs control exocytosis of vesicles from priming to fusion. *EMBO J* **24**: 2114-2126.
- Capogna M, McKinney RA, O'Connor V, Gähwiler BH, Thompson SM (1997) Ca^{2+} or Sr^{2+} partially rescues synaptic transmission in hippocampal cultures treated with botulinum toxin A and C, but not tetanus toxin. *J Neurosci* **17**: 7190-7202.
- Chen YA, Scales SJ, Patel SM, Doung YC, Scheller RH (1999) SNARE complex formation is triggered by Ca^{2+} and drives membrane fusion. *Cell* **97**: 165-174.
- Chen YA, Scales SJ, Scheller RH (2001) Sequential SNARE assembly underlies priming and triggering of exocytosis. *Neuron* **30**: 161-170.
- Fasshauer D (2004) Structural insights into the SNARE mechanism. *Biochim Biophys Acta* **1641**: 87-97.
- Fasshauer D, Antonin W, Subramaniam V, Jahn R (2002) SNARE assembly and disassembly exhibit a pronounced hysteresis. *Nat Struct Biol* **9**: 144-151.
- Fasshauer D, Margittai M (2004) A transient N-terminal interaction of SNAP-25 and syntaxin nucleates SNARE assembly. *J Biol Chem* **279**: 7613-7621.
- Fergestad T, Wu MN, Schulze KL, Lloyd TE, Bellen HJ, Broadie K (2001) Targeted mutations in the syntaxin H3 domain specifically disrupt SNARE complex function in synaptic transmission. *J Neurosci* **21**: 9142-9150.
- Fiebig KM, Rice LM, Pollock E, Brunger AT (1999) Folding intermediates of SNARE complex assembly. *Nat Struct Biol* **6**: 117-123.

Gerona RRL, Larsen EC, Kowalchuk JA, Martin TFJ (2000) The C terminus of SNAP25 is essential for Ca^{2+} -dependent binding of synaptotagmin to SNARE complexes. *J Biol Chem* **275**: 6328-6336.

Han X, Wang CT, Bai J, Chapman ER, Jackson MB (2004) Transmembrane segments of syntaxin line the fusion pore of Ca^{2+} -triggered exocytosis. *Science* **304**: 289-292.

Hanson PI, Heuser JE, Jahn R (1997) Neurotransmitter release – four years of SNARE complexes. *Curr Opin Neurobiol* **7**: 310-315.

Haro Ld, Ferracci G, Opi S, Iborra C, Quetglas S, Miquelis R, Lévêque C, Seagar M (2004) Ca^{2+} /calmodulin transfers the membrane-proximal lipid-binding domain of the v-SNARE synaptobrevin from cis to trans bilayers. *Proc Natl Acad Sci* **101**: 1578-1583.

Hu K, Carroll J, Fedorovich S, Rickman C, Sukhodub A, Davletov B (2002) Vesicular restriction of synaptobrevin suggests a role for calcium in membrane fusion. *Nature* **415**: 646-650.

Hua SY, Charlton MP (1999) Activity-dependent changes in partial VAMP complexes during neurotransmitter release. *Nat Neuroscience* **2**: 1078-1083.

Koh TW, Bellen HJ (2003) Synaptotagmin I, a Ca^{2+} sensor for neurotransmitter release. *Trends in Neurosci* **26**: 413-422.

Kweon DH, Kim CS, Shin YK (2003) Regulation of neuronal SNARE assembly by the membrane. *Nat Struct Biol* **10**: 440-447.

Lang T, Bruns D, Wenzel D, Riedel D, Holroyd P, Thiele C, Jahn R (2001) SNAREs are concentrated in cholesterol-dependent clusters that define docking and fusion sites for exocytosis. *EMBO J* **20**: 2202-2213.

Martin TF (2003) Tuning exocytosis for speed: fast and slow modes. *Biochim Biophys Acta* **1641**: 157-165.

Matos MF, Mukherjee K, Chen X, Rizo J, Südhof TC (2003) Evidence for SNARE zippering during Ca^{2+} -triggered exocytosis in PC12 cells. *Neuropharmacology* **45**: 777-786.

Melia TJ, Weber T, McNew JA, Fisher LE, Johnston RJ, Parlati F, Mahal LK, Söllner TH, Rothman JE (2002) Regulation of membrane fusion by the membrane-proximal coil of the t-SNARE during zippering of SNAREpins. *J Cell Biol* **158**: 929-940.

Nagy G, Milosevic I, Fasshauer D, Muller EM, de Groot BL, Lang T, Wilson MC, Sorensen JB (2005) Alternative Splicing of SNAP-25 Regulates Secretion through Nonconservative Substitutions in the SNARE Domain. *Mol Biol Cell* 2005 Sep 29; [Epub ahead of print]

Nonet ML, Saifee O, Zhao H, Rand JB, Wei L (1998) Synaptic transmission deficits in *Caenorhabditis elegans* synaptobrevin mutants. *J Neurosci* **18**: 70-80.

Rao SJ, Stewart BA, Rivlin PK, Vilinsky I, Watson BO, Lang C, Boulianne G, Salpeter MM, Deitcher DL (2001) Two distinct effects on neurotransmission in a temperature-sensitive SNAP-25 mutant. *EMBO J* **20**: 6761-6771.

Saifee O, Wei L, Nonet ML (1998) The *Caenorhabditis elegans unc-64* locus encodes a syntaxin that interacts genetically with synaptobrevin. *Mol Biol Cell* **9**: 1235-1252.

Sakaba T, Stein A, Jahn R, Neher E (2005) Distinct kinetic changes in neurotransmitter release after SNARE protein cleavage. *Science* **309**: 491-494.

Salaün C, James DJ, Greaves J, Chamberlain LH (2004) Plasma membrane targeting of exocytic SNARE proteins. *Biochim Biophys Acta* **1693**: 81-89.

Schoch S, Deak F, Königstorfer A, Mozhayeva M, Sara Y, Südhof TC, Kavalali ET (2001) SNARE function analyzed in synaptobrevin/VAMP knockout mice. *Science* **294**: 1117-1122.

Sørensen JB (2004) Formation, stabilisation and fusion of the readily-releasable pool of secretory vesicles. *Pflügers Arch* **448**: 347-362.

Sørensen JB, Nagy G, Varoqueaux F, Nehring RB, Brose N, Wilson MC, Neher E (2003) Differential control of the releasable vesicle pools by SNAP-25 splice variants and SNAP-23. *Cell* **114**: 75-86.

Sutton RB, Fasshauer D, Jahn R, Brunger AT (1998) Crystal structure of a SNARE complex involved in synaptic exocytosis at 2.4 Å resolution. *Nature* **395**: 347-353.

Trudeau LE, Fang Y, Haydon PG (1998) Modulation of an early step in the secretory machinery in hippocampal nerve terminals. *Proc Natl Acad Sci USA* **95**: 7163-7168.

Voets T (2000) Dissection of three Ca^{2+} -dependent steps leading to secretion in chromaffin cells from mouse adrenal slices. *Neuron* **28**: 537-545.

Washbourne P, Thompson PM, Carta M, Costa ET, Mathews JR, Lopez-Bendito G, Molnar Z, Becher MW, Valenzuela CF, Partridge LD, Wilson MC (2002) Genetic ablation of the t-SNARE SNAP-25 distinguishes mechanisms of neuroexocytosis. *Nat Neurosci* **5**: 19-26.

Weber T, Zemelman BV, McNew JA, Westermann B, Gmachl M, Parlati F, Söllner TH, Rothman JE (1998) SNAREpins: minimal machinery for membrane fusion. *Cell* **92**: 759-772.

Wei S, Xu T, Ashery U, Kollwe A, Matti U, Antonin W, Rettig J, Neher E (2000) Exocytotic mechanism studied by truncated and zero layer mutants of the C-terminus of SNAP-25. *EMBO J* **19**: 1279-1289.

Wu MN, Fergestad T, Lloyd TE, He Y, Broadie K, Bellen HJ (1999) Syntaxin 1A interacts with multiple exocytic proteins to regulate neurotransmitter release in vivo. *Neuron* **23**: 593-605.

Xu T, Binz T, Niemann H, Neher E (1998) Multiple kinetic components of exocytosis distinguished by neurotoxin sensitivity. *Nat Neurosci* **1**: 192-200.

Xu T, Rammner B, Margittai M, Artalejo AR, Neher E, Jahn R (1999) Inhibition of SNARE complex assembly differentially affects kinetic components of exocytosis. *Cell* **99**: 712-722.

FIGURE LEGENDS

Fig. 1. Alternative scenarios for SNARE action. Orange protein: synaptotagmin; blue: synaptobrevin, red: syntaxin; green: SNAP-25; red dots: Ca^{2+} . Note that the drawing is not to scale. In all scenarios we assume that a 1:1 SNAP-25:syntaxin receptor complex comprising both helices of SNAP-25 has already formed on the plasma membrane. *A.* SNARE complex assembly takes place before calcium-triggering of fusion. During the triggering step, the SNARE complex may therefore be dispensable (pale colors). *B.* SNARE complex assembly happens across the entire length after calcium-triggering by synaptotagmin. *C.* The SNARE complex partly assembles upstream of triggering. Calcium-triggering and final assembly of the SNARE complex are coupled. *D.* Sequence of the SNARE ‘core complex’, with mutated layer residues emphasized in red. Syb: synaptobrevin; syx: syntaxin; SN1: N-terminal helix of SNAP-25A; SN2: C-terminal helix of SNAP-25A.

Fig. 2. Alanine substitutions in the C-terminal end of the SNARE complex slow down the triggering phase of exocytosis.

A. a. Averaged results for SNAP-25 *null* cells overexpressing WT SNAP-25 (rescue, red) or SNAP-25 M202A (blue). Top panel: Mean \pm SEM $[\text{Ca}^{2+}]_i$ before (point on left ordinate axis) and after a brief flash of UV-light liberated calcium from the calcium-cage (at 0.5 s). Middle panel: mean capacitance increase; *insert*: capacitance traces scaled to similar amplitude 1 s after the flash to allow inspection of the fast phase of secretion. Bottom panel: Amperometric current (noisy traces, left ordinate axis) and cumulative amperometric charge (smooth traces, right ordinate axis) obtained simultaneously with the capacitance trace. Number of cells: N=38 (WT) and N=27 (M202A). The mean results show no obvious effect of the M202A mutation. *Ab-e*: results of the kinetic analysis of individual capacitance traces. *Ab*: The amplitude of the fast and slow burst of secretion corresponds to the size of the RRP and the SRP, respectively. *Ac*: The sustained rate of secretion defines the slope of the near-linear capacitance increase following the fast burst phase. *Ad*: Relationships between the fastest rate constant (1/ time constant) resolvable in the exponential fit and the post-flash $[\text{Ca}^{2+}]_i$. For WT SNAP-25 rescue this is an increasing relationship. *Ae*: Relationship between the secretory delay and the post-flash $[\text{Ca}^{2+}]_i$. For WT SNAP-25 rescue this is a decreasing relationship. *Ad-e*: Lines represent the

predictions of a sequential calcium-binding site model of the fast calcium-sensor for exocytosis (Voets, 2000) and describe the data in the WT situation.

These data show no major change in secretion upon mutation of M202 into alanine.

B. Double mutation in layer +8 (L81A/M202A) slows down the fast phase of secretion. *Ba*: the mean results show that the fast phase of secretion is slowed down in the mutant. *Bb*: capacitance (noisy traces) and cumulative amperometric charge (smooth traces) scaled to similar amplitude at 1 s after the flash. The slow-down of the fastest phase is seen in both traces. *Bc-d*: capacitance increase 0-1 s, and 1-5 s after the flash. *Be-f*: kinetic analysis. Displayed is the rate constant of the fastest resolvable phase (*e*) and the delay (*f*) for WT and mutant experiments. N=51 cells (L81A/M202A) and N=57 cells (WT).

C. Triple mutation in layers +7 and +8 (L78A/L81A/M202A) dramatically slows down the fast phase of secretion. For explanations, see *B*. With the triple mutation the secretion within the first second of stimulation is now depressed, and the secretory rates are even slower and the delays even longer than with the double mutation. N=49 cells (L78A/L81A/M202A) and N=51 cells (WT).

Fig. 3. C-terminal deletions of SNAP-25, or mutation in layer +5, display dramatic phenotypes.

A. Averaged results of deleting the C-terminal 9 ($\Delta 9$) or 26 ($\Delta 26$) last amino acids compared to SNAP-25 *null* cells. Capacitance measurements revealed no rescue of secretion by the deletions. Bottom panel: The amperometric currents were corrected for artifacts caused by illumination of the carbon fiber (Materials and methods) in order to allow quantitative analysis. Note that the amplitude of individual spikes is reduced, since these are averaged traces. The $\Delta 26$ mutation significantly reduced the amperometric charge released during the 5-s period. N=33 cells (*null*); N=27 cells ($\Delta 9$) and N=16 cells ($\Delta 26$). *B.* The same cells as in *A* were stimulated with a stronger uncaging flash, resulting in post-flash $[Ca^{2+}]_i > 100 \mu M$ (top panel). Fusion of catecholamine-containing vesicles was evaluated using the cumulative amperometric charge (bottom panel), revealing that at these higher $[Ca^{2+}]_i$ the $\Delta 9$ mutation supported significantly more secretion than the SNAP-25 *null*, whereas the $\Delta 26$ was still dominant negative.

C. Double mutation in layer +5 abolishes secretion (blue traces). Null cells from the same preparations rescued with SNAP-25 WT displayed normal secretion (black traces). D. A second flash to increase $[Ca^{2+}]_i$ to $>100 \mu M$ also did not recover secretion in the mutant. Compared to SNAP-25 *null* cells (red traces) the layer +5 mutation was dominant-negative. N=18 cells (layer +5), N=26 cells (WT rescue). The results from SNAP-25 *null* cells were obtained in separate experiments (those presented in Fig. 5B).

Fig. 4. C-terminal SNAP-25 mutations selectively destabilize the C-terminal region of the SNARE complex.

A. The assembly rates of C-terminal SNAP-25 mutants into a binary or ternary SNARE complex were similar compared to wild type SNAP-25. SNAP-25 and the SNARE motif of syntaxin were allowed to assemble first into a binary complex. The increase in α -helical signal upon complex formation was followed by CD spectroscopy at 222 nm. After complete assembly of the binary complex, synaptobrevin was added (arrow) and the formation of the ternary complex followed over time.

B. Thermal melts of purified ternary SNARE complexes containing SNAP-25 variants with C-terminal mutations or deletions. A clear deviation from a single, cooperative unfolding transition was observed for a triple alanine mutation in the last C-terminal layers (layer +7/+8 triple). Complexes containing a deletion of the last 9 C-terminal amino acids ($\Delta 9$), or a double alanine mutation in layer +5 unfolded in two separate steps. The first unfolding step probably represents the autonomous unfolding of the C-terminal region of the SNARE four-helix bundle. The unfolding temperature of the remaining SNARE bundle was only slightly reduced compared to the WT complex.

Fig. 5. Mutation of the interaction layers does not affect membrane targeting of over expressed SNAP-25.

A-B. SNAP-25 and syntaxin 1 specific immunostaining in the plasma membrane of mouse embryonic chromaffin cells. Plasma membrane sheets were generated from SNAP-25 null chromaffin cells expressing (A) SNAP-25a $\Delta 26$ and (B) SNAP-25a M71A/I192A. Sheets were immediately fixed with paraformaldehyde and

immunostained. The samples were imaged in three channels: membranes were identified in the presence of TMA-DPH dye in the blue (not shown), SNAP-25 signal was detected in the red and syntaxin 1 in the long red channel. C. Mean \pm SEM SNAP-25 immunofluorescence intensity from 4-10 WT and SNAP-25 null animals expressing SNAP-25a or SNAP-25a mutations. These experiments showed that incubation of null cells for 8 h with the Semliki Forest Virus increased the level of membrane-bound SNAP-25 to roughly 10-fold the level in SNAP-25 WT cells. A similar increase was found with all SNAP-25 mutations tested. Thus, mild disruption of SNAP-25 binding to its partners by mutation of the interaction layers, or C-terminal deletion, does not affect plasma membrane targeting or expression level.

Fig. 6. Mutation in the middle layers slow down the vesicular priming rate.

Double mutation in layer -1 (L50A/I171A) (*Aa*), layer 0 (Q53A/Q174A) (*Ba*), layer +1 (L57A/I178A) (*Ca*), and layer +2 (V60A/I181A) (*Da*) decreased mean secretion. *Ab-c*, *Bb-c*, *Cb-c*, *Cb-c*: the sustained rate of release was significantly decreased in all cases, whereas the amplitude of the fast burst was significantly depressed in layer -1, 0, and +1 mutations. *Ad-e*, *Bd-e*, *Cd-e*, *Dd-e*: time constants of fast and slow burst fusion were unchanged by these mutations. *Af*, *Bf*, *Cf*, *Df*: the mean capacitance and cumulative amperometric charge scaled to WT amplitude revealed no differences in the triggering phases of secretion. N=21 cells (layer -1), N=25 cells (WT); N=31 cells (layer 0), N=31 cells (WT); N=25 cells (layer +1), N=26 cells (WT); N=24 cells (layer +2), N=26 cells (WT).

Fig. 7. N-terminal alanine substitutions do not affect secretion.

Double mutation in layer -7 (T29A/L150A) (*Aa*) or layer -6 (M32A/V153A) (*Ba*) left mean secretion only slightly depressed. *Ab-c* and *Bb-c*: kinetic analysis showed that the size of both burst components and the sustained rates of secretion were not significantly changed. *Ad-e* and *Bd-e*: the time constants of fast and slow burst components were also unchanged. *Af* and *Bf*: The mean capacitance and cumulative amperometric charge scaled to WT amplitude at 1-s after the flash revealed no differences in the fast triggering phase of secretion. N=28 cells (layer -7), N=24 cells (WT); N=31 cells (layer -6), N=35 cells (WT).

Fig. 8. Assembly and stability of SNARE complexes with N-terminal and central double alanine layer mutations.

A. Mutations in the N-terminal and central layers perturbed the interaction of syntaxin and SNAP-25 (shown are layers -6, -1 and +2). Assembly into the ternary complex was also very slow with the layer -6 mutation, and moderately slowed down by the layer -1 mutation.

B. Central layer mutants (layer -1, 0, and +2) rendered the entire ternary SNARE complex somewhat less stable than N-terminal layer mutants (layer -7 and -6). Note that the 0-layer mutation appears to cause a slight two-step unfolding process. However, different than for the two-step unfolding processes observed for the $\Delta 9$ and +5 layer mutations (Fig. 4B), the two unfolding steps of the complex containing 0-layer mutations are only a few degrees apart ($T_{m1} \approx 73^\circ\text{C}$, $T_{m2} \approx 79^\circ\text{C}$), and it is not seen when mutating neighboring layers.

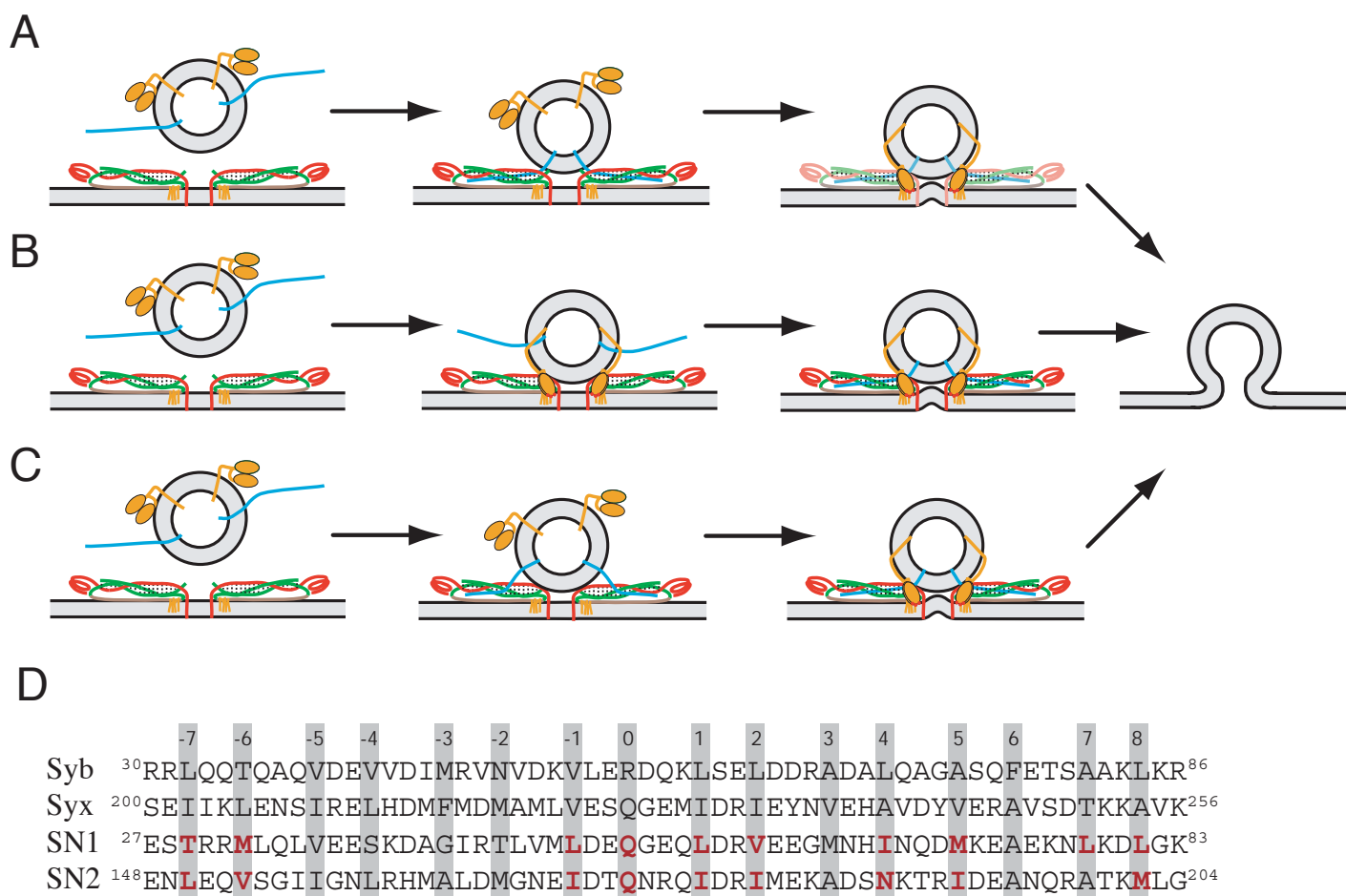


Figure 1

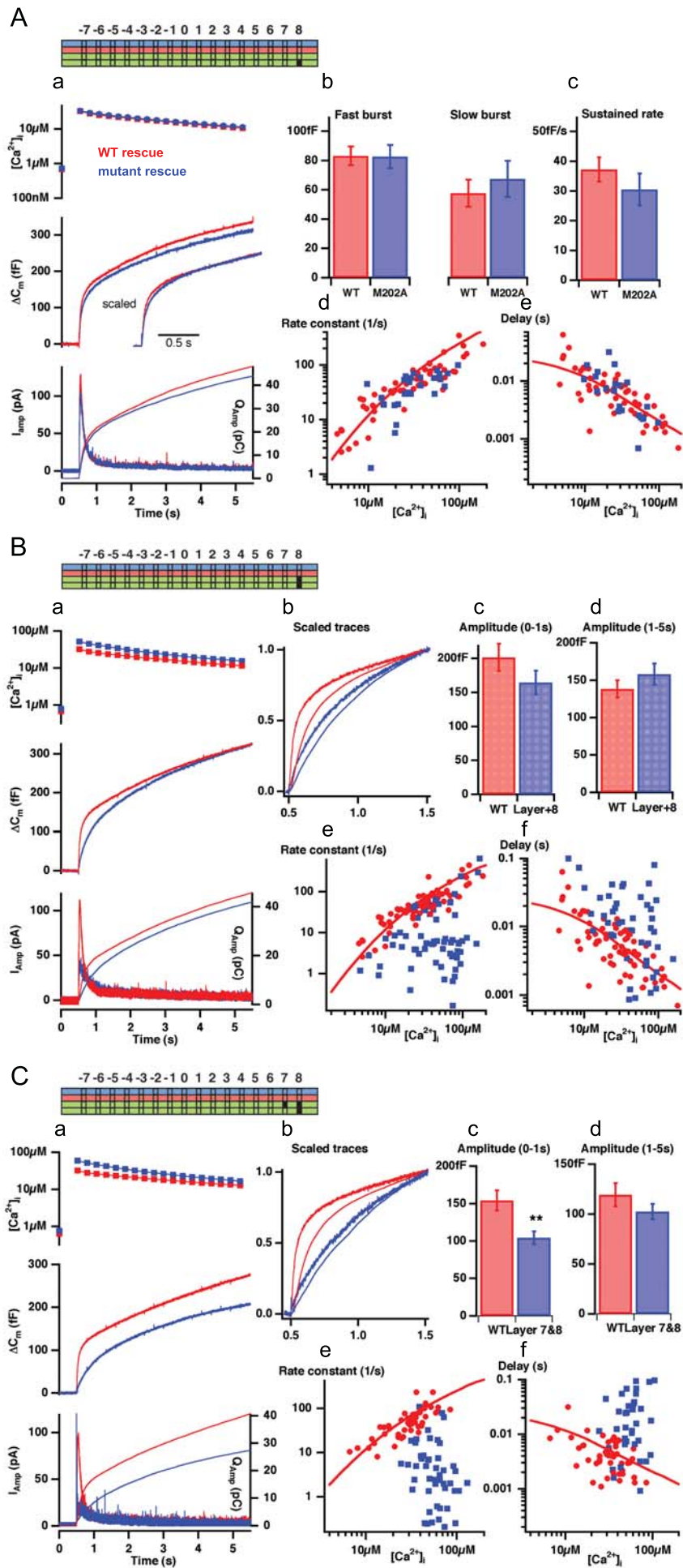


Figure 2

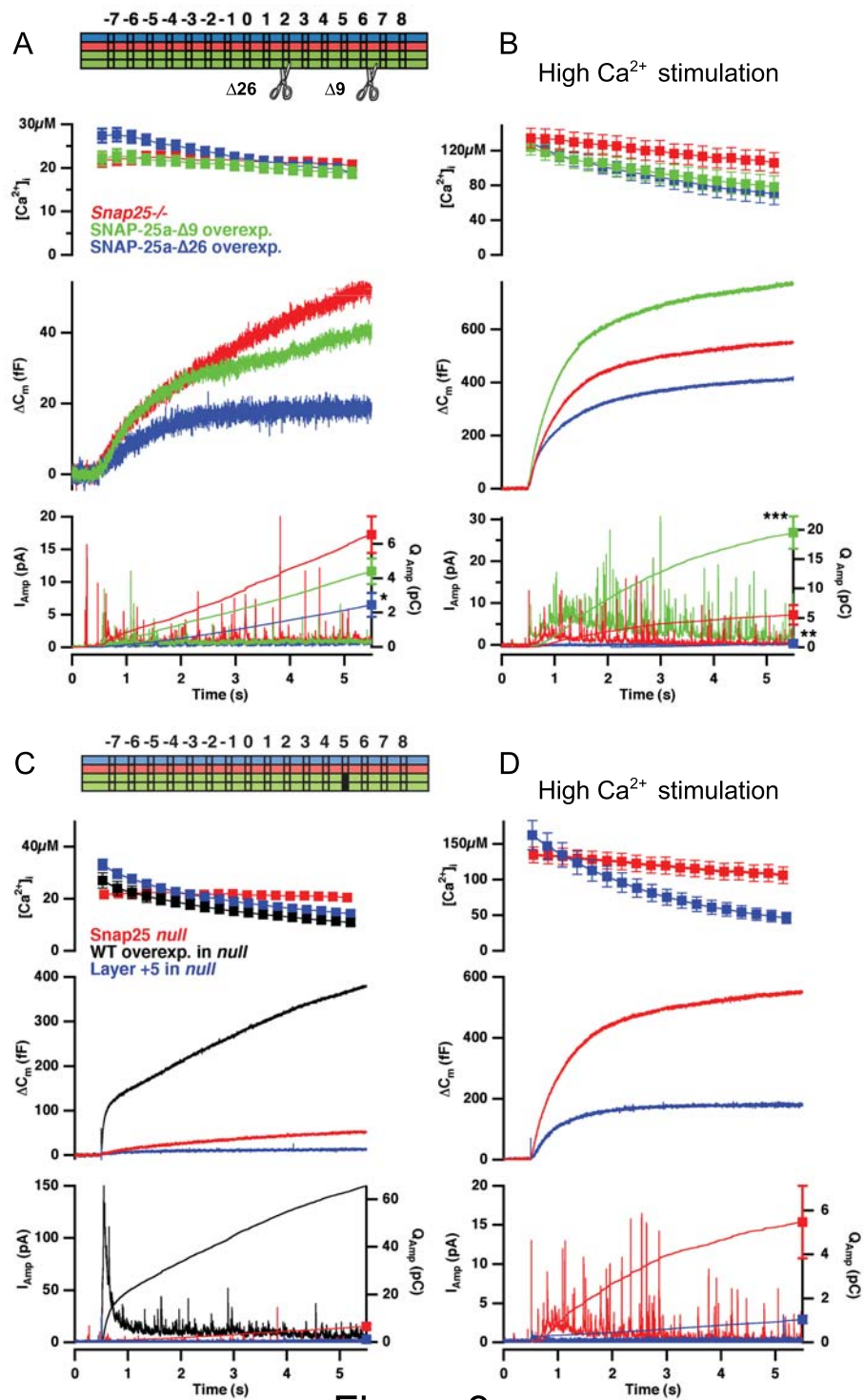


Figure 3

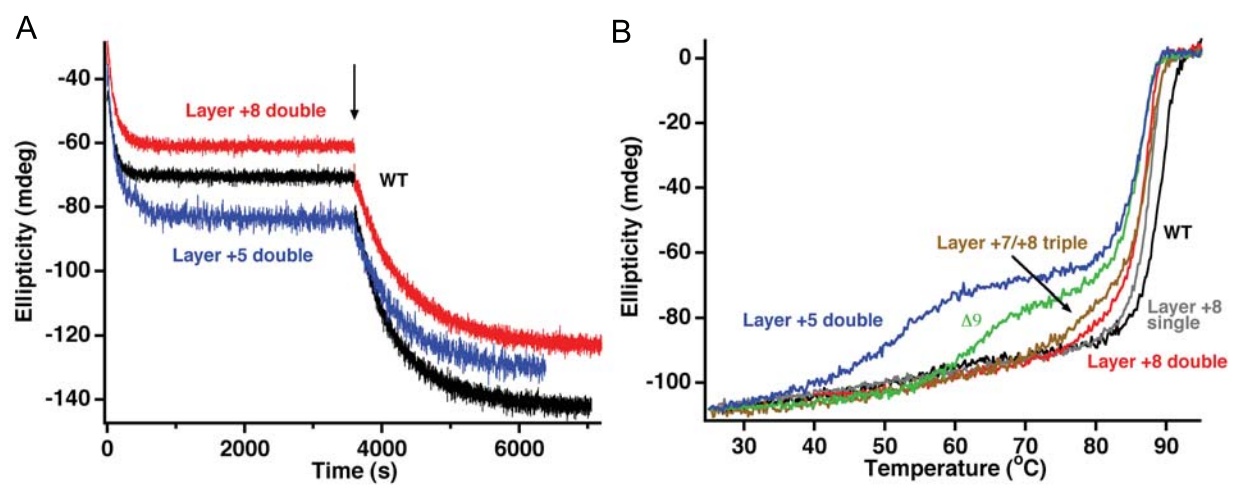


Figure 4

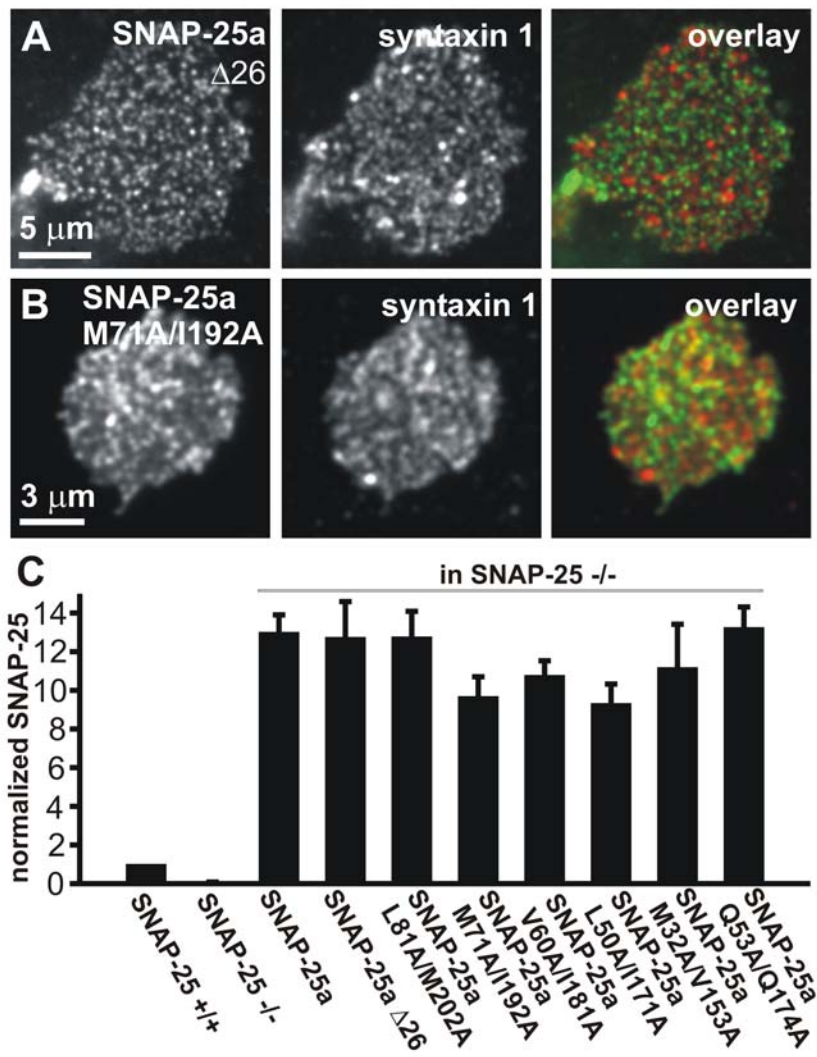


Figure 5

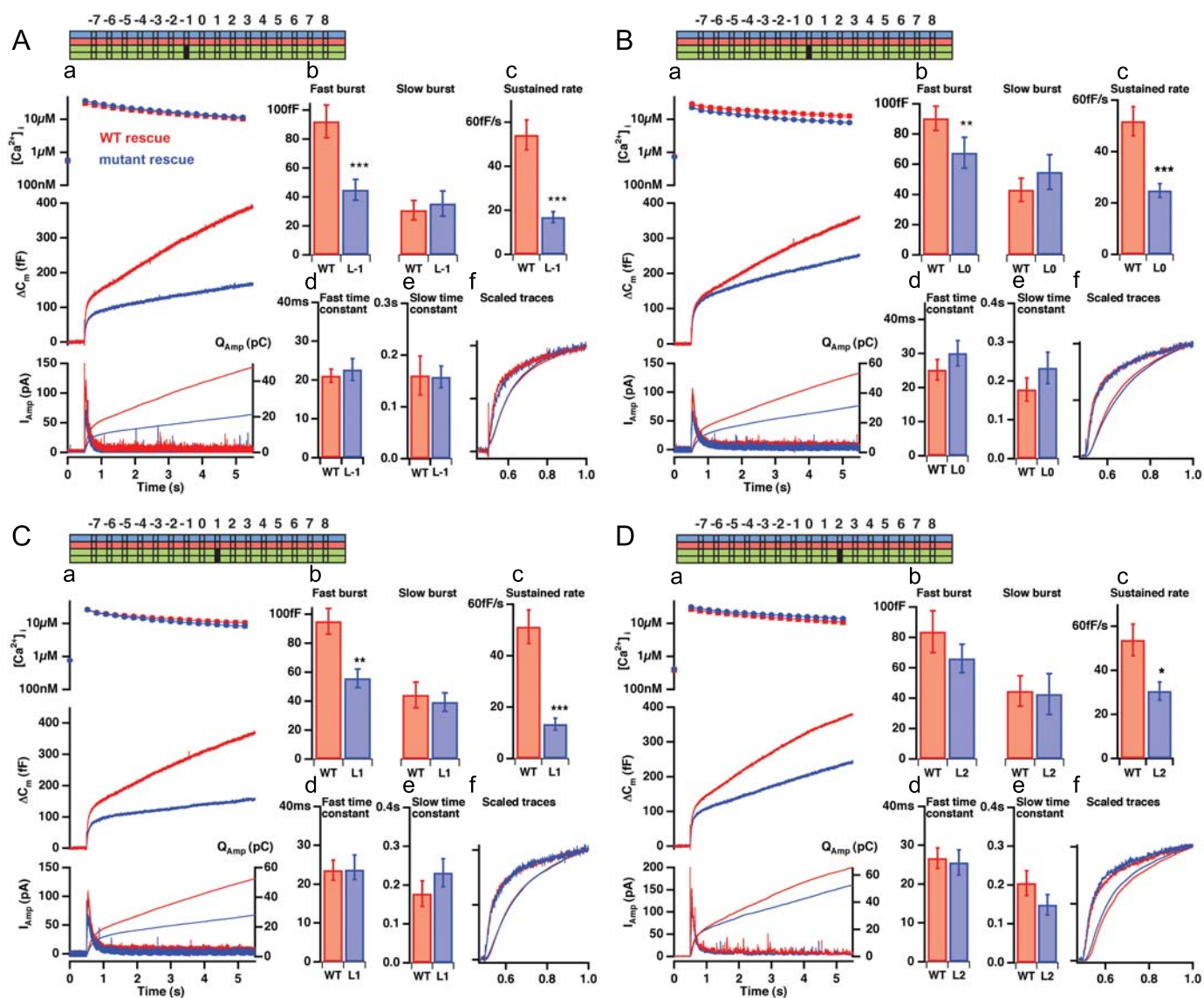


Figure 6

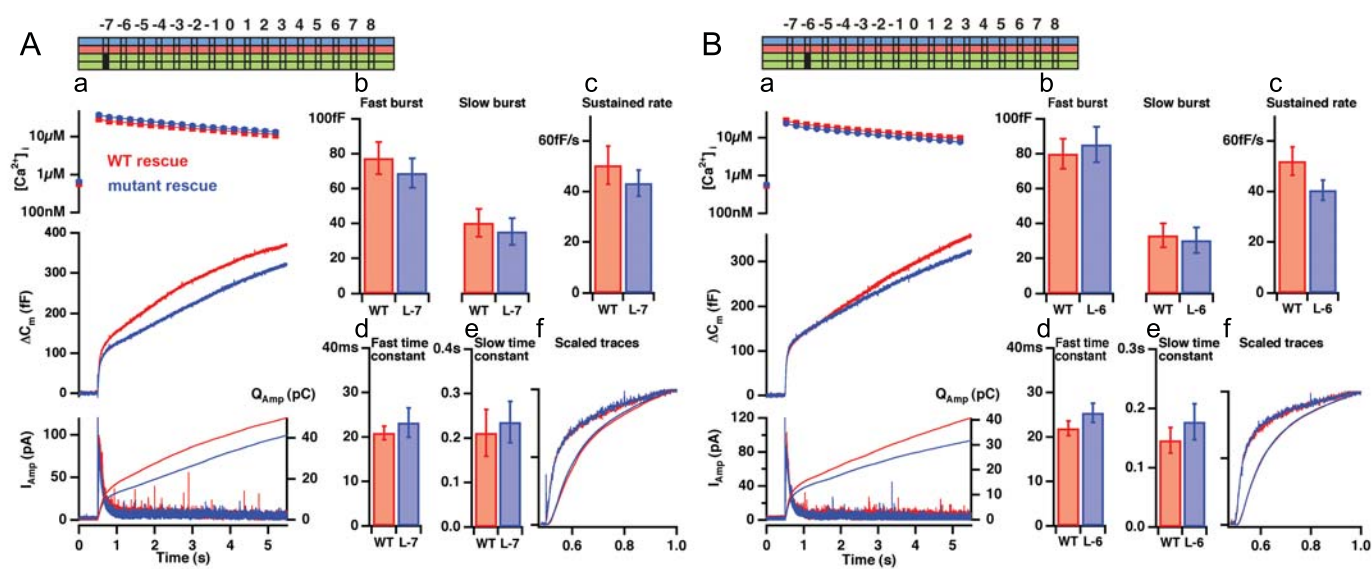


Figure 7

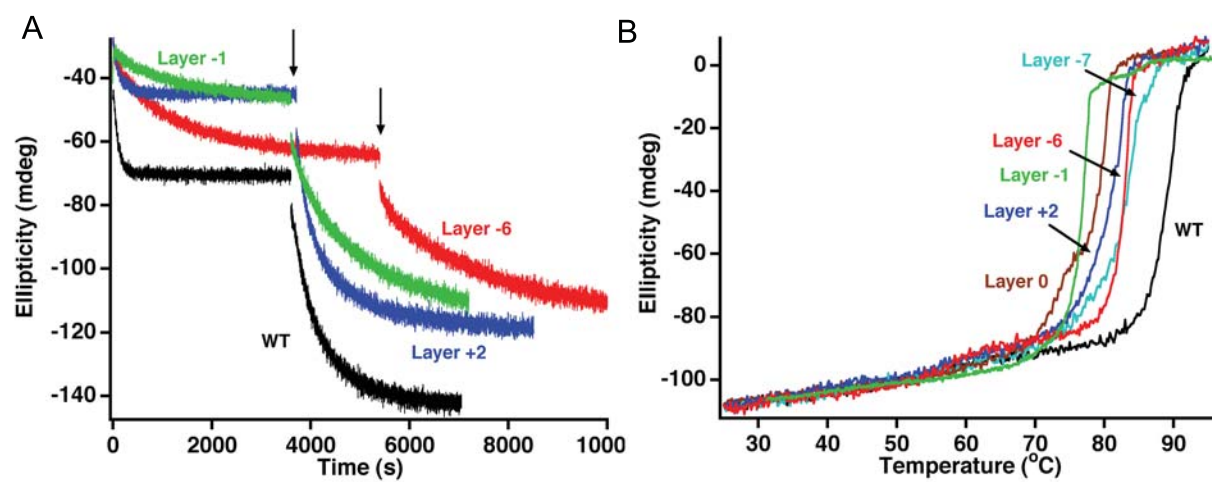


Figure 8

Table 1. Free energy perturbation calculations

Tripeptide				
	ΔG (forward) kJ/mol	ΔG (backward) kJ/mol	ΔG (average) kJ/mol	$\Delta\Delta G$ kJ/mol
L78A	1.7	5.7	3.7 ± 2.0	
L81A	3.2	4.0	3.6 ± 0.4	
M202A	7.1	6.3	6.7 ± 0.4	
Protein				
M202A	23.3	11.5	17.4 ± 5.9	10.8 ± 6.3
L81A/M202A	46.7	31.3	39.0 ± 7.7	28.7 ± 8.5
L78A/L81A/M202A	66.2	52.6	59.4 ± 6.8	45.4 ± 9.6

Table 1:

Free energy changes, ΔG , between WT and mutants for the unfolded and folded state, respectively, and differences, $\Delta\Delta G$, as an estimate of the effect of the mutation on the thermodynamic stability of the complex. An estimate for the uncertainty is obtained by comparing forward and backward ΔG values. The single, double and triple mutants display a progressive amount of destabilization with respect to the WT protein.

SUPPLEMENTAL DATA

Supplemental Figure legends

Suppl Fig. 1. Effect of the single mutation L81A in layer +8.

A. The mean results show no major effect of the mutation. *Insert:* Scaled capacitance (noisy trace) and integrated amperometry (smooth trace) reveal at most mild slow-down of secretion in the mutant cells. B. Kinetic analysis indicates that the fast burst is slightly, but significantly, reduced in the L81A mutant, whereas the slow burst and sustained components are not changed. C. The rate constant of fast release and the delay appear similar to WT in most cells, even though slower rates were found in a few cells. N=29 cells (L81A), N=30 cells (WT).

Overall, the mutation L81A in layer +8 only mildly affects secretion.

Suppl Fig. 2. Calcium ramp stimulation of double and triple mutations in layers 7 and 8.

The double (L81A/M202A) and triple (L78A/L81A/M202A) mutations were studied alongside with WT rescued cells by stimulation with Ca^{2+} -ramps (top panels). The capacitance increase (middle panels) was measured during slowly increasing calcium concentrations, and after appropriate smoothing the second derivative of the capacitance trace was used to find the point of maximal capacitance acceleration (bottom panel). This value (termed secretion threshold), was increased in the double mutation, and even more so in the triple mutation (right panel). This experiment indicates a graded effect of accumulating mutations in the C-terminal end of the SNARE complex. N=13 (WT), N=12 (L81A/M202A) and N=8 (L78A/L81A/M202A) cells.

Supplemental Materials and Methods

Energy perturbation calculations

Molecular dynamics (MD) simulations were started from the x-ray structure of the neuronal SNARE complex (chains A-D from PDB code: 1SFC (Sutton et al., 1998)). The simulation system contained 3,001 protein atoms, 8,275 SPC water molecules (Berendsen et al., 1981), and 16 sodium ions, resulting in a system size of 27,842 atoms.

MD simulations were carried out using the GROMACS simulation suite (Lindahl et al., 2001). Shake and Settle (Ryckaert et al., 1977; Miyamoto and Kollman, 1992) were applied to constrain covalent bond lengths, allowing an integration step of 2 fs. The temperature was kept constant by separately coupling ($\tau = 0.1$ ps) the protein and solvent to an external temperature bath (Berendsen et al., 1984). The pressure was kept at 1 bar by weak coupling ($\tau = 1.0$ ps) to a pressure bath (Berendsen et al., 1984). The GROMACS force field was applied, which is the GROMOS 87 force field (van Gunsteren and Berendsen, 1987) with slight modifications (Van Buuren et al., 1993) and explicit hydrogens on the aromatic side chains. Polar hydrogens were attached to the protein using the ADDHYD routine implemented in the WHAT IF package (Vriend, 1990). To equilibrate the system, 5 ns of conventional molecular dynamics were performed. At a distance smaller than 1.0 nm, electrostatic interactions were calculated explicitly, long-range electrostatic interactions were calculated by particle-mesh Ewald summation (Darden et al., 1993).

The free energy changes ΔG associated with the mutations (see Table 1) were calculated using free energy perturbation (FEP) simulations. Using a thermodynamic cycle, the difference in stability between the WT and mutant protein was estimated from difference $\Delta\Delta G$ in the free energy changes ΔG for the mutation in the folded protein and in a model of the unfolded state (modeled as a tripeptide in solution). All FEP simulations were carried out using the method of slow growth (Bash et al., 1987, Ossig et al., 2000), i.e. by gradually introducing the mutation into the simulated system (using soft-core parameters $\alpha=0$ (resulting in linear interpolation of the non-bonded interactions) and $\sigma=0.3$ nm) during a simulation period of 1 ns. For both the folded and unfolded state (tripeptide), forward and backward mutations were simulated to ensure reversibility and to quantify hysteresis effects for error estimation.

All FEP simulations started from the equilibrated structure, using a time step of 1 fs and cut-off radii of 1.0 and 1.4 nm for the van der Waals and electrostatic forces, respectively.

References for supplemental data

Avery J, Ellis DJ, Lang T, Holroyd P, Riedel D, Henderson RM, Edwardson JM, Jahn R (2000) A cell-free system for regulated exocytosis in PC12 cells. *J Cell Biol* **148**: 317-324.

Bash PA, Singh UC, Langridge R, Kollman PA (1987) Free energy calculations by computer simulation. *Science* **236**: 564-568.

Berendsen HJ, Postma JP, DiNola A, Haak JR (1984) Molecular dynamics with coupling to an external bath. *J Chem Phys* **81**: 3684-3690.

Darden T, York D, Pedersen L (1993) Particle mesh Ewald - an $N \log(N)$ method for Ewald sums in large systems. *J Chem Phys* **98**: 10089-10092.

Lindahl E, Hess B, van der Spoel D (2001) GROMACS 3.0: a package for molecular simulation and trajectory. *J Mol Model* **7**: 306-317.

Miyamoto S, Kollman PA (1992) SETTLE: an analytical version of the SHAKE and RATTLE algorithms for rigid water models. *J Comp Chem* **13**: 952-962.

Ossig R, Schmitt HD, de Groot B, Riedel D, Keränen S, Ronne H, Grubmüller H, Jahn R (2000) Exocytosis requires asymmetry in the central layer of the snare complex. *EMBO J* **19**: 6000-6010.

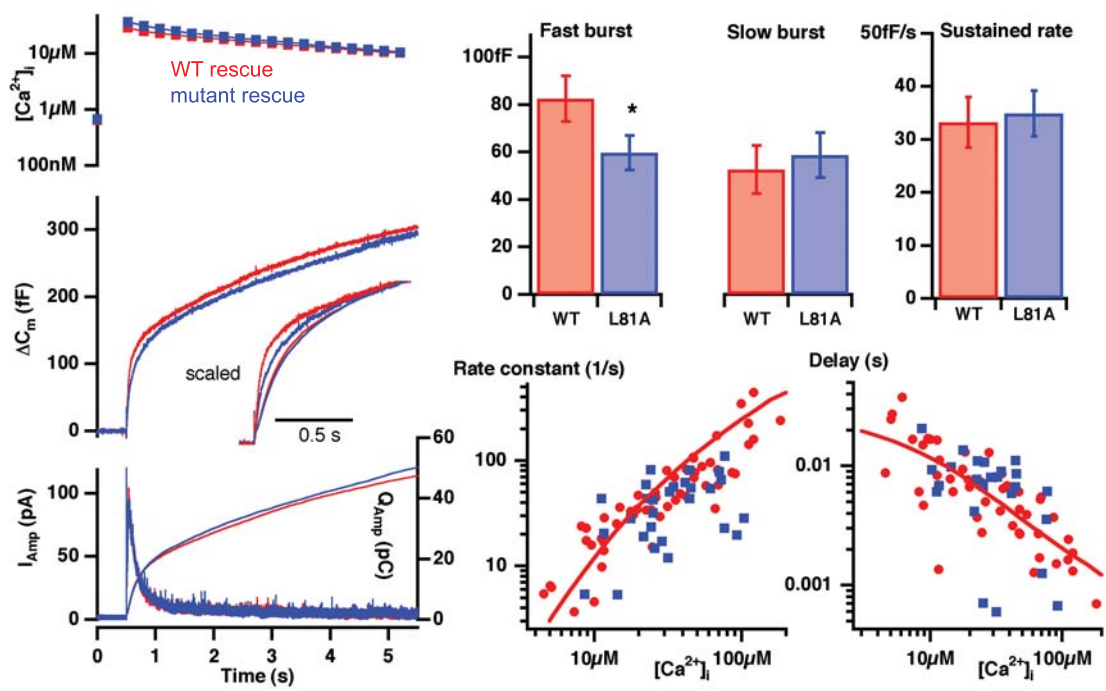
Ryckaert JP, Ciccotti G, Berendsen HJC (1977) Numerical integration of the cartesian equations of motion of a system with constraints; molecular dynamics of n-alkenes. *J Comp Phys* **23**: 327-341.

Sutton, R.B., Fasshauer, D., Jahn, R., and Brunger, A.T. (1998). Crystal structure of a SNARE complex involved in synaptic exocytosis at 2.4 Å resolution. *Nature* **395**, 347-353.

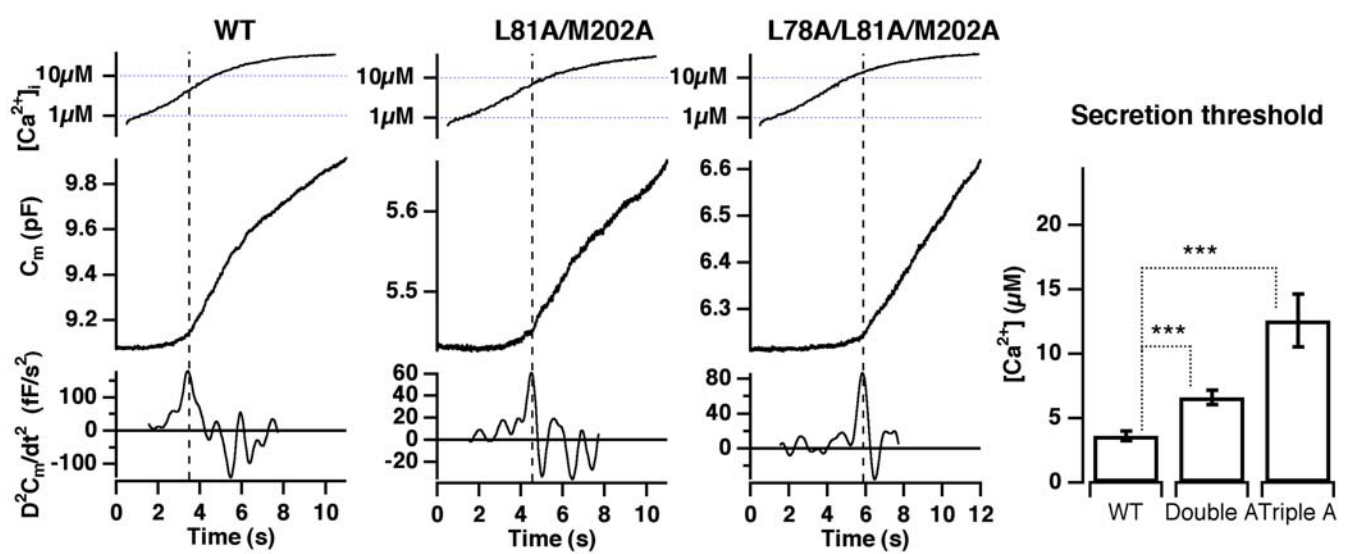
Van Buuren AR, Marrink SJ, Berendsen HJ (1993) A molecular dynamics study of the decane/water interface. *J Phys Chem* **97**: 9206-9212.

van Gunsteren WF, Berendsen H J (1987) *GROMOS manual*. BIOMOS biomolecular Software; Laboratory of Physical Chemistry, University of Groningen, The Netherlands.

Vriend G (1990) WHAT IF: a molecular modeling and drug design program. *J Mol Graph* **8**: 52-56.



Supplemental Fig. 1



Supplemental Fig. 2

3. GENERAL DISCUSSION

Over the last two decades, the studies of exocytosis have focused on membrane proteins. Only recently has the importance of the membrane lipids and their metabolism begun to be appreciated. Such late interest in the lipid contribution to the exocytic process may be largely due to the previously mentioned complexity of lipids (Introduction, chapter 1.2.2.) and the lack of powerful tools for the study of their function. However, this has changed recently with the availability of many new tools. Most of the lipid metabolising enzymes have been cloned, allowing the use of mutant and fusion proteins as well as overexpression and RNA interference techniques. The use of model transgenic organisms has revolutionised the studies of genetics and diseases. Furthermore, new pharmacological, chemical and analytical tools accompanied by mathematical modelling are also starting to be utilised (Wenk, 2005). This doctoral thesis employs some of cutting-edge methodology to study the roles of lipids in exocytosis.

The aim of my doctoral work was to explore the role of the phospholipid PI(4,5)P₂ and plasmalemmal SNARE proteins in the exocytic process. Since exocytosis is organised spatially and temporally, my goal was to address both spatial and temporal aspects of exocytic regulation by the aforementioned membrane constituents. This was challenging as the techniques then available for studying exocytosis only permitted the study of these aspects independently. Indeed the present knowledge of the field reflects this limitation. Functional studies of exocytic molecules using mainly electrophysiological techniques focus on the kinetic features of the molecular participants and cannot provide spatial information. In these studies the cell is often considered as a “black box” whose output is being analysed. On the other hand, biochemical studies provide spatial, but no temporal information. Examples of such approaches are studies addressing the lipid raft association of the SNARE proteins that will be discussed later in this section (Chamberlain *et al.*, 2001; Salaün *et al.*, 2005). In general, to overcome the limitation of single techniques, the combination of physiological and biochemical assays is highly desirable.

I used patch-clamp membrane capacitance and amperometric measurements accompanied by [Ca²⁺]_i measurements to obtain high temporal resolution. To acquire spatial information, I adapted the plasma membrane sheet technique to bovine and mouse chromaffin cells. The three studies presented in this doctoral thesis are based on the powerful combination of these methods.

Study I directly compared plasma membrane PI(4,5)P₂ levels with the extent of chromaffin cell exocytosis. The spatial distribution and the levels of PI(4,5)P₂ were investigated in plasma membrane sheets, while exocytosis was monitored in intact cells by measuring changes in membrane capacitance and catecholamine release by amperometry. The study revealed that the PI(4,5)P₂ level regulates the size and the refilling rate of the primed vesicle pools, but not the fusion rate constants. PI(4,5)P₂ was found in nanometric-sized cholesterol-dependent clusters, which partially colocalised with syntaxin 1 clusters to which secretory vesicles preferentially dock and fuse.

Study II investigated the molecular basis for the distinct secretory phenotypes of two SNAP-25 isoforms in chromaffin cells. As before, the spatial distribution and the levels of plasmalemmal SNAP-25 and syntaxin 1 were examined in plasma membrane sheets, while exocytosis was evaluated by electrophysiological measurements. The study demonstrated that the two non-conservative substitutions in the N-terminal SNARE domain, and not the different localisation of one palmitylated cysteine residues, caused the functional difference between the SNAP-25 isoforms. Biochemical and molecular dynamic simulation experiments revealed that the two substitutions probably do not regulate exocytosis by affecting the property of SNARE complex itself, but rather increase the availability of the SNAP-25b-containing SNARE complex to accessory factor(s).

Study III addressed the mechanism of the SNARE complex action in exocytosis. The combination of assays used above was again employed. This time membrane targeting and the levels of SNAP-25 mutated proteins were measured in the plasma membrane sheets and exocytosis was monitored by membrane capacitance change and amperometry. The analysis demonstrated that progressive N- to C-terminal zippering of the SNARE complex drives priming and fusion of chromaffin cell secretory vesicles.

Since most of my doctoral thesis concerns studies I and II the subsequent chapters will focus mainly on this work.

3.1. Plasma membrane sheet as an assay to study plasmalemmal lipids and proteins

We exploited the membrane sheet assay to inspect the spatial localisation of PI(4,5)P₂ in the plasma membrane and to quantify the plasmalemmal PI(4,5)P₂ level. As a PI(4,5)P₂ probe, we used the recombinant fluorescently tagged PH-domain from PLCδ₁. This proved to be very specific, in agreement with previous studies (Lemmon *et al.*, 1995; Stauffer *et al.*, 1998; Várnai and Balla 1998). With the ability to visualise PI(4,5)P₂, we tested the effect of acute and chronic manipulations of PI(4,5)P₂ concentration in chromaffin cells. Approaches to

lower available (free) PI(4,5)P₂ in the plasma membrane include activation of PLC via receptors, application of antibodies against PI(4,5)P₂ or poly-cations (e.g. neomycin, spermine or poly-lysine) to the inner leaflet of the plasma membrane, overexpression of PI(4,5)P₂ binding proteins or their binding modules, or the overexpression of PI phosphatases or their active domains. In addition, it is possible to interfere with the PI(4,5)P₂ synthesis by knocking down the respective kinases, or by blocking them with the pharmacological agents (e.g. phenylarsine oxide, wortmannine, LY294002). Alternatively, the manoeuvres to increase available PI(4,5)P₂ include addition of PI(4,5)P₂ to the inner leaflet of the plasma membrane, inhibition of PI phosphatases and overexpression of PIP5Ks. Furthermore, PI kinase activity can be stimulated through several signalling pathways (e.g. application of PA, see chapter 1.2.2.). Still, at the time no pharmacological tool was known to increase intracellular PI(4,5)P₂ by targeting its metabolising enzymes.

Study I however described the use of such a pharmacological tool to increase intracellular PI(4,5)P₂ for the first time. The acute application of LY294002, a potent PI3K inhibitor, quickly raised PI(4,5)P₂ level as detected by the transient increase in GFP-PH-PLCδ₁ binding to the membrane sheets. In general, the combination of fluorescently labelled PH-PLCδ₁ and the plasma membrane sheets provided a straightforward way to detect the relative changes in PI(4,5)P₂ concentration resulting from different manipulations. Furthermore, by using protein modules specific for other PIs (e.g. PX, ENTH, FERM, FYVE), it could be possible to determine their relative levels. Particularly interesting would be the detection of the plasmalemmal second messengers derived from PI(4,5)P₂, PI(3,4,5)P₃ and DAG, whose levels can increase dramatically in response to stimuli.

We used the described combination of GFP-PH-PLCδ₁ and the plasma membrane sheets to study the role of PI(4,5)P₂ in chromaffin cell exocytosis by determining the spatial distribution of PI(4,5)P₂ in the native plasma membrane, and by directly comparing the levels of secretion with the levels of the phospholipid. Besides the distribution and the semi-quantitative detection of membrane lipid, my doctoral work revealed another useful application of the membrane sheet assay – the quantification of plasmalemmal protein levels. This approach is valuable if only a limited amount of sample material is available, as it is the case with a primary culture of chromaffin cells derived from embryonic or new-born mice. Such a preparation yields only a few hundred of chromaffin cells, which is not sufficient for a classical biochemical protein analysis by *western* blot. Thus, we also employed plasma membrane sheets to analyse the membrane targeting and the level of virally encoded SNAP-

25 isoforms in SNAP-25 *null* cells. These examples of the applicability of this assay are thoroughly discussed in the next chapters.

We also used plasma membrane sheets to develop an *in vitro* assay for imaging single vesicle exocytosis in chromaffin cells. It was anticipated that this assay would not only provide spatial information but also temporal data with a resolution comparable to electrophysiological methods. We constructed a specific marker for chromaffin LDCVs, neuropeptide Y (NPY) conjugated to a yellow fluorescent protein (Venus), and expressed it in cells prior to the plasma membrane preparation. A sub-population of labelled vesicles that was retained on the membrane sheets underwent exocytosis. Exocytosis was found to be dependent on Ca^{2+} and SNARE proteins. Interestingly, we were able to observe a number of vesicles in which fluorescence was lost in small, incremental steps and a flickering effect was produced. This observation suggested occasional multi-step exocytic events in which LDCVs failed to empty their content rapidly. Interestingly, occasional amperometric signals were recorded in the chromaffin cells which resembled foot signals without spikes which suggested transient pore opening without complete fusion (Albillos *et al.*, 1997; Ales *et al.*, 1999). A similar explanation has been proposed for comparable findings in two other neuroendocrine cell types: PC12 cells (Taraska *et al.*, 2003) and pancreatic β -cells (Tsuboi and Rutter, 2003).

The utility of the above *in vitro* assay to obtain temporal data comparable to more standard electrophysiological means on single vesicle exocytosis was however limited. There are three main reasons for this: 1) only a small fraction of vesicles were actually labelled with NPY-Venus, possibly due to a short viral transfection interval, 2) an unexpectedly low number of exocytic events was detected, and 3) no exocytosis could be detected concomitantly with Ca^{2+} addition even with the improved temporal resolution of the assay. As this was the primary goal of my work, further experiments were abandoned.

To summarise, we developed an *in vitro* assay for imaging single vesicle exocytosis in chromaffin cells. Although not ideal to study the fast kinetic aspect of chromaffin cells secretion, the assay permitted direct experimental access to the plasma membrane. Consequently, a variety of studies of proteins and lipids were still possible in a preparation that largely reflected the physiological state of the molecules in the cell.

3.2. Plasma membrane clusters of proteins and lipids involved in exocytosis

The distribution of proteins and lipids in the plasma membrane attracts great interest (reviewed by Mukherjee and Maxfield, 2004; Helms and Zurzolo, 2004). Here I shall focus on the spatial organisation of the plasma membrane constituents essential for exocytosis. The

plasma membrane clustering of the SNARE proteins has been intensively studied in the last five years (reviewed by Lang, 2003; Salaün *et al.*, 2004). Spatial distribution of PI(4,5)P₂ is presently unclear and vigorously debated (Martin 2001; van Rheenen *et al.*, 2005).

3.2.1. PI(4,5)P₂ clusters

During most of my doctoral work I was occupied with the question how a single lipid molecule such as PI(4,5)P₂ could regulate so many different cellular responses, apparently with spatial and temporal precision. It is hypothetically possible that PI(4,5)P₂ serves as transient target for numerous proteins involved in the regulation of vesicle trafficking and actin cytoskeleton. However, I believe that another dimension besides time is needed, and in this chapter I discuss the possibility that the spatial organisation of plasmalemmal PI(4,5)P₂ may be vital for its multiple functions, particularly exocytosis and endocytosis.

Four years ago, several investigators simultaneously stressed the importance of understanding the lateral organization of PI(4,5)P₂ in the plasma membrane (Martin 2001; Cremona and de Camilli, 2001; Gillooly and Stenmark, 2001; Simonsen *et al.*, 2001; Caroni, 2001). In his review, Thomas Martin (2001) wrote “Dynamic PI(4,5)P₂-rich membrane microdomains on the plasma membrane, in the trans-Golgi network and on trafficking vesicles may be the principal structures that dictate where membrane fission and fusion machinery and cytoskeletal constituents act”. With respect to endocytosis in particular, Gillooly and Stenmark (2001) suggested that “the focal assembly of clathrin lattices implies that there may be PI(4,5)P₂ rich patches in the plasma membrane”. Caroni (2001) discussed the possibility that the actin cytoskeleton is regulated through modulation of PI(4,5)P₂ rafts. In short, PI(4,5)P₂-enriched clusters and their putative functions have been simultaneously proposed by several groups.

The distribution of PI(4,5)P₂ in the plasma membrane has been studied intensively since the development of specific probes a few years ago. The first overexpression studies using GFP-PH-PLCδ₁ reported a nearly uniform distribution of PI(4,5)P₂ over the plasma membrane (Stauffer *et al.*, 1998; Várnai and Balla 1998). Other experiments with GFP-PH-PLCδ₁ overexpression revealed that PI(4,5)P₂ accumulated in distinct dynamic structures in plasma membrane ruffles (Honda *et al.*, 1999; Tall *et al.*, 2000), or at sites of phagocytosis (Botelho *et al.*, 2000). Nevertheless, a subsequent study which challenged these findings showed a close correlation between the GFP-PH-PLCδ₁-signal and the staining with a number of lipophilic membrane dyes, implying that the apparent PI(4,5)P₂-enrichments in membrane ruffles were caused by a larger membrane area due to local invaginations (van Rheenen and

Jalink, 2002). Another study using anti-PI(4,5)P₂ antibody detected PI(4,5)P₂-clusters that were cholesterol-dependent and colocalised well with actin-binding GAP43, MARCKS and CAP23 (GMC)-proteins (Laux *et al.*, 2000). However, several objections can be raised to this work. Firstly, PI(4,5)P₂ distribution was investigated in aldehyde-fixed cells. One potential problem with such approach is that many lipids, including PIs, may not be effectively immobilised on aldehyde fixation (Griffiths, 1993). Secondly, the anti-PI(4,5)P₂ antibody can itself generate artificial clusters of PI(4,5)P₂ molecules. In this respect, the use of PH-PLCδ₁ which recognises PI(4,5)P₂ with a one-to-one stoichiometry thereby preventing probe-induced clustering or the coalescence of PI(4,5)P₂ clusters represents a better approach. However, even studies using overexpression of the PI(4,5)P₂-binding domain must be interpreted cautiously. It has been shown that the overexpression of specific protein domains can have deleterious effects on cell physiology, either by sequestration of lipid or by disruption of functionally important protein-protein interactions (Levine and Munro, 1998). In addition, in the cell PH-PLCδ₁ will bind both PI(4,5)P₂ and its hydrolysis product, I(1,4,5)P₃, making it harder to focus on the PI(4,5)P₂ molecule. Finally, all the discussed studies have the common disadvantage of investigating PI(4,5)P₂ distribution by light microscopy which is incompatible with studying structures smaller than ~220 nm.

An investigation by Watt and collaborators (2002) addressed the subcellular localisation of PI(4,5)P₂ with high resolution of electron microscopy and exogenously added PH-PLCδ₁. PI(4,5)P₂ signal was detected primarily in the plasma membrane, where it was clustered, but did not associate with lipid rafts. Lipid rafts are hypothetical small functional lipid domains in the membrane, enriched in cholesterol, sphingolipids and glycosylphosphatidylinositol (GPI)-anchored proteins (Simons and Ilkonen, 1997). Biochemically, rafts are characterised as resistant to solubilisation in detergents (e.g. Triton X-100) and by their dependence on cholesterol (Simons and Toomre, 2000). They have attracted much attention over the last few years as putative scaffolds for signalling transduction components. However, a consensus about their exact function, size, turnover, or whether they even exist is lacking and the methods by which they are studied can be questioned (Edidin, 2003b; Munro, 2003; Glebov and Nichols, 2004). Nevertheless, the enrichment of PI(4,5)P₂ in lipid rafts has been suggested by a number of studies (Hope and Pike, 1996; Pike and Casey, 1996; Pike and Miller, 1998; Waugh *et al.*, 1998; Laux *et al.*, 2000; Hilgemann *et al.*, 2001; Klopfenstein *et al.*, 2002). Some of these have though been challenged by a recent work showing that the treatment of intact cells with Triton X-100 itself induces strong PI(4,5)P₂ clustering (van Rheenen *et al.*, 2005). Therefore, despite detailed

investigations, it is still uncertain whether PI(4,5)P₂-enriched clusters exist, and if they do, whether PI(4,5)P₂ is enriched in lipid rafts or it is present in functionally-uncharacterised raft-independent clusters.

We addressed the question of PI(4,5)P₂ cluster existence with the plasma membrane sheet assay. As this is a clear plasma membrane preparation, no soluble cytoplasmic factors are present. Therefore, when we applied a purified recombinant GFP-PH-PLCδ₁ to the native plasma membranes and observed abundant, but distinct binding of the fluorescent probe, we assumed that PI(4,5)P₂, as the probe's only ligand, was spatially organised in clusters. In our case, the detected punctate pattern of the plasma membrane was not due to local increases in the membrane area as had been observed by van Rhee and Jalink (2002; I, Figure 1A-D). However, as considered in the Discussion of study I, the punctate staining of GFP-PH-PLCδ₁ may also reflect variable accessibility of the probe to plasma membrane PI(4,5)P₂, caused by steric hindrance of endogenous PI(4,5)P₂-associated proteins. In such a scenario the punctate distribution of GFP-PH-PLCδ₁ fluorescence may reflect a non-homogeneous protein distribution in the membrane, rather than a non-homogeneous PI(4,5)P₂ distribution.

The clusters we observed appear similar to those that were described to colocalise with PI(4,5)P₂ binding GMC proteins in neurons and PC12 cells (Laux *et al.*, 2000). However, the PI(4,5)P₂ clusters quantified in that study were larger and less abundant than the ones we visualised in chromaffin and PC12 cells (I, Figure 1A-D; Laux *et al.*, 2000, Fig. 1C). Procedural differences may account for the abundance of larger clusters - Laux and collaborators (2000) detected PI(4,5)P₂ by antibody in permeabilised cells, while we incubated freshly prepared membrane sheets with GFP-PH-PLCδ₁ for a short time followed immediately by imaging. Indeed, when we applied anti-PI(4,5)P₂ antibody to paraformaldehyde-fixed membrane sheets, we also observed an enrichment of larger clusters, implying that antibody mediated patching of lipids was occurring after aldehyde fixation. Despite of these methodological differences, our study, in agreement with Laux *et al.* (2000), also found that clusters disintegrated in the presence of methyl-β-cyclodextrin indicating that cholesterol is necessary for the non-uniform distribution of PI(4,5)P₂ in the plasma membrane.

Interestingly, cholesterol depletion by methyl-β-cyclodextrin strongly correlates with both the disruption of syntaxin 1 clusters and a reduction in the rate of exocytosis in PC12 cells (Lang *et al.*, 2001). The same treatment also causes dispersion of PI(4,5)P₂ clusters (I), implying that the high local concentrations of PI(4,5)P₂ may be required for efficient fusion.

This is nevertheless speculative as removal of cholesterol may generally alter membrane organisation. Another interesting aspect revealed by PI(4,5)P₂ detection in cholesterol depleted membranes is the occurrence of micrometric domains devoid of PI(4,5)P₂ (not shown). These clusters were not holes in the plasma membrane since the phospholipid staining by membrane dye was uniform. However, these non-physiological structures are probably the consequence of membrane reorganisation caused by cholesterol removal.

Our study of PI(4,5)P₂ clusters was followed by similar investigations by Aoyagi and collaborators (2005), who used the plasma membrane sheet assay to examine the relationship between PI(4,5)P₂ clusters and the exocytic machinery in PC12 cells. In contrast to previous reports of uniform GFP-PH-PLCδ₁ distribution upon its expression in the cells (Stauffer *et al.*, 1998; Várnai and Balla 1998; van Rheenen and Jalink, 2002), Aoyagi *et al.* (2005) overexpressed the same probe but detected clusters similar to ours and reported their partial colocalisation with lipid rafts and syntaxin 1 clusters. The colocalisation of PI(4,5)P₂ and clusters of syntaxin 1 increased with PI4P5K-I overexpression and decreased after stimulated exocytosis (Aoyagi *et al.*, 2005). Based on such data, the authors suggested that exocytic sites are activated by the formation of PI(4,5)P₂ clusters underneath syntaxin 1 clusters (Aoyagi *et al.*, 2005).

We have also detected significant colocalisation of PI(4,5)P₂ and syntaxin 1 clusters in chromaffin cells. However, we did not publish these results in the context of study I. They are presented as additional data in this thesis. In contrast to Aoyagi *et al.* (2005), who followed a previously published analysis (Lang *et al.*, 2001), we quantified the colocalization by calculating the correlation coefficient of the two images, which gave an objective estimation of the signal colocalisation. Nevertheless, intermediate degrees of colocalisation between PI(4,5)P₂ and syntaxin 1 clusters observed in both studies cannot entirely resolve the question of the function of PI(4,5)P₂ clusters in exocytosis. Most likely, exocytosis takes place at a subset of these clusters or at dynamically generated PI(4,5)P₂ clusters, which may not be fully accessible to the probe. Finally, several other physiological roles for the PI(4,5)P₂ clusters could be suggested, and the majority of the observed clusters may in fact serve other purposes, such as forming the sites for endocytosis and the regulation of actin cytoskeleton. However the presence of PI(4,5)P₂ clusters could explain, at least in part, the exquisite degree of spatial and temporal control exhibited by regulated exocytosis and endocytosis at the plasma membrane as these clusters may act as loci for the recruitment of functional protein complexes. In addition, these processes may not be independent but may instead be interconnected through such structures (see next chapter).

The mechanism(s) by which the PI(4,5)P₂ clusters are assembled and maintained is unknown. The spatial restriction could be driven by local synthesis or by clustering of the phospholipid, followed by recruitment of functional protein complexes through specific lipid binding domains. This remains to be explored. However, it is becoming apparent that the PI(4,5)P₂ clusters are plasmalemmal structures distinct from lipid rafts (Watt *et al.*, 2002; Aoyagi *et al.*, 2005). Consequently, they will require dedicated studies and methodologies that will attempt to preserve the natural molecular environment.

In conclusion, study I supports the hypothesis that lateral inhomogeneities of PI(4,5)P₂ exist in the plasma membrane. It goes beyond the similar studies reaching the same fundamental conclusion since it is the first to show the detection of PI(4,5)P₂ in native plasma membranes with a selective probe that binds with a one-to-one stoichiometry. Nevertheless, since the organization of the plasma membrane lipids is complex and only partially understood, many questions remain. Progress will depend upon the further development of lipid probes, better analytical techniques with improved spatial resolution (e.g. stimulated emission depletion (STED) microscopy, freeze-fracture electron microscopy in the plane of the membrane) and being able to assign a functional role to the observed structures.

3.2.2. SNARE protein clusters

There has been much interest in the distribution of exocytic SNARE proteins at the plasma membrane. Plasmalemmal SNAREs have been found to concentrate in clusters: syntaxin 1 and SNAP-25 (Lang *et al.*, 2001), syntaxin 4 and SNAP-23 (Chamberlain and Gould, 2002). The syntaxin 1 clusters represent the preferential fusion sites for secretory vesicles and exocytosis is dependent on their integrity (Lang *et al.*, 2001). Other studies have also suggested the regionalisation of release in neuroendocrine cells (Monck *et al.*, 1994; Schroeder *et al.*, 1994; Robinson *et al.*, 1996). However, the syntaxin 1 nanometric-sized clusters are much smaller than the detected specific release zones, also called “hot spots”, in neuroendocrine cells (1-2 µm in chromaffin cells; Monck *et al.*, 1994; Schroeder *et al.*, 1994). In addition, it was recently suggested that targeting of SNARE proteins to lipid rafts spatially controls exocytosis (Chamberlain *et al.*, 2001; Salaün *et al.*, 2005), but there is no consensus as to whether SNARE proteins are actually enriched in lipid rafts (Lang *et al.*, 2001). Altogether, these observations suggest that exocytosis in neuroendocrine cells is spatially controlled.

During my doctoral study I performed a detailed analysis of the spatial organisation of the SNARE proteins syntaxin 1 and SNAP-25 in the plasma membrane of bovine and mouse

chromaffin cells. In bovine chromaffin cells I characterised the SNARE protein distribution and found that the aforementioned proteins are clustered and constitutively active, in agreement with previously published data (Lang *et al.*, 2001; Lang *et al.*, 2002). By adapting the plasma membrane sheet technique to mouse chromaffin cells, I could combine use of transgenic cells and overexpression techniques to study SNARE protein organisation in a “clean” genetic background. Using this approach, the hypothesis that SNAP-25 isoforms may have an altered targeting efficiency to exocytic sites was investigated. As explained in the Introduction, the two SNAP-25 isoforms differ in the positioning of the four palmitylated cysteines which has been suggested to cause differences in their membrane localisation or targeting (Bark and Wilson, 1994; Bark *et al.*, 1995). We hoped that this might explain the different ability of SNAP-25a and SNAP-25b to support the primed pool of vesicles (Sørensen *et al.*, 2003a).

Yet, we found that both SNAP-25 splice variants are targeted to the plasma membrane with the same efficiency, are available in large excess and colocalise to the same extent with syntaxin 1 clusters (II). We objectively analysed colocalisation of SNAP-25 and syntaxin 1 in chromaffin cells by calculating the correlation coefficient of the two mean-subtracted images. We did not observe the nearly perfect colocalization of the two proteins reported by Rickman and collaborators (2004), but instead a partial overlap in agreement with studies in PC12 and pancreatic β -cells (Lang *et al.*, 2001; Ohara-Imaizumi *et al.*, 2004). However, our anti-SNAP-25 antibody is known to recognise SNAP-25 less efficiently when complexed with syntaxin 1 (Lang *et al.*, 2002), which might reduce the signal to noise ratio for the detection of this complex when compared to free SNAP-25.

We further determined that the levels of syntaxin 1 immunofluorescence were not affected by ablation or overexpression of SNAP-25 isoforms (II). Previous studies have suggested that co-expression with syntaxin 1 is required to retain SNAP-25 on the intracellular membranes (Rowe *et al.*, 1999; Vogel *et al.*, 2000; Washbourne *et al.*, 2001). However, a more recent work shows that targeting of SNAP-25 to the plasma membrane in neuronal cells does not require syntaxin 1 (Loranger and Linder, 2002). This model is in agreement with our finding that plasma membrane-associated SNAP-25 can be increased over tenfold, without changing the plasma membrane syntaxin 1 level.

In conclusion, our thorough analysis showed that the relocation of the cysteine does not affect the localisation of the different SNAP-25 isoforms in the plasma membrane and consequently does not contribute to the difference in secretory phenotype between SNAP-25 isoforms in chromaffin cells. Nevertheless, this question should be re-examined in polarized

neurons, as the work of Bark and collaborators (1995) indicated that SNAP-25b localised more to varicosities and terminals in nerve growth factor differentiated PC12 cells, whereas SNAP-25a was more diffuse.

3.3. The role of PI(4,5)P₂ in chromaffin cells exocytosis

Prior to my doctoral work several studies implied dependence of regulated exocytosis on PI(4,5)P₂ (Eberhard *et al.*, 1990; Hay and Martin, 1993; Hay *et al.*, 1995; Holz *et al.*, 2000; see Introduction). In the meantime, a few other studies indirectly stressed a PI(4,5)P₂ role: functional disruption of Arf6, a positive regulator of PI(4,5)P₂ synthesis via its action on PI4P5K-I (Krauss *et al.*, 2003), impaired neuroendocrine exocytosis (Lawrence and Birnbaum, 2003; Aikawa and Martin, 2003), while stimulation of Arf6 enhanced it (Vitale *et al.*, 2002). More recently, Olsen and collaborators (2003) showed that infusion of PI(4)P and PI(4,5)P₂ into pancreatic β -cells increased the size of the RRP.

Our study directly compared PI(4,5)P₂ levels in the plasma membrane with levels of chromaffin cell secretion. We observed that overexpression of a PI(4,5)P₂-kinase, PI4P5K-I γ , increased the plasma membrane PI(4,5)P₂ level and cellular exocytosis, whereas overexpression of a PI(4,5)P₂-phosphatase, IPP1-CAAX, eliminated plasmalemmal PI(4,5)P₂ and secretion. Thus we found that in addition to being essential, PI(4,5)P₂ regulates the extent of LDCV secretion from chromaffin cells. This is similar to the situation for SNARE proteins, which are also found both to be essential for and to regulate the exocytic process. However, PI(4,5)P₂ abundance limits exocytosis in the control situation and therefore changes in its level regulate secretion directly and dynamically. This is different from the situation for the SNARE complex member SNAP-25: although SNAP-25 is necessary for exocytosis (Sørensen *et al.*, 2003a), overexpression of SNAP-25a in wild-type bovine or mouse chromaffin cells does not change secretion (Nagy *et al.*, 2002; Sørensen *et al.*, 2003a). Likewise, secretion in the heterozygous *Snap-25* mouse, where only one *Snap-25* gene copy is present, was normal. PI(4,5)P₂ levels, but not SNAP-25 levels, are therefore limiting exocytosis in the normal situation.

The ability of the PI(4,5)P₂ level to directly regulate the extent of secretion on a minute time-scale was further confirmed in our experiments with LY294002, a potent PI3K inhibitor. Two studies had previously tested the effect of LY294002 on neuroendocrine secretion (Martin *et al.*, 1997; Chasserot-Golaz *et al.*, 1998). When applied for 30 minutes, LY294002 did not significantly affect secretion in permeable PC12 cells, although on average a small inhibition of secretion was seen (Martin *et al.*, 1997). However, Chasserot-Golaz and

collaborators (1998) described a dose-dependent inhibition of catecholamine secretion in chromaffin cells after a 30 minute long incubation with LY294002. The results of our experiments are in agreement with these latter findings, since we found that the short application of LY294002 caused a greater than twofold increase in the number of fused vesicles, while a longer preincubation inhibited secretion. The mechanism of the biphasic effect of LY294002 on secretion in chromaffin cells is unknown. We speculate that it might be elicited through inhibition of certain PI4K isoforms by LY294002 (Downing *et al.*, 1996, Sorensen *et al.*, 1998; see Discussion of I), and may simply be the result of changes in PI(4,5)P₂ levels, without invoking a role for 3-phosphorylated PIs in exocytosis.

Both acute and chronic manipulations of PI(4,5)P₂ level showed that PI(4,5)P₂ affected exocytosis by regulating both the number of vesicles residing in the releasable vesicle pools and the sustained rate of release. This is indicative of an increased filling rate of the releasable pools that is in agreement with the finding that PI(4,5)P₂ infusion into pancreatic β -cells increases the RRP size (Olsen *et al.*, 2003). Moreover, from our data it seems that the number of primed vesicles is proportional to the level of PI(4,5)P₂ in the membrane, with the resting cell having an intermediate PI(4,5)P₂ level.

Our study was followed by similar investigations by Gong and collaborators (2005), who examined the secretion in chromaffin cells obtained from mice lacking PI4P5K-I γ . The absence of this enzyme decreases PI(4,5)P₂ levels in neurons which causes defects in both exocytosis and endocytosis of synaptic vesicles (Di Paolo *et al.*, 2004). In chromaffin cells the absence of PI4P5K-I γ reduces the releasable pool and its refilling rate, with a small increase in morphologically docked vesicles (Gong *et al.*, 2005). Based on these observations, Gong and collaborators (2005) reached the same conclusion as our study: PI(4,5)P₂ regulates vesicle priming. In addition, Gong *et al.* (2005) used amperometry to analyse the kinetics of catecholamine release from individual vesicles and detected longer foot duration in PI4P5K-I γ *null* mice, implying a delay in fusion pore expansion. The other amperometric parameters including the quantal size, peak amplitude, half-width and the rise time were unchanged. Interestingly, no difference in fusion pore expansion was found in chromaffin cells overexpressing PI4P5K-I γ (Gong *et al.*, 2005). We also did not detect any difference in fusion rate constants when the plasmalemmal PI(4,5)P₂ level was increased by a number of manipulations. In addition, we did not detect any difference in fusion rate constants when the plasmalemmal PI(4,5)P₂ level was decreased upon prolonged application of LY294002. However, the releasable pools in this experimental group were either very small or even missing and it was difficult to reliably fit the cellular responses by the triple exponential

function (for explanation on method, see Introduction). Therefore, we reported that PI(4,5)P₂ is a key physiological regulator of the size and the refilling rate of the primed vesicle pools, but not of the fusion rate constants.

Having PI(4,5)P₂ as the regulator of primed vesicle pool size raises an interesting possibility that Ca²⁺-activated PI(4,5)P₂ synthesis by PI4P5K-I γ may underlie the Ca²⁺-dependent priming in chromaffin cells. Indeed, PI4P5K-I γ S264A, the mutant which presumably mimics the activated kinase form, additionally increased the primed pools and overall exocytosis (additional data). Yet, PI4P5K-I γ S264E, the mutant which presumably mimics the non-activated kinase form, also increased the exocytic burst when compared to control cell (additional data). However, it is not known whether PI4P5K-I γ S264E is indeed inactive, or it retained some residual activity which may be potentiated by strong viral overexpression. This can be tested by defining the plasmalemmal PI(4,5)P₂ level PI4P5K-I γ S264E overexpressing cells. In addition, plasmalemmal PI(4,5)P₂ levels can be measured in PI4P5K-I γ transfected chromaffin cells with altered [Ca²⁺]_i to directly examine the Ca²⁺ regulation of PI4P5K-I γ . Similar experiment may be performed in PI4P5K-I γ *null* cells to dissect the contribution of other enzymes to the plasmalemmal PI(4,5)P₂ level.

The molecular mechanism(s) of PI(4,5)P₂ function in exocytosis is unknown. As pointed out in the Discussion of study I, the molecular characterisation of the exocytic machinery revealed several proteins that specifically bound PI(4,5)P₂ *in vitro*, between others members of synaptotagmin family (Schiavo *et al.*, 1996), CAPS1 (Loyet *et al.*, 1998) and Mint (Okamoto and Südhof, 1997). It remains to be determined which of these interactions are physiologically relevant. My experimental data show that the amounts of synaptotagmin 1, synaptotagmin 7, Mint-interacting protein Munc18-1 and actin, but not CAPS1 and CAPS2, are significantly increased in the plasma membrane of chromaffin cells expressing PI4P5K-I γ (additional data).

The exocytic role of synaptotagmin 7 is not unclear (Andrews and Chakrabarti, 2005). On the other hand, the exocytic function of synaptotagmin 1 has been intensively studied (reviewed by Südhof, 2004). Fusion of LDCVs from the RRP depends on synaptotagmin 1 (Voets *et al.*, 2001), and the release rate constant is modified by synaptotagmin 1 R233Q mutation (Sørensen *et al.*, 2003b). Synaptotagmin 1 binds to PI(4,5)P₂-containing membranes via its C₂B-domain and thereby increases its speed of insertion into the membrane, suggesting that changes in PI(4,5)P₂ level can regulate fusion rates (Bai *et al.*, 2004). Gong and collaborators (2005) reported that reduction of PI(4,5)P₂ level causes a delay in fusion pore expansion, while increased PI(4,5)P₂ level does not affect fusion kinetics. Therefore, the

physiological concentration of PI(4,5)P₂ is not rate-limiting for triggering fusion. An appealing possibility would be that PI(4,5)P₂-binding of synaptotagmin 1 is involved in upstream reactions, specifically in the recruitment of vesicles into the releasable vesicle pools. Interestingly, overexpression of synaptotagmin 1 in chromaffin cells results in a larger RRP and a smaller SRP, without changing the overall secretion and fusion rates (Nagy *et al.*, 2006). However, these data also suggest that synaptotagmin 1 is not the likely mediator of the twofold increase in chromaffin cell secretion detected upon PI(4,5)P₂ elevation.

At difference with synaptotagmin 1, but similarly to PI4P5K-I γ , overexpression of Munc18-1 increases the exocytic burst, the rate of sustained release and overall BCC secretion without affecting fusion rates (Voets *et al.*, 2001). Taken together with the significant increase in the Munc18-1 level in the plasma membrane of PI4P5K-I γ overexpressing cells, these results imply that the effect of PI(4,5)P₂ on exocytosis may be mediated through Munc18-1 protein. Nevertheless, Munc18-1 does not bind PI(4,5)P₂ directly, but the interaction can be mediated through Mint (Okamoto and Südhof, 1997) or another adaptor protein. In any case, further investigations will be required to answer this question.

Originally discovered as an essential cytosolic factor in Ca²⁺-triggered exocytosis from cracked PC12 cells, CAPS1 exhibits specific PI(4,5)P₂ binding *in vitro* (Walent *et al.*, 1992; Loyet *et al.* 1998). Anti-CAPS1 antibody inhibition studies reported disruption of LDCV, but not SV exocytosis and indicated that CAPS1 functions selectively in LDCV exocytosis (Berwin *et al.*, 1998; Tandon *et al.*, 1998; Elhamdani *et al.*, 1999; Rupnik *et al.*, 2000; Olsen *et al.*, 2003). Furthermore, these investigations involved CAPS1 both in priming and fusion steps. In chromaffin cells and melanotrophs, it was found that CAPS1 modulates fusion pore formation and dilation (Elhamdani *et al.*, 1999; Rupnik *et al.*, 2000). Olsen *et al.* (2003) reported CAPS1 involvement in priming of chromaffin cell LDCVs. Grishanin *et al.* (2004) proposed that priming of secretory vesicles consists of two sequential steps and modelled the CAPS1 function. The first faster priming step depends on Mg²⁺-ATP and involves synthesis of PI(4,5)P₂, while the second slower priming step requires Ca²⁺ and CAPS binding of PI(4,5)P₂ (Grishanin *et al.*, 2004). Nevertheless, the exact role of PI(4,5)P₂ binding in CAPS function is still not understood. Since the protein has two membrane-association domains, the functionally important PI(4,5)P₂-binding site needs be identified. Interestingly, the recent analysis of CAPS1 *null* mice suggested a different function for the CAPS1 protein – a role in the biogenesis or maintenance of mature secretory vesicles upstream of priming and fusion (Speidel *et al.*, 2005). In addition, no increase in CAPS1 or CAPS2 level was

detected in the plasma membrane of PI4P5K-I γ overexpressing chromaffin cells (additional data). Therefore, the function of CAPS proteins in exocytosis remains unresolved and requires additional studies.

As a secretion regulator, PI(4,5)P₂ would have several advantages over proteins with the same task. PI(4,5)P₂ molecules in the plasma membrane could recruit and activate a large number of different proteins in the cells to create a local environment where certain cellular processes could take place (Martin, 2001; Cremona and de Camilli, 2001). At the same time, however, the rapid enzymatic production and degradation of PI(4,5)P₂ would allow the cell to remain flexible: by changing the PI(4,5)P₂-level cells could change the distribution of entire sets of proteins within seconds or minutes, thereby modifying physiological function without the need for protein synthesis or degradation. Apart from the essential role in exocytosis discussed here, PI(4,5)P₂ is also intimately involved in clathrin-mediated endocytosis (reviewed by Cremona and de Camilli, 2001). The means by which exocytosis and compensatory endocytosis are spatially and temporally coupled remains unclear (Gundelfinger *et al.*, 2003). An interesting possibility is that in neuroendocrine cells PI(4,5)P₂ could act as a physiological regulator to balance these two processes.

3.4. The roles of SNAP-25 isoforms in chromaffin cell exocytosis

The main aim of study II was to find the molecular mechanism underlying the functional difference between two splice variants of SNAP-25. In the previous sections, I have discussed our results from the plasma membrane sheet assay which failed to explain the different secretory phenotypes of the SNAP-25 isoforms. Since the relevant changes were not localised within the SNAP-25 linker region, they had to be in the SNARE domain. Therefore, we focused on the next striking difference between the isoforms: the three charge substitutions in the N-terminal SNARE domain. These changes are notable since similar substitutions in the SNARE domains of both syntaxin 1 and synaptobrevin isoforms are either conserved or do not exist (Bennett *et al.*, 1992; Archer *et al.*, 1990). We thus performed systematic swapping of these residues and in the “clean” genetic background of SNAP-25 *null* mice we found that two out of three non-conservative substitutions (H66Q, Q69K) were both necessary and sufficient to provide SNAP-25a with the secretory properties of SNAP-25b. The complementary substitution study in SNAP-25b indicated that even the single K69Q mutation was sufficient to provide the reversion to the SNAP-25a phenotype. When considering this together with the observation that the Q69K mutation in SNAP-25 leads to an

intermediate phenotype, it implies that the amino acids in positions 66 and 69 do not have additive effects on secretion.

The principle of thermal denaturation studies to inspect the stability of the SNARE complex was elaborated in the study II. This approach revealed that the SNAP-25b-containing complex was somewhat more stable than the SNAP-25a-containing complex, and that the difference in stability could be attributed to the same two amino acid substitutions on position 66 and 69. However, further experiments revealed that the conserved neighbouring aspartate residue (D70) is necessary to confer the SNAP-25b secretory phenotype. If D70 is mutated to alanine in SNAP-25b, secretion is reduced to that of SNAP-25a, although the stability of the SNARE complex was unchanged. These results imply that the complex stability change is probably not the cause for the functional difference between the isoforms. This suggestion was further supported by computer-assisted molecular dynamics simulations, which showed that the SNAP-25b residues Q66 and K69 participate less frequently in intra-complex interactions than the SNAP-25a residues H66 and Q69. Based on these results we hypothesised that the function of these residues is mediated through an interaction with accessory factor(s) that may influence the stabilization or formation of the primed vesicle state (see II). The identity of such putative binding partner(s) is unknown. However, our characterisation of the amino acid polar stretch at the N-terminus of SNARE domain should allow the identification of the binding partner(s) by biochemical interaction experiments. Since both isoforms have a secretory phenotype with a secretory burst, a tentative scenario suggests binding of an accessory factor to both the SNAP-25a and the SNAP-25b containing SNARE complex, but with different affinities. The D70A mutation may change the affinity of the interaction in the case of the SNAP-25b containing complex, resulting in a SNAP-25a-like phenotype. Naturally, this is speculative and the actual mechanism remains unknown.

Interestingly, from the crystal structure analysis it is known that complexin binds to the groove between syntaxin 1 and synaptobrevin 2 (Chen *et al.*, 2002). The residues Q66, K69 and D70 however face the external surface of the coiled-coil SNARE structure. Furthermore, synaptotagmin 1 has been shown to bind to charged amino acids in the C-terminal end of the SNARE complex, but the residues responsible for binding are found in the second SNARE domain of SNAP-25 (Zhang *et al.*, 2002). Thus, both complexin and synaptotagmin 1 are not good candidates for our proposed accessory factor. A novel protein which binds SNAP-25 splice variants with different affinity has recently been identified (Hiroshi Kawabe, personal communication). However, it remains to be investigated whether

the protein has a role in exocytosis and whether the different affinity for SNAP-25 isoforms is physiologically relevant.

Finally, our data demonstrate that the difference of only two amino acids underlies the distinct exocytic phenotypes of SNAP-25 isoforms. In this case, nature found a simple way to construct a gain-of-function phenotype. The physiological importance of the SNAP-25 isoforms and the significance of the developmental expression switch have yet to be resolved. It is interesting to note that SNAP-25b is the main isoform in adult neurons (Bark *et al.*, 1995). Similar to chromaffin cells, it seems that the SNAP-25b isoform supports the higher level of exocytosis and produces a more efficient neurotransmission in hippocampal neurons (Ignacio Delgado, personal communication). The relevance of such regulation of neurotransmitter release in neuronal adaptation and synaptic plasticity remains to be explored.

3.5. The mechanism of the SNARE complex action in exocytosis

The incorporation of different SNAP-25 isoforms into the SNARE complex regulates the size of the exocytic burst i.e. the number of primed vesicles in releasable pools (Sørensen *et al.*, 2003a). Importantly, the fusion kinetics of the releasable pools (either the SRP or the RRP) is not changed. This is consistent with the previous studies focusing on SNAP-25 phosphorylation sites which modulate the priming reactions without affecting the fusion rates of the primed vesicle pools (Nagy *et al.*, 2002; Nagy *et al.*, 2004). These results establish a function of SNARE proteins in regulating the priming reaction. However, in addition to the regulation of priming, study III implies that the SNARE complex also functions in triggering exocytosis - a role that has been demonstrated in several other studies (Gil *et al.*, 2002; Sørensen *et al.*, 2003a; Han *et al.*, 2004; Borisovska *et al.*, 2005). Taken together, these observations suggest that the SNARE proteins are involved in both vesicle priming and fusion triggering. Moreover, they can regulate the priming reaction without compromising the speed or fidelity of the downstream fusion step. This arrangement allows the economical organization of the exocytic machinery in which the same molecules mediate sequential steps.

Study III sought to determine how the sequential SNARE complex zippering drives priming and fusion of secretory vesicles. The zippering of the hydrophobic layers of the SNARE complex was systematically examined by mutagenesis. All SNAP-25 mutants were correctly targeted to the plasma membrane and expressed in the similar amounts - over tenfold the endogenous SNAP-25 level in wild-type cells. Interestingly, also the C-terminal deletion mutant of SNAP-25a, $\Delta 26$, which corresponds to the larger cleavage products of BoNT/E, was correctly targeted to the plasma membrane and expressed at a similar level as

the wild-type protein. In contrast, Bajohrs and collaborators (2004) could not detect BoNT/E cleaved SNAP-25 at the plasma membrane. The authors suggest that this is due to the lost interaction with syntaxins 1 and 2, which provide the molecular basis for retention of SNAP-25 at the plasma membrane (Bajohrs *et al.*, 2004). However, the results presented here and from study II imply that targeting of SNAP-25 to the plasma membrane does not require syntaxin 1.

The electrophysiological measurements of secretion mediated by SNAP-25 mutants and corresponding studies of SNARE complex assembly led to the proposal of a model for the SNARE complex action in exocytosis. According to this model, the SNARE complex zippers up in two steps. The first step involves priming of the vesicles by an N-terminal nucleation reaction of the SNAREs, which is followed by zippering across the “0-layer”. Therefore, the primed vesicles are characterised by a stable, partially zippered intermediate of the SNARE complex. In the second step exocytosis triggering requires the complete zippering of the SNARE complex, resulting in fusion pore formation and finally, full membrane fusion. This model offers a simple explanation as to how SNARE complex formation, which is the rate limiting *in vitro*, can drive the fast Ca^{2+} -triggered secretion with millisecond time constants *in vivo*. However, a few open questions remain. What prevents the partially zippered SNARE complex from zippering up prematurely? How is the second zippering step coupled to the Ca^{2+} -trigger? It may be possible that the SNARE complex is intrinsically unable to zipper up entirely, but instead it is locked in an intermediate form due to the energy barrier created by the repulsion of two approaching membranes. In this case an additional input, possibly Ca^{2+} -mediated binding of synaptotagmin family members to the target membrane, would be required to allow complete zippering and membrane fusion. Alternatively, synaptotagmin itself may prevent the SNARE complex from zippering up entirely, and only upon its Ca^{2+} -mediated removal can the complex be zippered all the way to permit fusion of the membranes. Which of the two possibilities resemble the situation *in vivo* remains to be elucidated.

3.6. Future perspectives

Much has been learned about exocytosis and a lot remains unknown. The core features of the basic mechanism of exocytosis have been established. As pointed out in the Introduction, the present research is mainly focused on the regulation of the exocytic process. It is still enigmatic how the pace of the process is controlled and how its flexibility is maintained in different cell types, neurons in particular. Many regulatory proteins and some

lipids seem to be involved in this task. A higher level of understanding of the SNARE proteins and their regulators may be achieved through physiological investigations performed using gene-ablated model animals. This thesis provides two examples of such studies using SNAP-25 *null* mice. Both these studies show the importance of analysing protein function in a “clean” genetic background. Future work along these lines may focus on the characterisation of protein(s) which interact with different affinities for the two SNAP-25 splice variants, and on functional characterisation of other SNAP-25 homologues, namely SNAP-23 and SNAP-29. Interestingly, overexpression of SNAP-23 in SNAP-25 *null* chromaffin cells can partially rescue secretion, but the exocytic burst is missing suggesting that SNAP-23 cannot support a pool of primed vesicles (Sørensen *et al.*, 2003a). I am presently investigating chromaffin cell secretion mediated by chimeras between SNAP-25a and SNAP-23 proteins in order to elucidate the mechanism by which SNAP-25 protein supports priming of secretory vesicles.

The spatial organisation of the exocytic machinery probably also contributes to the regulation of the process. I believe that plasmalemmal clusters of proteins and lipids will attract more scientific interest in the future. Most of the basic aspects of their formation and function are unknown. Understanding the cause of lipid clustering is a matter of relevance. Lipid sorting may be partially influenced by their structural properties (for example, lipids with various alkyl chain lengths are differently sorted to late endosomes; Mukherjee *et al.*, 1999) and the tendency of some lipids to associate with each other (accumulation of shingolipid in lysosomes leads to co-accumulation of cholesterol and *vice versa*, for example; Puri *et al.*, 1999). It may also be possible that the lipid clustering is mediated by proteins, as may be the case with PI(4,5)P₂. Nonetheless, very little is currently known, and the field of lipid microdomains would definitely benefit from better experimental approaches and more advanced methodology. The progress in revealing the dynamics and function of PI(4,5)P₂ clusters will also depend on additional methodological and technological breakthroughs, particularly concerning *in vivo* imaging with an improved spatial and temporal resolution.

This thesis does not provide an answer on the molecular mechanism that mediates the effect of PI(4,5)P₂ on exocytosis. As detailed earlier in the Discussion, several proteins with a high affinity for PI(4,5)P₂ exist, but it is unclear whether this interaction has a physiological role. Indeed, whether PI(4,5)P₂ mediates the role of synaptotagmin family members and CAPS proteins remains questionable. Further experiments are needed to resolve this. The complexity of PI(4,5)P₂ functions is highlighted by the fact that this lipid is involved in both vesicle fusion and retrieval, implying that PI(4,5)P₂ turnover itself may determine the direction of the membrane flow. This also suggests a key role for PI(4,5)P₂ metabolising

enzymes, such as PI4P5K and synaptojanin. Animals in which these genes have been knocked-out have defective PI(4,5)P₂ metabolism and provide valuable information on the regulation of membrane flow (Cremona *et al.*, 1999; Di Paolo *et al.*, 2004). Nevertheless, there is no animal model completely devoid of PI(4,5)P₂. The present models have either decreased (PI4P5K-I γ null mouse, Di Paolo *et al.*, 2004) or increased PI(4,5)P₂ level (synaptojanin 1 null mouse, Kim *et al.*, 2002).

Another unclear aspect is the role of other PI molecules in exocytosis. It would be particularly important to understand the regulation of PI(4)P, which serves as the substrate for the generation of PI(4,5)P₂. Interesting questions include the contribution of PI(4)K type II α (a vesicle-associated enzyme) and PI4K type III α (a plasma membrane-associated enzyme) to the generation and regulation of PI(4)P pools. A strategy similar to that used in this thesis could be applied to studying the role other PIs involved in exocytosis.

Finally, I would like to stress the critical role of lipids in cellular physiology. The importance of lipids is demonstrated by a large number of genetic studies and by the many human diseases associated with the disruption of lipid metabolic enzymes and pathways. Furthermore, mammalian cells have several hundred different lipids - all of which are synthesised by enzymes. This implies that there are many proteins involved in the formation and maintenance of cellular lipid diversity, and that a significant part of the genome is devoted to encode them. Cellular membranes share common classes of lipid constituents, but differ in the relative proportions of the individual molecular species. The most apparent reason for such organisation is to confer membrane identity. Therefore, cells spend considerable amounts of energy to specifically distribute the lipid populations across the membranes and to preserve the non-homogeneity of its membrane leaflets. How this is achieved is largely unknown. In the case of proteins, sorting is achieved via recognition of peptide tags that direct components to the correct location. For lipids, no such targeting motifs have been identified. In light of the rapid transport between membranes via vesicles, selectivity must exist. It could be also possible that cells use different lipid composition as an additional level of control to ensure correct vesicular trafficking.

Although we are currently unaware of the cause, evolution has created lipid diversity for a reason. In addition, we do not understand why the PI family of lipids is present in such a small proportion. Given this characteristic, it would be possible to assign them a signalling function. The signalling and regulatory potential of PIs is enormous and it is well suited to the regulation of the complex cellular process of vesicle cycling. Such a constant and rapid changing lipid environment could mediate changes in plasma membrane structure and

dynamics, and regulate protein localisation and activity. However, the explosion of information obtained from the fields of genomics and proteomics remains to be matched by a corresponding advance of knowledge in the field of lipids. The development of novel approaches for analysis of lipids and their interacting partners will benefit lipid research. A parallel analysis of cellular lipid and protein levels (i.e. the convergence of lipidomics and proteomics) will provide, for example, a better understanding of the molecular significance of the temporal relationship between enzyme and metabolite fluctuations. This may facilitate the identification of new targets for therapeutic intervention in human diseases. Thus, I believe that the richness of lipid-dependent activities will keep many investigators busy for years to come.

Despite the growing richness of science, some basic questions remain essentially untouched. One of these questions comprises the nature of human mind. The mind emerges from the activities of the brain, whose structure and function are currently being intensively studied. Hopefully one day the diverse knowledge derived from the various levels of brain analyses will be integrated into a coherent understanding of the human mind. This doctoral work is insignificant in these terms; however, it has been conducted with the goal of addressing some aspects of exocytosis - the process underlying communication between the basic units of the brain. I hope it has succeeded in giving an impression of the wonderful molecular life present at the cellular interface.

4. SUMMARY

Ca^{2+} -triggered exocytosis is a highly regulated process and the proteinaceous machinery mediating and regulating it has been studied in detail over the last decade. However, the participation of membrane lipids and their roles in this important process remain unclear. Therefore, in addition to studying the plasmalemmal members of a protein family central to the late steps of exocytosis, the soluble N-ethylmaleimide-sensitive factor attachment protein receptors or SNAREs, I also explored the function of one plasmalemmal lipid, phosphatidylinositol 4,5-bisphosphate or $\text{PI}(4,5)\text{P}_2$.

Exocytosis is organised spatially and temporally and my aim was to examine both these aspects of exocytic regulation with respect to SNAREs and $\text{PI}(4,5)\text{P}_2$. To obtain the high temporal resolution, I used patch-clamp membrane capacitance and amperometric measurements while monitoring intracellular Ca^{2+} -levels. To acquire the spatial information, I adapted the plasma membrane sheet technique: the spatial distribution and level of $\text{PI}(4,5)\text{P}_2$ was studied using adult bovine cells and embryonic mouse chromaffin cells were employed to investigate that of SNARE proteins. The results I obtained using this powerful combination of electrophysiological and imaging assays are summarised in the following points:

1) $\text{PI}(4,5)\text{P}_2$, a signalling phospholipid with a dynamically fluctuating concentration, is spatially organised in the plasma membrane of chromaffin and pheochromocytoma cells. It is enriched in nanometric-sized clusters which require the presence of cholesterol. The $\text{PI}(4,5)\text{P}_2$ clusters partially co-localise with SNARE protein syntaxin 1 clusters to which secretory vesicles preferentially dock and fuse.

2) The level of $\text{PI}(4,5)\text{P}_2$ in the inner leaflet of the plasma membrane can be semi-quantitatively measured and manipulated. Using a $\text{PI}(4,5)\text{P}_2$ -specific monovalent probe and the plasma membrane sheet assay, I detected a twofold increase in $\text{PI}(4,5)\text{P}_2$ level upon overexpression of phosphatidylinositol-4-phosphate-5-kinase $\text{I}\gamma$ ($\text{PI4P5K-I}\gamma$), and a nearly complete elimination of $\text{PI}(4,5)\text{P}_2$ from the membrane upon overexpression of a membrane-targeted inositol 5'-phosphatase domain of synaptojanin 1 (IPP1-CAAX). I also determined a dual effect for the pharmacological drug LY294002 on $\text{PI}(4,5)\text{P}_2$ abundance: short-term LY294002 application caused a twofold increase, while long-term LY294002 application resulted in a significant decrease of plasmalemmal $\text{PI}(4,5)\text{P}_2$.

3) $\text{PI}(4,5)\text{P}_2$ is necessary for secretion, and moreover, its level directly controls the extent of exocytosis by regulating the releasable vesicle pool size but not the fusion kinetics.

If PI(4,5)P₂ is depleted from the plasma membrane by long-term LY294002 application or phosphatase overexpression, exocytosis is abolished or reduced, respectively. In contrast, when PI(4,5)P₂ levels are increased by short-term LY294002 application, PI4P5K-I γ overexpression or PI(4,5)P₂ infusion, exocytosis is increased. Collectively, these findings imply that first, the cells do not compensate for a change in PI(4,5)P₂ level, but employ it as an input signal to determine the extent of exocytosis; and second, in the resting chromaffin cells the PI(4,5)P₂ level is limiting, so that an increase in PI(4,5)P₂ concentration can up-regulate secretion. These features suggest that PI(4,5)P₂ is a potential key physiological regulator of exocytosis.

4) In a separate study, Gabor Nagy and I investigated the basis for the different secretory phenotypes associated with two SNAP-25 isoforms which differ by 9 amino acids. Using the plasma membrane sheet assay and chromaffin cells derived from SNAP-25 *null* mice, we found that both SNAP-25 splice variants are targeted to the plasma membrane with the same efficiency, are available in large excess and co-localise to the same extent with syntaxin 1 clusters. This allowed us then to investigate the role of the specific amino acid alterations in more detail. The results can be summarised as follows. The repositioning of one of the four palmitylated cysteines does not alter isoform targeting efficiency to exocytic sites. Systematic swapping of the three charge substitutions in the N-terminal SNARE domain was undertaken which indicated that two of the three non-conservative substitutions (H66Q, Q69K) are both necessary and sufficient to provide SNAP-25a with the secretory properties of SNAP-25b. The complementary substitution study in SNAP-25b revealed that the single K69Q mutation is sufficient to induce reversion to the SNAP-25a phenotype. If this is considered together with the observation that the Q69K mutation in SNAP-25 results in an intermediate phenotype, it implies that the amino acids in positions 66 and 69 do not have additive effects on exocytosis. Further biochemical and molecular dynamic stimulation experiments suggested that these two substitutions probably do not regulate exocytosis by affecting the SNARE complex properties, but rather they may play a role in the interaction with an accessory factor that could influence the stabilisation or formation of the primed vesicle state.

5) Minor perturbations of SNAP-25 binding to its SNARE partners achieved by mutating residues within the interaction layers or through C-terminal deletion does not affect plasma membrane targeting or protein expression level. Jakob B. Sørensen was then able to use these mutated proteins to demonstrate that sequential N- to C-terminal “zippering-up” of the SNARE complex drives priming and fusion of secretory vesicles.

5. REFERENCES

- Aharonovitz O, Zaun HC, Balla T, York JD, Orlowski J, Grinstein S (2000) Intracellular pH regulation by Na^+/H^+ -exchange requires phosphatidylinositol 4,5-bisphosphate. *J Cell Biol* 150, 213-224
- Aikawa Y, Martin TFJ (2003) ARF6 regulates a plasma membrane pools of phosphatidylinositol(4,5)bisphosphate required for regulated exocytosis. *J Cell Biol* 162, 647-659
- Alberts B, Johnson A, Lewis J, Raff M, Roberts K, Walter P (2002) Internal organisation of the cell. In *Molecular Biology of the Cell*. Garland Science, New York, USA, pp 583-766
- Albillos A, Dernick G, Horstmann H, Almers W, Alvarez de Toledo G, Lindau M (1997) The exocytotic event in chromaffin cells revealed by patch amperometry. *Nature* 389, 509-512
- Ales E, Tabares L, Poyato JM, Valero V, Lindau M, Alvarez de Toledo G (1999) High calcium concentrations shift the mode of exocytosis to the kiss-and-run mechanism. *Nat Cell Biol* 1, 40-44
- An S, Zenisek D (2004) Regulation of exocytosis in neurons and neuroendocrine cells. *Curr Opin Neurobiol* 14, 522-530
- Andrews NW, Chakrabarti S (2005) There's more to life than neurotransmission: the regulation of exocytosis by synaptotagmin VII. *Trends Cell Biol* 15, 626-631
- Ann K, Kowalchuk JA, Loyet KM, Martin TFJ (1997) Novel Ca^{2+} -binding protein (CAPS) related to UNC-31 required for Ca^{2+} -activated exocytosis. *J Biol Chem* 272, 19637-19640
- Antonin W, Fasshauer D, Becker S, Jahn R, Schneider TR (2002) Crystal structure of the endosomal SNARE complex reveals common structural principles of all SNAREs. *Nat Struct Biol* 9, 107-111
- Aoyagi K, Sugaya T, Umeda M, Yamamoto S, Terakawa S, Takahashi M (2005) The activation of exocytic sites by the formation of phosphatidylinositol 4,5-bisphosphate microdomains at syntaxin clusters. *J Biol Chem* 280, 17346-17352
- Aravamudan B, Fergestad T, Davis WS, Rodesch CK, Broadie K (1999) *Drosophila* UNC-13 is essential for synaptic transmission. *Nat Neurosci* 2, 965-971
- Aravanis AM, Pyle JL, Tsien RW (2003) Single synaptic vesicles fusing transiently and successively without loss of identity. *Nature* 423, 643-47
- Archer BT, Özcelik T, Jahn R, Francke U, Südhof, TC (1990) Structures and chromosomal localizations of two human genes encoding synaptobrevins 1 and 2. *J Biol Chem* 265, 17267-17273
- Ashery U, Varoqueaux F, Voets T, Betz A, Thakur P, Koch H, Neher E, Brose N, Rettig J (2000) Munc13-1 acts as a priming factor for large dense-core vesicles in bovine chromaffin cells. *EMBO J* 19, 3586-3896

- Augustin I, Rosenmund C, Südhof TC, Brose N (1999) Munc13-1 is essential for fusion competence of glutamatergic synaptic vesicles. *Nature* 400, 457-461
- Avery J, Ellis DJ, Lang T, Holroyd P, Riedel D, Henderson RM, Edwardson JM, Jahn R (2000) A cell-free system for regulated exocytosis in PC12 cells. *J Cell Biol* 148, 317-324
- Bader MF, Holz RW, Kumakura K, Vitale N (2002) Exocytosis: the chromaffin cell as a model system. *Ann NY Acad Sci* 971, 178-183
- Bai J, Chapman ER (2004) The C2 domains of synaptotagmin - partners in exocytosis. *Trends Biochem Sci* 29, 143-151
- Bai, J, Tucker, WC, Chapman ER (2004) PIP₂ increases the speed of response of synaptotagmin and steers its membrane-penetration activity toward the plasma membrane. *Nat Struct Mol Biol* 11, 36-44
- Bajohrs M, Rickman C, Binz T, Davletov B (2004) A molecular basis underlying differences in the toxicity of botulinum serotypes A and E. *EMBO Rep* 5, 1090-1095
- Balla T (2001) Pharmacology of phosphoinositides, regulators of multiple cellular functions. *Curr Pharm Des* 7, 475-507
- Bark IC, Wilson MC (1994) Human cDNA clones encoding two different isoforms of the nerve terminal protein SNAP-25. *Gene* 139, 291-292
- Bark IC, Hahn KM, Ryabinin AE, Wilson MC (1995) Differential expression of SNAP-25 protein isoforms during divergent vesicle fusion events of neural development. *Proc Natl Acad Sci USA* 92, 1510-1514
- Bark C, Bellingier FP, Kaushal A, Mathews JR, Partridge LD, Wilson MC (2004) Developmentally regulated switch in alternatively spliced SNAP-25 isoforms alters facilitation of synaptic transmission. *J Neurosci* 24, 8796-8805
- Baumert M, Maycox PR, Navone F, De Camilli P, Jahn R (1989) Synaptobrevin: an integral membrane protein of 18,000 daltons present in small synaptic vesicles of rat brain. *EMBO J* 8, 379-384
- Bennett MK, Calakos N, Scheller RH (1992) Syntaxin: a synaptic protein implicated in docking of synaptic vesicles at presynaptic active zones. *Science* 257, 255-259
- Berridge MJ, Irvine RF (1984) Inositol trisphosphate, a novel second messenger in cellular signal transduction. *Nature* 312, 315-321
- Berwin B, Floor E, Martin TF (1998) CAPS (mammalian UNC-31) protein localizes to membranes involved in dense-core vesicle exocytosis. *Neuron* 21, 137-145
- Betz A, Okamoto M, Benseler F, Brose N (1997) Direct interaction of the rat unc-13 homologue Munc13-1 with the N terminus of syntaxin. *J Biol Chem* 272, 2520-2526

- Betz A, Ashery U, Rickmann M, Augustin I, Neher E, Südhof TC, Rettig J, Brose N (1998) Munc13-1 is a presynaptic phorbol ester receptor that enhances neurotransmitter release. *Neuron* 21, 123-136
- Beutner D, Voets T, Neher E, Moser T (2001) Calcium dependence of exocytosis and endocytosis at the cochlear inner hair cell afferent synapse. *Neuron* 29, 681-690
- Bittner MA, Holz RW (2005) Phosphatidylinositol-4,5-bisphosphate: actin dynamics and the regulation of ATP-dependent and -independent secretion. *Mol Pharmacol* 67, 1089-1098
- Blasi J, Chapman ER, Yamasaki S, Binz T, Niemann H, Jahn R (1993a) Botulinum neurotoxin C1 blocks neurotransmitter release by means of cleaving HPC-1/syntaxin. *EMBO J* 12, 4821-4828
- Blasi J, Chapman ER, Link E, Binz T, Yamasaki S, De Camilli P, Südhof TC, Niemann H, Jahn R (1993b) Botulinum neurotoxin A selectively cleaves the synaptic protein SNAP-25. *Nature* 365, 160-163
- Bock JB, Matern HT, Peden AA, Scheller RH (2001) A genomic perspective on membrane compartment organization. *Nature* 409, 839-841
- Borisovska M, Zhao Y, Tsytysura Y, Glyvuk N, Takamori S, Matti U, Rettig J, Südhof T, Bruns D (2005) v-SNAREs control exocytosis of vesicles from priming to fusion. *EMBO J* 24, 2114-2126
- Boschert U, O'Shaughnessy C, Dickinson R, Tessari M, Bendotti C, Catsicas S, Pich EM (1996) Developmental and plasticity-related differential expression of two SNAP-25 isoforms in the rat brain. *J Comp Neurology* 367, 177-193
- Botelho RJ, Teruel M, Dierckman R, Anderson R, Wells A, York JD, Meyer T, Grinstein S (2000) Localized biphasic changes in phosphatidylinositol-4,5-bisphosphate at sites of phagocytosis. *J Cell Biol* 151, 1353-1368
- Brose N, Petrenko AG, Südhof TC, Jahn R (1992) Synaptotagmin: a calcium sensor on the synaptic vesicle surface. *Science* 256, 1021-1025
- Brose N, Hofmann K, Hata Y, Südhof TC (1995) Mammalian homologues of *Caenorhabditis elegans* unc-13 gene define novel family of C2-domain proteins. *J Biol Chem* 270, 25273-25780
- Brose N, Rosenmund C, Rettig J (2000) Regulation of transmitter release by Unc-13 and its homologues. *Curr Opin Neurobiol* 10, 303-311
- Caroni (2001) New EMBO members' review: actin cytoskeleton regulation through modulation of PI(4,5)P(2) rafts. *EMBO J* 20, 4332-6
- Chasserot-Golaz S, Hubert P, Thierse D, Dirrig S, Vlahos CJ, Aunis D, Bader M.-F. (1998) Possible involvement of phosphatidylinositol 3-kinase in regulated exocytosis: studies in chromaffin cells with inhibitor LY294002. *J Neurochem* 70, 2347-2355

Chamberlain LH, Burgoyne RD, Gould GW (2001) SNARE proteins are highly enriched in lipid rafts in PC12 cells: implications for the spatial control of exocytosis. *Proc Natl Acad Sci USA* 98, 5619-5624

Chamberlain LH, Gould GW (2002) The vesicle- and target-SNARE proteins that mediate Glut4 vesicle fusion are localized in detergent-insoluble lipid rafts present on distinct intracellular membranes. *J Biol Chem* 277, 49750-49754

Chapman ER (2002) Synaptotagmin: a Ca^{2+} sensor that triggers exocytosis? *Nat Rev Mol Cell Biol* 3, 498-508

Chen YA, Scales SJ, Scheller RH (2001) Sequential SNARE assembly underlies priming and triggering of exocytosis. *Neuron* 30, 161-170

Chen YA, Scheller RH (2001) SNARE-mediated membrane fusion. *Nat Rev Mol Cell Biol* 2, 98-106

Chen X, Tomchick DR, Kovrigin E, Arac D, Machius M, Südhof TC, Rizo J (2002) Three-dimensional structure of the complexin/SNARE complex. *Neuron* 33, 397-409

Chung SH, Song WJ, Kim K, Bednarski JJ, Chen J, Prestwich GD, Holz RW (1998) The C2 domains of Rabphilin3A specifically bind phosphatidylinositol 4,5-bisphosphate containing vesicles in a Ca^{2+} -dependent manner. In vitro characteristics and possible significance. *J Biol Chem* 273, 240-248

Cisternas FA, Vincent JB, Scherer SW, Ray PN (2003) Cloning and characterization of human CADPS and CADPS2, new members of the Ca^{2+} -dependent activator for secretion protein family. *Genomics* 81, 279-291

Clapham DE (1995) Calcium signaling. *Cell* 80, 259-268

Craxton M (2004) Synaptotagmin gene content of the sequenced genomes. *BMC Genomics* 5, 43

Cremona O, Di Paolo G, Wenk MR, Luthi A, Kim WT, Takei K, Daniell L, Nemoto Y, Shears SB, Flavell RA, McCormick DA, De Camilli P Essential role of phosphoinositide metabolism in synaptic vesicle recycling. *Cell* 99, 179-188

Cremona O, De Camilli P (2001) Phosphoinositides in membrane traffic at the synapse. *J Cell Sci* 114, 1041-1052

Czech MP (2000) PIP_2 and PIP_3 : complex roles at the cell surface. *Cell* 100, 603-666

Davis S, Rodger J, Stephan A, Hicks A, Mallet J, Laroche S (1998) Increase in syntaxin 1B mRNA in hippocampal and cortical circuits during spatial learning reflects a mechanism of trans-synaptic plasticity involved in establishing a memory trace. *Learn Mem* 5, 375-390

De Camilli P, Jahn R (1990) Pathways to regulated exocytosis in neurons. *Annu Rev Physiol* 52, 625-645

- De Matteis MA, Godi A (2004) PI-loting membrane traffic. *Nat Cell Biol* 6, 487-492
- Deak F, Schoch S, Liu X, Südhof TC, Kavalali ET (2004) Synaptobrevin is essential for fast synaptic-vesicle endocytosis. *Nat Cell Biol* 6, 1102-1108
- Di Paolo G, Moskowitz HS, Gipson K, Wenk MR, Voronov S, Obayashi M, Flavell R, Fitzsimonds RM, Ryan TA, De Camilli P (2004) Impaired PtdIns(4,5)P₂ synthesis in nerve terminals produces defects in synaptic vesicle trafficking. *Nature* 431, 415-422
- Dittmer JC, Dawson RM (1960) The isolation of a new complex lipid: triphosphoinositide from ox brain. *Biochim Biophys Acta* 40, 379-380
- Douglas WW (1968) Stimulus-secretion coupling: The concept and clues from chromaffin and other cells. *Br J Pharmacol* 34, 451-474
- Downing GJ, Kim S, Nakanishi S, Catt KJ, Balla T (1996) Characterization of a soluble adrenal phosphatidylinositol 4-kinase reveals wortmannin sensitivity of type III phosphatidylinositol kinases. *Biochemistry* 35, 3587-94
- Dulubova I, Sugita S, Hill S, Hosaka M, Fernandez I, Südhof TC (1999) A conformational switch in syntaxin during exocytosis: role of Munc18. *EMBO J* 18, 4372-4382
- Eberhard DA, Cooper CL, Low MG, Holz RW (1990) Evidence that the inositol phospholipids are necessary for exocytosis. Loss of inositol phospholipids and inhibition of secretion in permeabilised cells caused by a bacterial phospholipase C and removal of ATP. *Biochem J* 268, 15-25
- Efanov AM, Zaitsev SV, Berggren PO (1997) Inositol hexakisphosphate stimulates non-Ca²⁺-mediated and primes Ca²⁺-mediated exocytosis of insulin by activation of protein kinase C. *Proc Natl Acad Sci USA* 94, 4435-4439
- Elferink LA, Trimble WS, Scheller RH (1989) Two vesicle-associated membrane protein genes are differentially expressed in the rat central nervous system. *J Biol Chem* 264, 11061-11064
- Elhamdani A, Martin TF, Kowalchuk JA, Artalejo CR (1999) Ca²⁺-dependent activator protein for secretion is critical for the fusion of dense-core vesicles with the membrane in calf adrenal chromaffin cells. *J Neurosci* 19, 7375-7383
- Edidin M (2003a) Lipids on the frontier: a century of cell-membrane bilayers. *Nat Rev Mol Cell Biol* 4, 414-418
- Edidin M (2003b) The state of lipid rafts: from model membranes to cells. *Annu Rev Biophys Biomol Struct* 32, 257-283
- Fasshauer D, Sutton RB, Brunger AT, Jahn R (1998) Conserved structural features of the synaptic fusion complex: SNARE proteins reclassified as Q- and R-SNAREs. *Proc Natl Acad Sci USA* 95, 15781-15786

- Fisher RJ, Revsner J, Burgoyne RD (2001) Control of fusion pore dynamics during exocytosis by Munc18. *Science* 291, 875-878
- Fruman DA, Meyers RE, Cantley LC (1998) Phosphoinositide kinases. *Annu Rev Biochem* 67, 481-507
- Folch J (1949) Brain diposphoinositide, a new phosphatide having inositol metadiphosphate as a constituent. *J Biol Chem* 177, 505-519
- Ford MG, Pearse BM, Higgins MK, Vallis Y, Owen DJ, Gibson A, Hopkins CR, Evans PR, McMahon HT (2001) Simultaneous binding of PtdIns(4,5)P₂ and clathrin by AP180 in the nucleation of clathrin lattices on membranes. *Science* 291, 1051-1055
- Fukuda M, Kanno E, Satoh M, Saegusa C, Yamamoto A (2004) Synaptotagmin VII is targeted to dense-core vesicles and regulates their Ca²⁺-dependent exocytosis in PC12 cells, *J Biol Chem* 279, 52677-52684
- Gandhi SP, Stevens CF (2003) Three modes of synaptic vesicular recycling revealed by single-vesicle imaging. *Nature* 423, 607-613
- Gamper N, Reznikov V, Yamada Y, Yang J, Shapiro MS (2004) Phosphatidylinositol 4,5-bisphosphate signals underlie receptor specific Gq/11-mediated modulation of N-type Ca²⁺ channels. *J Neurosci* 24, 10980-10992
- Geppert M, Goda Y, Hammer RE, Li C, Rosahl TW, Stevens CF, Südhof TC (1994) Synaptotagmin I: a major Ca²⁺ sensor for transmitter release at a central synapse. *Cell* 79, 717-727
- Gil A, Rueda J, Viniegra S, Gutierrez LM (2000) The F-actin cytoskeleton modulates slow secretory components rather than readily releasable vesicle pools in bovine chromaffin cells. *Neurosci* 98, 605-614
- Gil A, Gutierrez LM, Carrasco-Serrano C, Alonso MT, Viniegra S, Criado M (2002) Modifications in the C terminus of the synaptosome-associated protein of 25 kDa (SNAP-25) and in the complementary region of synaptobrevin affect the final steps of exocytosis. *J Biol Chem* 277, 9904-9910
- Gillooly DJ, Stenmark H (2001) Cell biology. A lipid oils the endocytosis machine. *Science* 291, 993-994
- Glebov OO, Nichols BJ (2004) Lipid rafts proteins have a random distribution during localised activation of the T-cell receptor. *Nat Cell Biol* 6, 238-243
- Gong LW, Di Paolo G, Diaz E, Cestra G, Diaz ME, Lindau M, De Camilli P, Toomre D (2005) Phosphatidylinositol phosphate kinase type I gamma regulates dynamics of large dense-core vesicle fusion. *Proc Natl Acad Sci USA* 102, 5204-5209
- Gonzalo S, Linder ME (1998) SNAP-25 palmitoylation and plasma membrane targeting require a functional secretory pathway. *Mol Biol Cell* 9, 585-597

- Graham ME, Sudlow AW, Burgoyne RD (1997) Evidence against an acute inhibitory role of nSec-1 (munc-18) in late steps of regulated exocytosis in chromaffin and PC12 cells. *J Neurochem* 69, 2369-2377
- Grant NJ, Hepp R, Krause W, Aunis D, Oehme P, Langley K (1999) Differential expression of SNAP-25 isoforms and SNAP-23 in the adrenal gland. *J Neurochem* 72, 363-37
- Griffiths G (1993) Fine structure preservation. In *Fine structure immunocytochemistry*. Eds. Griffiths G, Burke B and Lucocq J, Springer-Verlag, Berlin, pp 26-80
- Grishanin RN, Klenchin VA, Loyet KM, Kowalchuk JA, Ann K, Martin TF (2002) Membrane association domains in Ca^{2+} -dependent activator protein for secretion mediate plasma membrane and dense-core vesicle binding required for Ca^{2+} -dependent exocytosis. *J Biol Chem* 277, 22025-22034
- Grishanin RN, Kowalchuk JA, Klenchin VA, Ann K, Earles CA, Chapman ER, Gerona RR, Martin TF (2004) CAPS acts at a pre-fusion step in dense-core vesicle exocytosis as a PIP_2 binding protein. *Neuron* 43, 551-562
- Gross SD, Hoffman DP, Fisette PL, Baas P, Anderson RA (1995) A phosphatidylinositol 4,5-bisphosphate-sensitive casein kinase I α associates with synaptic vesicles and phosphorylates a subset of vesicle proteins. *J Cell Biol* 130, 711-724
- Gundelfinger ED, Kessels MM, Qualmann B (2003) Temporal and spatial coordination of exocytosis and endocytosis. *Nat Rev Mol Cell Biol* 4, 127-139
- Hammond G, Thomas CL, Schiavo G (2004) Nuclear phosphoinositides and their functions. *Curr Top Microbiol Immunol* 282, 177-206
- Han X, Wang CT, Bai J, Chapman ER, Jackson MB (2004) Transmembrane segments of syntaxin line the fusion pore of Ca^{2+} -triggered exocytosis. *Science* 304, 289-292
- Hanson PI, Heuser JE, Jahn R (1997) Neurotransmitter release - four years of SNARE complexes. *Curr Opin Neurobiol* 7, 310-315
- Hay JC, Martin TF (1993) Phosphatidylinositol transfer protein required for ATP-dependent priming of calcium activated secretion. *Nature* 366, 572-575
- Hay JC, Fisette PL, Jenkins GH, Fukami K, Takenawa T, Anderson RA, Martin TF (1995) ATP-dependent inositide phosphorylation required for calcium activated secretion. *Nature* 374, 173-177
- Helms JB, Zurzolo C (2004) Lipids as targeting signals: lipid rafts and intracellular trafficking. *Traffic* 5, 247-254
- Hess DT, Slater TM, Wilson MC, Skene JH (1992) The 25 kDa synaptosomal-associated protein SNAP-25 is the major methionine-rich polypeptide in rapid axonal transport and a major substrate for palmitoylation in adult CNS. *J Neurosci* 12, 4634-4641

Hilgemann DW, Ball R (1996) Regulation of cardiac Na^+ , Ca^{2+} exchange and KATP potassium channels by PIP_2 . *Science* 273, 956-959

Hilgemann DW, Feng S, Nasuhoglu C (2001) The complex and intriguing lives of PIP_2 with ion channels and transopters. *Sci STKE* 2001, RE 19

Hirono M, Denis CS, Richardson GP, Gillespie PG (2004) Hair cells require phosphatidylinositol 4,5-bisphosphate for mechanical transduction and adaptation. *Neuron* 44, 309-320

Hokin M, Hokin L (1953) Enzyme secretion and the incorporation of ^{32}P into phospholipids of pancreas slices. *J Biol Chem* 203, 967-977

Holroyd P, Lang T, Wenzel D, De Camilli P, Jahn R (2002) Imaging direct, dynamin-dependent re-capture of fusing secretory granules on plasma membrane lawns from PC12 cells. *Proc Natl Acad Sci USA* 99, 16806-16811

Holz RW, Bittner MA, Peppers SC, Senter RA, Eberhard DA (1989) MgATP-independent and MgATP-dependent exocytosis. Evidence that MgATP primes adrenal chromaffin cells to undergo exocytosis. *J Biol Chem* 264, 5412-5419

Holz RW, Hlubek MD, Sorensen SD, Fisher SK, Balla T, Ozaki S, Prestwich GD, Stuenkel EL, Bittner MA (2000) A pleckstrin homology domain specific for phosphatidylinositol 4,5-bisphosphate (PtdIns-4,5-P_2) and fused to green fluorescent protein identifies plasma membrane PtdIns-4,5-P_2 as being important in exocytosis. *J Biol Chem* 275, 17878-17885

Honda A, Nogami M, Yokozeki T, Yamazaki M, Nakamura H, Watanabe H, Kawamoto K, Nakayama K, Morris AJ, Frohman MA, Kanaho Y (1999) Phosphatidylinositol 4-phosphate 5-kinase α is a downstream effector of the small G protein ARF6 in membrane ruffle formation. *Cell* 99, 521-532

Hope HR, Pike LJ (1996) Phosphoinositides and phosphoinositide-utilising enzymes in detergent-insoluble lipid domains. *Mol Biol Cell* 7, 843-851

Hu K, Carroll J, Fedorovich S, Rickman C, Sukhodub A, Davletov B (2002) Vesicular restriction of synaptobrevin suggests a role for calcium in membrane fusion. *Nature* 415, 646-650

Hu C, Ahmed M, Melia TJ, Sollner TH, Mayer T, Rothman JE (2003) Fusion of cells by flipped SNAREs. *Science* 300, 1745-1749

Hui E, Bai J, Wang P, Sugimori M, Llinas RR, Chapman ER (2005) Three distinct kinetic groupings of the synaptotagmin family: Candidate sensors for rapid and delayed exocytosis. *Proc Natl Acad Sci USA* 102, 5210-5214

Huisamen B, Lochner A (1996) Inositolpolyphosphates and their binding proteins - a short review. *Mol Cell Biochem* 157, 229-232

Hurley JH, Misra S (2000) Signaling and subcellular targeting by membrane binding domains. *Annu Rev Biophys Biomol Struct* 29, 49-79

- Hurley JH, Mayer T (2001) Subcellular targeting by membrane lipids. *Curr Opin Cell Biol* 13, 146-152
- Irvine RF (2005) Inositide evolution - towards turtle domination? *J Physiol* 566, 295-300
- Jain MK (1972) The bimolecular lipid membranes. Van Nostrand Reinhold Company, New York, USA
- Jahn R, Lang T, and Südhof TC (2003) Membrane fusion. *Cell* 112, 519-533
- Janssens PM (1988) The evolutionary origin of eukaryotic transmembrane signal transduction. *Comp Biochem Physiol* 90, 209-223
- Jost M, Simpson F, Kavran JM, Lemmon MA, Schmid SL (1998) Phosphatidylinositol-4,5-bisphosphate is required for endocytic coated vesicle formation. *Curr Biol* 8, 1399-1402
- Kandel ER, Schwartz JH, Jessell TM (2000) Elementary interactions between neurons: Synaptic transmission. In *Principles of neuronal science*. Eds. Butler J, Lebowitz H, McGraw-Hill, Palatino, USA
- Kim WT, Chang S, Daniell L, Cremona O, Di Paolo G, De Camilli P (2002) Delayed reentry of recycling vesicles into the fusion-competent synaptic vesicle pool in synaptotagmin 1 knockout mice. *Proc Natl Acad Sci USA* 99, 17143-17148
- Klopfenstein DR, Tomishige M, Stuurman N, Vale RD (2002) Role of phosphatidylinositol 4, 5-bisphosphate organisation in membrane transport by the Unc104 kinesin motor. *Cell* 109, 347-358
- Krauss M, Kinuta M, Wenk MR, De Camilli P, Takei K, Haucke V (2003) ARF6 stimulates clathrin/AP-2 recruitment to synaptic membranes by activating phosphatidylinositol phosphate kinase type Igamma. *J Cell Biol* 162, 113-124
- Kweon DH, Kim CS, Shin YK (2003) Regulation of neuronal SNARE assembly by the membrane. *Nat Struct Biol* 10, 440-447
- Lane SR, Liu Y (1997) Characterization of the palmitoylation domain of SNAP-25. *J Neurochem* 69, 1864-1869
- Lang T, Wacker I, Steyer J, Kaether C, Wunderlich I, Soldati, T, Gerdes HH, Almers W (1997) Ca^{2+} -triggered peptide secretion in single cells imaged with green fluorescent protein and evanescent-wave microscopy. *Neuron* 18, 857-863
- Lang T, Bruns D, Wenzel D, Riedel D, Holroyd P, Thiele C, Jahn R. (2001), SNAREs are concentrated in cholesterol-dependent clusters that define docking and fusion sites for exocytosis. *EMBO J* 20, 2202-2213
- Lang T, Margittai M, Hölzler H, Jahn R (2002) SNAREs in the native plasma membranes are active and readily form core complexes with endogenous and exogenous SNAREs. *J Cell Biol* 158, 751-760

Lang T (2003) Imaging SNAREs at work in “unroofed” cells – approaches that may be of general interest for functional studies on membrane proteins. *Biochem Soc Trans* 31, 861-864

Larrabee MG, Klingman JD, Leicht WS (1963) Effects of temperature, calcium and activity on phospholipid metabolism in a sympathetic ganglion. *J Neurochem* 10, 549-570

Laux T, Fukami, K, Thelen M, Golub T, Frey D, Caroni P (2000) GAP43, MARCKS, and CAP23 modulate PI(4,5)P₂ at plasmalemmal rafts, and regulate cell cortex actin dynamics through a common mechanism. *J Cell Biol* 149, 1455-1472

Lawrence JT, Birnbaum MJ (2003) ADP-ribosylation factor 6 regulates insulin secretion through plasma membrane phosphatidylinositol 4,5-bisphosphate. *Proc Natl Acad Sci USA* 100, 13320-13325

Lemmon MA, Ferguson KM, O'Brien R, Sigler PB, Schlessinger J (1995) Specific and high-affinity binding of inositol phosphates to an isolated pleckstrin homology domain. *Proc Natl Acad Sci USA* 92, 10472-10476

Lemmon MA (2003) Phosphoinositide recognition domains. *Traffic* 4, 201-213

Leung S-M, Chen D, DasGupta BR, Whiteheart SW, Apodaca G (1998) SNAP-23 requirement for transferrin recycling in streptolysin-O-permeabilised MDCK cells. *J Biol Chem* 273, 34171-34179

Levine TP, Munro S (1998) The pleckstrin homology domain of oxysterol-binding protein recognises a determinant specific to Golgi membranes. *Curr Biol* 8, 729-39

Liscovitch M, Chalifa V, Pertile P, Chen CS, Cantley LC (1994) Novel function of phosphatidylinositol 4,5-bisphosphate as a cofactor for brain membrane phospholipase D. *J Biol Chem* 269, 21403–21406

Littleton JT, Barnard RJ, Titus SA, Slind J, Chapman ER, Ganetzky B (2001) SNARE-complex disassembly by NSF follows synaptic-vesicle fusion. *Proc Natl Acad Sci USA* 98, 12233-12238

Loranger SS, Linder ME (2002) SNAP-25 traffics to the plasma membrane by a syntaxin-independent mechanism. *J Biol Chem* 277, 34303-9

Loyet KM, Kowalchuk JA, Chaudhary A, Chen J, Prestwich GD, Martin TF (1998) Specific binding of phosphatidylinositol 4,5-bisphosphate to calcium-dependent activator protein for secretion (CAPS), a potential phosphoinositide effector protein for regulated exocytosis. *J Biol Chem* 273, 8337-8343

McMahon HT, Missler M, Li C, Südhof TC (1995) Complexins: cytosolic proteins that regulate SNAP receptor function. *Cell* 83, 111-119

Martin TF, Loyet KM, Barry VA, Kowalchuk JA (1997) The role of PtdIns(4,5)P₂ in exocytotic membrane fusion. *Biochem Soc Trans* 25, 1137-1141

- Martin TF (2001) PI(4,5)P(2) regulation of surface membrane traffic. *Curr Opin Cell Biol* 13, 493-499
- Martin TF (2003) Tuning exocytosis for speed: fast and slow modes. *Biochim Biophys Acta* 1641, 157-165
- Mansvelder HD, Kits KS (2000) Calcium channels and the release of large dense core vesicles from neuroendocrine cells: spatial organisation and functional coupling. *Prog Neurobiol* 62, 427-441
- Matos MF, Mukherjee K, Chen X, Rizo J, Südhof TC (2003) Evidence for SNARE zippering during Ca^{2+} -triggered exocytosis in PC12 cells. *Neuropharmacology* 45, 777-786
- McNew JA, Parlati F, Fukuda R, Johnston RJ, Paz K, Paumet F, Sollner TH, Rothman JE (2000) Compartmental specificity of cellular membrane fusion encoded in SNARE proteins. *Nature* 407, 153-159
- Melia TJ, Weber T, McNew JA, Fisher LE, Johnston RJ, Parlati F, Mahal LK, Sollner TH, Rothman JE (2002) Regulation of membrane fusion by the membrane-proximal coil of the t-SNARE during zippering of SNAREpins. *J Cell Biol* 158, 929-940
- Micheva KD, Holz RW, Smith SJ (2001) Regulation of presynaptic phosphatidylinositol 4,5-bisphosphate by neuronal activity. *J Cell Biol* 154, 355-368
- Misura KM, Scheller RH, Weis WI (2000) Three-dimensional structure of the neuronal-Sec1-syntaxin 1a complex. *Nature* 404, 355-362
- Mitchell CA, Brown S, Campbell JK, Munday AD, Speed CJ (1996) Regulation of second messengers by the inositol polyphosphate 5-phosphatases. *Biochem Soc Trans* 24, 994-1000
- Monck JR, Robinson IM, Escobar AL, Vergara JL, Fernandez JM (1994) Pulsed laser imaging of rapid Ca^{2+} -gradients in excitable cells. *Biophys J* 67, 505-514
- Mukherjee S, Soe TT, Maxfield FR (2004) Endocytic sorting of lipid analogues differing solely in the chemistry of their hydrophobic tails. *J Cell Biol* 144, 1271-1284
- Mukherjee S, Maxfield FR (2004) Membrane domains. *Annu Rev Cell Dev Biol* 20, 839-866
- Munro S (2003) Lipid rafts: elusive or illusive? *Cell* 115, 377-388
- Nagy G, Matti U, Nehring RB, Binz T, Rettig J, Neher E, Sørensen JB (2002) Protein kinase C-dependent phosphorylation of synaptosome-associated protein of 25 kDa at Ser187 potentiates vesicle recruitment. *J Neurosci* 22, 9278-9286
- Nagy G, Reim K, Matti U, Brose N, Binz T, Rettig J, Neher E, Sørensen JB (2004) Regulation of releasable vesicle pool sizes by protein kinase A-dependent phosphorylation of SNAP-25. *Neuron* 41, 417-429

- Nagy G, Kim JH, Matti U, Sørensen JB (2006) Differential control of the calcium-dependence of exocytosis by synaptotagmin 1 and 2 isoforms, but not by synaptotagmin 1 phosphorylation. *J Neurosci (in press)*
- Nasuhoglu C, Feng S, Mao J, Yamamoto M, Yin HL, Earnest S, Barylko B, Albanesi JP, Hilgemann DW (2002) Nonradioactive analysis of phosphatidylinositides and other anionic phospholipids by anion-exchange high-performance liquid chromatography with suppressed conductivity detection. *Anal Biochem* 301, 243-254
- Niemann H, Blasi J, Jahn R (1994) Clostridial neurotoxins: new tools for dissecting exocytosis. *Trends Cell Biol* 4, 179-185
- Neher E, Zucker RS (1993) Multiple calcium-dependent processes related to secretion in bovine chromaffin cells. *Neuron* 10, 21-30
- Ninomiya Y, Kishimoto T, Yamazawa T, Ikeda H, Miyashita Y, Kasai H (1997) Kinetic diversity in the fusion of exocytotic vesicles. *EMBO J* 16, 929-934
- Ohara-Imaizumi M, Nishiwaki C, Nakamichi Y, Kikuta T, Nagai S, Nagamatsu S (2004) Correlation of syntaxin-1 and SNAP-25 clusters with docking and fusion of insulin granules analysed by total internal reflection fluorescence microscopy. *Diabetologia* 47, 2200-2207
- Oheim M, Loerke D, Stuhmer W, Chow RH (1998) The last few milliseconds in the life of a secretory granule. Docking, dynamics and fusion visualized by total internal reflection fluorescence microscopy (TIRFM). *Eur Biophys J* 27, 83-98
- Olsen HL, Hoy M, Zhang W, Bertorello AM, Bokvist K, Capito K, Efanov AM, Meister B, Thams P, Yang SN, Rorsman P, Berggren PO, Gromada J (2003) Phosphatidylinositol 4-kinase serves as a metabolic sensor and regulates priming of secretory granules in pancreatic beta cells. *Proc Natl Acad Sci USA* 100, 5187-92
- Okamoto M, Südhof TC (1997) Mints, Munc18-interacting proteins in synaptic vesicle exocytosis. *J Biol Chem* 272, 31459-31464
- Oliver D, Lien CC, Soom M, Baukrowitz T, Jonas P, Fakler B (2004) Functional conversion between A-type and delayed rectifier K⁺ channels by membrane lipids. *Science* 304, 265-270
- Oyler GA, Higgins GA, Hart RA, Battenberg E, Billingsley M, Bloom FE, Wilson MC (1989) The identification of a novel synaptosomal-associated protein, SNAP-25, differentially expressed by neuronal subpopulations. *J Cell Biol* 109, 3039-3052
- Pabst S, Hazzard JW, Antonin W, Südhof TC, Jahn R, Rizo J, Fasshauer D (2000) Selective interaction of complexin with the neuronal SNARE complex. Determination of the binding regions. *J Biol Chem* 275, 19808-19818
- Pan PY, Cai Q, Lin L, Lu PH, Duan S, Sheng ZH (2005) SNAP-29-mediated modulation of synaptic transmission in cultured hippocampal neurons. *J Biol Chem* 280, 25769-25779
- Parsons TD, Coorssen JR, Horstmann H, Almers W (1995) Docked granules, the exocytic burst, and the need for ATP hydrolysis in endocrine cells. *Neuron* 15, 1085-1096

- Parlati F, McNew JA, Fukuda R, Miller R, Sollner TH, Rothman JE (2000) Topological restriction of SNARE-dependent membrane fusion. *Nature* *407*, 194-198
- Perin MS, Fried VA, Mignery GA, Jahn R, Südhof TC (1990) Phospholipid binding by a synaptic vesicle protein homologous to the regulatory region of protein kinase C. *Nature* *345*, 260-263
- Pevsner J, Hsu SC, Scheller RH (1994) n-Sec1: a neural-specific syntaxin-binding protein. *Proc Natl Acad Sci USA* *91*, 1445-1449
- Plattner H, Artalejo AR, Neher E (1997) Ultrastructural organization of bovine chromaffin cell cortex-analysis by cryofixation and morphometry of aspects pertinent to exocytosis. *J Cell Biol* *139*, 1709-1717
- Pike LJ, Casey L (1996) Localisation and turnover of phosphatidylinositol 4,5-bisphosphate in caveolin-enriched membrane microdomains. *J Biol Chem* *271*, 26453-26456
- Pike LJ, Miller JM (1998) Cholesterol depletion delocalised phosphatidylinositol bisphosphate and inhibits hormone-stimulated phosphatidylinositol turnover. *J Biol Chem* *273*, 22298-22304
- Puri V, Watanabe R, Dominguez M, Sun X, Wheatley CL, Marks DL, Pagano RE (1999) Cholesterol modulates membrane traffic along the endocytic pathway in sphingolipid-storage diseases. *Nat Cell Biol* *1*, 386-388
- Rana RS, Hokin LE (1990) Role of phosphoinositides in transmembrane signaling. *Physiol Rev* *70*, 115-164
- Raucher D, Stauffer T, Chen W, Shen K, Guo S, York JD, Sheetz MP, Meyer T (2000) Phosphatidylinositol 4,5-bisphosphate functions as a second messenger that regulates cytoskeleton-plasma membrane adhesion. *Cell* *100*, 221-228
- Ravichandran V, Chawla A, Roche PA (1996) Identification of a novel syntaxin- and synaptobrevin/VAMP-binding protein, SNAP-23, expressed in non-neuronal tissues. *J Biol Chem* *271*, 13300-13303
- Rea S, Martin LB, McIntosh S, Macaulay SL, Ramsdale T, Baldini G, James DE (1998) Syndet, an adipocyte target SNARE involved in insulin-induced translocation of GLUT4 to the cell surface. *J Biol Chem* *273*, 18784-18792
- Reim K, Mansour M, Varoqueaux F, McMahon HT, Südhof TC, Brose N, Rosenmund C (2001) Complexins regulate a late step in Ca²⁺-dependent neurotransmitter release. *Cell* *104*, 71-81
- Rettig J, Neher E (2002) Emerging roles of presynaptic proteins in calcium triggered exocytosis. *Science* *298*, 781-785
- Rhee SG, Bae YS (1997) Regulation of phosphoinositide-specific phospholipase C isozymes. *J Biol Chem* *272*, 15045-15048

- Richmond JE, Broadie KS (2002) The synaptic vesicle cycle: exocytosis and endocytosis in *Drosophila* and *C. elegans*. *Curr Opin Neurobiol* 12, 499-507
- Rickman C, Meunier FA, Binz T, Davletov B (2004) High affinity interaction of syntaxin and SNAP-25 on the plasma membrane is abolished by botulinum toxin E. *J Biol Chem* 279, 644-651
- Rizo J, Südhof TC (2002) SNAREs and Munc18 in synaptic vesicle fusion. *Nat Rev Neurosci* 3, 641-653
- Robinson IM, Yamada M, Carrion-Vazquez M, Lennon VA, Fernandez JM (1996) Specialized release zones in chromaffin cells examined with pulsed-laser imaging. *Cell Calcium* 20, 181-201
- Rohacs T, Lopes CM, Jin T, Ramdya PP, Molnar Z, Logothetis DE (2003) Specificity of activation by phosphoinositides determines lipid regulation of Kir channels. *Proc Natl Acad Sci USA* 100, 745-750
- Rosenmund C, Clements JD, Westbrook GL (1993) Nonuniform probability of glutamate release at a hippocampal synapse. *Science* 262, 754-757
- Rowe J, Corradi N, Malosio ML, Taverna E, Halban P, Meldolesi J, Rosa P (1999) Blockade of membrane transport and disassembly of the Golgi complex by expression of syntaxin 1A in neurosecretion-incompetent cells: prevention by rbSEC1. *J Cell Sci* 112, 1865-1877
- Rosenmund C, Sigler A, Augustin I, Reim K, Brose N, Rhee JS (2002) Differential control of vesicle priming and short-term plasticity by Munc13 isoforms. *Neuron* 33, 411-424
- Ruiz-Montasell B, Aguado F, Majo G, Chapman ER, Canals JM, Marsal J, Blasi J (1996) Differential distribution of syntaxin isoforms 1A and 1B in the rat central nervous system. *Eur J Neurosci* 8, 2544-2552
- Rupnik M, Kreft M, Sikdar SK, Grilc S, Romih R, Zupancic G, Martin TF, Zorec R (2000) Rapid regulated dense-core vesicle exocytosis requires the CAPS protein. *Proc Natl Acad Sci USA* 97, 5627-5632
- Salaün C, James DJ, Greaves J, Chamberlain LH (2004) Plasma membrane targeting of exocytic SNARE proteins. *Biochim Biophys Acta* 1693, 81-89
- Salaün C, Gould GW, Chamberlain LH (2005) Lipid raft association of SNARE proteins regulates exocytosis in PC12 cells. *J Biol Chem* 280, 19449-19453
- Sankaranarayanan S, Atluri PP, Ryan TA (2003) Actin has a molecular scaffolding, not propulsive, role in presynaptic function. *Nat Neurosci* 6, 127-135
- Schneggenburger R, Neher E (2000) Intracellular calcium dependence of transmitter release rates at a fast central synapse. *Nature* 406, 889-893

Schiavo G, Gu QM, Prestwich GD, Sollner TH, Rothman JE (1996) Calcium-dependent switching of the specificity of phosphoinositide binding to synaptotagmin. *Proc Natl Acad Sci USA* 93, 13327-13332

Schroeder TJ, Jankowski JA, Senyshyn J, Holz RW, Wightman RM. (1994) Zones of exocytotic release on bovine adrenal medullary cells in culture. *J Biol Chem* 269, 17215-17220

Schoch S, Deak F, Königstorfer A, Mozhayeva M, Sara Y, Südhof TC, Kavalali ET (2001) SNARE function analyzed in synaptobrevin/VAMP knockout mice. *Science* 294, 1117-1122

Schulze KL, Littleton JT, Salzberg A, Halachmi N, Stern M, Lev Z, Bellen HJ (1994) rop, a *Drosophila* homolog of yeast Sec1 and vertebrate n-Sec1/Munc-18 proteins, is a negative regulator of neurotransmitter release in vivo. *Neuron* 13, 1099-1108

Sechi AS, Wehland J (2000) The actin cytoskeleton and plasma membrane connection: PtdIns(4,5)P(2) influences cytoskeletal protein activity at the plasma membrane. *J Cell Sci* 113, 3685-3695

Shao X, Li C, Fernandez I, Zhang X, Südhof TC, Rizo J (1997) Synaptotagmin-syntaxin interaction: the C2 domain as a Ca²⁺-dependent electrostatic switch. *Neuron* 18, 133-42

Shears SB, Yang L, Qian X (2004) Cell signaling by a physiologically reversible inositol phosphate kinase/phosphatase. *Adv Enzyme Regul* 44, 265-277

Sherry DM, Wang MM, Frishman LJ (2003) Differential distribution of vesicle associated membrane protein isoforms in the mouse retina. *Mol Vis* 9, 673-688

Simons K, Ilkonen E (1997) Functional rafts in cell membranes. *Nature* 387, 569-572

Simons K, Toomre D (2000) Lipid rafts and signalling transduction. *Nat Rev Mol Cell Biol* 1, 31-39

Simonsen A, Wurmser AE, Emr SD, Stenmark H (2001) The role of phosphoinositides in membrane transport. *Curr Opin Cell Biol* 13, 485-492

Singh AK (1992) Quantitative analysis of inositol lipids and inositol phosphates in synaptosomes and microvessels by column chromatography: comparison of the mass analysis and the radiolabelling methods. *J Chromatogr* 581, 1-10

Slepnev VI, De Camilli P (2000) Accessory factors in clathrin-dependent synaptic vesicle endocytosis. *Nat Rev Neurosci* 1, 161-172

Sorensen SD, Linseman DA, McEwen EL, Heacock AM, Fisher SK (1998). A role for a wortmannin-sensitive phosphatidylinositol-4-kinase in the endocytosis of muscarinic cholinergic receptors. *Mol Pharmacol* 53, 827-836

Söllner T, Whiteheart SW, Brunner M, Erdjument-Bromage H, Geromanos S, Tempst P, Rothman JE (1993) SNAP receptors implicated in vesicle targeting and fusion. *Nature* 362, 318-324

- Sørensen JB, Matti U, Wei SH, Nehring RB, Voets T, Ashery U, Binz T, Neher E, Rettig J (2002) The SNARE protein SNAP-25 is linked to fast calcium triggering of exocytosis. *Proc Natl Acad Sci USA* 99, 1627-1632
- Sørensen JB, Nagy G, Varoqueaux F, Nehring RB, Brose N, Wilson MC, Neher E (2003a) Differential control of the releasable vesicle pools by SNAP-25 splice variants and SNAP-23. *Cell* 114, 75-86
- Sørensen JB, Fernandez-Chacon R, Südhof TC, Neher E (2003b) Examining synaptotagmin 1 function in dense core vesicle exocytosis under direct control of Ca^{2+} . *J Gen Physiol* 122, 265-276
- Sørensen JB (2004) Formation, stabilisation and fusion of the readily releasable pool of secretory vesicles. *Eur J Physiol* 448, 347-362
- Speidel D, Varoqueaux F, Enk C, Nojiri M, Grishanin RN, Martin TF, Hofmann K, Brose N, Reim K (2003) A family of Ca^{2+} -dependent activator proteins for secretion: comparative analysis of structure, expression, localization, and function. *J Biol Chem* 278, 52802-52809
- Speidel D, Bruederle CE, Enk C, Voets T, Varoqueaux F, Reim K, Becherer U, Fornai F, Ruggieri S, Holighaus Y, Weihe E, Bruns D, Brose N, Rettig J (2005) CAPS1 regulates catecholamine loading of large dense-core vesicles. *Neuron* 46, 75-88
- Stauffer TP, Ahn S, Meyer T (1998) Receptor-induced transient reduction in plasma membrane $\text{PtdIns}(4,5)\text{P}_2$ concentration monitored in living cells. *Curr Biol* 8, 343-346
- Steegmaier M, Yang B, Yoo JS, Huang B, Shen M, Yu S, Luo Y, Scheller RH (1998) Three novel proteins of the syntaxin/SNAP-25 family. *J Biol Chem* 273, 34171-34179
- Steyer JA, Horstmann H, Almers W. (1997) Transport, docking and exocytosis of single secretory granules in live chromaffin cells. *Nature* 388, 474-478
- Steyer JA, Almers W (2001) A real-time view of life within 100 nm of the plasma membrane. *Nat Rev Mol Cell Biol* 2, 268-275
- Südhof TC (1995) The synaptic vesicle cycle: a cascade of protein-protein interactions. *Nature* 375, 645-653
- Südhof TC (2002) Synaptotagmins: why so many? *J Biol Chem* 277, 7629-7632
- Südhof TC (2004) The synaptic vesicle cycle. *Annu Rev Neurosci* 27, 509-547
- Suh BC, Hille B (2005) Regulation of ion channels by phosphatidylinositol 4,5-bisphosphate. *Curr Opin Neurobiol* 15, 370-378
- Sugita S, Han W, Butz S, Liu X, Fernandez-Chacon R, Lao Y, Südhof TC (2001) Synaptotagmin VII as a plasma membrane Ca^{2+} sensor in exocytosis. *Neuron* 30, 459-473

- Sugita S, Shin OH, Han W, Lao Y, Südhof TC (2002) Synaptotagmins form a hierarchy of exocytotic Ca^{2+} sensors with distinct Ca^{2+} affinities. *EMBO J* 21, 270-280
- Sutton RB, Fasshauer D, Jahn R, Brunger AT (1998) Crystal structure of a SNARE complex involved in synaptic exocytosis at 2.4 Å resolution. *Nature* 395, 347-353
- Tall EG, Spector I, Pentyala SN, Bitter I, Rebecchi MJ (2000). Dynamics of phosphatidylinositol 4,5-bisphosphate in actin-rich structures. *Curr Biol* 10, 743-746
- Takei K, Haucke V, Slepnev V, Farsad K, Salazar M, Chen H, De Camilli P (1998) Generation of coated intermediates of clathrin-mediated endocytosis on protein-free liposomes. *Cell* 94, 131-141
- Tandon A, Bannykh S, Kowalchuk JA, Banerjee A, Martin TF, Balch WE (1998) Differential regulation of exocytosis by calcium and CAPS in semi-intact synaptosomes. *Neuron* 21, 147-154
- Taraska JW, Perrais D, Ohara-Imaizumi M, Nagamatsu S, Almers W (2003) Secretory granules are recaptured largely intact after stimulated exocytosis in cultured endocrine cells. *Proc Natl Acad Sci USA* 100, 2070-2075
- Teng FY, Wang Y, Tang BL (2001) The syntaxins. *Genome Biol* 2, REVIEWS3012
- Terrian DM, White MK (1997) Phylogenetic analysis of membrane trafficking proteins: a family reunion and secondary structure predictions. *Eur J Cell Biol* 73, 198-204
- Traub LM (2003) Sorting it out: AP-2 and alternate clathrin adaptors in endocytic cargo selection. *J Cell Biol* 163, 203-208
- Trimble WS, Cowan DM, Scheller RH (1988) VAMP-1: a synaptic vesicle-associated integral membrane protein. *Proc Natl Acad Sci USA* 85, 4538-4542
- Tomlinson RV, Ballou CE (1961) Complete characterization of the myo-inositol polyphosphates from beef brain phosphoinositide. *J Biol Chem* 236, 1902-1906
- Toonen RF (2003) Role of Munc18-1 in synaptic vesicle and large dense-core vesicle secretion. *Biochem Soc Trans* 31, 848-850
- Trimble WS, Gray TS, Elferink LA, Wilson MC, Scheller RH (1990) Distinct patterns of expression of two VAMP genes within the rat brain. *J Neurosci* 10, 1380-1387
- Tsuboi T, Rutter GA (2003) Multiple forms of “kiss and run” exocytosis revealed by evanescent wave microscopy. *Curr Biol* 13, 563-567
- Xu T, Binz T, Niemann H, Neher E (1998) Multiple kinetic components of exocytosis distinguished by neurotoxin sensitivity. *Nat Neurosci* 1, 192-200
- Vaidyanathan VV, Puri N, Roche PA (2001) The last exon of SNAP-23 regulates granule exocytosis from mast cells. *J Biol Chem* 276, 25101-25106

- van Rheenen J, Jalink K (2002) Agonist-induced PIP₂ hydrolysis inhibits cortical actin dynamics: Regulation at a global but not at a micrometer scale. *Mol Biol Cell* 13, 3257-3267
- van Rheenen J, Achame EM, Janssen H, Calafat J, Jalink K (2005) PIP₂ signaling in lipid domains: a critical re-evaluation. *EMBO J* 24, 1664-1673
- Vanhaesebroeck B, Leervers SJ, Ahmadi K, Timms J, Katso R, Driscoll PC, Woscholski R, Parker PJ, Waterfield MD (2001) Synthesis and function of 3-phosphorylated inositol lipids. *Annu Rev Biochem* 70, 535-602
- Varnai P, Balla T (1998) Visualization of phosphoinositides that bind pleckstrin homology domains: calcium- and agonist-induced dynamic changes and relationship to myo-[3H]inositol-labeled phosphoinositide pools. *J Cell Biol* 143, 501-510
- Veit M, Söllner TH, Rothman JE (1996) Multiple palmitoylation of synaptotagmin and the t-SNARE SNAP-25. *FEBS Letters* 385, 119-123
- Verhage M, Maia AS, Plomp JJ, Brussaard AB, Heeroma JH, Vermeer H, Toonen RF, Hammer RE, van den Berg TK, Missler M, Geuze HJ, Südhof TC (2000) Synaptic assembly of the brain in the absence of neurotransmitter secretion. *Science* 287, 864-869
- Vitale ML, Seward EP, Trifaro J-M (1995) Chromaffin cell cortical actin network dynamics control the size of the release-ready vesicle pool and the initial rate of exocytosis. *Neuron* 14, 353-363
- Vitale N, Chasserot-Golaz S, Bailly Y, Morinaga N, Frohman MA, Bader MF (2002) Calcium-regulated exocytosis of dense-core vesicles requires the activation of ADP-ribosylation factor (ARF)6 by ARF nucleotide binding site opener at the plasma membrane. *J Cell Biol* 159, 79-89
- Voets T, Neher E, Moser T (1999) Mechanisms underlying phasic and sustained secretion in chromaffin cells from mouse adrenal slices. *Neuron* 23, 607-615
- Voets T (2000) Dissection of three calcium-dependent steps leading to secretion in chromaffin cells from mouse adrenal slices. *Neuron* 28, 537-545
- Voets T, Toonen RF, Brian EC, de Wit H, Moser T, Rettig J, Südhof TC, Neher E, Verhage M (2001) Munc18-1 promotes large dense-core vesicle docking. *Neuron* 31, 581-591
- Vogel K, Cabaniols J-P, Roche PA (2000) Targeting of SNAP-25 to membranes is mediated by its association with the target SNARE syntaxin. *J Biol Chem* 275, 2959-2965
- Wang G, Witkin JW, Hao G, Bankaitis VA, Scherer PE, Baldini G (1997) Syndet ia a novel SNAP-25 related protein expressed in many tissues. *J Cell Sci* 110, 505-513
- Walent JH, Porter BW, Martin TF (1992) A novel 145 kd brain cytosolic protein reconstitutes Ca²⁺-regulated secretion in permeable neuroendocrine cells. *Cell* 70, 765-775

Washbourne P, Cansino V, Mathews JR, Graham M., Burgoyne RD, Wilson MC (2001) Cysteine residues of SNAP-25 are required for SNARE disassembly and exocytosis, but not for membrane targeting. *Biochem J* 357, 625-634

Waugh MG, Lawson D, Tan SK, Hsuan JJ (1998) Phosphatidylinositol 4-phosphate synthesis in immunisolated caveolae-like vesicles and low buoyant density non-caveolar membranes. *J Biol Chem* 273, 17115-17121

Waters MG, Hughson FM (2000) Membrane tethering and fusion in the secretory and endocytic pathways. *Traffic* 1, 588-597

Watt SA, Kular G, Fleming IN, Downes CP, Lucocq JM (2002) Subcellular localization of phosphatidylinositol 4,5-bisphosphate using the pleckstrin homology domain of phospholipase C δ_1 . *Biochem J* 363, 657-666

Weber T, Zemelman BV, McNew JA, Westermann B, Gmachl M, Parlati F, Sollner TH, Rothman JE (1998) SNAREpins: minimal machinery for membrane fusion. *Cell* 92, 759-772

Weimbs T, Mostov K, Low SH, Hofmann K (1998) A model for structural similarity between different SNARE complexes based on sequence relationships. *Trends Cell Biol* 8, 260-262

Weernink PA, Meletiadis K, Hommeltenberg S, Hinz M, Ishihara H, Schmidt M, Jakobs KH (2004) Activation of type I phosphatidylinositol 4-phosphate 5-kinase isoforms by the Rho GTPases, RhoA, Rac1, and Cdc42. *J Biol Chem* 279, 7840-7849

Wenk MR, Pellegrini L, Klenchin VA, Di Paolo G, Chang S, Daniell L, Arioka M, Martin TF, De Camilli (2001) PIP kinase Igamm is the major PI(4,5)P(2) synthesizing enzyme at the synapse. *Neuron* 32, 79-88

Wenk MR, De Camilli P (2004) Protein-lipid interactions and phosphoinositide metabolism in membrane traffic: insights from vesicle recycling in nerve terminals. *Proc Natl Acad Sci USA* 101, 8262-8269

Wenk MR (2005) The emerging field of lipidomics. *Nat Rev Drug Discov* 4, 594-610

Woscholski R, Finan PM, Radley E, Totty NF, Sterling AE, Hsuan JJ Waterfield MD, Parker PJ (1997) Synaptojanin is the major constitutively active phosphatidylinositol 3,4,5-triphosphate 5-phosphatase in rodent brain. *J Biol Chem* 272, 9625-9628

Wölfel M, Schneggenburger R (2003) Presynaptic capacitance measurements and Ca²⁺ uncaging reveal submillisecond exocytosis kinetics and characterize the Ca²⁺ sensitivity of vesicle pool depletion at a fast CNS synapse. *J Neurosci* 23, 7059-7068

Wu L, Bauer CS, Zhen XG, Xie C, Yang J (2002) Dual regulation of voltage gated calcium channels by PtdIns(4,5)P2. *Nature* 419, 947-952

Xu T, Binz T, Niemann H, Neher E (1998) Multiple kinetic components of exocytosis distinguished by neurotoxin sensitivity *Nature Neurosci* 1, 192-200

- Xu T, Rammner B, Margittai M, Artalejo AR, Neher E, Jahn R (1999) Inhibition of SNARE complex assembly differentially affects kinetic components of exocytosis. *Cell* 99, 713-722
- Yang B, Steegmaier M, Gonzalez LC Jr, Scheller RH (2000) nSec1 binds a closed conformation of syntaxin1A. *J Cell Biol* 148, 247-252
- Yin HL, Janmey PA (2003) Phosphoinositide regulation of the actin cytoskeleton. *Annu Rev Physiol* 65, 761-789
- Zhang X, Kim-Miller MJ, Fukuda M, Kowalchuk JA, Martin TF (2002) Ca^{2+} -dependent synaptotagmin binding to SNAP-25 is essential for Ca^{2+} -triggered exocytosis. *Neuron* 34, 599-611
- Zhang H, Craciun LC, Mirshahi T, Rohacs T, Lopes CM, Jin T, Logothetis DE (2003) PIP_2 activates KCNQ channels and its hydrolysis underlies receptor mediated inhibition of M currents. *Neuron* 37, 963-975

Abbreviations

ATP	adenosine 5'-triphosphate
BCC	bovine chromaffin cell
BoNT	botulinum neurotoxin
°C	degree Celsius
Ca ²⁺	calcium cation
[Ca ²⁺] _i	intracellular Ca ²⁺ concentration
CAPS	Ca ²⁺ -dependent activator protein for secretion
C _m	membrane capacitance
DAG	diacylglycerol
DNA	deoxyribonucleic acid
EGTA	ethylene glycol-O,O'-bis(2-aminoethyl)-N,N,N',N'-tetraacetic acid
GDP	guanosine 5'-bisphosphate
GFP	green fluorescent protein
GTP	guanosine 5'-triphosphate
I(1,4,5)P ₃	inositol (1,4,5)-triphosphate
K ⁺	potassium cation
LDCV	large dense-core vesicle
MARCKS	myristoylated alanine-rich C kinase substrate
Mg ²⁺	magnesium cation
NPY	neuropeptide Y
NSF	N-ethylmaleimide-sensitive fusion protein
PC12	pheochromocytoma cell line
PA	phosphatidic acid
PH	pleckstrin homology domain
PH-PLCδ ₁	pleckstrin homology domain of phospholipase C-δ ₁
PI	phosphatidylinositide
PI(4)P	phosphatidylinositol 4-phosphate
PI(4,5)P ₂	phosphatidylinositol 4,5-bisphosphate
PI4P5K-I _γ	phosphatidylinositol 4-phosphate 5-kinase I _γ
PI3K	phosphatidylinositol 3-kinase
PITP	phosphatidylinositol transfer protein
PKC	protein kinase C
PLCδ ₁	phospholipase C-δ ₁
PLD	phospholipase D
RRP	rapidly releasable pool
SFV	Semliki Forest Virus
SM	Sec1/Munc18-like protein
SNAP	soluble NSF attachment protein
SNAP-25	synaptosomal-associated protein of 25 kDa
SNARE	soluble NSF attachment protein receptor
SRP	slowly releasable pool
SV	synaptic vesicle
TIRF	total internal reflection microscopy
UPP	unprimed pool

Acknowledgements

I wish to express my sincere gratitude to:

My supervisor Prof. Erwin Neher, head of the Membrane Biophysics Department at the MPIbpc, for giving me an opportunity to work in his laboratory and making this study possible, for continuous support and sharing his vision of science with me, for an ideal scientific environment to grow and evolve.

My supervisor Prof. Reinhard Jahn, head of the Neurobiology Department at the MPIbpc, for giving me an opportunity to work in his laboratory, for his support and interest as well as his contribution to make me a better scientist.

Dr. Jakob B. Sørensen, my “daily” supervisor, for his encouragement and enthusiasm, for endless patience and support, for his readiness to always find the time to help me and discuss the data. Jakob, I enjoyed working with you. Thank you for that!

Dr. Thorsten Lang for sharing with me the early steps in the laboratory and the challenging moments of refining the membrane sheet assay for PI(4,5)P₂ measurements.

My colleagues Dr. Gabor Nagy, Dr. Attila Gulyas-Kovacs, Dr. Jean-Sebastian Schonn, Ignacio Delgado and Dr. Marcin Barszczewski for all help over the years and stimulating discussions.

Prof. Volker Haucke and Dr. Michael Krauss for a fruitful collaboration on the role of PI(4,5)P₂ in exocytosis.

Dr. Ralf Nehring for help with cloning in the moments of despair, Ina Herfort for numerous bovine chromaffin cell preparations and Dirk Reuter for Semliki Forest Virus preparations.

All previous and present members of the Departments of Membrane Biophysics and Neurobiology, for assistance in developing this thesis in a pleasant working atmosphere.

Boehringer Ingelheim Fonds and Max Planck Society for the financial support.

Nuno Raimundo for sharing all my ups and downs and his infinite patience and support.

My parents and sister for their love and support throughout my life. *Mama, tata, Nina, hvala od srca za sve!*

CURRICULUM VITAE

Name	Ira Milosevic
Gender	female
Born	January 19 th , 1978, Sinj, Croatia (27 years old)
Citizenship	Croatian citizen
Marital status	single
Private address	Karl-Grünekle-Str. 6a, 37073 Göttingen Phone: +49 179 685 8231
Work address	Max Planck Institute for Biophysical Chemistry (MPIbpc), Am Fassberg 11, 37077 Göttingen, Germany Dept. of Membrane Biophysics; Tel. +49 551 201 1022 Dept. of Neurobiology; Tel. +49 551 201 1658 E-mail: imilose@gwdg.de http://www.gpneuro.uni-goettingen.de/students/stud2001/stud_13.html http://www.mpibpc.gwdg.de/abteilungen/140/groups/mme/index.html
Education	2003 – present Ph.D. student, MPIbpc, Göttingen, Germany 2001 – present International Ph.D. Program in Neuroscience, Göttingen, Germany 2001 – 2003 M.Sc. student, MPIbpc, Göttingen, Germany 1999 – 2000 Diploma student, Eötvös Lorand University, Budapest, Hungary 1996 – 2001 University of Zagreb, Faculty of Natural Sciences and Mathematics, Zagreb, Croatia
Degree	2003 M.Sc. in Neuroscience, Georg August University Göttingen, Germany 2001 Diploma in Molecular Biology (Dipl. Ing.), University of Zagreb, Croatia
Research experience	04/2003 – present Ph.D. student Temporal and spatial aspects of chromaffin cell exocytosis, collaborative project within two departments of MPIbpc in Göttingen: Dept. of Membrane Biophysics, supervisors: Prof. Dr. Erwin Neher, Dr. Jakob B. Sørensen and Dept. of Neurobiology, supervisor: Prof. Dr. Reinhard Jahn 10/2002 – 04/2003 M.Sc. student Plasma membrane microdomains of proteins and lipids involved in neuroendocrine cell exocytosis, Dept. of Membrane Biophysics, supervisor: Prof. Dr. Erwin Neher and Dept. of Neurobiology, supervisor: Prof. Dr. Reinhard Jahn 01/2001 – 07/2002 four 7-8 weeks long “laboratory rotations” within the International Ph.D. Program in Neuroscience, Göttingen, Germany: 1. Morphological analysis of Bassoon distribution in the plasma membrane of the PC-12 cells, MPIbpc, Dept. of Neurobiology; supervisors Prof. Dr. R. Jahn, Dr. T. Lang 2. Effect of inositol-1,3,4,5,6-pentakisphosphate on calcium triggered secretion in bovine chromaffin cells, MPIbpc, Dept. of Membrane Biophysics; supervisors Prof. Dr. E. Neher, Dr. J. B. Sørensen

3. Effect of lithium salts on CREB/CRE-directed transcription in cell culture system, University Hospital Göttingen, Dept. of Molecular Pharmacology; supervisor Prof. Dr. W. Knepel

4. α_{2B} -adrenergic receptors in the tree shrew (*Tupaia belangeri*) brain: regional expression and immunohistochemical detection, German Primate Center, Dept. of Neurobiology; supervisors Prof. Dr. E. Fuchs, Dr. G. Flügge

07/2001 – 09/2001 Transformation of *Deinococcus radiodurans* with *cyt1Aa* gene from *Bacillus thuringiensis* subsp. *israelensis*, Ben Gurion University of the Negrev, Beer-Sheva, Israel; supervisor: Prof. Dr. A. Zaritsky

07/1999 – 11/2000 Diploma student
Construction of molluscan myosin with a structurally altered regulatory light chain, Eötvös Lorand University, Dept. of Biochemistry, Budapest, Hungary; supervisor: Prof. Dr. L. Nyitrai and Rudjer Boskovic Institute, Dept. of Molecular Genetics, Zagreb, Croatia; supervisor Prof. Dr. I. Weygand-Durasevic

Awards/Scholarships	05/2003 – 10/2005 Boehringer Ingelheim Fond Scholarship 10/2002 – 04/2003 Max Planck Society Scholarship 10/2001 – 09/2002 DeveloGen Scholarship 2000, 2003 FEBS Travel Funds 2000 Rector's Award for the year 2000, University of Zagreb, Croatia 1997 – 2000 Croatian Ministry of Science and Technology Merit Scholarship
Membership in Society	German Society for Biochemistry and Molecular Biology, since 2003 American Society for Neuroscience, since 2004
Teaching responsibility	04/2001 – 10/2001 Teaching assistant in "Practicum in molecular biology" (1 semester), University of Split, Faculty of Science and Education, Split, Croatia
Languages	Croatian language (mother tongue) English language German language

International symposia and courses

International Summer School on Biophysics, September 2000, Rovinj, Croatia
(FEBS Scholarship)

FEBS Advanced Course on Lipid Signalling and Membrane Traffic, June 2003, S. Maria Imbaro, Italy
(FEBS Scholarship); Own contribution: 10 min talk and poster

12th International Symposium on Chromaffin Cell Biology, September 2003, La Palma, Spain
(B.I.F. Scholarship); Own contribution: 10 min talk and poster

International Titisee Conference, October 2003, Titisee, Germany
(B.I.F. Scholarship); Own Contribution: Poster

Synaptic transmission: From ion channels to neuronal network function, June 2004, Göttingen, Germany
Own contribution: Poster

FEBS Special Meeting on Cytoskeletal Dynamics, June 2004, Helsinki, Finland
Own contribution: Poster

Biophysical Society Discussions: Probing Membrane Microdomains, October 2004, Asilomar, CA, USA
(B.I.F. Scholarship); Own contribution: Poster

Neurizons: Interdisciplinary Ph.D. Student Symposium, November 2004, Göttingen, Germany
Own contribution: Co-organiser and poster

Science: Get it across, Cold Spring Harbor, NY, USA
(B.I.F. Scholarship); Own contribution: 10 min talk

FEBS Advanced Course on Lipid-protein interaction in signalling and membrane traffic, June 2005, S. Maria Imbaro, Italy
(IMPRS Travel Funds by the Ph.D. Program in Neuroscience); Own contribution: 10 min talk and poster

35th Annual Meeting of Society of Neuroscience: Neuroscience 2005, November 2005, Washington DC, USA
(B.I.F. Scholarship); Own contribution: 10 min talk

List of publications

Milosevic I, Sørensen JB, Lang T, Krauss M, Nagy G, Haucke V, Jahn R, Neher E (2005) Plasmalemmal phosphatidylinositol-4,5-bisphosphate level regulates the releasable vesicle pool size in chromaffin cells. *J Neurosci* 25 (10), 2557-2565

Nagy G*, Milosevic I*, Fasshauer D, Müller M, de Groot B, Lang T, Wilson MC, Sørensen JB (2005) Alternative splicing of SNAP-25 regulates secretion through non-conservative substitutions in the SNARE domain. *Mol. Biol. Cell* 16, 5675-5685

*equal contribution

Sørensen JB, Wiederhold K, Müller M, Milosevic I, Nagy G, de Groot B, Grubmüller H, Fasshauer D (2006) Sequential N- to C-terminal „zippering-up“ of the SNARE complex drives priming and fusion of secretory vesicles. *EMBO J.*